TIME-DEPENDENT LOSSES IN

POST-TENSIONED PRESTRESSED CONCRETE

A thesis presented for the Degree of

Doctor of Philosophy

By

Waheeb Ahmed Amin Al-khaja

The Department of Civil Engineering

The University of Leeds

August, 1986

To my parents

and my wife

SYNOPSIS

An investigation has been undertaken into the factors affecting the time-dependent deformations, prestress losses and deflections of Class 1 uncracked prestressed concrete beams. The main influencing factors considered were environmental conditions, loading conditions, size and shape of members and concrete mix composition. Twenty seven beams consisting of both I- and rectangular sections with different concrete mixes, and tested under different environmental and loading conditions, were monitored for a period of one year. Tests were also conducted on short I- and rectangular beams and cylindrical control specimens to determine the shrinkage and creep properties of various concrete mixes including some with PFA and admixtures.

Results indicated that a significant reduction in prestress losses was observed for beams of different sections stored in the variable humidity condition, although camber and deflection values for loaded and non-loaded beams stored in constant and variable environments were comparable.

A comprehensive assessment has been undertaken to determine the reliability of various methods of predicting deformations, prestress losses and deflections by comparing current prediction methods with experimental results obtained during this research programme. The use of experimentally determined material parameters for creep and shrinkage, is also considered in the prediction methods. Proposals are made for improving prediction by the current British Code: BS8110:1985.

ACKNOWLEDGEMENTS

I would like to thank Professor A.R. Cusens, Head of Civil Engineering Department of the University of Leeds, for allowing the use of the facilities for this investigation.

I am greatly indebted to Mr. A.E. Gamble and Dr. J.J. Brooks for their unfailing help and supervision during my study in Leeds University and especially their constructive criticism, constant guidance and encouragement throughout the course of this research.

I would like to extend my appreciation and thanks to the technical staff for their assistance in the preparation of test, and Miss Nemes for typing the manuscript.

I would also like to express my deep gratitude to my wife, Wedad Nass, for the love, patience and support she gave me during my study.

I am also indebted to my parents for their encouragement and support so that I have the opportunity to study in this country.

Notation

A_c = Cross-sectional area of member

A_g = Area of gross section

A_t = Area of transformed section

a_t = Deflection at any time

d = Average thickness of concrete member

$E_c, E_c(t_o)$ = Static modulus of elasticity at the age of application of load

$E_{c_d}(t_o)$ = Dynamic modulus of elasticity at the age of application of load

E_e, E_{eff} = Effective modulus of elasticity of concrete

E_s = Modulus of elasticity of steel

E' = Fictitious modulus of elasticity of concrete

e = Eccentricity (in mm)

f_c = Net concrete compressive stress at tendon level

$f_{cyl_{28}}$ = 28-day cylinder strength

f_{pu} = Guaranteed ultimate tensile strength of prestressing steel

f_s = Remaining stress at time t after prestressing

f_{si} = Initial stress of steel

f_y = Yield strength of steel

I = Second moment of area of section

I_g = Moment of inertia of gross section

I_t = Moment of inertia of transformed section

M_D = Bending moment due to dead load

M_s = Moment due to the superimposed load

P = Prestres force after all losses

P_o = Prestress force at transfer

R = Relaxation coefficient

U = Circumference exposed to drying

$\sigma_{ap,o}$ = Initial tension in the steel

$\Sigma_{sh}(t,t_o)$ = Shrinkage of concrete at any time (10^{-6})

$\Sigma_{sh\infty}$ = Ultimate shrinkage of concrete (10^{-6})

$\phi(t,t_o)$ = Creep coefficient of concrete

$\Phi(t,t_o)$ = Creep function (10^{-3} per MPa)

Φ_∞ = Ultimate creep function

TABLE OF CONTENTS

CHAPTER 4 PREDICTION AND ANALYSIS METHODS OF CREEP AND SHRINKAGE DEFORMATIONS

CHAPTER 1 - INTRODUCTION

1.1 General

Prestressed concrete members undergo time-dependent deformations as a result of creep and shrinkage of the concrete and relaxation of the prestressing steel wires or strands. The rate of creep and shrinkage of concrete and relaxation of the prestressing steel are greatest during the early ages, and decrease continuously with time.

During the last decade, there has been considerable renewed interest in the amount of prestress losses which occur during the lifetime of prestressed concrete structures. As a result, some long-term investigations into the behaviour of prestressed concrete members have been carried out under field conditions where varying environmental conditions play an important factor in the behaviour of the structure.

Now that some experience has been gained under both laboratory and field conditions, it can be used to determine new factors for the prediction of prestress losses, recognizing the complex interrelationships which exist between shrinkage, creep of concrete and relaxation of the prestressing steel. Recently, attention has been given to the time-dependent camber and deflection of flexural members, which while not affecting ultimate capacities of structures, may be critical for serviceability criteria.

1.2 Definition of Terms

Some of the basic terminology may be defined as follows:

Prestressed concrete member : A prestressed concrete member is a structural member in which a permanent predetermined force system is established in such a manner that the stresses resulting from any anticipated condition of external loading are counteracted to a predetermined and desired degree.

Tendon: A tendon is a steel (cable, wire, strand or bar) used to impart prestress to the concrete.

Grouted tendons: The tendons are "Bonded tendons" if bonded to the concrete either directly or through grouting throughout its length to the surrounding concrete.

Ungrouted tendons: The tendons are "Unbonded tendons" if free relative to the surrounding concrete.

Post-tensioning: An application of prestress to the concrete in which the tendons are tensioned after the concrete is placed and cured.

Class 1 prestressed member: Member with no tensile stresses allowed in the concrete (uncracked member) in order to prevent corrosion of steel caused by severe exposure conditions such as sea water or alternate wetting and drying condition.

Transfer: Transfer is the operation of transferring the tendon force to the concrete.

Shrinkage of concrete: Shrinkage of concrete is the time-dependent contraction of concrete due to loss of evaporable water; shrinkage is independent of external load.

Creep of concrete: Creep of concrete is the time-dependent deformation which occurs under a constant sustained load as distinguished from the elastic deformation which occurs when the load is first applied.

Relaxation of steel: Relaxation is the reduction in tensile stress that occurs as a consequence of creep of steel throughout the length of the wire or bar when the length is kept constant

Camber of beam: is the upward midspan deflection due to prestressing force, self weight load.

Deflection in beam: is the downward midspan deflection due to superimposed sustained load

1.3 Objectives of Present Investigation

A programme of research has been undertaken on class 1 uncracked prestressed concrete beams with grouted and ungrouted tendons with the following objectives:

(1) To investigate the effect of variable humidity conditions on concrete strength and elastic modulus, creep and shrinkage, strain-time relationship, and time-dependent loss of prestress and deflection of concrete members.

(2) To identify the influence of different loading conditions (no loading, cyclic and sustained loadings) on the time-dependent behaviour of prestress losses and deflections.

(3) To investigate the influence of shape and size of members on time-dependent deformation, loss of prestress and deflection.

(4) To study the effect of different concrete mix compositions including PFA and a superplasticizing admixture on concrete strength and elastic modulus, creep and shrinkage, and time-dependent prestress losses and deflections.

(5) To investigate the stabilization period of camber and deflection with time.

(6) To appraise the recommendations of present Codes and Specifications concerning the calculation of elastic strain, creep and shrinkage, and long-term prestress losses and deflections by using general or experimental material parameters.

1.4 Outline of Thesis

The thesis consists of eight chapters as follows:

Following the general introduction in the present chapter, Chapter Two gives a detailed survey of past research on time-dependent deformations, prestress losses and camber and deflection of members.

In Chapter Three, the experimental programme, materials, instrumentation, testing measurements and procedures are outlined and discussed in detail.

In Chapter Four, the methods of prediction and analysis of creep and shrinkage are reviewed.

In Chapter Five, experimental investigation of factors affecting creep and shrinkage are presented and comparisons are made and discussed between the experimental and predicted results.

In Chapter Six, experimental observations of time-dependent prestress losses and a comparison with current prediction methods are presented.

In Chapter Seven, the behaviour of time-dependent deflection and camber for prestressed concrete beams is described and discussed. Comparisons are made between the experimental and predicted results.

In Chapter Eight, the conclusions from the investigation are summarised and recommendations for further study are made.

CHAPTER 2 - REVIEW OF LITERATURE

2.1. Long-Term Prestress Losses

2.1.1 General

In recent years prestressed concrete has rapidly developed into an important structural system. One of the problems in the analysis and design of a prestressed member is the accurate determination of the loss of prestress over an extended period of time. Unsatisfactory performance, or possibly failure, may result from underestimation of losses, while undesirable camber could result from overestimation.

Various design specifications include widely different provisions for prestress loss estimation. At one extreme, some codes of practice simply specify a straight percentage or constant value for prestress loss. In contrast, other specifications involve lengthy procedures requiring the use of many equations, graphs, and numerical constants.

This section is primarily concerned with the long-term prestress loss components, namely creep and shrinkage of concrete, and relaxation in steel. These three time-dependent components are very heavily interdependent and hence cannot be considered completely separately. Furthermore, accurate estimation of these long-term losses is difficult on account of the many factors affecting them, such as the quality and composition of concrete, the quality of steel, the environment in which the structure is kept,

the curing process of concrete, etc. A few suggested prediction procedures are briefly described and compared in the following paragraphs.

In 1967 Ghali, Neville and Jha (1) developed an expression for the loss of prestress in which elastic and creep recoveries of concrete strain induced by steel relaxation were taken into account, as well as the increase in the modulus of elasticity of concrete with time. Ghali et al. (1) believed that previous investigators had ignored at least one of these factors. Consequently, a step-by-step procedure was used incorporating an estimate of the concrete modulus of elasticity, as well as several other assumptions. The prestress loss at the end of any interval can be calculated, provided that the loss at the beginning of the same interval is known. In the above process the loss in any interval is assumed to act from the middle of the interval up to the time at which the loss is determined. Each loss component -shrinkage, creep and relaxation - is considered separately only for each interval.

In 1973 Ghali and Dilger (2) simplified the previous method (1). An interaction of the three time-dependent components is accounted for by the use of graphs intended for practical design. Assumptions include a constant modulus of elasticity of concrete (equal to the value at the time of application of prestress) and that prestress is applied at one stage only.

The step-by-step procedure used in developing the graphs and other design aids, incorporate the strain compatibility

condition that the total strain in the steel and concrete due to all causes must be equal at the end of each interval in order to determine the loss during that interval. Only the final value of the loss is given by this method. It was believed that the final value of loss was sensitive only to the final values of creep, shrinkage and relaxation, not to their variation with time.

In 1971 Branson and Kripanarayanan (3) conducted a systemmatic investigation at the University of Iowa into the material and structural response of prestressed concrete members and developed a procedure for estimating prestress losses. This method includes equations with separate terms for the prestress loss components. Some component interaction is recognised in the expression for creep loss, but not in any other terms. Continuous time functions are provided for all required parameters, as well as some approximate equations and several correction factors. All correction factors are applied to ultimate values.

This procedure used by Branson and Kripanarayanan for predicting time-dependent material and structural behaviour represents a nominal approach for design purposes. These procedures are neither definitive nor statistical and therefore they concluded that probabilistic methods should be used for an accurate estimation of the loss.

Glodowski and Lorenzetti (4) presented in 1972 an "interaction" method for prestress loss prediction. The basis of this method is a stress-strain balancing technique in which the

service life is divided into small time intervals during which the relaxation, creep and shrinkage can be assumed to be independent of each other.

Since interaction between steel and concrete is considered, a procedure for determining steel relaxation losses under conditions of changing strain is established. The procedure developed involves transfer from one stress level relaxation curve to another for each change in strain. The accuracy of the interaction method is dependent upon the accuracy of the material property determinations, as well as proper descriptions of actual stress levels and environment of the structure during its life. As concluded by Glodowski and Lorenzetti, the interaction method yielded lower total prestress losses than if loss causes were treated independently. The reduction is generally more significant for steel stress relaxation.

2.1.2 Creep and Shrinkage

2.1.2.1 General

Creep and shrinkage are two important parameters to be considered in prestressed concrete when estimating prestress loss. Prestressed concrete can be considered as a more general case of reinforced concrete, but the presence of prestress in a member increases the importance of both creep and shrinkage effects. Both these phenomena, in common with other losses, reduce the compressive stresses which prestress induces in a member. The serviceability of a member could thus be impaired by such a reduction in prestress

perhaps resulting in undesirable formation of cracks.

Although creep and shrinkage phenomena are commonly known, they have not been uniformly defined. Researchers have usually supplied definitions for specific use in their experiments.

Abeles (5) described creep thus: "If concrete is subject to any kind of stress for some considerable time, then the initially produced deformation will continue to increase and this increase will go on for years". Abeles also mentions that creep is primarily a permanent phenomenon and attributes it to the plastic properties of gels contained in the concrete while they are still moist.

Even when no stress is acting, concrete undergoes a gradual deformation with time. This is due to the movement of water from the concrete to the surrounding medium, and is commonly referred to as shrinkage.

The two phenomena, creep and shrinkage, are considered additive. Thus, the total increase in strain is assumed to be the sum of shrinkage (equal in magnitude to that of an unstressed member) and of a change in strain due to stress (creep). This assumption proved suitable for those applications where both creep and shrinkage occured simultaneously.

Neville (6) gives definitions for creep of drying concrete members subjected to a sustained stress, which enhances the understanding of the creep phenomenon. The creep occurring under

conditions of no moisture movement into or out of the surrounding medium is termed basic creep, whereas the additional strain caused by the concurrent drying process is called drying creep. Neville mentions that by separating creep into these two components, the real phenomenon can be interpreted correctly. He describes three stages of creep under a constant applied stress: primary (decreasing rate of creep), secondary (steady-state creep), and tertiary (associated with increasing strain rate, cracking and increased actual stress, and finally resulting in failure of material). In prestressed concrete members, however, the concrete stress does not remain constant. Herein lies the difficulty in accurately estimating creep of concrete. Also it should be noted that the effect of shrinkage in post-tensioned members is reduced, since an appreciable amount of shrinkage occurs before the prestress is applied to the member. Similarly, as the prestress is usually applied at a later stage, the loss due to creep is also smaller than that in pretensioned member. Consequently, a smaller loss is frequently allowed for in post-tensioned members.

2.1.2.2 Influencing Factors

There are many factors known to influence creep and shrinkage of prestressed concrete members.

This section is primarily concerned with the influencing factors which are experimentally investigated and discussed in this research project. Such influencing factors are: effect of environmental condition, effect of shape and size of members, effect

of stress level and loading condition and effect of cement, superplasticizers and PFA on long term deformations.

In ACI Special Publications-27 and 76 (7, 8), "Prediction of creep Shrinkage and Temperature Effects in Concrete Structures" (1971, 1982), the principal variables affecting both creep and shrinkage, in most cases, are listed. The variables considered were: time of initial loading and time of initial shrinkage, environmental humidity, minimum thickness of member, water/cement ratio in the form of slump and cement content, and mix proportions in the form of percent fines and air content. Most researchers generally agree with the above listing. In accordance with the factors mentioned above, ACI also presented several correction factors to account for deviations from a carefully chosen "normal" condition. These factors are normally not excessive and tend to offset each other. In general, for design purpose, these may normally be neglected with the possible exception of the effect of member size and slump.

In 1964, Neville and Meyers (9) listed the following factors as affecting creep: age of member, elastic modulus of the aggregate used, relative humidity, drying process, moisture movement and temperature. As was previously explained, the effect of creep is greatest and therefore of largest importance at early age. At later ages, however, Neville and Meyers asserted that the rate of creep becomes independent of the ambient relative humidity, and that shrinkage is essentially completed.

2.1.2.2.1 Effect of Environmental Conditions

There have been few investigations into the effects of varying the relative humidity on the creep and shrinkage of concrete, and thus the incorporation of this information into engineering practice has been slow.

In 1942 Pickett (10) demonstrated that the rate of creep deformation of 51 mm by 51 mm plain concrete flexural specimens increased each time the specimens were either submerged in water or removed from water.

Later in 1961, Hansen (11) subjected a series of 20-mm deep flexural specimens to cycles of changing humidity, and found that while the shrinkage of unstressed specimens corresponded to shrinkage at the average relative humidity; the creep corresponded approximately to creep of specimens maintained at the lower limit of the relative humidity cycle. The length of the humidity cycle was significant, as was the initial moisture state of the specimens.

Corley and Sozen (12) developed a numerical method based on the rate of creep and superposition methods for calculating long-time behaviour of sustained load tests on prestressed concrete beams carried out under laboratory conditions. They found that the computed results were in good agreement with laboratory measurements.

Corley and Sozen indicated that since actual bridge structures are subjected to the changes in humidity and temperature

of the environment, using creep and shrinkage values based on laboratory tests, even if conducted on the materials used for a given structure, could lead to erroneous predictions. Therefore, the effect of environment on creep and shrinkage should be taken into account in order to make a reliable estimation of time-dependent deformations in structural members.

The loss-of-prestress provisions in the American Association of State Highway and Transportation Officials (AASHTO-1977) Bridge Specification (13) implicitly take into account the effects of variable environment, as do some recommendations of Prestressed Concrete Institute (PCI-1975) Committee on Prestress Losses (14). The American Concrete Institute (ACI-1982) Committee 209 (8) and Comite Europeen du Beton (CEB-FIP 1970, 1978) International Recommendations (15, 16) reviewed many factors which influence time-dependent response, but their discussions do not include any information about the effect of variations in relative humidity with time. Gamble and Parrott (17) conducted creep tests on specimens which were allowed to dry and were then rewetted. Both drying and rewetting lead to significant increases in the rates of creep. Rewetting of the accompanying unstressed shrinkage specimens also leads to recovery of much of the shrinkage strain.

There have been a few other investigations, as reviewed by Neville, Dilger and Brooks (18), under controlled cyclic changes in humidity, and two series of test reported by Gamble in 1982 (19) and L'Hermite and Mamillan (20) in which specimens were stored both outdoors and in a constant environment laboratory. The effect of a

varying environment on the creep and shrinkage of concrete was studied by Kingham, Fisher and Viest (21) by the AASHTO Road Test. Their investigation involved cylindrical specimens stored outdoors over a period of about three years. A cyclic variation in the growth of shrinkage was noted, reflecting the seasonal changes of the environmental conditions (most importantly relative humidity). In contrast, the growth of creep strain appeared to be notably unaffected by these same seasonal changes. These findings were consistent with those of Hansen and Mattock (24) that shrinkage was directly related to moisture movement while creep was not. In addition, Kingham et al. reported that the growth of the shrinkage and creep strains practically stopped after one and two years, respectively. These periods for stabilization were very short as compared to the thirty years or longer observation reported by Troxell, Raphael and Davis (22).

In 1976, Parrott (23) also measured shrinkage strains in outdoor exposed specimens and found seasonal variations of the same nature.

Shrinkage is known to be dependent on time and existing moisture conditions, but not on stresses. The amount of shrinkage of a concrete member is proportional to the quantity of water incorporated into the mix. Weather conditions are thus the most important factors influencing the rate of shrinkage.

There apparently has been no systemmatic investigation of the effects of variable environment exposure on creep and shrinkage

in which a range of possible environments has been taken into account.

2.1.2.2.2 Effect of Size and Shape of Concrete Specimen

The effect of size and shape of specimens on the time-dependent strain have been recognized by many researchers. Hansen and Mattock (24) presented the results of the first four years of this study in 1966. Most of the specimens were either cylindrical or I-shaped. The cylinders had diameters from 100 to 610 mm and lengths from 457 to 1470 mm. The depth of the I-shaped members varied from 290 to 1170 mm while their lengths changed from 1600 to 3350 mm. The volume to surface ratio, which was used as a measure of the relative thickness of the specimens, lay within the range of 250 to 1520 mm. The creep specimens were loaded to about 25% of their ultimate strengths. Results showed that when de-watering was permitted, creep and shrinkage of concrete were influenced greatly by the volume to surface ratio. However, the influence of this ratio on the rate of creep appeared to be restricted to an initial period of about three months only. After this initial period, the rate of creep of all members was equal to that of a sealed specimen which had an effective volume/surface ratio of infinity. These authors also recommended that the volume/surface ratio could be used as a practical, though not perfect, design parameter reflecting the effects of size and shape. This recommendation of theirs has received general acceptance.

J.R. Keeton (25) made an extensive study of the effects of the size of specimens and relative humidity of storage on creep and

shrinkage of concrete, and reported his findings in 1965. Five different controlled relative humidity environments were used and four different stress levels were applied, while the design strength was 35 N/mm^2 after 7 days in 100% curing. The specimens were cylinders of three different sizes. His findings on the size of specimens were essentially the same as those by Hansen and Mattock. Relative humidity of storage environment was observed to have an inverse but non-linear influence on the volumetric change in concrete. The results of similar tests on hollow box and other shapes showed the same results.

2.1.2.2.3 Effect of Stress Level and Loading Condition

The effect of loading conditions on creep of concrete structures have been observed by many researchers. Such structures under repeated loads must be designed to control deformations due to so-called static and cyclic creep, i.e. creep resulting from both dead load and cyclically varying live load. Cyclic creep is a function of many variables, e.g. minimum and maximum stress ratios, duration and interval of loading and type of concrete mix and specimen.

Many experiments have been reported on the influence of the magnitude of the applied stress on creep. One of the most extensive studies was done by Keeton (25) in 1965. The relationship between the applied stress and the creep strain was found to be non-linear for all storage humidities except at 100% R.H. where linearity was reached beginning at 175 days. Keeton concluded that the curvature

of the creep versus applied stress diagram, for all storge conditions, was very small and could be neglected for all practical purposes. Lyse (26) also found creep strain to be directly proportional to the applied stress.

Creep of concrete under varying stress is of special interest in prestressed concrete design. Ross (27) conducted a test to study this phenomenon in 1958. One series of specimens was subjected to constant stresses at various ages. Test results showed that creep strain was approximately proportional to stress, and the total creep strain decreased with an increase in the age of concrete at the time of the application of stress. In a second series, stress was altered at various time intervals. The residual strain that remained after the removal of all loads was greater for a declining stress than for an increasing stress.

In 1931, Davis and Davis (28) conducted a series of tests on the creep behaviour of concrete under very slow load-cycling for three duration cycles of 2, 10 and 60 days. From the test results, it appears that the rate of creep and rate of creep recovery decrease with each successive cycle but their relative magnitude was such that for any given cycle the rate of creep was greater than the rate of creep recovery, although the difference became less pronounced with an increase in the number of cycles.

Berhardt (29) also subjected concrete to periodically varying stresses at the Cement and Concrete Research Institute (NORWAY). In the test series the stresses were varied within

periods of lengths, 7 or 14 days. It has been observed that the long-term deformation under a variable stress is equal to that under a constant stress of considerably higher magnitude than the mean stress under variable conditions, thus indicating that a variable stress favours high creep.

The influence of loading on grouted and ungrouted post-tensioned concrete members was studied by Breckenridge et al. (30) in 1967. Test over a period of 10 years indicated that the prestress losses of the non-loaded beams were nearly 50 percent larger than the beams loaded with 1.0 design live load. Moreover, the grouted beams deflected essentially the same as those that were ungrouted, whereas the time-dependent prestress losses of the grouted beams were slightly lower than ungrouted beams.

Mossiossian (31) conducted a series of test to study the effect of loading condition on prestress losses. It was indicated that when beams are loaded over a period of 2 years, a reduction in prestress losses of 14 percent was observed when compared with the values of unloaded beams exposed to actual field conditions with an average of 70% relative humidity.

In 1975, Hernandez (32) observed that the effects of deck load on the total prestress losses are significant, with the total prestress losses being smallest for the heaviest deck load and greatest for the case of no deck load.

2.1.2.2.4 Effect of Cement, Superplasticizers and PFA on Long Term Deformations

The influence of types of Portland cement on creep and shrinkage was studied by Hummel in 1959 (33). Hummel conducted a series of tests on creep behaviour of ordinary Portland cement (Type I) and rapid hardening Portland cement (Type III), for three ages of application of load: 3, 28 and 90 days. The creep specimens were loaded to about one-third of the cube strength and a 0.55 water/cement ratio was used. It seems from the test results that OPC (Type I) cement always exhibited a higher specific creep (creep per unit of stress), than RHPC (Type III) cement, while the observed specific creep from the first day of loading was lower for a higher initial strength. Glanville and Thomas (34) indicated that the difference in basic creep between OPC (Type I) and RHPC (Type III) cements is smaller than the difference in the drying creep condition.

In 1968, Petersen and Watstein (35) conducted a test on pre-tensioned prestressed concrete beams made with OPC (Type I) and RHPC (Type III) cements. The test indicated that there is almost no difference in long term loss after 500 days.

In recent years, interest has grown in the use of superplasticizing admixtures and pulverised fuel ash (PFA) in prestressed concrete members especially in connection with long term deformations and strength of concrete.

The Cement and Concrete Association (36) presented a test report on concrete with a naphthalene superplasticizer. The test specimens were sealed and then loaded at the age of 28 days with a surrounding relative humidity of 65 per cent. It appeared from the 40 days test period that the superplasticizer had no significant effect on creep, for both flowing concrete and high-strength concrete.

In 1980, Alexander at al. (37) conducted tests on concrete specimens with a melamine superplasticizer stored at 50 per cent relative humidity and 23°C for a test period of 20 months. The test results show that creep at constant 0.25 stress/strength ratio was 10 per cent greater than that of the control concrete mix in spite of the increased strength of the admixture concrete with age. Such an increase in creep can be explained by the amount of drying shrinkage of the admixture concrete which was 10 to 25 per cent greater than shrinkage of the control concrete.

An investigation by Brooks et al. (38) in 1981 was carried out on two concretes made with RHPC (Type III) and having the same workability, but with one mix containing a superplasticizing admixture and having a lower water/cement ratio. Tests over a period of one year show that creep at a given stress-strength ratio is higher for the admixture concrete than for the control concrete, but the values of specific creep are similar for the two concretes. The difference in creep behaviour can be explained by the development of strength under load which varies for the two concretes.

Pulverised fuel ash (PFA) has been used successfully for several years as a part-replacement of cement to make Portland-pozzolana cement concrete.

In 1960, Ross (39) found that, for a replacement of cement by fly ash of 25 per cent in a surrounding environment of 90 per cent relative humidity and temperature of 17.5°C, the fly ash had little effect on creep. This indicates that there was a slight reduction in creep based upon a constant initial stress/strength ratio.

Bamforth (40) carried out tests to study the creep behaviour of fly ash concrete with a replacement of cement from 15 to 25 per cent, stored at a relative humidity of 90 per cent and temperature of 27°C. Bamforth found that there was a slight increase in creep ranging from 6 to 14 per cent. However, both Bamforth (40) and Gifford et al. (41) have observed a reduction in basic creep at a constant stress/strength ratio.

Brooks et al. (42) made an extensive study on the effect of superplasticizing admixture and fly ash on creep and shrinkage of concrete, and reported their findings in 1982. All mixes tested had a similar workability and were loaded up to 0.2 of the 28-day cylinder compressive strength. The test results showed that when 30 per cent of cement was replaced by fly ash, there was a reduction in both shrinkage and in total creep. For specimens stored in water, the creep and swelling for the ordinary Portland cement and fly ash concrete were higher than plain concrete. Moreover, when fly ash

and superplasticizers were used in combination it led to significant reductions in shrinkage, in basic creep and in total creep. The effect of such a combination is to improve the low early-age development of strength of ordinary Portland cement and fly ash concrete through a reduction in mixing water content. As expressed by Brooks et al., the beneficial effects of high-early strength and long-term strength, coupled with low shrinkage and creep, are of benefit in decreasing the long-term losses occuring in prestressed concrete elements.

2.1.3 Relaxation in Steel Tendons

Relaxation in steel tendons refers to stress loss in the steel without strain changes. Most of the reported relaxation studies referred to tests under the "constant length" condition. Under this strain condition, it is generally acceptd that the total amount of stress relaxation for a given steel is a function of the initial stress, temperature and the stressing procedure. It should be pointed out that the conditions of the prestressing steel in a prestressed concrete member is somewhat more complicated. The steel strain gradually decreases with time on account of creep and shrinkage of the concrete. On the other hand, the steel strain could increase with an addition of load to the member.

In the following paragraphs, the work of four separate researchers will be described. It should be emphasized that in all cases, the basic tests used by the researchers were under the constant length condition. For application in the analysis of

prestressed concrete members, the basic relaxation expressions were extended to deal with varying strain conditions. The extension is discussed in Section 2.1.3.2.

2.1.3.1 Constant Length Tests

Magura, Sozen and Siess (43) presented a paper describing a comprehensive research programme on the stress relaxation of prestressing wires, which was concluded in 1964. Their studies included the relationship between relaxation loss and the initial stress level and time, as well as the effect of prestressing. In addition, they made an extensive review of relaxation information available in literature.

Based on their own tests as well as data from previous investigators, Magura et al. arrived at the following conclusions:

1. The significance of relaxation loss of prestress lies in its effect on the service performance of the structural member. Therefore, the estimate of loss should not be viewed as an end by itself, but a means to estimate the prestress remaining.

2. Relaxation loss is strongly influenced by the initial stress-yield strength ratio (initial stress ratio). For initial stress ratios less than 0.5, relaxation loss may be neglected.

3. The effect of pre-stretching on relaxation loss is insignificant if the pre-stretching time is short.

4. Within the ordinary temperature range, the effect of temperature on relaxation loss is negligible.

Using all of the available data, Magura et al. derived the following expression relating the remaining stress at any time to the initial stress and yield strength of the steel

$$\frac{f_s}{f_{si}} = 1 - \frac{\log t}{10}\left(\frac{f_{si}}{f_y} - 0.55\right), \text{ for } \frac{f_{si}}{f_y} \geq 0.55 \qquad \text{Eq.(2.1)}$$

where f_s = remaining stress at time t after prestressing

f_{si} = initial stress of steel, t = time, in hours

f_y = yield strength of steel, defined by the 0.1% offset.

Podolny and Melville (44) presented a paper describing the several variables affecting relaxation losses in prestressing steel wire. Their study, concluded in 1969, involved an investigation of research concerning the relaxation characteristics of steel. As a result of the study, Podolny and Melville reached the following conclusions: "At normal initial stress levels and temperatures, relaxation is predictable and is of relatively minor significance in terms of other losses imposed upon the structure or member. At elevated temperatures, the losses due to relaxation of the prestressing steel are of greater significance ..."

In 1972, Glodowski and Lorenzetti (4) presented a paper dealing with a method for prestress loss prediction. These authors

reviewed the literature and concluded that Magura's straight-line, semi-log expression mentioned earlier was not sufficiently accurate for short periods of time less than 1000 hours. This conclusion is understandable in light of the fact that Magura utilized relatively long-term data in deriving the stress relaxation expression.

Glodowski and Lorenzetti conducted their own relaxation tests on prestressing steel wires, and developed a method for extrapolating short-term data to predict steel stress relaxation losses at much longer times. Their steel relaxation expression takes the following quadratic form:

$$\%SR = A + B\ (\ln t) + C\ (\ln t)^2 \qquad \text{Eq.(2.2)}$$

where %SR = percent stress relaxation

t = time in hours

A, B and C are functions of the initial stress ratio.

As in Magura's expression, the Glodowski et al. equation predicts higher relaxation for higher initial stress ratios. The authors showed tht the quadratic expression was quite accurate for short times, and also fairly consistent with other methods of long-term stress relaxation prediction.

Relaxation properties of prestressing strands were studied at Lehigh University over a five year duration (45, 46). The tests involved seven-wire stress-relieved strands, under a constant length condition. The controlling variables studied were type and size of strand and the initial stress level.

In the study, particular attention was paid to the selection of suitable time functions so that an extrapolation of long-term relaxation loss for periods up to 100 years would be feasible. The investigations developed the following expression for the prediction of relaxation loss as a function of initial stress and time:

$$\% SR = \frac{f_{si}}{f_{pu}} (B_1 + B_2 \log(t+1)) + (\frac{f_{si}}{f_{pu}})^2 (B_3 + B_4 \log(t+1) \qquad \text{Eq.(2.3)}$$

where %SR = relaxation loss, in % of initial stress

$\frac{f_{si}}{f_{pu}}$ = initial stress, in fractions of guaranteed ultimate strength

t = time in days.

B_1, B_2, B_3 and B_4 are constants which depend on the type and size of strand.

The form of this expression very closely resembles the quadratic equation developed by Glodowski and Lorenzetti. In fact Batel and Huang (45) examined a quadratic logarithmic function, but found this function to be overly sensitive to variations of data at the beginning and also at the end of the testing period. In view of this, they eliminated this function for further long-term estimation (46).

2.1.3.2 Effect of Varying Strain

In actual prestressed concrete members there is an interaction between steel and concrete, hence conditions of changing strain in steel are always prevalent. Glodowski and Lorenzetti (4) established a procedure for determining steel stress relaxation under these conditions. As mentioned in an earlier section, they developed a "curve transfer" procedure to account for varying strain. Curves corresponding to different initial stress levels were first constructed, showing percent steel stress relaxation vs. time. For each change in strain, a transfer is made from one stress level relaxation curve to another, by maintaining the same percent loss (horizontal transfer). Relaxation loss during the next time interval is then estimated following the new curve. The authors suggested that the best choice of the two alternatives of horizontal and vertical curve transfer is the horizontal method which is based on equivalent stress relaxation losses.

In 1975 the PCI Committee on Prestress Losses (14) suggested a modified form of Magura's expression to be used in a step-by-step calculation. The expression is used over a finite time interval with the steel stress at the beginning of the interval substituted for the initial stress. The expression takes the following form

$$RET = f_{st}\left(\frac{\log 24t - \log 24t_1}{10}\left(\frac{f_{st}}{f_{py}} - 0.55\right)\right) \qquad \text{Eq.(2.4)}$$

where $(f_{st}/f_{py} - 0.55) \geq 0.05$ and $f_{py} = 0.85\ f_{pu}$

RET = relaxation over time interval t_1 to t, psi

f_{st} = steel stress at t_1, psi; f_{py} = 0.1% offset stress, psi

t and t_1 = time at end and beginning of time interval, days.

In 1979, the ACI-ASCE Committee (47) proposed a reasonable equation as follows:

$$RE = (k_{re} - J\ (SH + CR + ES))C \qquad \text{Eq.(2.5)}$$

where RE = stress loss due to relaxation of tendons

K_{re} and J = constants related to type and grade of steel

C = constant (accounts for the ratio f_{pi}/f_{pu})

SH, CR and ES = stress losses due to shrinkage, creep and elastic shortening of concrete

In order to facilitate the solution of the problem of the time-dependent variation of strain, Schultchen, Ying, and Huang (46) developed the concept of a stress-strain-time relationship. Geometrically speaking, their expression describes a three-dimensional surface in a stress-strain-time coordinate system. The contour lines parallel to the stress-time plane indicate the gradual decrease of stress under a constant length condition. The expression is as follows:

$$f_s = D_1 + D_2S + D_3S^2 - S(C_1 + C_2 \log(t+1)) - S^2(c_3+C_4 \log(t+1)) \qquad \text{Eq.(2.6)}$$

where f_s = remaining stress in strand

s = steel strain in 10^{-2}

t = time in days.

D_1, D_2, D_3, C_1, C_2, C_3, C_4 are constants which depend on the type and size of strand

The applicability of the three-dimensional surface is restricted to initial stress values in the range of 0.5 fpu to 0.8 fpu. Also, time values may vary from approximately one day to 100 years.

To summarize, at the present time, researchers continue to experiment on the relaxation behaviour of steel. The phenomenon of steel stress relaxation has been described and its characteristics experimentally verified. Researchers have identified the various factors affecting relaxation behaviour, and expressions have been developed for prediction of stress loss due to relaxation (constant length). In addition, the actual phenomenon of a varying strain has been investigated by several researchers and expressions have been formulated to help predict the stress loss under these conditions. Most of the proposed expressions agree with the test data used by the particular investigators.

2.2 Camber and Deflection

2.2.1 General Remarks

Camber refers to the upward deflection of beams under the influence of prestress as well as other loads. Because of the time-

dependent nature of the concrete strains, camber and deflection also vary with time. Several researchers had commented on the difficulty in accurately predicting the deflection of concrete flexural members (48, 49, 50). The actual quality of the concrete, particularly the modulus of elasticity, is usually quite different from design value, and it is usually impossible to separate the creep effect completely from the instantaneous response. On the time-dependent behaviour of concrete members, researchers have generally concentrated their attention on two aspects: the effect of the humidity and temperature of the environment, and the length of time before the fluctuations of camber or deflection becomes sufficiently small so that a stabilized condition may be assumed.

2.2.2 Effect of Environmental Condition

As early as 1942, Pickett (10) reported his finding that environmental humidity affected the deflection characteristic of concrete structural members. This effect of environmental condition was given recognition by the ACI-ASCE Joint Committee (51) in their recommendations for the design of prestressed concrete members, published in 1958. The time-dependent concrete strain was specified as varying from 100 per cent of the initial elastic value for very humid environments, to 300 per cent of the initial value for a very dry environment.

In a 1961 paper by Corley, Sozen and Seiss (12), reference was made to deflections measured by Delarue (52) on a highway bridge in Morocco, North Africa. These measurements were compared with

values computed using material properties determined in the laboratory and seasonal pattern of deviation was noticed. It was suggested that this seasonal variation, which was of nearly the same magnitude as the computed time-dependent deflection, may be attributed to changes in relative humidity and possibly temperature in the field.

Also in 1961, Branson and Ozell (48) reported their findings from a relatively short-term study. Ten post-tensioned beams were tested, of which two were stored outdoors. The effect of ambient relative humidity on the total camber (initial plus time-dependent) was found to be small. Corresponding to a change of ambient relative humidity from 72 to 90 percent, the total camber at the end of ninety days changed only by approximately 7%. As expected, the more humid environment outdoors induced the lower total camber. The relatively small influence of humidity on the total camber was attributed to the tendency for the effect of shrinkage on camber growth to be offset by that of the corresponding decrease of prestress.

2.2.3 Duration for Stabilization

Researchers agree that the rate of camber or deflection growth diminishes with time, and would become negligible after a certain initial period, but at the current time, there is no agreement on the length of this initial period for stabilization. In their 1961 report, Corley, Sozen and Siess (12) observed that camber growth, like the creep strain of concrete, was a long-term

phenomenon and would continue for many years, but the increase after two years is small. More recently, several indications have shown that camber would become stabilized much sooner. Branson and Ozell (48) maintained that the camber growth in prestressed concrete members would reach its maximum relatively early compared to the time-dependent strains, because of the significant decrease of prestress. Based on their test data over a period of 150 days, they speculated for a stabilization period of from 100 to 200 days. Furr et al. (53) made the same general observation from their studies on an in-service highway bridge, and reportedastabilization period of from 100 to 150 days. In 1971, Pauw (54) made field measurements of deflections of an in-service box-girder highway bridge over a period of about 500 days, and found essentially no change after the first eight months. It is worth noting that the first two investigations, by Corley et al. and Branson and Ozell, were based primarily on laboratory stored small specimens, while the other two studies were carried out outdoors on full size in-service bridge members.

One of the most extensive investigations with regard to the duration for stabilization were reported by Gamble on his study since 1965 of two in-service highway bridges in Illinois (49, 50, 55). He also found the duration for stabilization to be rather short. For one bridge located in Douglas Country (build in 1969), the camber was essentially stabilized six months after fabrication with a total growth of about 75 per cent of the initial camber. For the other bridge, located in Jefferson County and constructed in 1966, camber growth practically stopped after two to three months, with a total growth also about 75 percent. Gamble observed that the

early exposure conditions for the two sets of beams were different, and suggested that as the reason for the difference in the camber stabilization. The Douglas County bridge beams were fabricated in December, and were moved outdoors into sub-zero temperatures three days after casting. In contrast, the Jefferson County bridge beams were fabricated in the summer month of August, and were kept inside a building for nearly three weeks.

An unexpected finding by Gamble was that after a period of apparent stability, the camber started once again to show a small but persistent growth. For both bridges, the changes in deflection were extremely small after the casting of the concrete deck, as the stress distribution in the beam at midspan was almost uniform over the depth. But after a period of time, the camber started to increase again. Gamble explained that this small increase in camber was consistent with the expected differential shrinkage between the beam and the deck concrete, when the continuity of the composite structure over the interior supports was taken into consideration.

2.3 Summary

This chapter gives a detailed survey of previous research on the behaviour of time-dependent deformations, prestress losses and deflections of prestressed concrete members.

From the literature review presented in this chapter it can be concluded that:

1. There has apparently been no systemmatic investigation of the effects of variable environments or outdoor condition exposure on time-dependent deformation, prestress losses and camber and deflections in which a range of possible environments has been taken into account. Many tests under controlled cyclic conditions are needed before all aspects of behaviour under random variable conditions can be understood.

2. Further tests are required to investigate the influence of size and shape of concrete members on long-term deformations for various environmental conditions.

3. Despite the fact that there have been a fair number of tests conducted on the effect of loading condition on time-dependent prestress losses, camber and deflections, there have been no attempts to investigate the effect of cyclic loading on prestress losses and deflections of prestressed concrete members.

4. There has not been a significant amount of research in the material response of prestressed concrete members. More work needs to be done to define the variables of the concrete mix composition especially when using PFA and admixtures, and the possible range of effects. This aspect needs further investigation to identify areas where additional research may be needed.

5. To appraise the recommendations of prediction methods, concerning the calculation of time-dependent deformations, prestress losses and camber and deflections, a re-examination is needed to provide a better

understanding and careful study of the variation between prediction methods and the experimental results obtained.

6. Further tests are needed to investigate the stabilization period of camber and deflection of post-tensioned concrete members.

CHAPTER 3 - EXPERIMENTAL PROGRAMME, MATERIALS, INSTRUMENTATION, TESTING AND MEASUREMENT OF DEFORMATION AND STRAIN

3.1 Scope of the Experimental Programme

The main purpose of this experimental programme was to examine and study the major factors effecting the long term losses of post-tensioned prestressed concrete members over a period of at least one year. The important parameters which were examined in this investigation are as follows:

(1) Environmental conditions (Relative humidity)

(2) Shape and size of section (Volume-to-surface ratio)

(3) Type of loading condition (e.g. self-weight, cyclic or sustained)

(4) Different concrete mixes (e.g. OPC, RHPC, admixtures and PFA)

Twenty seven beams of effective span 2.7 metres and overall depth 180 mm were designed with varying selected parameters as fully detailed in Table 3.1. Two different sections of beams (rectangular and I shaped) having different loading conditions were prestressed with one post-tensioned high tensile steel wire, and were placed in a simply supported condition. Of the twenty seven beams, fifteen beams were kept in a constant environmental condition of 65 percent relative humidity and a temperature of 20°C, and the remaining beams were kept in a variable relative humidity condition ranging from 65

percent to 100 percent relative humidity and a constant temperature of $20^{o}C$. The geometrical and material properties will be described in detail in this chapter, together with details of the instrumentation and test arrangements.

3.2 Description of Test Beams, Creep Cylinders and Control Specimens

3.2.1 Test Beams

The basic consideration for the test beams was that they should represent class 1 prestressed concrete which allows no flexural tensile stresses at the top or bottom fibres of the concrete member. The test beams, 180 mm deep and 100 mm wide, were designed for a total length of 2.7 metres to allow an effective span of 2.6 metres. Full details of the beams are shown in Figure 3.1.

3.2.2 Control Shrinkage Beams

The control shrinkage beams had the same shape as the prestressed concrete beams (Rectangular or I-shaped) except that the length was only one metre. Eleven shrinkage beams were utilized for each variable condition of environment, shape of beam and concrete mix. For concrete mix 1 (RHPC) and mix 2 (OPC), one rectangular and one I-shaped shrinkage beam was utilized for each environmental condition. However, one I-shaped shrinkage beam was used for mix 3 (RHPC/Admx.), mix 4 (RHPC/PFA) and mix 5 (RHPC/Admx. & PFA) in a constant environmental condition. Plate 3.1 shows a general view of control shrinkage beams placed in the vertical direction.

3.2.3 Creep and Control Shrinkage Cylinders

Test specimens were cylinders 76 mm diameter and 267 mm long, and were partially sealed with bitumen sealant and covered with a polythene sheet to represent the volume-surface ratios of the rectangular and I-shaped prestress beams. Plate 3.2 gives a general view of loaded creep and control shrinkage cylinders inside the constant environment room. The full details of the scheme of creep and shrinkage cylinders tests are shown in Table 3.2.

3.3 Designation of Beams

A special code was used to identify each test beam as shown in Table 3.1. The first two letters represent the loading condition of the prestressed concrete beam and the series is detailed as follows:

NG - Self weight only loaded beam with grouted tendon.

N - Self weight only loaded beam without grouted tendon

CY - Cyclic service loaded beam without grouting

C - Constant sustained service load beam without grouting

The letters R and I represent the shape of the rectangular and I shaped beams respectively. After the / a letter is used to identify the environmental condition such as /C for constant environment and /V for variable environment. Finally, a number is used to identify the type of concrete mix and the series of mixes are detailed as follows:

1 - Plain rapid hardening Portland cement

2 - Plain ordinary Portland cement

3 - Rapid hardening Portland cement and admixture

4 - Rapid hardening Portland cement and pulverized fuel ash

5 - Rapid hardening Portland cement, admixture and pulverised fuel ash.

Thus, for example, beam NGR/C1 is a self weight only loaded rectangular beam with grouted tendon, having a plain rapid hardening Portland cement mix and stored in constant environment.

3.4 Materials

3.4.1 Cement

Two type of cement were used in this research study: ordinary Portland cement (Type I) and 'Ferrocrete' rapid hardening Portland cement (Type III). The composition of the ordinary and Ferrocrete cements conformed to B.S. 12:1958. Rapid hardening Portland cement was used for almost 70 percent of the total number of beams and specimens, whereas ordinary Portland cement was used for the remaining 30 per cent of beams and specimens.

3.4.2 Aggregate

The fine aggregate was quartzite sand supplied from North Nottinghamshire and conformed with the requirements of B.S. 882:1985 Group M. The coarse aggregate was also from Nottinghamshire, having a 10 mm nominal maximum size and complying with B.S. 882.

3.4.3 Concrete Mixes

Five different concrete mixes were utilized in this research investigation, with rapid hardening Portland cement being used in four mixes and ordinary Portland cement being used in one mix. The concrete mixes had similar workability as measured by slump (5-12 mm) and by Vebe time (9-11 seconds), except for ordinary Portland cement mix which had a higher workability of 30 mm slump and 3 seconds of Vebe time. All concrete mixes were designed to achieve a minimum strength of 45 MPa at transfer. The full details are presented in Table 3.3 and compared in the following sections.

3.4.3.1 Plain Ordinary Portland Cement Mix

The concrete mix was designed for a nominal 7-day cube (100 mm) strength of 45 N/mm^2, using a cement content of 340 kg/m^3 and a water/cement ratio of 0.5 as shown in Table 3.3. The aggregate/cement ratio was 5.4 and the coarse/fine aggregate ratio was 1.70. A total of eight post-tensioned beams along with creep and control specimens were cast using ordinary Portland cement and stored in two different environmental conditions as indicated in Table 3.1.

3.4.3.2 Plain Rapid Hardening Portland Cement Mix

The mix proportion for this mix was chosen to produce a low workability mix (Table 3.3) and the cement content of 420 kg/m^3 being typical of that used in the prestressed concrete industry in

the United Kingdom. The concrete was found to develop the required transfer strength of 45 MPa at 2 days. The aggregate/cement ratio was 4.4 and the coarse/fine aggregate ratio was 1.67. Sixteen post-tensioned beams accompanied by creep and control specimens were cast using plain rapid hardening Portland cement and stored in two environmental conditions as shown in Table 3.1.

3.4.3.3 Admixture (Superplasticizers) and Rapid Hardening Portland Cement Mix

The RHPC/Admixture mix had the same proportions as the plain RHPC mix with the exception of a reduced water/cement ratio of 12.82 percent. A naphthalene type superplasticizer (CORMIX 2000) was used with a dosage of 0.6 percent by mass of cement. CORMIX 2000 conforms to type G materials of ASTM designation C494-81, and to the new British Standard B.S. 5075:Part3:1985 Specification for Superplasticising Admixture. The admixture was added to achieve a similar workability to that having plain RHPC, as measured by slump and Vebe consistometer (Table 3.3). The superplasticizer mix was found to achieve the required transfer strength of 45 N/mm^2 in one day. One post-tensioned beam accompanied by creep and control specimens were cast and stored in the constant environment.

3.4.3.4 Pulverized Fuel Ash (PFA) and Rapid Hardening Portland Cement Mix

The RHPC/PFA mix had 30 percent of cement replaced by 37.5 percent by mass of PFA at a reduced water/cement ratio of 7.7 per

cent and adjusted fine and coarse aggregte contents to produce an equivalent yield to the plain RHPC mix as shown in Table 3.3. The PFA was obtained via the Ash Marketing Division of the Central Electricity Generating Board and came from the power station of Radcliffe, Nottingham.

The concrete was found to develop the required transfer strength of 45 N/mm^2 at 8 days. One post-tensioned beam accompanied by creep and control specimens were cast and stored in the constant environment.

3.4.3.5 Admixture, Pulverized Fuel Ash and Rapid Hardening Portland Cement Mix

The RHPC/PFA & admixture mix was proportioned identically to the RHPC/PFA mix but had a lower water/cement plus PFA ratio to offset the superplasticizing effect of the admixture. The dosage of superplasticizer was the same as the RHPC/Admixture mix of 0.6 per cent by mass of cement. A transfer strength of 45 N/mm^2 was achieved in 5 days. One post-tensioned beam, accompanied by creep and control specimens, was cast and stored in the constant environment.

3.4.3.6 Grouting Mix for Tendons

The grouting mix used in this investigation was a mixture of two parts of rapid hardening Portland cement to one part of water by mass. The grouting mix was used to grout six post-tensioned beams as shown in Table 3.1.

3.4.4 Characteristics and Relaxation of Steel Wire

The prestressing tendon used in this study was 7 mm diameter, plain cold-drawn high tensile wire of specified characteristic strength of 1793 N/mm^2 (69.0 KN) supplied by Johnson and Nephew (Ambergate) Ltd. The properties and dimensions of the steel wire conformed with the requirements of B.S. 5896 (1980) and ASTM A421-74.

In determining the loss of prestress for a concrete member, it is important to know the modulus of elasticity of the prestressing steel and stress relaxation characteristics. The experimental stress-strain curve for 7 mm cold drawn wire is shown in Figure 3.2. The measured modulus of elasticity was 206.4 KN/mm^2 and the 0.2% proof stress was 1564 MPa. The manufacturer specified the maximum relaxations after 1000 hour at 20^{o} as 4.5%, 8.0% and 12.0% for the percentage of initial load to breaking load of 60, 70 and 80 percent respectively.

3.5 Beams and Test Specimens Formwork, Casting, Compaction and Curing

3.5.1 Formwork

The sides of the formwork consisted of steel channels 180 mm deep, placed back to back and bolted to a steel base plate lined with seasoned wood. Steel plates with accurately located perforations were placed at the ends of the unit to keep the 15 mm diameter P.V.C. duct in the correct position. A wedge-shaped steel

cone was fixed to form a void to allow the flaring of the tendons at the anchorages.

For post-tensioned beams two beams were cast in two moulds 2.7 metre long. Two shrinkage beam moulds were used having the same dimensions of prestressed beam moulds, but they were one metre long. For all moulds, similar base and channels were used, but to form the web of I-section beams, varnished timber checks were fixed to the inside of the channels. For ease in removing the form, the moulds were oiled before casting.

3.5.2 Casting and Compaction

Mixing of concrete was carried out mechanically in a horizontal rotating pan-type mixer of 250 kg capacity and constituents were batched by mass. After turning the mixer dry for about 30 seconds, the water was gently added and the mix turned for another 2 minutes.

The concrete was then placed in the moulds in layers and compacted by means of a vibrating table at a frequency of 50 Hz. All precautions were taken to ensure that the concrete flowed freely around the P.V.C. duct especially in the bottom flange of the I beams. For each batch of concrete, control specimens were cast and slump and Vebe time tests were carried out. The exposed surfaces of the beams and specimens were then trowelled off after the initial set had taken place and covered with wet hessian mats and polythene sheets for one day, after which they were released from the moulds.

The full details of the casting programme for all post-tensioned beams are shown in Table 3.4.

3.5.3 Curing

After demoulding, the beams and specimens were transferred to the curing room on the day after casting and kept at a constant temperature of about 18°C to 20°C and a relative humidity of 95-99%. The beams together with the control specimens were stored in the curing room until the time of stressing. Table 3.4 indicates the duration of curing for all the post-tensioned concrete beams at different days for different mixes.

3.6 Test Apparatus, Instrumentation and Experimental Measurements

3.6.1 Details and Description of Beam Loading Rig

In this investigation, there were several variables to be considered, such as type of loading and different environmental conditions. Therefore, to accommodate these conditions, six steel rigs were designed and utilized to carry twenty-seven prestressed beams having variable conditions as indicated in Table 3.1. As shown in Fig.3.3, each rig was designed to carry four or five prestressed concrete beams at the same time, five beams being carried by each constant environment rig and four beams being carried by each variable environment rig.

The rigs were designed in such a way that it was possible

to obtain the desired applied load needed for the loaded concrete beams by means of the self weight of the concrete beam above, together with that of the steel joist hinged at the far end of the rig and a number of weights used at the other end of the rig as shown in Fig.3.3 and Plate 3.3. Plate 3.4 gives a general view of beams loading rigs inside the control room. The desired load applied at the mid-span point of the prestressed concrete beam was between 4 to 4.8 kN, depending upon the shape of the loaded concrete beam used. The non-loaded (with grouting) and cyclic loaded concrete beams were placed in the two upper berths of the rig whereas the two other beams, non-loaded (without grouting) and sustained loaded concrete beams were placed in the lower berths of the rig. The fifth beam of the constant environment rigs was placed at the top of the steel rig as shown in Plate 3.3. The full details of the steel rig components are indicated in Fig. 3.3.

3.6.2 Description of Creep Loading Frame

The loading apparatus used in the creep test and the method of measurement of strain was developed at the Department of Civil Engineering, The University of Leeds (56).

The creep frame was designed to hold two 76 x 267 mm cylindrical concrete specimens and a calibrated steel-tube load dynamometer by four tie rods each 25 mm. in diameter with an overall length of 1.02 metre and two end plates of 25 mm thickness. One of the plates was fixed to the rods and the other was movable. Two steel trunnions of 100 mm in length and 25 mm in diameter were

screwed into the centres of the top and bottom plates so that the loading frame could be held horizontally.

Due to creep of concrete, the loss of load was compensated manually by tightening the four nuts. The details of the loading frame are shown in Fig. 3.4.

3.6.3 Loading of Creep Specimens and Scheme of Tests

The creep specimens were partially sealed and loaded at the same day of prestressing the post-tensioned concrete beams. The steel dynamometer was used to check the required load applied which corresponded to 0.15 of the cylinder compressive strength at transfer of prestressing force giving a nominal axial stress of 5.0 MPa. The stress imposed on the concrete specimens was maintained for the duration of the test by manually tightening the four nuts as mentioned earlier and were adjusted until the value of strain reading across eight reference 200 mm Demec points was within ± 4 divisions of strain. Thirteen creep frames representing three environmental conditions having the same applied load were used within this study. The creep specimens conditions of the three environments were as follow: specimens stored in water tank of 18 $\pm$ 2°C, specimens stored in dry control room of 20 $\pm$ 2°C and 65% R.H. and specimens stored in cyclic environment of 20°C $\pm$ 4°C and a relative humidity ranging from 65 to 100%. The full details of the scheme of creep and shrinkage tests are shown in Table 3.2.

3.6.4 Experimental Strain and Deflection Measurements

3.6.4.1 Steel Tendon Strain Measurements

The strain of the steel tendon was measured by using electrical resistance strain gauges installed on the steel wire itself and on a load cell at the end of the tendon. The strain gauges were connected to the Intercole Compulog IV data logging system as shown in Plate 3.6. The system has a maximum input connection of 100 strain channels and was programmed to read to 1 microstrain resolution and at a rate of 33 1/3 channels per second. The details of the electrical strain gauges measurements are described in the following sections.

3.6.4.1.1 Steel Wire Electrical Strain Gauge

The strain in the tendon was measured by one EA-06-240LZ-12^{o} electrical resistance strain gauge which was mounted at the centre of the prestressing wire. The gauge is manufactured with self-temperature compensation characteristics to compensate the apparent strain produced by changes in temperature. A layer of protective coating of M-Coat D was used to cover the strain gauges and all the exposed electrical connections to provide an insulation against any possible electrical leakage. A second protective coating of M-Coat G was then utilized to act as a sealant against moisture and contaminants. Finally, the treated area was enclosed with a heat shrinkable rubber tube to protect the coating from any physical damage. The strain gauge was connected to the data logging system to obtain the strain reading in microstrains.

3.6.4.1.2 Load Cell Electrical Strain Gauges

The load cell dynamometer was designed and calibrated to measure the total force in the steel tendon. The details of steel dynamometer is shown in Fig.3.5. A full bridge circuit consisting of four PL-10 electrical resistance strain gauges were used for the dynamometer in order to compensate the strain due to temperature variation. Two layers of M-Coat D and G were applied to provide the dynamometer strain gauges with a protective coating. The force in the steel wire was monitored throughout the test period by wiring up the dynamometer strain gauges to the data logging system. The dynamometer measurements were used as an alternative stress reading for the steel tendon as a back-up in case of damage occurring to the electrical strain gauge mounted on the steel wire.

3.6.4.2 Concrete Beams and Cylinders Strain Surface Measurements

3.6.4.2.1 Attachment of Demec Points for Strain Measurement

Demec points, made up of small stainless steel discs, were fixed to the concrete surface with Amco F88 dental cement mixed with dichloro-methane. The gauge length for all prestress and shrinkage beams and cylinder specimens was 200 mm with a gauge resolution of 8.0 microstrain. The same demountable mechanical extensometer of 200 mm gauge length was used to measure the concrete strain as was used to measure the steel dynamometer strains (see 3.6.3).

3.6.4.2.2 Prestressed and Shrinkage Beams Strain Measurements

For each rectangular and I shaped prestressed and shrinkage beam, seven gauge lines were used on each side of the beams. The levels and locations of gauge lines are shown in Fig. 3.6. The strain readings were taken more frequently during the first month of testing and gradually less frequently from one month to one year of the experimental period. The strain reading intervals were based on the developments of creep and shrinkage of the concrete mixes, shape of beams and environmental conditions used in this study.

3.6.4.2.3 Cylinder Creep and Shrinkage Strain Measurements

Four Demec gauge lengths of 200mm at four circumferential positions were used for each cylinder strain measurements. These locations were dictated by an arrangement of four rods on the loading frame as shown in Fig. 3.4. The zero readings were taken for the creep and shrinkage test specimens just before applying the loads on the different specimens of the creep test. The time intervals of the strain reading were similar to those used for prestressed and shrinkage beams.

3.6.4.3 Measurement of Deflection

Deflection at the mid-span position of the beams was measured by means of two removable Baty dial gauges with a 14 mm and 8 mm maximum travel and a resolution of 0.025 mm. The positions of the dial gauges are shown in Plate 3.5 and Fig. 3.6.

3.6.4.4 Strength and Modulus of Elasticity Tests

The control specimens were tested in accordance with B.S.1881:1983. The following control tests were carried out for each beam for measuring the strength and modulus of elasticity of concrete.

(a) Cube Compressive Strength

100 mm cubes were used to obtain the compressive strength of two storage conditions (in dry room 65% R.H. and cyclic environment of 65-100% R.H.) having different concrete mixes. The ages of testing were: the time of stressing, 7 days, 28 days, 3 months, 6 months and one year. For each strength testing period at least 3 cubes were tested.

(b) Cylinder Compressive Strength

For each creep frame three (267 x 76 mm dia.) cylinders were tested for strength at the loading time of creep specimens and three more cylinders were tested after one year of age.

(c) Modulus of Elasticity

This test was performed on a 100 x 100 x 500 mm prism in a 500 KN Denison Universal Hydraulic testing machine. The strain deformation was measured with a 200 mm Demec extensometer on opposite sides of the prism. The modulus of elasticity tests were performed at the same time as the cube strength tests.

3.7 Experimental Procedures

3.7.1 Prestressimg Procedure

The stressing operation for the prestressed beam took place after a sufficient strength development to the transfer strength of 45 N/mm^2 at the specified duration of curing. Table 3.4 illustrates the programme of casting and stressing for the sets of beams utilized and also gives the duration of curing and age at stressing.

The beam and the accompanied control specimens were brought out from the curing room to dry for about 5 hours before stressing and the testing of control specimens. About 1 hour before stressing, the stainless steel discs for the demountable mechanical extensometer of 200 mm gauge length were fixed at the specified centre positions on the beam. Before the stressing operation the initial measurements on the gauge points and initial deflection were taken, with the full length of the beam supported on a flat steel channels.

The prestressing wire was cleaned and lightly greased for the non-grouted beam or degreased with methylchloroform for the grouted beam and then inserted into the duct through the holes in the steel anchorage plate and dynamometer. Precautions were taken to prevent twisting of the wire inside the duct. The end anchorage plates were positioned at the far ends of the prestressing beam and followed by placing the dynamometer and the anchor grips in position, before securing the wire in the anchor grips with wedges at one end. A force of 1 KN was applied to the wire by means of

mono-wire jack in order to secure the end plates and dynamometer in position. The jacking force in the wire was then increased to 48.3 KN and the extension on the scale attached to the jack was measured and checked against calculated value. The force applied corresponded to the 70% ultimate tensile strength of the prestressing wire. The actual force was measured by means of three different reading as follows: pressure gauge reading of the jack which had previously been calibrated, the electrical gauges readings of the steel wire and the load cell dynamometer. When the required force was applied to the wire, the split wedges were hammered into position and the jack pressure released. The stressing operation was then repeated in the same order and shims of different thickness were used to take up the slippage and the movement of tendon during anchoring. After the stressing had been completed, the Demec strain gauge measurements and mid-span deflection were taken. Then the projecting wire was cut off and the beam was lifted and transferred to the loading rig and then placed at its ends.

3.7.2 Grouting Procedure

The grouting procedure took place immediately after tensioning the steel wire. The tensioned wire was grouted into the duct by injecting a mixture of two parts of rapid-hardening Portland cement to one part of water at a pressure of 0.35-0.42 N/mm^2 until it flowed freely at the other end. All the holes in the end plates and dynamometer were then sealed with "plasticine". After the grouting had been completed, the beams were transferred to the loading rig.

3.7.3 Loading Cycle and Procedure

Three types of loading conditions were adopted in this study as illustrated in Fig. 3.7. The first one was the self-weight loading condition (no external load) which represents a mid-span triangular stress distribution in the beam, with a zero stress at the top. The second one was a sustained service loading condition which represents a mid-span concrete triangular stress distribution in the beam, with a zero stress at the bottom. The applied service loads used for rectangular and I shaped beams were 4.02 kN and 4.79 KN respectively, and were maintained for a period of one year. The third loading condition was the cyclic loading condition which represented a fluctuation between the loading and the non-loading conditions. The cyclic loading was applied twice a week (loading Monday, unloading Wednesday, loading Friday and so on), for a period of 12 months.

All prestressed concrete beams were loaded at the age of 8 days. Beams having OPC and RHPC mixes were loaded at 1 and 6 days after prestressing, respectively.

3.7.4 Environmental Cycle and Procedure

In this investigation, two types of environmental conditions were considered. The first environment maintains a constant control environment of 65 $\pm$ 5% relative humidity and a temperature of 20 $\pm$ 2^{o}C. Temperature and humidity were continuously monitored on a chart recorder. The second environment simulated a

field or outdoor environment. The environmental cycle was based on one week at 100% relative humidity and two weeks at 65 $\pm$ 5% relative humidity; a temperature of 20 $\pm$ 2°C was maintained throughout the testing period of one year (see Fig. 3.8).

Table 3.1 - Conditions of Prestressed Concrete Beams Tested

Concrete Mix	Shape of Beam	Environmental Conditions			
		Constant Environment (C) (65% R.H. and 20°C)	Beam Designation	Variable Environment (V) (from 65 to 100% R.H., 20°C)	Beam Designation
Mix 1: (RHPC) Plain Rapid Hardening Portland Cement	I - Shaped Beam (I)	(I) Grouted Tendon: Self weight loading condition	NGI/C1	(I) Grouted Tendon: Self weight loading Condition	NGI/V1
		(II) Non-Grouted Tendon:		(II) Non-Grouted Tendon:	
		(1) Self weight loading	NI/C1	(1) Self weight loading	NI/V1
		(2) Cyclic loading	CYI/C1	(2) Cyclic loading	CYI/V1
		(3) Sustained loading	CI/C1	(3) Sustained loading	CI/V1
	Rectangular Shaped Beam (R)	(I) Grouted Tendon: Self weight loading condition	NGR/C1	(I) Grouted Tendon: Self weight loading condition	NGR/V1
		(II) Non-Grouted Tendon:		(II) Non-Grouted Tendon:	
		(1) Self weight loading	CR/C1	(1) Self weight loading	NR/V1
		(2) Cyclic loading	CYR/C1	(2) Cyclic loading	CYR/V1
		(3) Sustained loading	CR/C1	(3) Sustained loading	CR/V1
Mix 2: (OPC) Plain Ordinary Portland Cement	I - Shaped Beam (I)	(I) Grouted Tendon: Self weight loading	NGI/C2	(I) Grouted Tendon: Self weight loading	NGI/V2
		(II) Non-grouted Tendon: Self weight loading	NI/C2	(II) Non-Grouted Tendon: Self weight loading	NI/V2
	Rectangular Shaped Beam (R)	(II) Non-Grouted Tendon:		(II) Non-Grouted Tendon:	
		(1) Cyclic loading	CYR/C2	(1) Cyclic loading	CYR/V2
		(2) Sustained loading	CR/C2	(2) Sustained loading	CR/V2
Mix 3: (RHPC/Admixture) Rapid Hardening Portland Cement and Admixtures (Superplasticizers)	I - Shaped Beam (I)	(II) Non-Grouted Tendon: Self weight loading	NI/C3	*	
Mix 4: (RHPC/PFA) Rapid Hardening Portland Cement and Pulverised Fuel Ash	I - Shaped Beam (I)	(II) Non-Grouted Tendon: Self weight loading	NI/C4	*	
Mix 5: (RHPC/Admx, PFA) Rapid Hardening Portland Cement, Admixture & Pulverized Fuel Ash	I - Shaped Beam (I)	(II) Non-Grouted Tendon: Self weight loading	NI/C5	*	

* No variable Environmental Investigation for this condition

N = NO LOAD/SELF WT. I = I-SHAPE
C = CONSTANT SERVICE LOAD R = RECT. SHAPE
CY = CYCLIC SERVICE LOAD /C = CONSTANT ENVIRONMENT
G = GROUTED TENDONS /V = VARIABLE ENVIRONMENT

Table 3.2 - Scheme of Creep and Shrinkage Tests

Environmental Condition	Frame No.	Type of Concrete mix	Vol./Surface Ratio (mm)	No. of Specimens	
				Creep	Shrinkage
Specimen in water of 20°C & 100% R.H. (Basic creep)	1	Plain RHPC	31.4	2	1
	2	Plain OPC	31.4	2	1
Specimen in dry room of 20°C & 65% R.H. (Total creep of constant environment)	3	Plain RHPC	31.4	2	1
	4	Plain RHPC	21.8	2	1
	5	Plain OPC	31.4	2	1
	6	Plain OPC	21.8	2	1
	7	RHPC/Admix.	21.8	2	1
	8	RHPC/PFA	21.8	2	1
	9	RHPC/Admix & PFA	21.8	2	1
Specimen in variable environment of 20°C & 65 to 100% RH. (Total creep of variable environment)	10	Plain RHPC	31.4	2	1
	11	Plain RHPC	21.8	2	1
	12	Plain OPC	31.4	2	1
	13	Plain OPC	21.8	2	1

Remarks:

(1) Test specimens were cylinders 76 mm diameter and 267 mm height

(2) Nominal compressive stress at loading is 5 N/mm^2

(3) Volume/Surface ratio of 31.4 and 21.8 mm represent rectangular and I shaped beams respectively

Table 3.3 - Details of Concrete Mixes Used

PARAMETER	TYPE OF MIX				
	MIX 1 RHPC	MIX 2 OPC	MIX 3 RHPC/ADMX.	MIX 4 RHPC/PFA	MIX 5 RHPC/PFA & ADMX.
CEMENT CONTENT kg/m^3	420	340	420	294	294
PFA CONTENT kg/m^3 (30% REPLACEMENT)	-	-	-	157.5	157.5
AGGREGATE/CEMENT RATIO	4.4	5.4	4.4	-	-
AGGREGATE/CEMENT PLUS PFA RATIO	-	-	-	4.0	4.0
PERCENTAGE FINES	37.5	37.0	37.5	35.0	35.0
WATER/CEMENT RATIO (FREE)	0.39	0.50	0.34	-	-
WATER/CEMENT & PFA RATIO (FREE)	-	-	-	0.36	0.30
ADMIXTURE, % BY WEIGHT OF CEMENT	-	-	0.6	-	-
ADMIXTURE, % BY WEIGHT OF CEMENT & PFA	-	-	-	-	0.6
SLUMP (mm)	7	30	5	10	12
VEBE TIME (seconds)	11	3	10	9	9

Table 3.4 Programme of casting and prestessing

Remarks: C= Concrete Casting ; P= Prestressing

Beams \ Date	Jan 30	February 1984 1	6	8	20	22	27	29	March 5	7	9	12	14	16	April 9	11	16	18	25	30	May 2	7	9	16	30	Jun 6	November 12	13	20	27	28	Dec 3	Age At Transfer In Days	Duration Of Curing In Days
CR/C2	C		P																														7	7
CYR/C2		C		P																													7	7
NGI/C2					C		P																										7	7
NI/C2						C		P																									7	7
NGI/C1 & NGR/C1									C	P																							2	2
CI/C1 & CYR/C1										C	P																						2	2
NI/C1 & NR/C1												C	P																				2	2
CR/C1 & CYI/C1													C	P																			2	2
NGI/V1 & NGR/V1															C	P																	2	2
NI/V1 & NR/V1																	C	P															2	2
NGI/V2																		C	P														7	7
CI/V1 & CYR/V1																				C	P												2	2
CR/V1 & CYI/V1																						C	P										2	2
NI/V2 & CYR/V2																							C	P									7	7
CR/V2																									C	P							7	7
NI/C3																											C	P					1	1
NI/C4																													C		P		8	8
NI/C5																														C		P	5	5

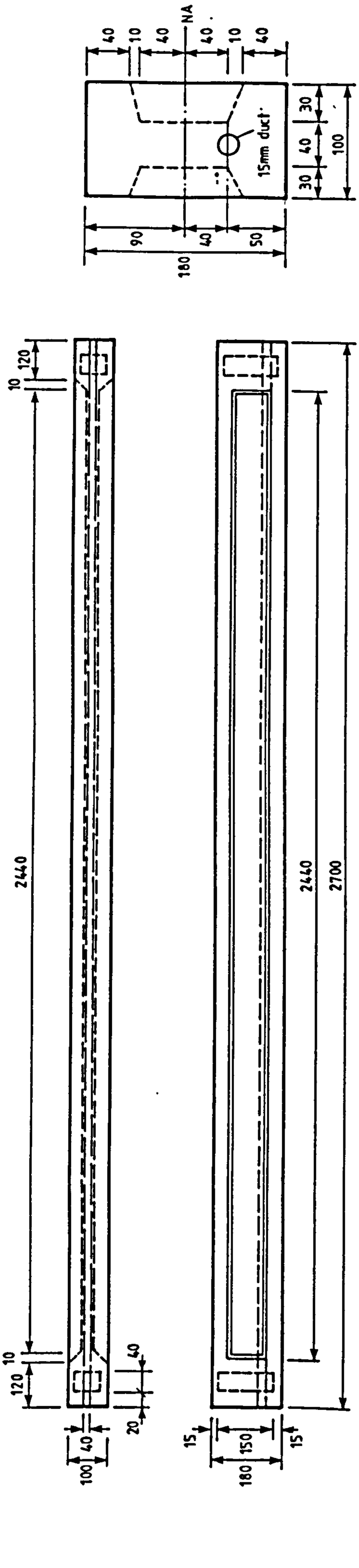

Fig.3.1 Prestress beams dimensional properties

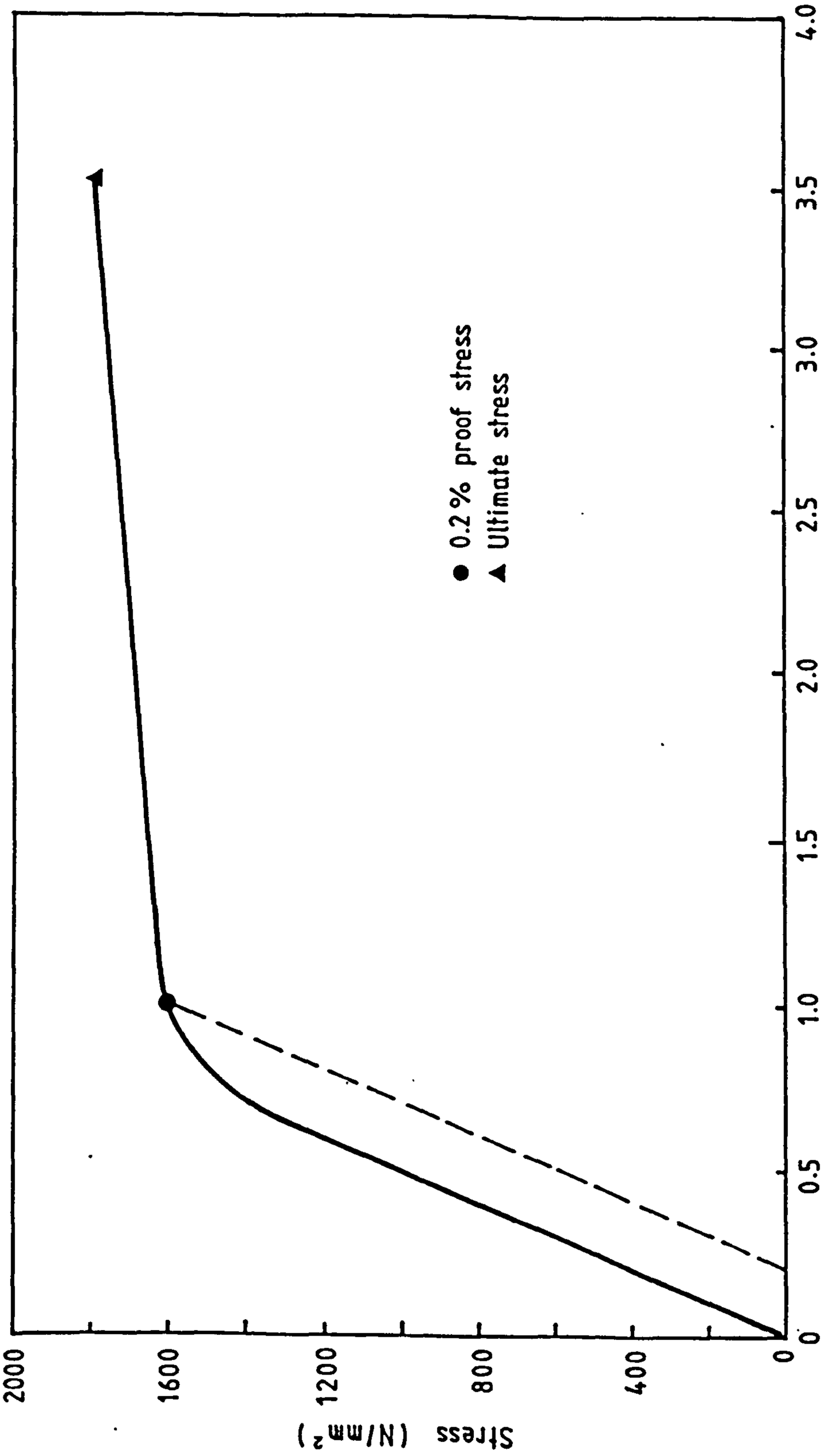

Fig. 3.2 Stress-strain relationship of 7mm high tensile wire

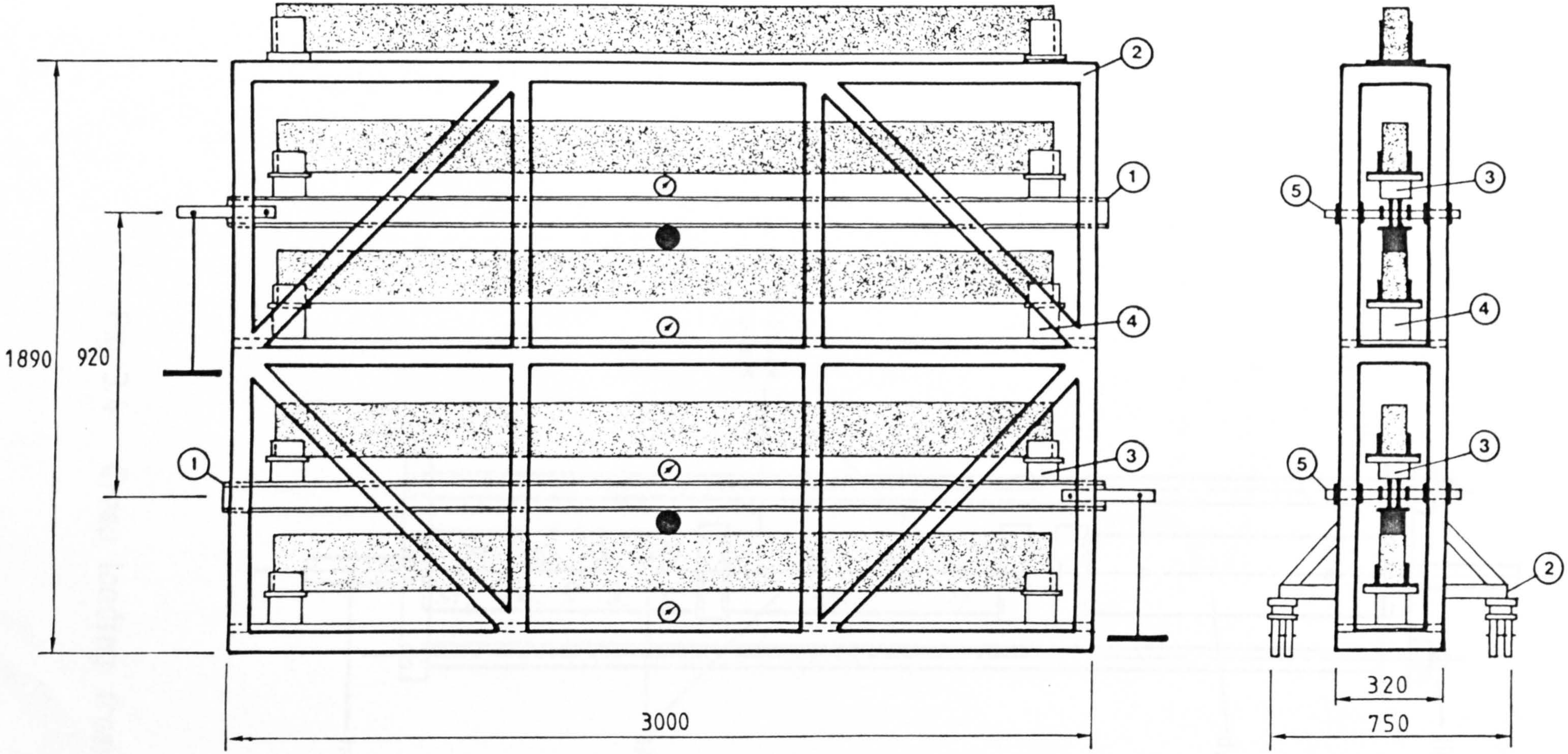

Dimensions in millimetres

SECTION No	SECTION	REFERENCE	NOMINAL SIZE
①	Joist	RSJ	102 × 102 × 23.07 kg/m
②	Square hollow section	SHS	50 × 50 × 6.97 kg/m
③	Rectangular hollow section	RHS	100 × 98 × 35.7 kg/m
④	Square hollow section	SHS	150 × 150 × 35.4 kg/m
⑤	Round bar	RB	30 o.d. × 5.55 kg/m

Fig. 3.3 Details of beam loading rig

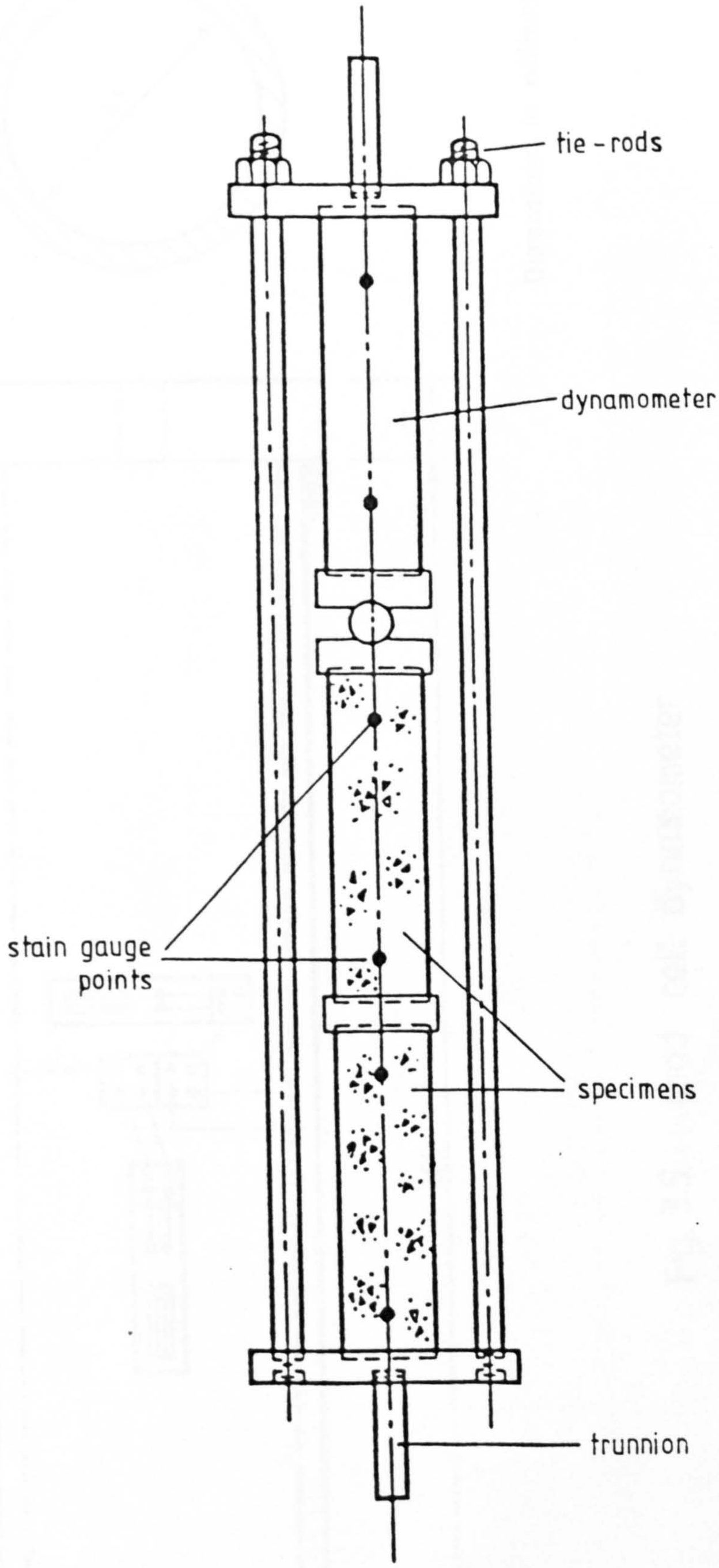

Fig. 3.4 Creep loading frame [56]

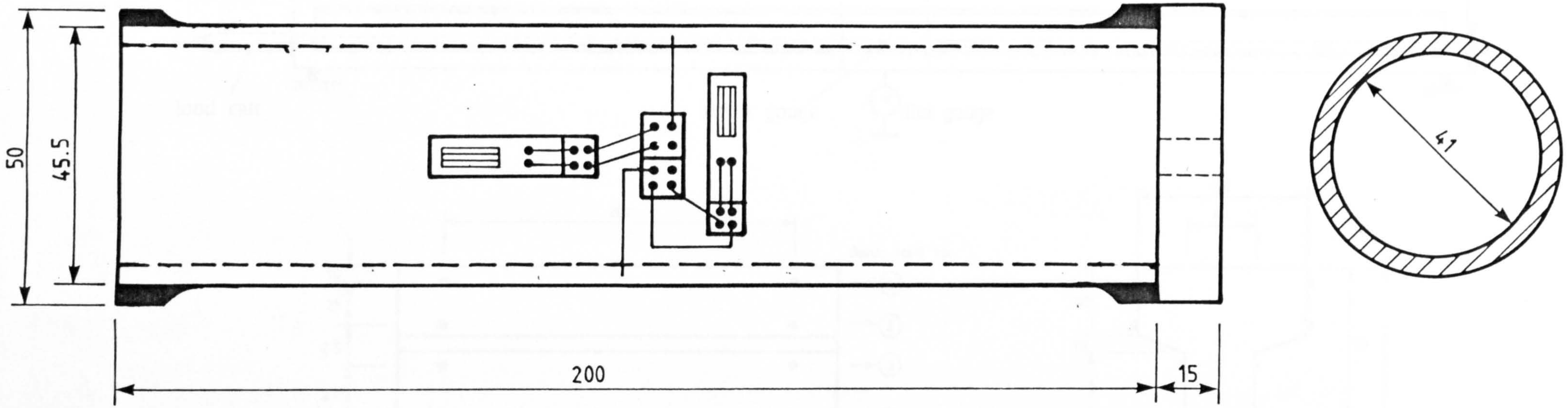

Dimensions in millimetres

Fig. 3.5 Load cell dynamometer

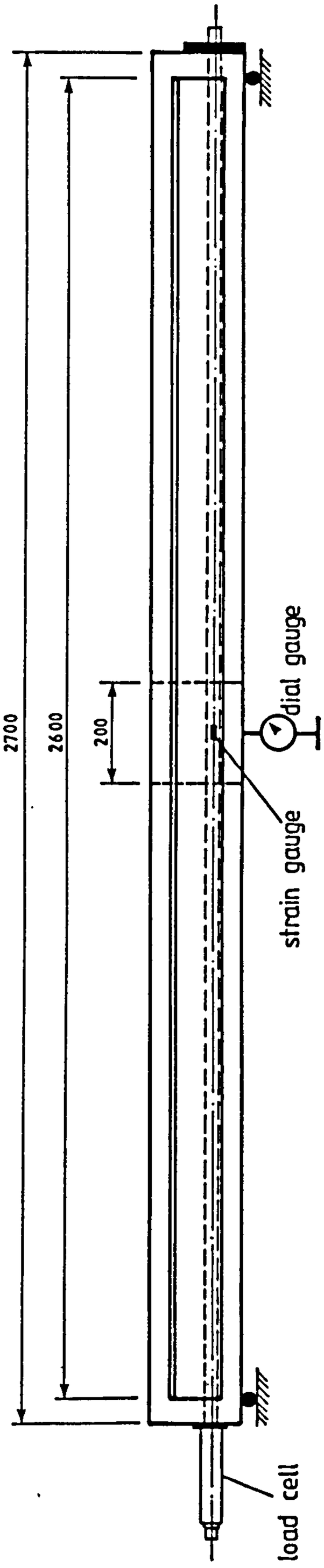

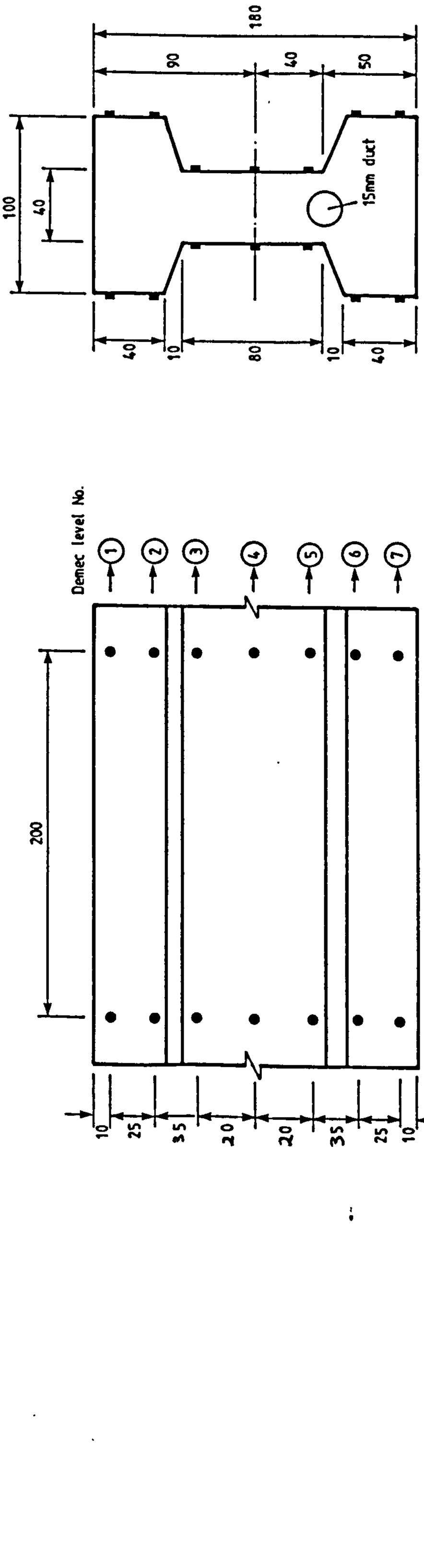

Beam section

Dimensions in millimetres

Position of Demec points

Fig.3.6 Locations of concrete and steel experimental measurements for prestress beams

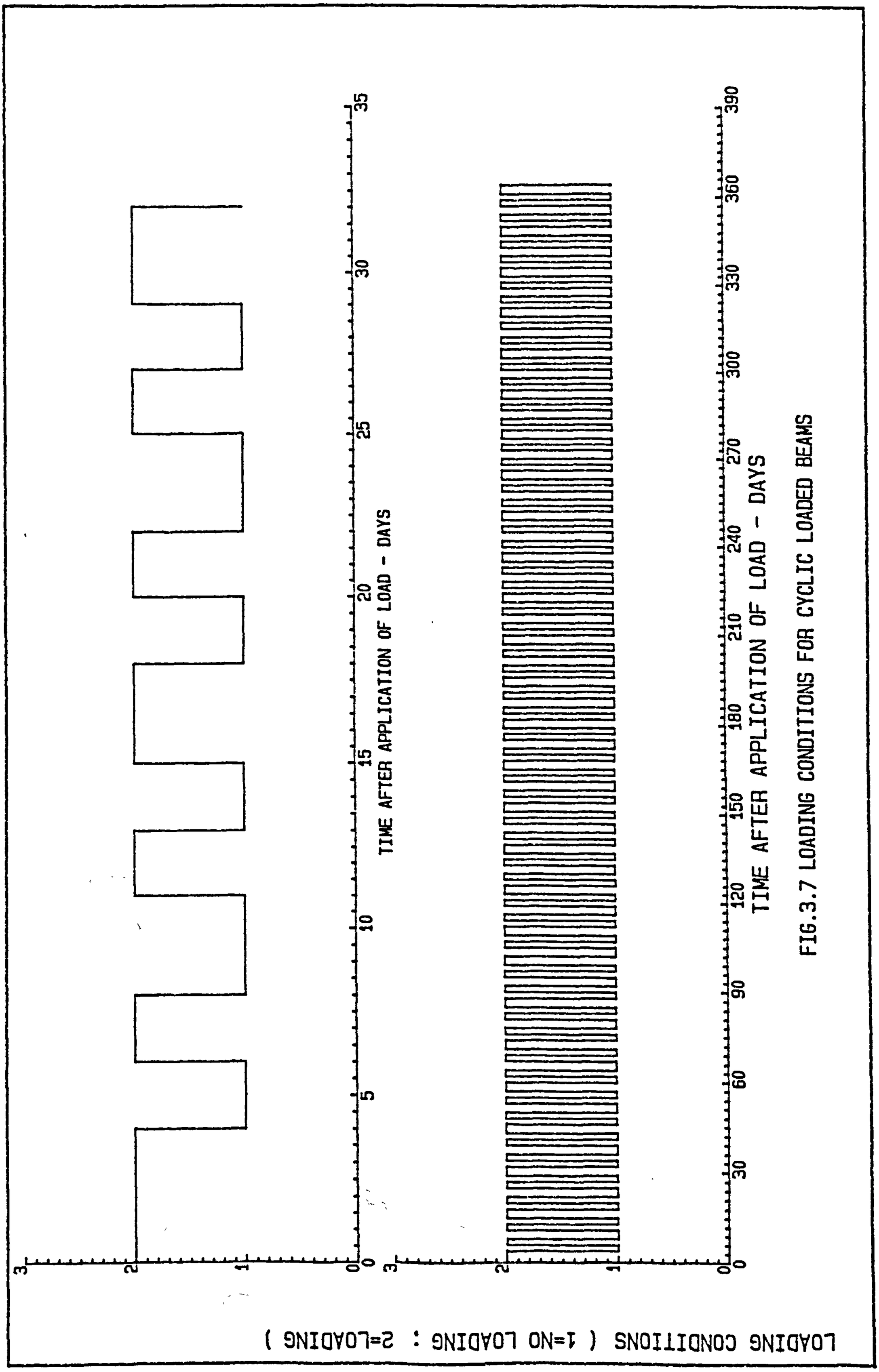

FIG.3.7 LOADING CONDITIONS FOR CYCLIC LOADED BEAMS

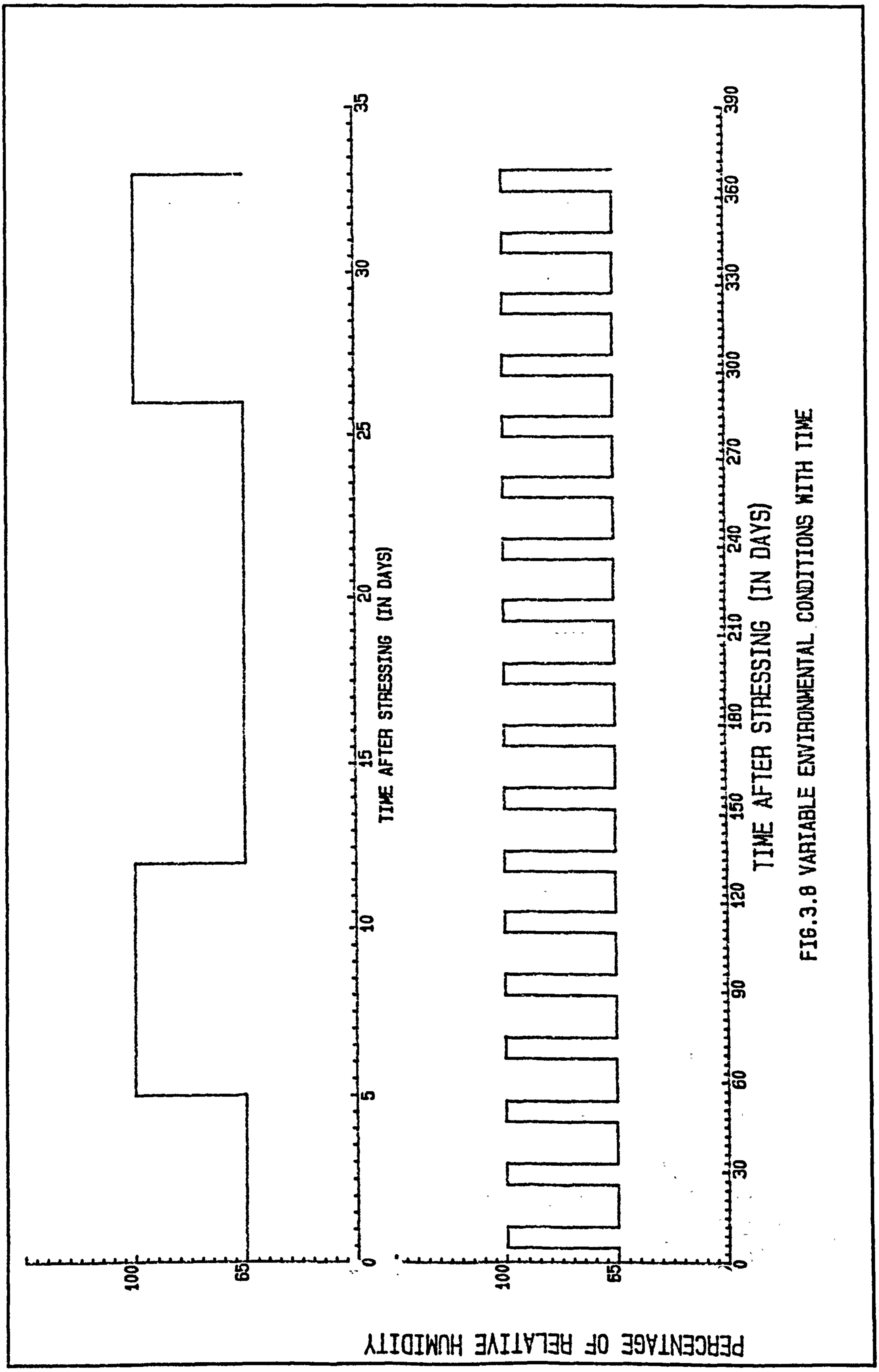

FIG.3.8 VARIABLE ENVIRONMENTAL CONDITIONS WITH TIME

Plate 3.1 Control shrinkage rectangular and I-shaped beams placed in the vertical direction

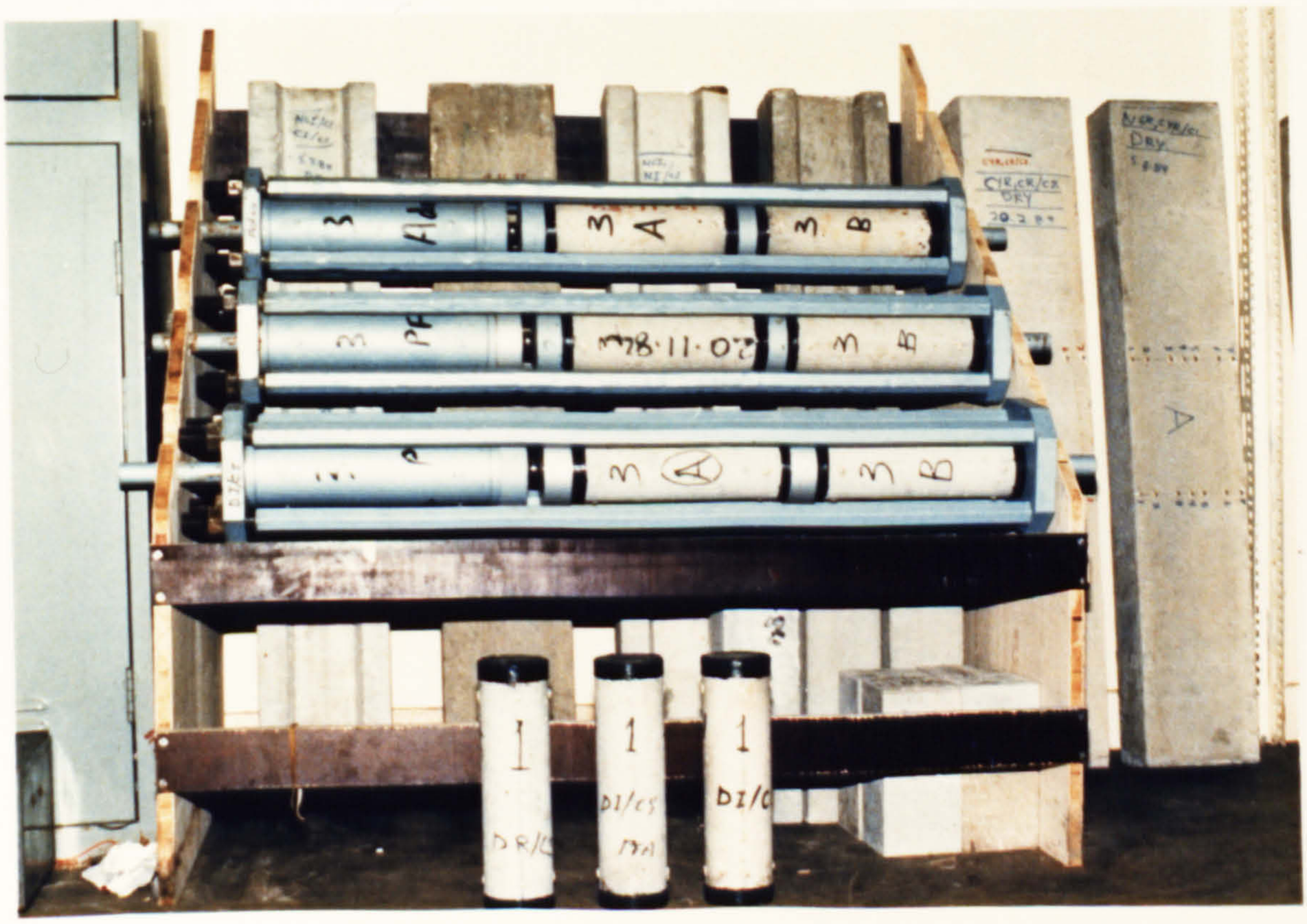

Plate 3.2 Typical view of creep rigs and shrinkage beams and cylinders

Plate 3.3 Beams loading rig inside control dry room

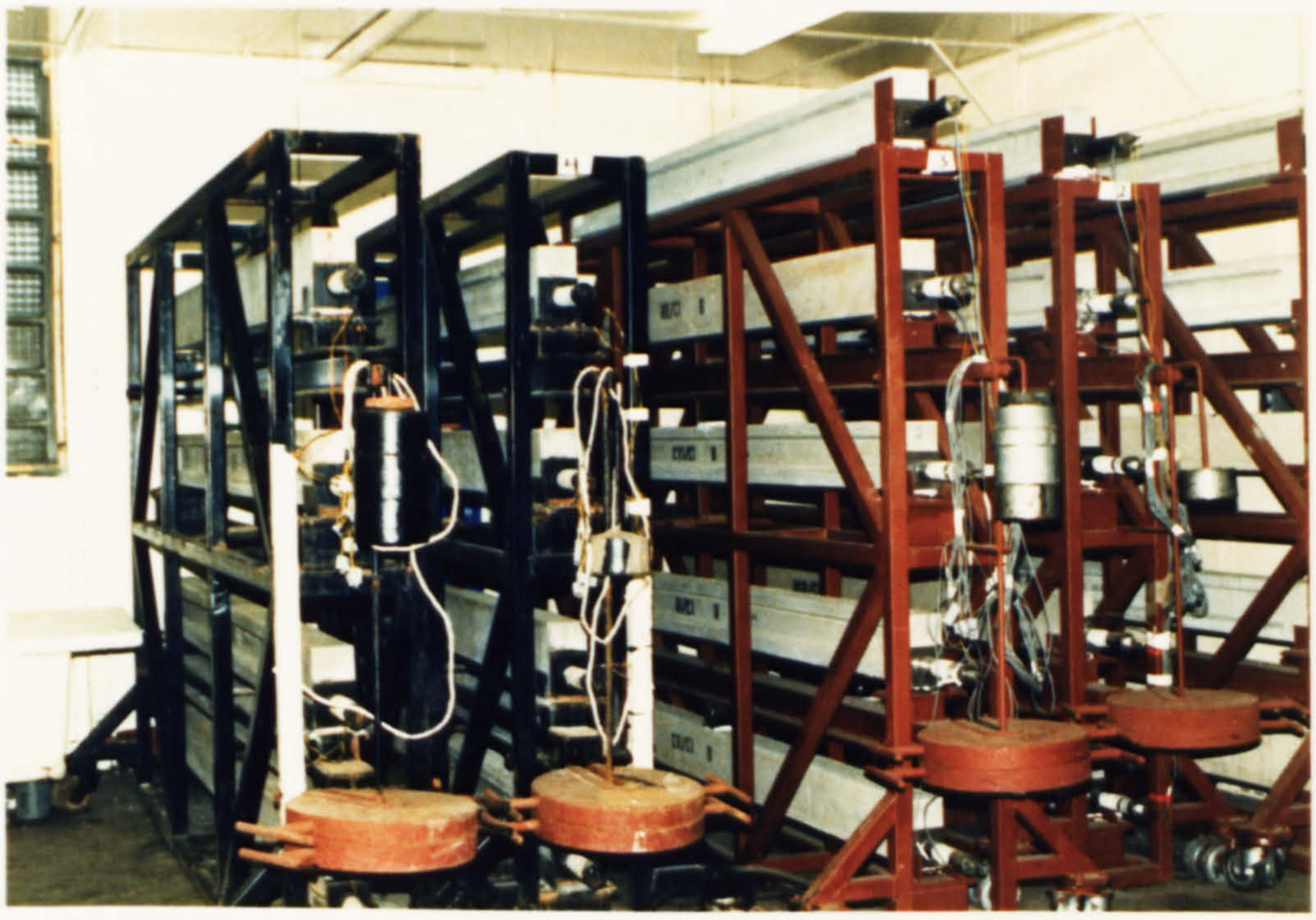

Plate 3.4 General view of beams loading rigs inside control room of 20°C and 65% R.H.

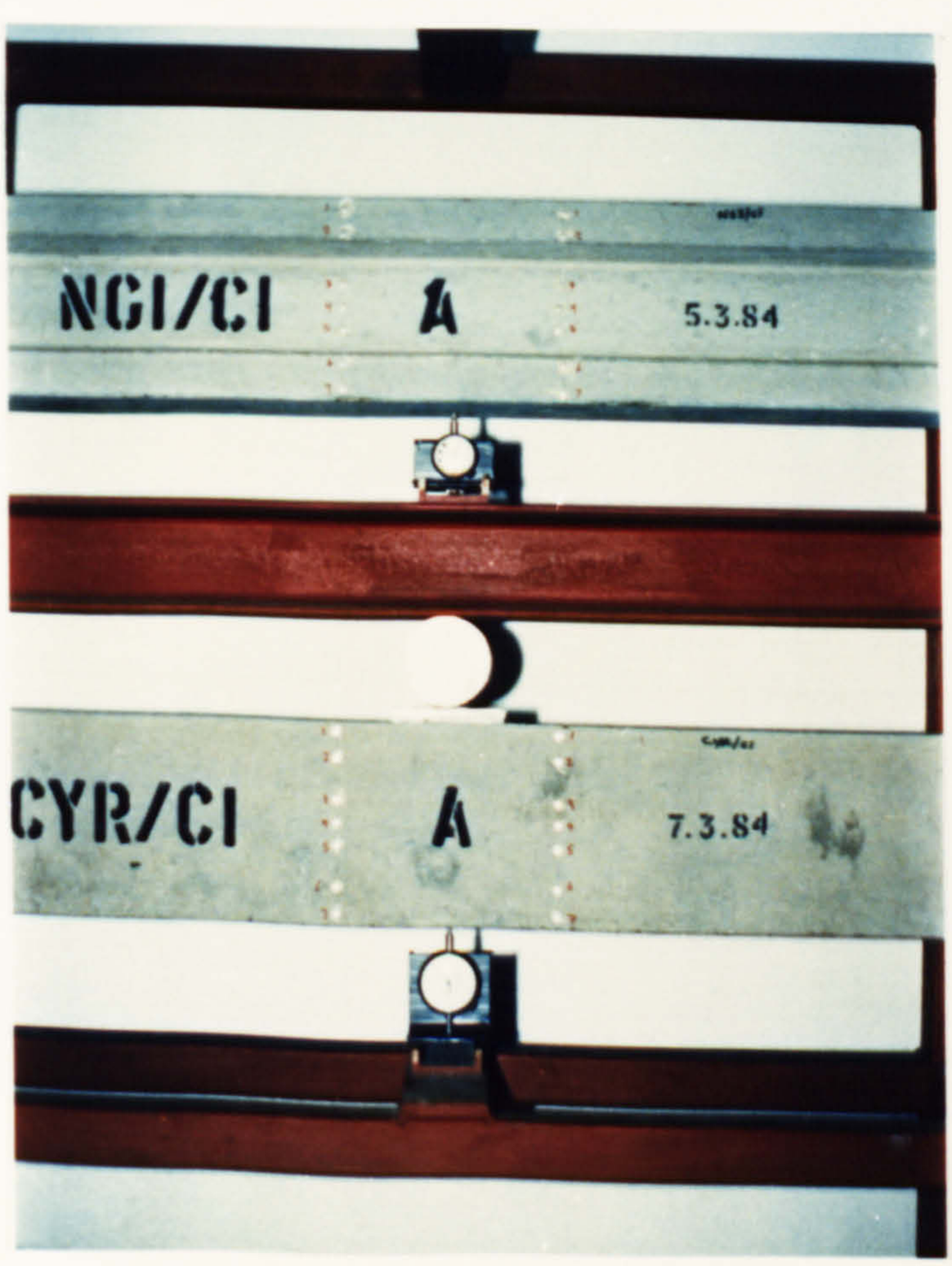

Plate 3.5 View of post-tensioned beams deflection measurement using the movable deflection dial gauges

Plate 3.6 The Intercole Compulog IV data logging system

CHAPTER 4 - PREDICTION AND ANALYSIS METHODS OF CREEP AND SHRINKAGE DEFORMATIONS

4.1 Introduction

The subject of time-dependent stresses and deformations in materials that exhibit creep and shrinkage properties has been under intensive study for the past few decades. When an applied stress is sustained in a structural member, it produces instantaneous strain and then creep. Creep starts to develop at the time of stress application and increases as time progresses. This time-dependent strain is known as creep which may amount to several times the instantaneous elastic strain. It is widely accepted that, for stresses within service limits, both the instantaneous strain and the creep are linearly proportional to the applied stress. The creep can be determined by conducting tests on the particular concrete used. Alternatively, the designer must resort to one of the available methods for creep prediction in the absence of test data. The most widely used methods for structural design purposes are given by CEB-FIP Recommendations (15,16), ACI committee 209 (8), Bazant and Panul's Model II (57) and Concrete Society (58,59) which is recently adopted by the new British code of practice BS8110 (60). Several analytical methods have been established to use creep data from tests under constant stress to analyse structures subjected to variable stress regimes.

In this chapter, the prediction methods of creep strains are reviewed along with the methods of creep analysis and their

approximations and limitations. Full treatment of these topics are given by Neville et al. (18).

4.1.1 Classification of Deformation of Concrete

Concrete undergoes instantaneous as well as time-dependent deformation. The time-dependent deformation encompasses two types, stress-dependent deformation or creep and stress-independent deformation caused by shrinkage and thermal dilation.

4.1.1.1 Instantaneous Elastic Strain

This strain occurs upon load application and depends on the value of Young's modulus, E, which is a function of the concrete age. The instantaneous recovery of strain due to unloading is usually less than the instantaneous strain increase resulting from previous loading: this is attributed to the fact that the modulus of elasticity of concrete increases due to aging of concrete. However it is a reasonable assumption to consider the elastic modulus of concrete to be constant for mature concretes over 28 days of age.

4.1.1.2 Recoverable and Irrecoverable Creep

An experimental investigation by Glucklich and Ishai (61) led to the first systematic examination of creep components. The study consisted of measurements of deflection in beams made of hardened cement paste, all loaded at the same age but for different durations of load. Further tests were performed by Illston on young

concrete (62) and on mature concrete (63) loaded uniaxially in compression or tension. Following these studies it has become well established that creep under sustained compressive stress may be divided into two distinct components:

(i) Recoverable creep (delayed elastic), which develops rapidly and reaches a limiting value in a relative short time, as short as two weeks for young concrete. This limiting value was shown to be little affected by age of concrete or by previous stress history. The time of development of limiting, on the other hand, increases with age. Furthermore, it has been shown by Rusch et al. (64) that the recoverable creep component is only slightly temperature dependent, independent of thickness of structural member and, according to Parrott (65) does not change appreciably with humidity.

The delayed elastic strain may be divided into rapid and slow components each of which follows an exponential law with time.

(ii) Irrecoverable creep (flow), which develops less rapidly than the recoverable creep at a decreasing rate with time and has no limiting value. The rate of flow declines as the age of concrete at loading increases but is independent of previous loading history. According to Illston (62,63) creep flow is highly dependent on tempertaure and humidity. Rusch et al. (64) divided the flow into three parts as follows: (a) rapid flow, and (b) basic flow, which are dependent on temperature and degree of hydration but independent of the size of structural member, and (c) drying flow which is partly reversibe in case of moisture change and dependent on

temperature and member size but is only slightly affected by degree of hydration. Therefore for static humidity fields one can treat the creep flow as one component without loss of accuracy.

4.1.1.3 Stress-Independent Deformation

This includes two types of volume changes:

(i) Shrinkage and swelling

When concrete loses moisture to the ambient environment, it exhibits a decrease in volume called free shrinkage and when the moisture movement is from the environment to the concrete it experiences an increase in volume called swelling. The magnitude of shrinkage is highly dependent on the humidity of the surrounding atmosphere as well as the size of the structural member and temperature.

(ii) Thermal dilation

When concrete is subjected to rising temperature, it expands, and when subjected to falling temperature it contracts. The magnitude of thermal movement depends on the coefficient of thermal dilation.

4.2 Prediction of Creep and Shrinkage

4.2.1 Formulation According to CEB-FIP Recommendations, 1970 (15)

The prediction method for the creep coefficient and the shrinkage is given in terms of coefficients accounting for different

coefficients depend on factors allowing for the composition of the mix, effective thickness of member, relative humidity of storage, age at loading and variation with time under load. The values of these coefficients are represented graphically in the form of curves.

4.2.1.1 Creep

The creep coefficient is equal to the product of five partial coefficients as follows:

$$\phi_{28}(t, to) = K_c\ K_d\ K_b\ K_e\ K_t \qquad \text{Eq.(4.1)}$$

where K_c is the ambient humidity coefficient (Fig.4.1a)

K_d is the age of loading coefficient (Fig.4.1b)

K_e is the theoretical thickness coefficient (Fig.4.1d)

The theoretical thickness h_o is defined as:

$$h_o = 2\frac{Ac}{u}$$

where h_o is the theoretical thickness which is the quotient of the area of the section A_c divided by the semi-perimeter u/2 in contact with the atmosphere.

K_b is the composition coefficient (Fig.4.1c)

K_t indicates the development of creep with time coefficient (Fig.4.1e).

The coefficient K_d is based on the hardening of Portland cement at an average temperature of $20^{o}C$ with protection against

excessive losses of moisture. If the temperature is other than $20^{o}C$, the age at loading (Fig.4.1b) is substituted by the corresponding degree of hardening;

$$D = \Sigma \Delta t(T + 10^{o})$$

in which D represents the degree of hardening at loading

Δt represents the number of days during which hardening has taken place at $T^{o}C$.

The total strain is given as:

$$\varepsilon_c(t, t_o) = \delta_{co} \left[\frac{1}{E_c(t_o)} + \frac{\phi_{28}(t, t_o)}{E_{c28}} \right] \qquad \text{Eq. (4.2)}$$

where δ_{co} is the applied stress in MPa.

$E_c(to)$ is the modulus of elasticity at the age at application of load to

4.2.1.2 Shrinkage

The shrinkage strain, $\Sigma_{sh}(t,to)$ measured from the start of drying (to), is expressed as:

$$\Sigma_{sh}(t, to) = K'_c K_b K'_e K_t \qquad \text{Eq.(4.3)}$$

where K'_c is the ambient humidity coefficient (Fig.4.2a)

K'_e is the theoretical thickness coefficient (Fig.4.2b)

K_b and K_t are as for creep

4.2.1.3 Modulus of Elasticity

The modulus of elasticity, E_c(GPa) is related to concrete cylinder compressive strength, f_c (MPa) by:

$$E_c(t) = 5.94 \quad f(t)^{\frac{1}{2}} \qquad \text{Eq.(4.4)}$$

and the development of strength with age is given in Table 4.1.

4.2.2 Formulation According to CEB-FIP Recommendations, 1978 (16)

A comparison of measured creep and shrinkage with values calculated according to the CEB-FIP Recommendations (1970) showed some deficiencies and led to the new CEB-FIP Recommendations (1978). According to Rusch et al. (64), the essential difference between the new and the old formulations is the separation of the creep strain into recoverable and irrecoverable components.

4.2.2.1 Creep

The creep coefficient ϕ_{28} (t, to) is given by:

$$\phi_{28}(t,to) = \beta_a(to) + \phi_d \beta_d(t-to) + \phi_f [\beta_f(t) - \beta_f(to)] \qquad \text{Eq.(4.5)}$$

and $\beta_a(to) = 0.8 \left[1 - \frac{f_c(t_o)}{f_{c\infty}}\right]$

where β_a = the initial flow

$\frac{f_c(t_o)}{f_{c\infty}}$ = strength ratio which obtained from Fig.4.3a

ϕ_d = ratio of limiting delayed elastic strain to the initial elastic strain at 28 days which is equal to 0.4

β_d = a function representing the development of delayed elastic strain with time (Fig.4.3b)

ϕ_f = flow coefficient = $\phi_{f1} \cdot \phi_{f2}$

ϕ_{f1} = ambient humidity coefficient (Table 4.2) for fresh concrete of normal consistency (slump). For low consistency, ϕ_{f1} should be reduced by 25% and, for high consistency ϕ_{f1} should be increased by 25%

ϕ_{f2} = notational thickness coefficient which takes into account the member size (Fig.4.3c)

The notational thickness (h_o) is given by:

$$h_o = \frac{\lambda \cdot 2A_c}{u}$$

where A_c = cross-sectional area of member (mm^2)

U = circumference exposed to drying (mm)

and λ = coefficient for ambient humidity obtained from Table 4.2.

The plastic flow parameters of the creep coefficient equations are:

$\beta_f(t)$ = a function describing the development of delayed plastic strain with time, and depends on h_o (Fig. 4.3d).

$\beta_f(to)$ = as above but at time $t = t_o$ to account for the age at application of loads.

To account for the temperature during curing, if it is appreciably different from 20°C, and cement type, the age of concrete must be adjusted i.e.

$$t_e = \frac{\alpha}{30} \sum_{o}^{tm} [T(t_m) + 10] \Delta t_m$$

where α = 1, 2 or 3 for normal and slowly-hardening cements, for rapid-hardening cements, and for rapid-hardening high strength cement, respectively; T is the mean daily temperature of concrete (°C) and Δt_m is the number of days when the mean daily temperature has assumed the value T.

The total deformation under a unit stress (creep function) is given by:

$$\Phi(t,t_o) = \frac{1}{E_c(t_o)} + \frac{\phi_{28}(t,t_o)}{E_{c28}} \qquad \text{Eq.(4.6)}$$

4.2.2.2 Shrinkage

The shrinkage strain, which develops in an interval of time $(t-t_o)$ is given by:

$$\Sigma_{sh}(t, t_o) = \Sigma_{sho} [\beta_{sh}(t) - \beta_{sh}(t_o)] \qquad \text{Eq.(4.7)}$$

where Σ_{sh0} is the basic shrinkage coefficient = $\Sigma_{sh1} \cdot \Sigma_{sh2}$

Σ_{sh1} depends on the environment (Table 4.2)

Σ_{sh2} depends on notational thickness h_o (Fig. 4.4a)

β_{sh} is a function corresponding to the change of shrinkage with time and depends on h_o (Fig. 4.4b)

t is the observation time, and t_o is the age of concrete at the moment from which the influence of shrinkage is considered.

4.2.2.3 Modulus of Elasticity

The modulus of elasticity at any time related to concrete strength is given by:

$$E_c(t_o) = 9.5[f_c(t_o)]^{1/3} \qquad \text{Eq.(4.8)}$$

where $E_c(t_o)$ and $f_c(t_o)$ are the modulus of elasticity (GPa) and stength (MPa), respectively, at the age of loading (t_o). $E_c(t_o)$ is the modulus for a load applied in a time of 1-5 min. For all other times, adjustments are necessary.

4.2.3 Formulation According to ACI-Committee 209, 1982 (8)

The ACI Committee 209 has proposed approximate equations for the prediction of strength and deformations properties on concrete based on the work of Branson and Christiason (66). The prediction of creep and shrinkage depends on many factors such as the method of curing, the coefficient for age at application of

load, the humidity coefficient and the coefficients which allow for the composition of the concrete. This method is similar to CEB-1970 but it is in algebraic form instead of a graphical one. For simplicity, the notations used are those adopted by Neville et al. (18).

4.2.3.1 Creep

The creep coefficient is given by:

$$\phi(t,t_o) = \frac{(t-t_o)^{0.06}}{10+(t-t_o)^{0.6}}\,\phi_\infty(t_o) \qquad \text{Eq.(4.9)}$$

where $(t-t_o)$ = time since application of load

and $\phi_\infty\ (t_o)$ = ultimate creep coefficient which is given by:

$$\phi_\infty(t_o) = 2.35\ K'_2K'_1K'_4K'_3K'_6K'_7 \qquad \text{Eq.(4.10)}$$

For ages at application of load greater than seven days for moist curing, or greater than 1 to 3 days for steam curing, the correction factor for age at application of load K'_2 is given by:

$$K'_2 = 1.25\ t_o^{-0.118} \quad \text{(moist curing)}$$

$$K'_2 = 1.13\ t_o^{-0.094} \quad \text{(steam curing)}$$

For relative humidity greater than 40 percent, the correction factor K'_1 is given by:

$$K'_1 = 1.27 - 0.006\ h, \text{ for } h \geq 40$$

Two methods are offered for estimating the correction factor of the member thickness (K'_4):

(a) Average thickness method

For average thickness < 150 mm, K'_4 is given in Table 4.4.

For average thickness between 150 and 380 mm,

$$K'_4 = 1.14 - 0.00092\ d, \text{ for } (t-t_o) \leq 1 \text{ year}$$

$$K'_4 = 1.10 - 0.00067\ d, \text{ for } (t-t_o) > 1 \text{ year}$$

where d is the average thickness of the concrete member under consideration (mm).

(b) Volume/surface ratio Method

$$K'_4 = 2/3(1 + 1.13\ e^{-(0.0213(v/s))})$$

where v/s = volume/surface ratio in mm = d/4

The correction factors which allow for the composition of the concrete are:

$$K'_3 = 0.82 + 0.00264\ s_f$$

where s_f = slump of fresh concrete (mm).

$$K'_6 = 0.88 + 0.0024\ s/a$$

where s/a = ratio of the fine aggregate to total aggregate by mass expressed as percentage.

$$K'_7 = 0.46 + 0.09A \geq 1$$

where A = air content in percent

4.2.3.2 Shrinkage

Shrinkage at time t, measured from the start of drying $t_{sh,o}$ is expressed as follows:

For moist curing

$$\Sigma_{sh}(t,t_{sh,o}) = \frac{(t - t_{sh,o})}{35 + (t-t_{sh,o})} \Sigma_{sh,\infty} \qquad \text{Eq.(4.11)}$$

or steam curing,

$$\Sigma_{sh}(t,t_{sh,o}) = \frac{(t - t_{sh,o})}{55 + (t-t_{sh,o})} \Sigma_{sh\infty} \qquad \text{Eq.(4.12)}$$

where Σ_{sh} = shrinkage strain (10^{-6})

The ultimate shrinkage Σ_{sh_∞} is given by:

$$\Sigma_{sh_\infty} = 780 \times 10^{-6} K'_5 K'_1 K'_4 K'_3 K'_6 K'_8 K'_7 \qquad \text{Eq.(4.13)}$$

The correction factor K'_5 for curing times different from 7 days for moist-cured concrete is given in Table 4.5. For steam curing in a period of one to three days, $K'_5 = 1$.

The humidity correction factor K'_1 is:

$$K'_1 = 1.40 - 0.010\ h, \text{ for } 40 \leq h \leq 80$$

$$K'_1 = 3.00 - 0.030\ h, \text{ for } 80 \leq h \leq 100$$

where h is relative humidity in percent.

Two methods are offered for estimating the correction factor of the member thickness (K'_4)

(a) Average thickness

For average thickness < 150 mm, K'_4 is given in Table 4.4.

For average thickness between 150 and 380 mm,

$$K'_4 = 1.23 - 0.0015\ d, \text{ for } (t-t_{sh,o}) \leq 1 \text{ year}$$

$$K'_4 = 1.17 - 0.0015\ d, \text{ for } (t-t_{sh,o}) > 1 \text{ year}$$

where d is the average thickness of the concrete member under consideration (mm).

(b) Volume/surface ratio (d > 380 mm)

$$K'_4 = 1.2\ e^{-0.00472(v/s)}$$

The correction factors which allow for the composition of the concrete are:

$$K'_3 = 0.89 + 0.00161\ s_f$$

where s_f = slump of fresh concrete (mm),

$$K'_6 = 0.30 + 0.014\ F, \text{ for } F \leq 50$$

$$K'_6 = 0.90 + 0.002\ F, \text{ for } F > 50$$

where F = fine aggretate/total aggregate ratio by mass percent.

$$K'_8 = 0.75 + 0.00061\gamma$$

where γ = cement content (kg/m^3)

and $K'_7 = 0.95 + 0.008\ A$

where A is the percentage of air content

4.2.3.3 Modulus of Elasticity

The relation of the elastic modulus, $E_c\ (t_o)$ to the strength (f_{cyl}) and the dependence of the elastic modulus age are given by the following equation:

$$E_c(t_o) = 42.8 \times 10^{-6}(\rho^3 f_{cyl}(t_o))^{\frac{1}{2}} \qquad \text{Eq.(4.14)}$$

and

$$f_{cyl}(t_o) = \frac{t_o}{A + B\ t_o} f_{cyl28} \qquad \text{Eq.(4.15)}$$

where $f_{cyl}(t_o)$ and f_{cyl28} are compressive strengths of concrete cylinders in MPa, E_c is in GPa, ρ = density of concrete (kg/m^3),

and A and B depend on the type of cement and curing conditions as shown in Table 4.6.

4.2.4 Bazant and Panula's Model II (BaP), 1978 (57)

This model is a simplified version of an earlier model proposed for estimating basic creep, total creep and shrinkage. The input data required are similar to those for the CEB-1970 and ACI methods. Total creep is considered separately from basic creep by introducing a drying creep term in the creep function, and this term is a function of shrinkage.

4.2.4.1 Basic Creep

The basic creep function at any time t for concrete loaded at the age of t_o is given by:

$$\Phi(t, t_o) = \frac{1}{E'}(1 + \phi'_b(t, t_o)) \qquad \text{Eq.(4.16)}$$

where $\Phi(t, t_o)$ = basic creep function (10^{-3} per MPa), and $\phi'_b(t, t_o)$ = basic creep coefficient which is expressed as:

$$\phi'_b(t, t_o) = B((t_o)^{-m} + 0.05)(t-t_o)^n \qquad \text{Eq.(4.17)}$$

where ϕ'_b is based on a fictitious modulus, E', which merely represents the inverse of the left-side asymptote of the creep curve in log-time. The parameters E', B, m and n are all functions of the 28-day strength and expressed as:

$$\frac{1}{E'} = 0.01306 + 3.203\ (f_{cyl28})^{-2} \text{ in } (10^{-3}/\text{MPa})$$

$$B = 0.3 + 152.2\ (f_{cyl28})^{-1.2}$$

$$m = 0.28 + 47.541\ (f_{cyl28})^{-2}$$

$$n = 0.115 + 0.183 \times 10^{-6}\ (f_{cyl28})^{3.4}$$

where f_{cyl28} = 28-day cylinder strength (MPa).

The basic creep coefficient $\phi_b(t, t_o)$, as based on the static modulus at the age of loading (t_o), is given by:

$$\phi_b(t, t_o) = E_c(t_o)\ \Phi_b(t, t_o) - 1 \qquad \text{Eq/(4.18)}$$

4.2.4.2 Total Creep

The total creep function at any time t for concrete loaded at the age of t_o is expressed as:

$$\Phi(t, t_o) = \Phi_b(t, t_o) + \frac{\phi'_d(t, t_o, t_{sh,o})}{E'} \qquad \text{Eq.(4.19)}$$

where $\Phi_b(t, t_o)$ = basic creep function

and the drying creep coefficient $\phi'_d(t, t_o, t_{sh,o})$ is given by the following equations:

$$\phi'_d(t, t_o, t_{sh,o}) = \bar{B}_d \, K''_1 (t_o)^{-(m/2)} \left(1 + \frac{3t_{(1/2)sh}}{t - t_o}\right)^{-c_d n}$$

Eq.(4.20)

$$\bar{B}_d = \left(1 + \frac{t_o - t_{sh,o}}{10\, t_{(1/2)sh}}\right)^{-(1/2)} B_d \Sigma_{sh\infty}$$

$$B_d = 0.0056 + \frac{0.0189}{1 + 0.7\, r^{-1.4}}$$

$$r = 0.56\left(\left(\frac{s}{a}\right) f_{cy/28}\right)^{0.3} \times \left(\frac{g}{s}\right)^{1.3} \left(1610 \frac{\left(\frac{w}{c}\right)}{\Sigma_{sh\infty}}\right)^{1.5} - 0.85$$

where $t_{(\frac{1}{2})sh}$ = half-time shrinkage

$\Sigma_{sh\infty}$ = ultimate shrinkage (section 4.2.4.3)

s/a = fine aggregate/total aggregate ratio by mass

g/s = coarse aggregate/fine aggregate ratio by mass

w/s = water/cement ratio by mass

If $r > o$ then $B_d = 0.0056$

and K''_1 in Eq.(4.20) depends on relative humidity (h) is given by:

$$K''_1 = 1 - 10^{-3} h^{1.5}$$

factor $c_d n$ is taken as 0.35

The coefficient $t_{(\frac{1}{2})sh}$ is given by the following equation:

$$t_{(1/2)sh} = 4\left(K'' \frac{V}{S}\right)^2 \frac{1}{D(t_{sh,o})} \qquad \text{Eq.(4.21)}$$

where K" = shape factor equal to 1.0, 1.15, 1.25, 1.30 and 1.55 for slab, cylinder, square prism, sphere and cube, respectively.

v/s = volume/surface ratio (mm)

$D(t_{sh,o})$ = drying diffusivity which is given by:

$$D(t_{sh,o}) = 2.4 + \frac{120}{\sqrt{t_{sh,o}}}$$

The total creep coefficient based on $E_c(t_o)$ is

$$\phi\ (t, t_o) = E_c(t_o)\ \Phi\ (t, t_o) - 1 \qquad \text{Eq.(4.22)}$$

4.2.4.3 Creep of Cyclic Humdity

For cyclic humidity conditions, Bazant et al. (67) have suggested a correction factor K to be multiplied by the creep coefficient $\phi'_d\ (t, t_o, t_{sh,o})$ presented earlier in Eq.(4.20), using however the time-average environmental humidity for h.

The $c_d n$ factor of Eq.(4.20) is given by:

$$c_d n = 2.8 - 7.5\ n$$

The total creep function at any time t for concrete stored in cyclic humidity condition is expressed as:

$$\Phi(t, t_o) = \Phi_b(t, t_o) + \frac{K \phi'_d(t, t_o, t_{sh,o})}{E'} \qquad \text{Eq.(4.23)}$$

where coefficient K represents an increase in creep due to humidity cycling and given by:

$$K = 1 + K_1\ (\Delta_h)\ \frac{D_p}{D_p + 0.5\ D} \qquad \text{Eq.(4.23)}$$

in which:

D represents the wall thickness

D_p represents the depth of penetration

$$D_p \simeq \sqrt{6\, C_1\, T}$$

where C_1 = 0.1 cm^2/day and T represents the period of humidity cycle in days.

The factor $K_1(\Delta_h)$ is a certain empirical function of the amplitude Δ_h of environmental humidity h and k_1 is a factor given by:

$$K_1 = 2.5\, \Delta_h (1-e^{-(t-t_o)/10})(1-e^{-T/5}) \qquad \text{Eq.(4.25a)}$$

in which t, t_o and T must be given in days.

For load durations $t - t_o > 10$ days, K_1 is expressed as:

$$K_1 \simeq 2.5\, \Delta_h\, (1-e^{-t/5}) \qquad \text{Eq.(4.25b)}$$

For $D_p > D/2$ the expression for coefficient K is given by:

$$K = 1 + K_1 \qquad \text{Eq.(4.26a)}$$

while for $D_p < D/2$ the coefficient K is given by:

$$K = 1 + 2\, K_1 \frac{D_p}{D} \qquad \text{Eq.(4.26b)}$$

4.2.4.4 Shrinkage

Shrinkage deformation of concrete $\Sigma_{sh}\,(t,\, t_{sh,o})$ at any

time t, measured from the start of drying $t_{sh,o}$ is given by:

$$\Sigma_{sh}(t, t_{sh,o}) = K''_1 \; \Sigma_{sh\infty} \left(\frac{(t - t_{sh,o})}{t_{(1/2)sh} + (t - t_{sh,o})} \right)^{\frac{1}{2}} \qquad \text{Eq.(4.27)}$$

where K''_1 = a coefficient which depends on the relative humidity h which is expressed by:

$$K''_1 = 1\text{-}10^{-6} \; h^3 \text{ for } h \leq 98 \text{ percent}$$

$$K''_1 = -0.2 \text{ for } h = 100 \text{ percent}$$

The ultimate shrinkage, $\Sigma_{sh\infty}$ (10^{-6}), is related to the mix parameters by the following expressions:

$$\Sigma_{sh\infty} = 1330 - 970 \; y \qquad \text{Eq.(4.28)}$$

$$y = (390 \; z^{-4} + 1)^{-1}$$

$$Z = 0.381(f_{cy/28})^{\frac{1}{2}} \; (1.25(\frac{a}{a})^{\frac{1}{2}} + 0.5(\frac{g}{s})^2] \; x \; (\frac{1 + \frac{s}{c}}{w/c})^{1/3} \; -12$$

where z must be > 0, otherwise Z = 0,

$\frac{a}{c}$ = total aggregate/cement ratio by weight

$\frac{s}{c}$ = fine aggregate/cement rtio by weight

4.2.4.5 Modulus of elasticity

The static and dynamic modulus of elasticity are given by the following equations:

$$\frac{1}{E_c(t_o)} = \frac{1}{E'} \left(1 + B((t_o)^{-m} + 0.05)\ 10^{-n}\right) \qquad \text{Eq.(4.29a)}$$

$$\frac{1}{E_{cd}(t_o)} = \frac{1}{E'} \left(1 + B((t_o)^{-m} + 0.05)\ 10^{-7n}\right) \qquad \text{Eq.(4.29b)}$$

where $E_c(t_o)$ = static modulus at time t_o measured in a time of 10^{-1} days

$E_{cd}(t_o)$ = dynamic modulus at time t_o measured in a time of 10^{-7} days.

4.2.5 Concrete Society, CS-1978 (58, 59) and British Code of Practice BS8110-1985 (60)

4.2.5.1 Creep

Following an earlier prediction method (58, 59) based on the CEB-1970, a simplified method for estimating the ultimate creep and modulus of elasticity is recommended by the British Concrete Society. This method applies only to ultimate values. The ultimate creep function Φ_∞ (10^{-3} per MPa) is given by:

$$\Phi_\infty = \frac{1}{E_c(t_o)} \left(1 + \phi_\infty\right) \qquad \text{Eq.(4.30)}$$

where $E_c(t_o)$ = modulus of elasticity at the age of application of load t_o

and ϕ_∞ is the ultimate creep coefficient which is obtained from Fig. 4.5a. It is based on CEB-1970 and relates to the

ambient humidity, age at loading and effective section thickness.

Although there is no provision for estimating creep coefficient as a continuous function of time, the Concrete Society suggests that approximately 80, 50 and 30 percent of the ultimate creep coefficient occurs after six months under load for effective thickness of <200, 300 and >400 mm, respectively. For no moisture exchange, basic creep will develop at the rate corresponding to an effective thickness of >400 mm.

The new British code BS8110-1985 suggests that 40%, 60% and 80% of the final creep develops during the first month, 6 months and 30 months under load, respectively, when concrete is exposed to conditions of constant relative humidity.

4.2.5.2 Shrinkage

Values of shrinkage and swelling after exposure periods of 6 months and 30 years are given in Fig. 4.5b for various relative humidities of storage and effective section thickness. The given values apply to concrete made with high-quality, dense, non-shrinking aggregates and to concrete having an effective water content of 8 percent of the original weight of concrete. For concretes with an original water content different from this value, the shrinkage of Fig.4.5b is adjusted in proportion to the water content.

4.2.5.3 Modulus of Elasticity

The modulus of elasticity at the age of loading $E_c(t_o)$ is estimated from strength as follows:

$$E_c(t_o) = E_{c28}\,(0.4 + 0.6\,\frac{f_{cu}(t_o)}{f_{cu28}}) \qquad \text{Eq.(4.31a)}$$

and $$E_{c28} = 20 + 0.2\,f_{cu28} \qquad \text{Eq.(4.31b)}$$

where $E_c(t_o)$ and $f_{cu}(t_o)$ = modulus of elasticity (6Pa) and cube strength (MPa), respectively, at the age at application of load t_o, and E_{c28} and f_{cu28} = corresponding values at the age of 28 days.

The strength ratio $(f_{cu}(t_o)/f_{cu28})$ is obtained either from measurement or from Table 4.7.

4.2.6 Comparison of Prediction Methods

For all the prediction methods described previously, a number of effecting parameters are summarised in Table 4.8. From this it follows that the methods differ considerably in the number of parameters which are taken into account. The methods ACI, CEB70 and BaP can only be applied accurately if concrete composition is known.

Muller and Hilsdrof (68) and Brooks (69) have made a comparison of prediction methods for instantaneous and time-dependent deformations of structural concrete with experimental

data. The methods studied were the CEB-70, CEB-78, ACI-82, British Concrete Society (CS-78) and Bazant and Panula (BaP-78) methods. They concluded that all methods do not satisfactory predict elastic strain. Muller and Hilsdrof concluded that the difference in accuracy between the various method is minor with the exception of the method BaP-78 and the method CS-78 gives good results. Also the methods CEB-70 and CEB-78 show relatively poor results for drying creep but they are in good agreement with creep data for basic creep. Brooks generally concluded that when predicting from strength and mix composition, the strains are underestimated, there being little difference between the five methods for estimating basic strain. However, for total strain, the BaP-78, CEB-70 and CS-78 methods are better than the CEB-78 and ACI-82 methods.

4.3 Methods of Analysis for Variable Stress Conditions

4.3.1 Effective Modulus Method (EM)

The effective modulus method is the oldest, simplest and most widespread method (70, 71, 72, 18). The total deformation at any age, $\varepsilon(t)$, for a history of varying stress under conditions of drying, is expressed as follows:

$$\varepsilon(t) = \frac{\sigma(t)}{E_c} + \Sigma_{sh}(t) \qquad \text{Eq.(4.32)}$$

where $\sigma(t)$ = applied stress,

$\Sigma_{sh}(t)$ = shrinkage strain,

and E_e = effective modulus as given by:

$$E_e = \frac{E(t_o)}{1 + \phi(t,t_o)} \qquad \text{Eq.(4.33)}$$

where $E(t_o)$ = modulus of elasticity at the age at first application of load, t_o,

and $\phi(t,t_o)$ = creep coefficient as expressed by

$$\phi(t,t_o) = C(t,t_o) \times E(t_o) \qquad \text{Eq.(4.34)}$$

where $C(t,t_o)$ = creep per unit of stress (specific creep)

The main shortcomings of the method are: it neglects the aging of concrete, it gives erroneous results in cases of severe stress variation, and it predicts complete recovery of strains on the removal of stress.

4.3.2 Rate of Creep Method (RC)

The method was introduced by Glanville (72) and the mathematical formulation was first developed by Whitney (73) for a constant modulus of elasticity. The main assumption is that the creep curves for various ages of loading are all identical but mutually vertically translated. Dischinger (74) extended Whitney's formulation, taking into account a variable modulus of elasticity of concrete. This method admits simple solutions by assuming the creep law in the form of a first-order differential equation:

$$d\Sigma(t) = \frac{\sigma(t)}{E(t_o)}\, d\phi + \frac{1}{E(t)}\, d\sigma(t) + d\Sigma_{sh}(t) \qquad \text{Eq.(4.35)}$$

in which $\Sigma(t)$ being the instant the permanent load or enforced deformation is introduced into the structure.

By integrating Eq. (4.35):

$$\Phi\ t,t_1) = \frac{1}{E(t_1)} + \frac{1}{E(t_o)}\ (\phi(t,t_o) - \phi(t_1,t_o)) \qquad \text{Eq.(4.36a)}$$

where t, t_1 are time elapsed from loading, in days.

The creep function for the initial application of load at age (t_o):

$$\Phi(t,t_o) = \frac{1}{E(t_o)}\ (1 + \phi(t,t_o)) \qquad \text{Eq.(4.36b)}$$

The advantage of this method is that it requires as data only a unit creep curve and a variation of elastic modulus with time if taken into consideration. On the removal of the stress, no recovery is predicted which is a shortcoming of the method.

4.3.3 Rate of Flow Method (RF)

The method was introduced by England and Illston (75), and developed by Illston (63) and Rusch et al. (64).

They suggested that creep is represented as in the rate of creep method which is irrecoverable and a delayed elastic component which is recoverable (see Section 4.1.1.2). Each of the two components has its own characteristics.

For a numerical solution which is the same procedure as the rate of creep method, the time period of prediction is divided into finite intervals of time during each of which the stress and the

modulus of elasticity are assumed to be constant (75). Considering two consecutive intervals, Δt_1 and Δt_2, for the case of a varying stress history, the change in total deformation Δ_ε at the end of Δt_2 is given by

$$\Delta\varepsilon = \frac{1}{E(t)}(\sigma_2 - \sigma_1) + \frac{\sigma_2}{E(t_o)}\Delta\phi_f + \Delta\Sigma_d + \Delta\Sigma_{sh} \qquad \text{Eq.(4.37)}$$

where $E(t)$ = modulus of elasticity during Δt_2,

σ_1 and σ_2 = the mean stresses during Δt_1 and Δt_2, respectively,

$\Delta\phi_f$ = change in flow coefficient during Δt_2 (flow coefficient = $E(t_o)$ x specific flow).

$\Delta\Sigma_{sh}$ = change in shrinkage during Δt_2, and

$\Delta\Sigma_d$ = change in delayed elastic strain during Δt_2 and given by:

$$\Delta\Sigma_d = (\sigma_2 C_{d1\infty} - \Sigma_{d1})(1 - e^{-(\Delta\phi_f/E(t_o)\phi_1)}) + \sigma_2 C_{d2\infty} - \Sigma_{d2}) \times (1 - e^{-[\Delta\phi_f/E(t_o)Q_2)}) \qquad \text{Eq.(4.38)}$$

where $C_{d1\infty}$ and $C_{d2\infty}$ = limiting values of specific delayed elastic strain for the rapid and slow periods, respectively.

and

Q_1 and Q_2 = rate parameters which are obtained from the delayed elastic strain slopes of the rapid and slow lines of the recovery curve as shown in Fig.4.6.

The creep function for the initial application of load at age (t_o) is given by:

$$\Phi(t,t_o) = \frac{1}{E(t_o)} + \frac{\phi_d(t-t_o)}{E(t_o)} + \frac{\phi_f(t)-\phi_f(t_o)}{E(t_o)} \qquad \text{Eq.(4.39)}$$

in which ϕ_d and ϕ_f denote creep coefficients for the delayed elastic strain and for the flow, respectively.

4.3.4 Improved Dischinger Method (ID)

Nielsen (76) proposed an improvement of the rate of creep method by recognizing the recoverable creep strain. For simplicity, Nielsen suggested that the ultimate value of the recoverable creep strain is to be taken as a constant and to be treated as part of the instantaneous deformation. This can be represented in practice by the inclusion of the recoverable creep strain in the immediate elastic strain, i.e., using a reduced value of the concrete modulus E_r such that:

$$E_r = E(t_o)/(1 + \phi_d) \qquad \text{Eq.(4.40)}$$

where ϕ_d is the ultimate recoverable creep coefficient which was suggested initially by Nielsen (76) to be approximated by 1/3. Later Nielsen (77, 78) indicated that this value needs more investigation because it is not the same from concrete to another concrete.

According to the method, the creep function is given by:

$$\Phi(t,t_o) = \frac{1}{E_d} + \frac{\phi_f(t) - \phi_f(t_o)}{E(t_o)} \qquad \text{Eq. (4.41)}$$

where $\frac{1}{E_d} = \frac{1}{E(t')} + \frac{\phi_d}{E(t_o)}$

and $E_d = 0.75\ E\ (t_o)$ when $\phi_d = 1/3$

in which E_d and ϕ_f are fictitious elastic modulus and creep coefficient, respectively. A later investigation by Rusch et al. (64) supported this method and suggested that $\phi_d = 0.4$ for load duration more than 90 days, which was adopted in the CEB-FIP, 1978 Model Code.

From a practical point of view, the method does not give serious errors and the prediction is generally good after the lapse of sufficient time after loading.

4.3.5 Superposition Method

McHenry (79) in 1943 proposed the theory of reversibility of creep which generally referred to as the principle of superposition. For a variable stress history, each stress increment produces a resulting deformation component continuing for an infinite time, while a stress decrement is considered as an increment with a negative sign. The total strain is estimated by superimposing creep curves of virgin concrete. The creep-time data are required fo the various ages at application of load at which an increment or decrement of stress is applied, and since the method requires a new creep curve whenever there is a change of stress, the amount of experimental data can be considerable.

The formulation of total strain at time t, due to a varying stress starting from an initial value σ_o, is

$$\Sigma(t) = \frac{\sigma_o}{E(t_o)} (1 + \phi(t,t_o)) + \int_{t_o}^{t} \Phi(t,t') \frac{\partial\sigma(t')}{\partial t'} dt' \qquad \text{Eq. (4.42)}$$

in which $\Phi(t,t')$ is the creep function given by

$$\Phi(t,t') = \frac{1}{E(t')} + C(t,t') = \frac{1}{E(t')}\ (1 + \phi(t,t') \qquad \text{Eq. (4.42a)}$$

4.3.6 Age-Adjusted Effective Modulus Method

Bazant (80) reformulated Trost's method (81) and extended it to the case of a variable elastic modulus and renamed it "Age-Adjusted Effective Modulus Method". The stress-strain relations were given by Bazant in the form of an incremental elastic law. The aging coefficient X (relaxation coefficient) is given by:

$$X(t,t_o) = \frac{E(t_o)}{E(t_o) - R(t,t_o)} - \frac{1}{\phi(t,t_o)} \qquad \text{Eq. (4.43)}$$

where $R(t,t_o)$ is the relaxation function at time t for an initial stress equal to $E(t_o)$ applied at age t_o.

Bazant (80) used two different creep functions to define the numerical values of aging coefficients, namely the ACI, 1971 (7) creep functions for structural concrete and for mass concrete. The creep function for structural concrete is given by:

$$\Phi(t,t') = \frac{1}{E(t')}\ (1 + \phi_u(t')\ \frac{(t-t')^{0.6}}{10 + (t-t')^{0.6}} \qquad \text{Eq. (4.44a)}$$

and the creep function for mass concrete expressed by:

$$\Phi(t,t') = \frac{1}{E(t')}\ (1 + \phi_u(t')0.113\ \log_e(1 + t - t')) \qquad \text{Eq. (4.44b)}$$

where $E(t') = E(28) \left(\frac{t'}{4+0.85t'} \right)^{\frac{1}{2}}$

and $\phi_u(t') = \phi(t_\infty, 7)\ 1.25\ t'^{-0.118}$

According to Bazant (80), in contrast with Trost et al. (82), the aging coefficient X is dependent on the duration of loading. This has been verified by Brugger (83) by solving some numerical examples using the ACI Committee 209 (7) creep functions.

In order to enable the designer to apply the method, values of aging coefficients should be available for different variables encountered in practical problems. So far, however, a very limited number of tables and charts of X values are available.

Table 4.1 - The effect of age on the ratio of strength at any age to the 28-day strength according to CEB-FIP, 1970 (15)

Age of concrete (days)		3	7	28	30	360
Portland cement strength ratio	normal	0.40	0.65	1.00	1.20	1.35
	rapid-hardening	0.55	0.75	1.00	1.15	1.20

Table 4.2 - CEB-FIP 1978 coefficients of creep and shrinkage (16)

Ambient environment	Relative humidity (per cent)	Coefficients of		Coefficient
		Creep ϕ_{fl}	Shrinkage $\varepsilon_{shl}(10^{-6})$	λ
Water	-	0.8	+100	30
Very damp atmosphere	90	1.0	-130	5
Outside in general	70	2.0	-320	1.5
Very dry atmosphere	40	3.0	-520	1

Table 4.3 - CEB-FIP, 1978 Values for H_f (16)

Notional thickness h_o (mm)	H_f (days)
50	330
100	425
200	570
400	870
800	1500
1600	2500

Table 4.4 - ACI, 1982 creep and shrinkage correction factors for average thickness of member (8)

Average thickness of member (mm)	Creep correction factor K'_4	Shrinkage correction factor K'_4
50	1.30	1.35
75	1.17	1.25
100	1.11	1.17
125	1.04	1.08
150	1.00	1.00

Table 4.5 - ACI 1982 age correction factors for shrinkage (K'_5) (8)

Period of moist curing (days)	Shrinkage age correction factor K'_5
1	1.2
3	1.1
7	1.0
14	0.93
28	0.86
90	0.75

Table 4.6 - Values of the constants A and B for use in the ACI, 1982 modulus-age expression (8)

Type of cement	curing condition	Constants	
		A	B
I	Moist	4.00	0.85
	Steam	1.00	0.95
III	Moist	2.30	0.92
	Steam	0.70	0.98

Table 4.7 - Development of strength with age: values of strength ratio for use in Eq.4.31a (58)

Age to (days)	Strength ratio	
	Ordinary Portland Cement	Rapid-hardening Portland cement
7	0.65	0.75
28	1.00	1.00
90	1.20	1.15
365	1.35	1.20

TABLE 4.8 - Required Input Data for Various Prediction Methods

Required input data	Prediction method				
	CEB 70	CEB 78	ACI 82	BaP 78	BCS 78
Size and shape of member	x	x	x	x	x
Age at loading	x	x	x	x	x
Humidity of environment	x	x	x	x	x
Compressive strength of concrete	x	x	x	x	x
Consistency of fresh concrete		x	x		
temperature	x†	x		x	
Type of cement	x	x	x	x	x
Cement content	x			x	
Unit weight of concrete			x	x	
Water-cement ratio	x			x	
Sand-aggregate ratio			x	x	
Aggregate-cement ratio				x	
Air content of concrete			x		
Curing conditions (humidity and beginning of drying)				x	

† During the curing period prior to loading

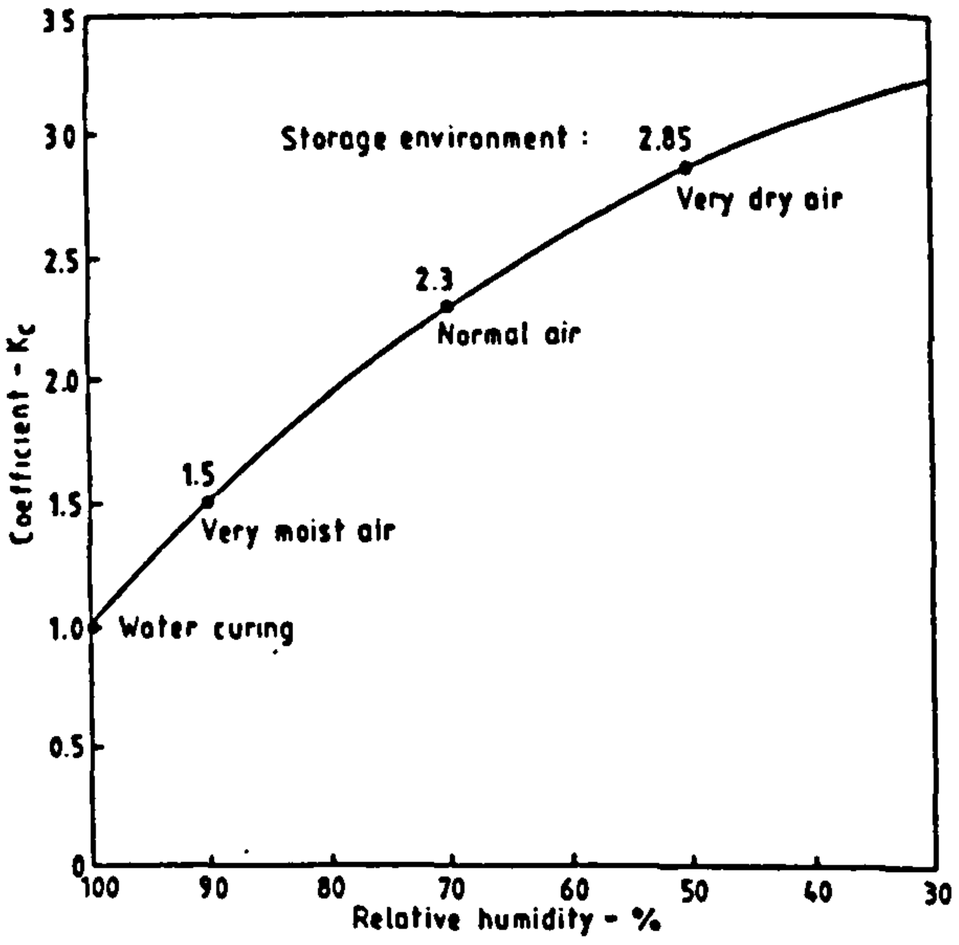

Fig.4.1(a) CEB-1970 creep prediction: ambient humidity coefficient (K_c)

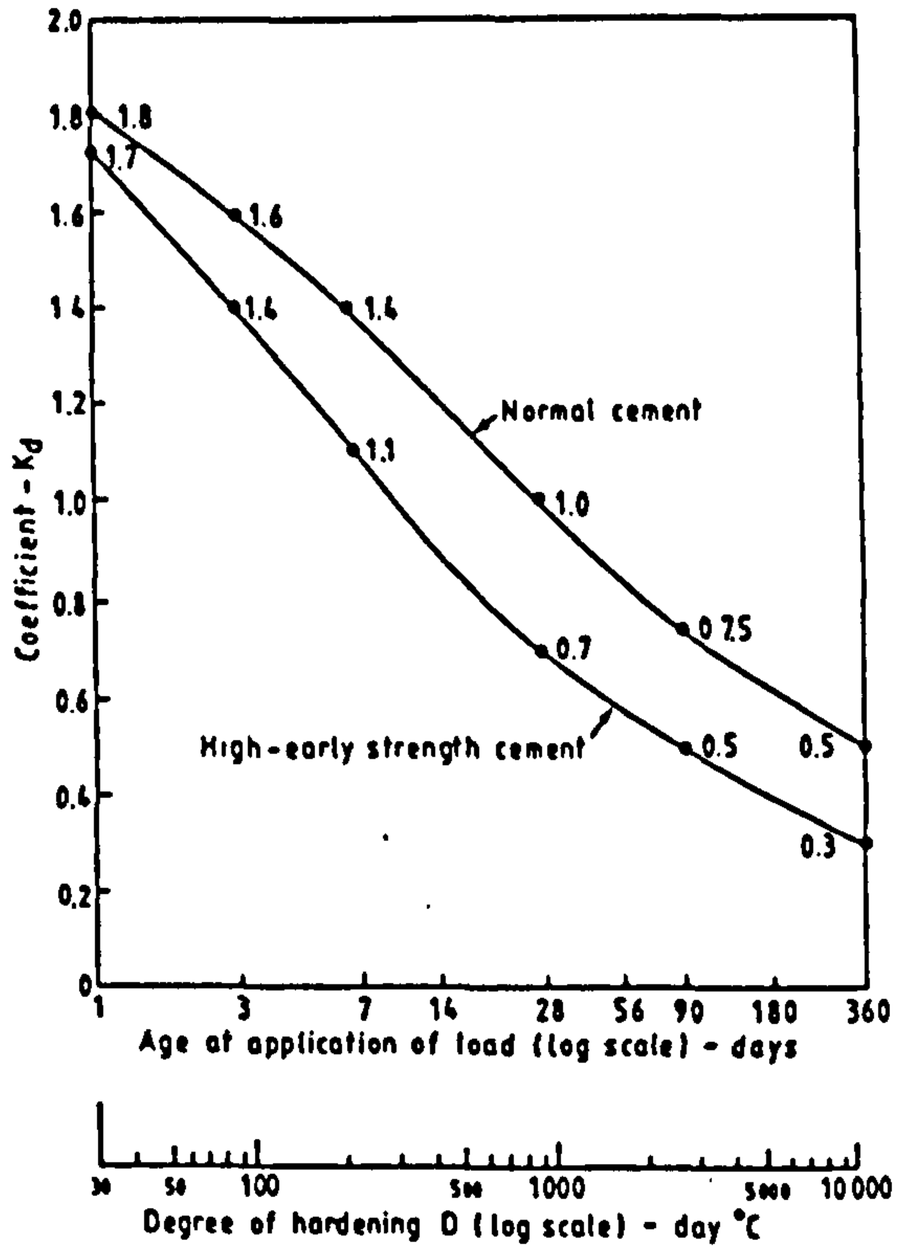

Fig.4.1(b) CEB-1970 creep prediction: age at application of load coefficient (K_d)

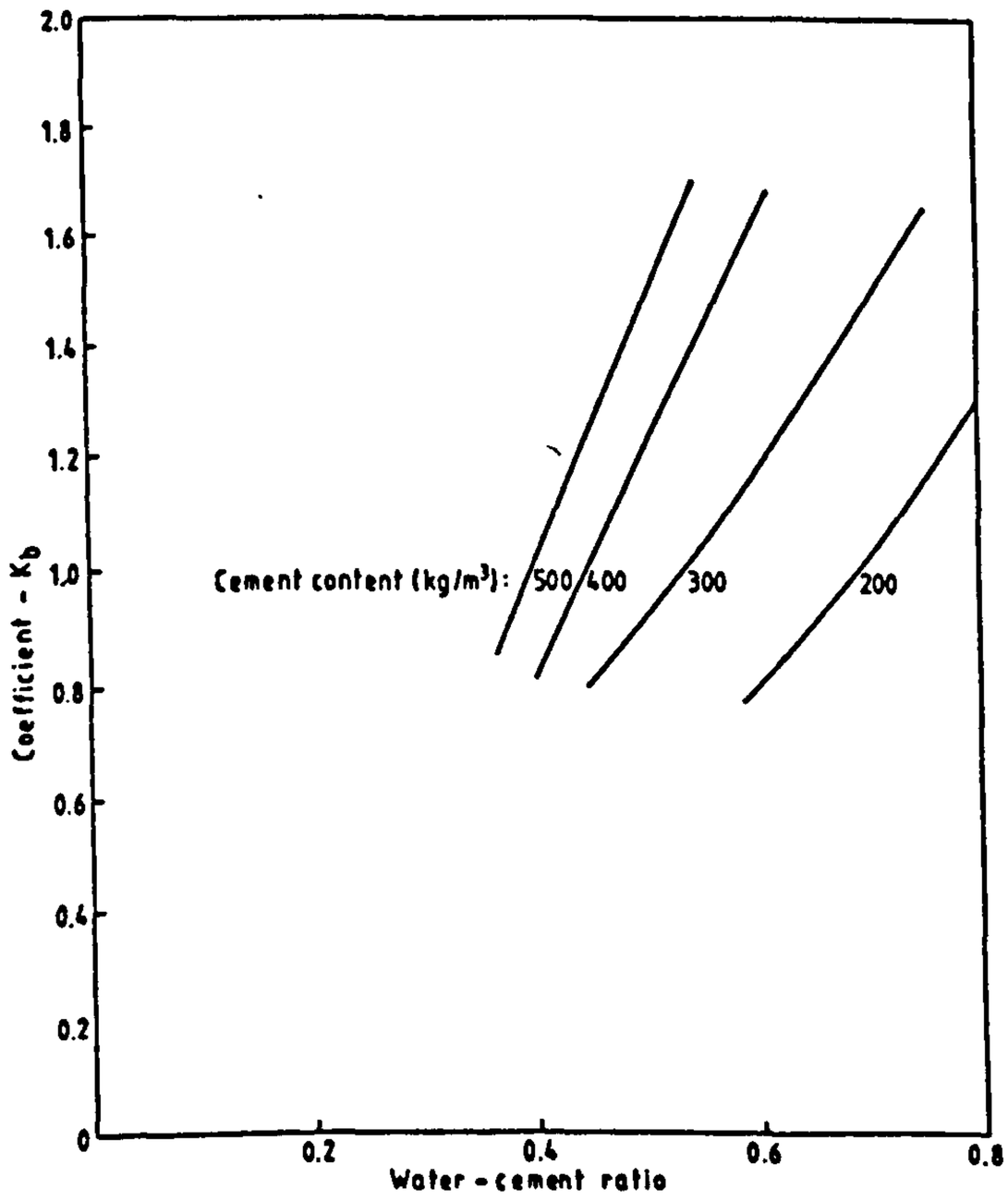

Fig. 4.1(c) CEB-1970 creep prediction: composition of concrete coefficient (K_b)

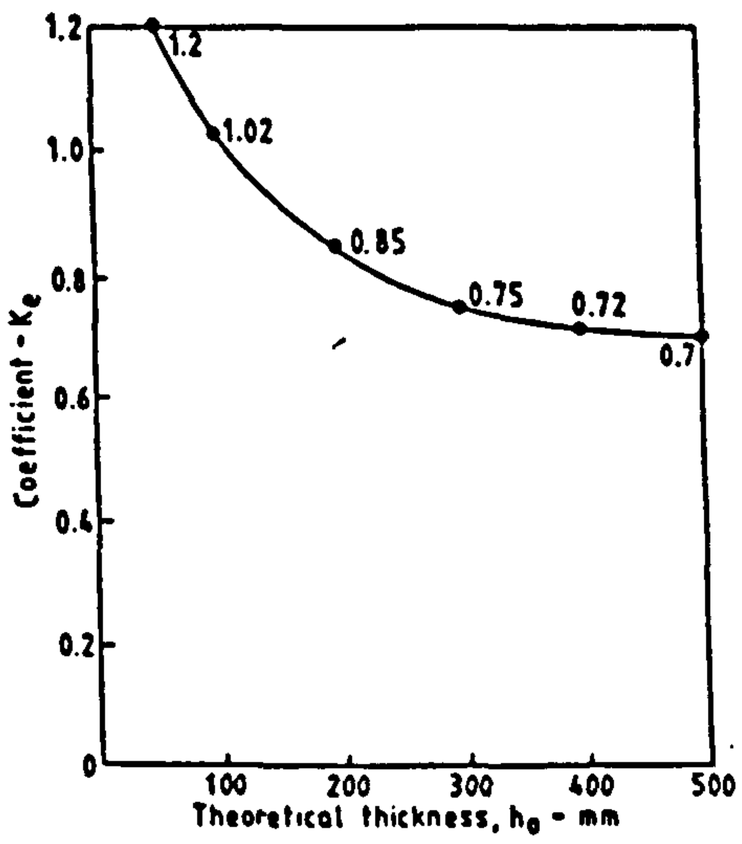

Fig. 4.1(d) CEB-1970 creep prediction: theoretical thickness coefficient (K_e)

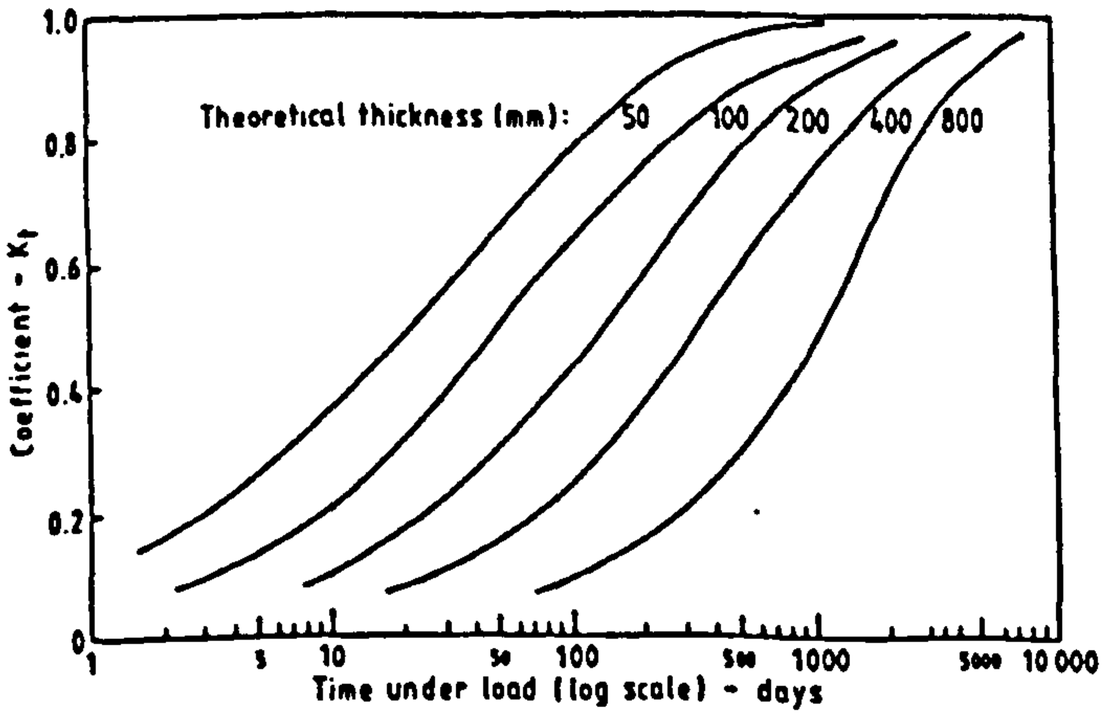

Fig. 4.1(e) CEB-1970 creep prediction: development of coefficient (K_f) with time

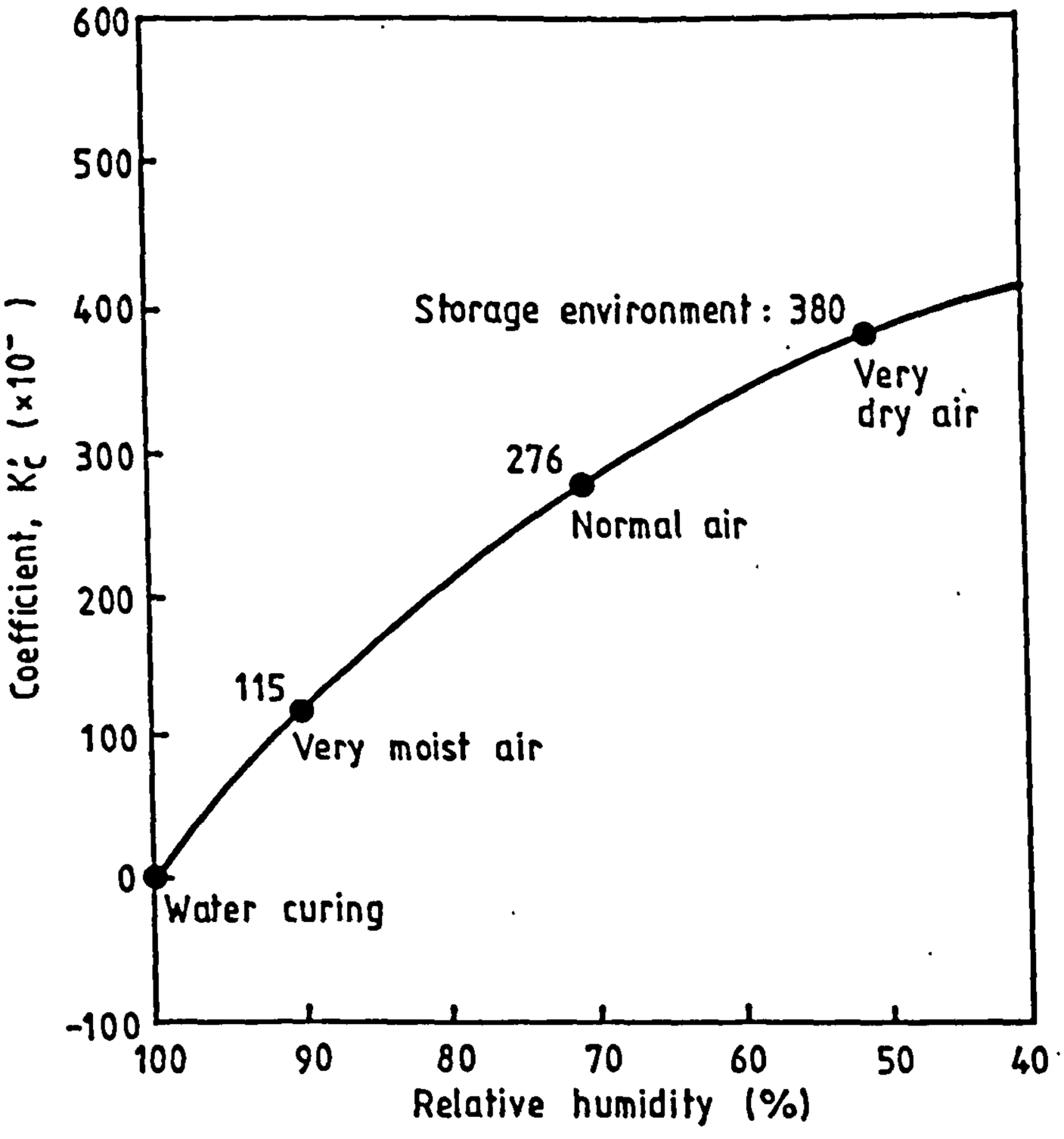

Fig. 4.2(a) CEB-1970 shrinkage prediction: ambient humidity coefficient (K'_c)

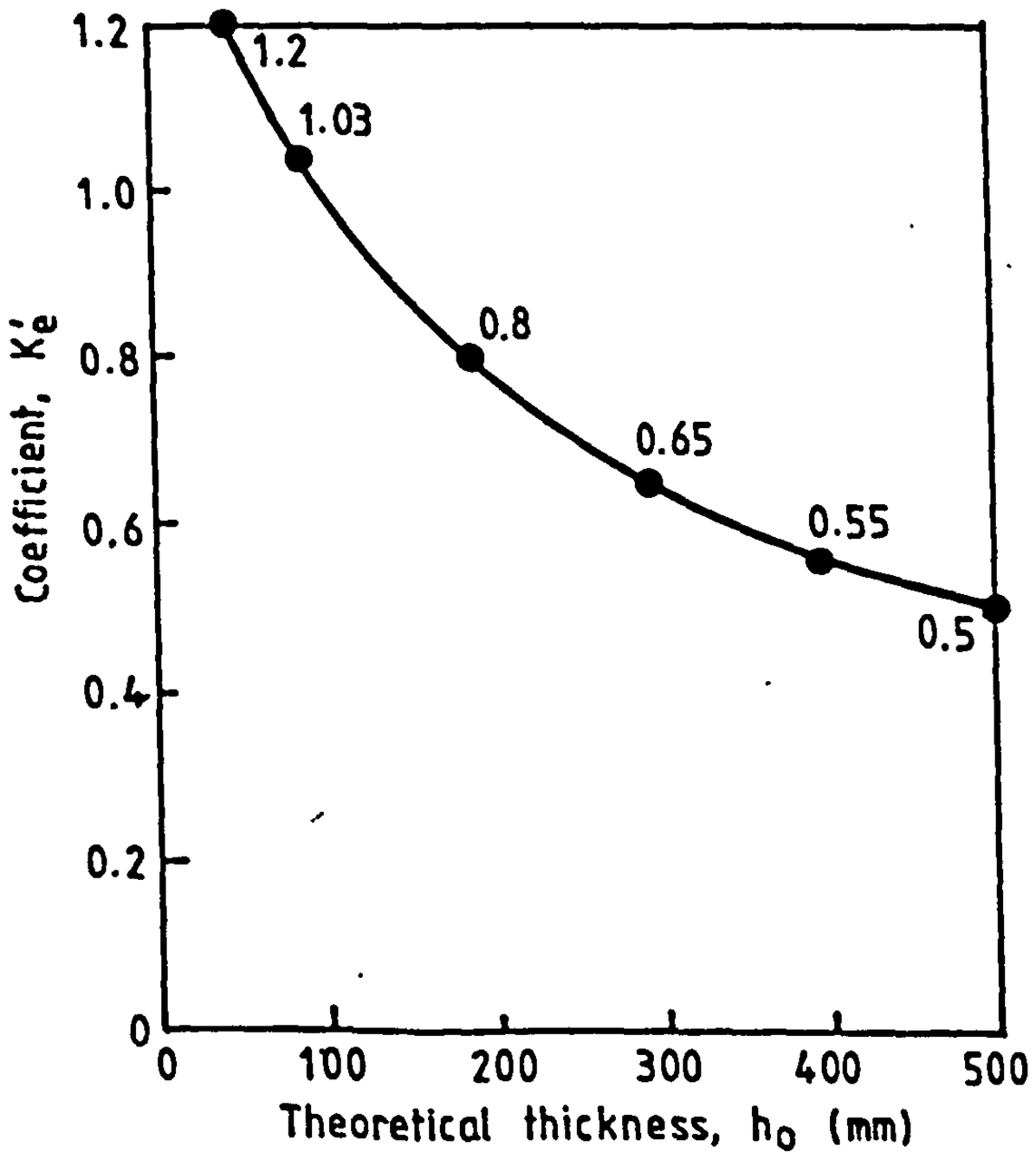

Fig. 4.2(b) CEB-1970 shrinkage prediction: theoretical thickness coefficient (K'_e)

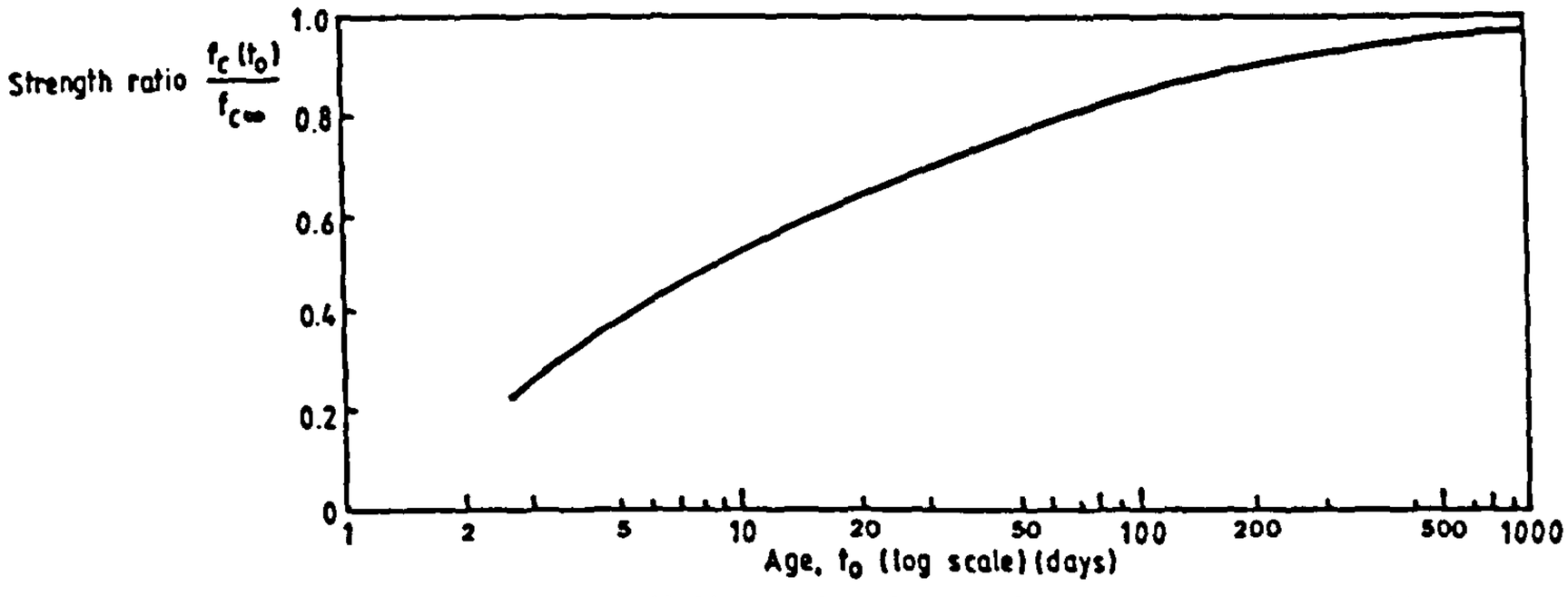

Fig. 4.3(a) CEB-1978 creep prediction: development of strength with time

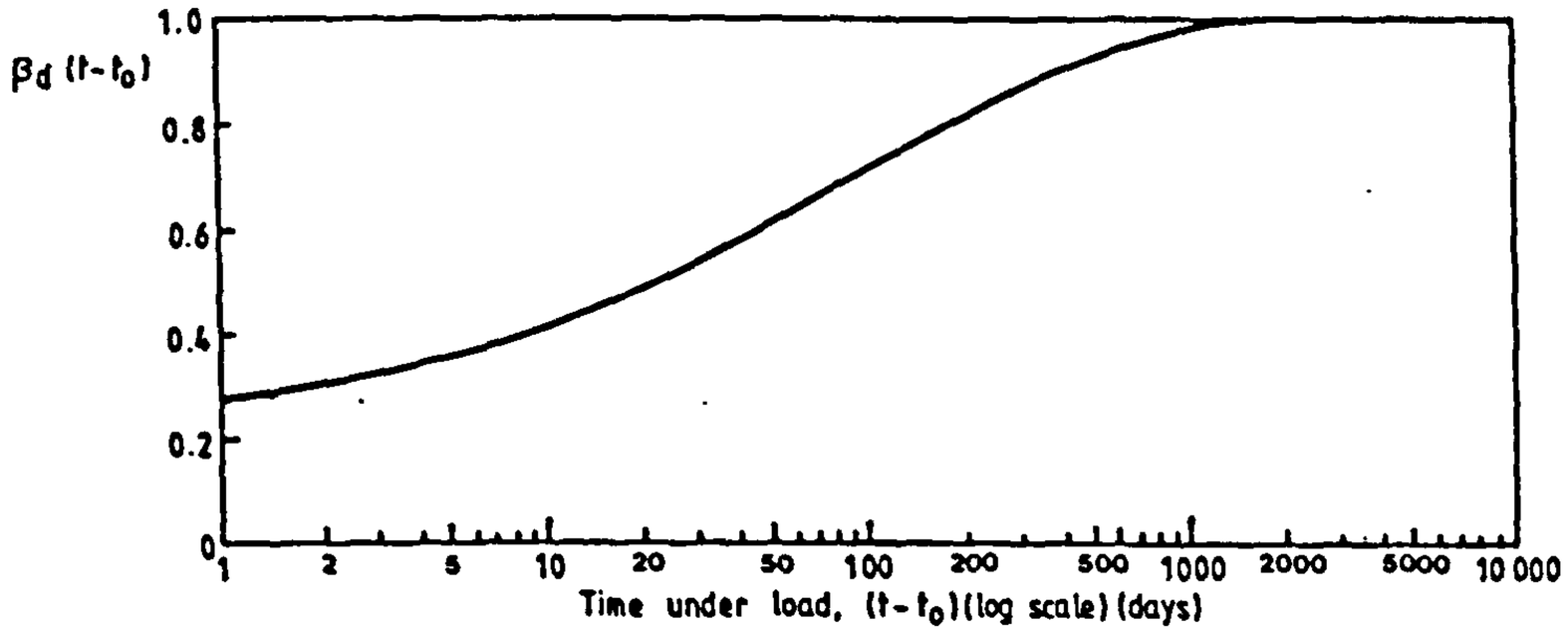

Fig. 4.3(b) CEB-1978 creep prediction: development of delayed elastic strain with time

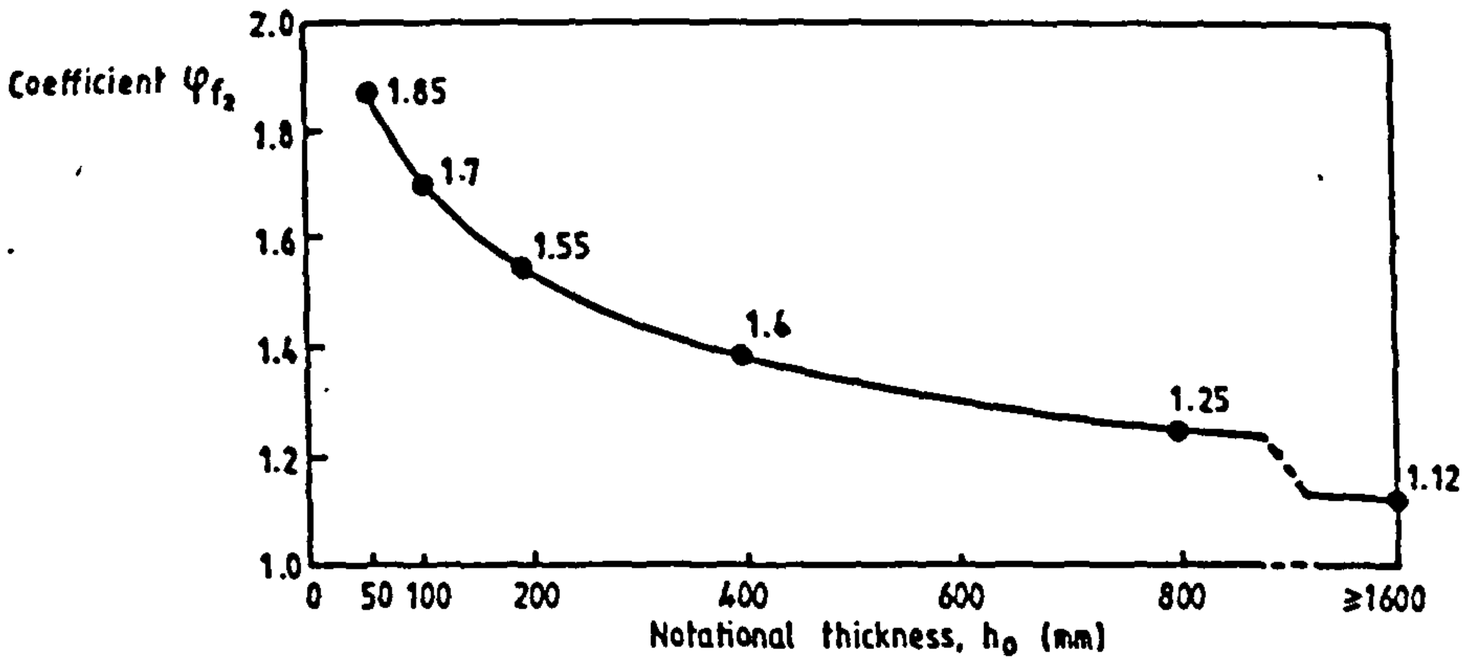

Fig. 4.3(c) CEB-1978 creep prediction: influence of notational thickness on creep

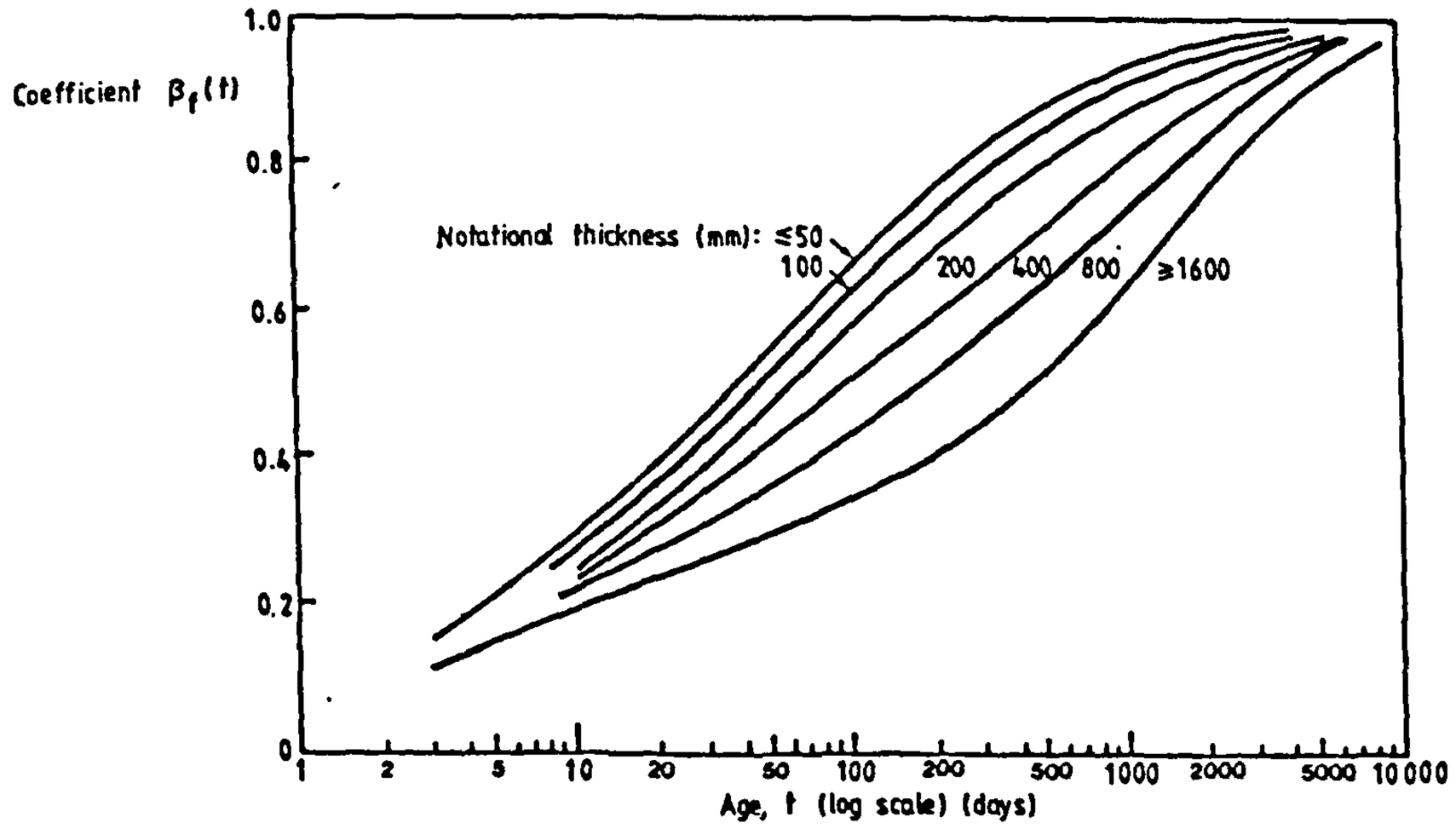

Fig. 4.3(d) CEB-1978 creep prediction: development of delayed plastic strain with time

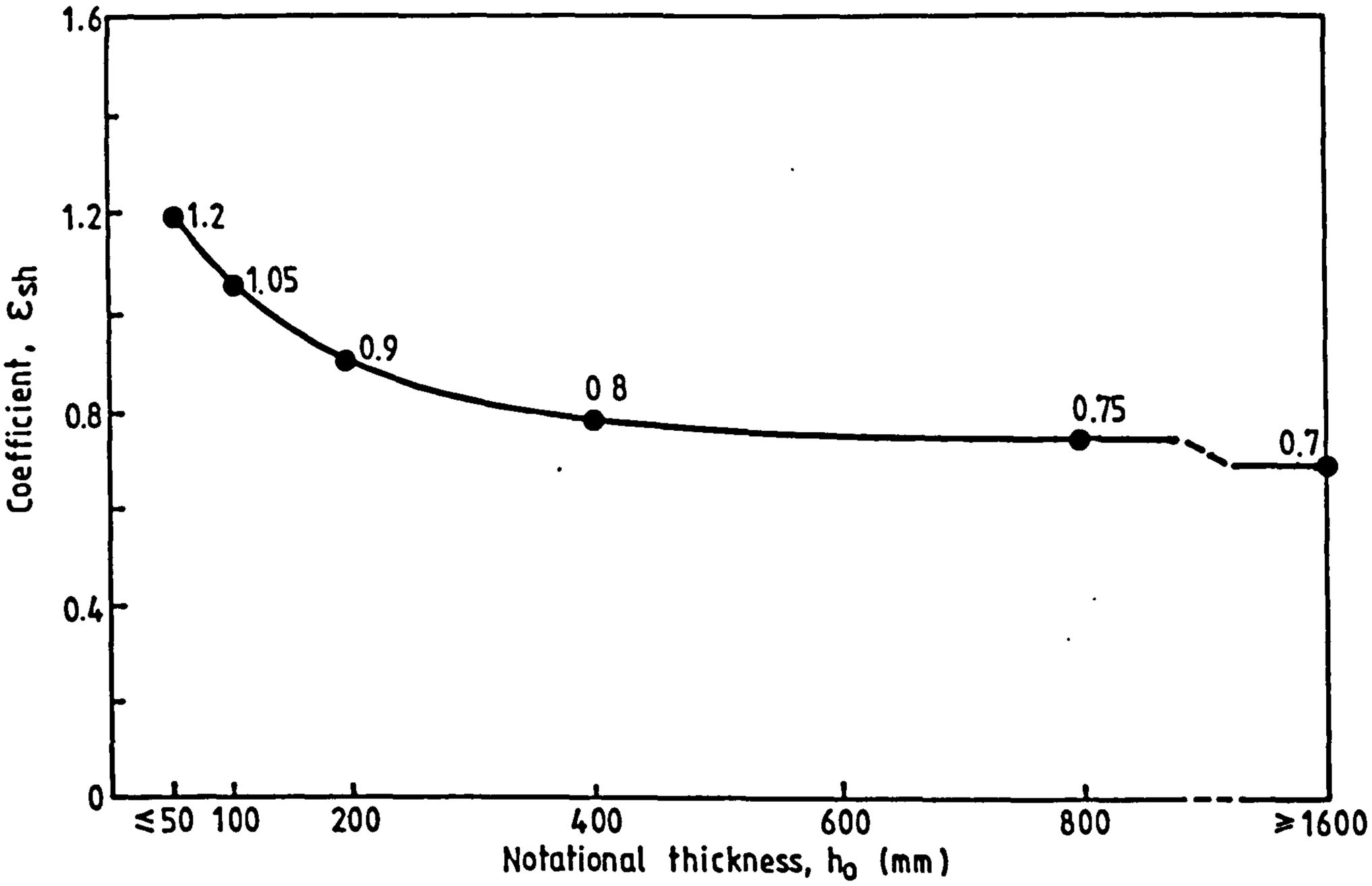

Fig. 4.4 (a) CEB-1978 shrinkage prediction: influence of notational thickness on shrinkage

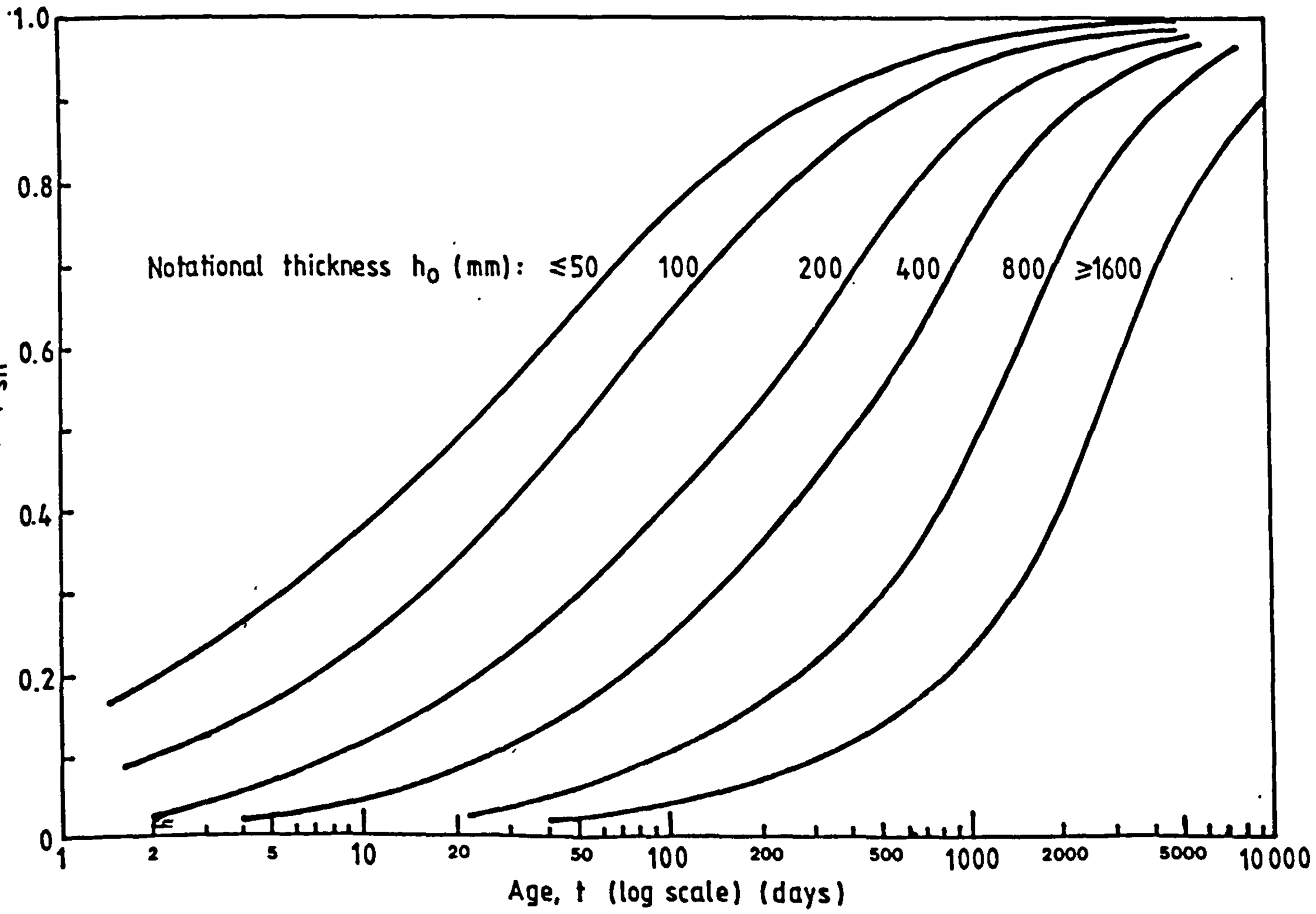

Fig. 4.4 (b) CEB-1978 shrinkage prediction: development of shrinkage with time

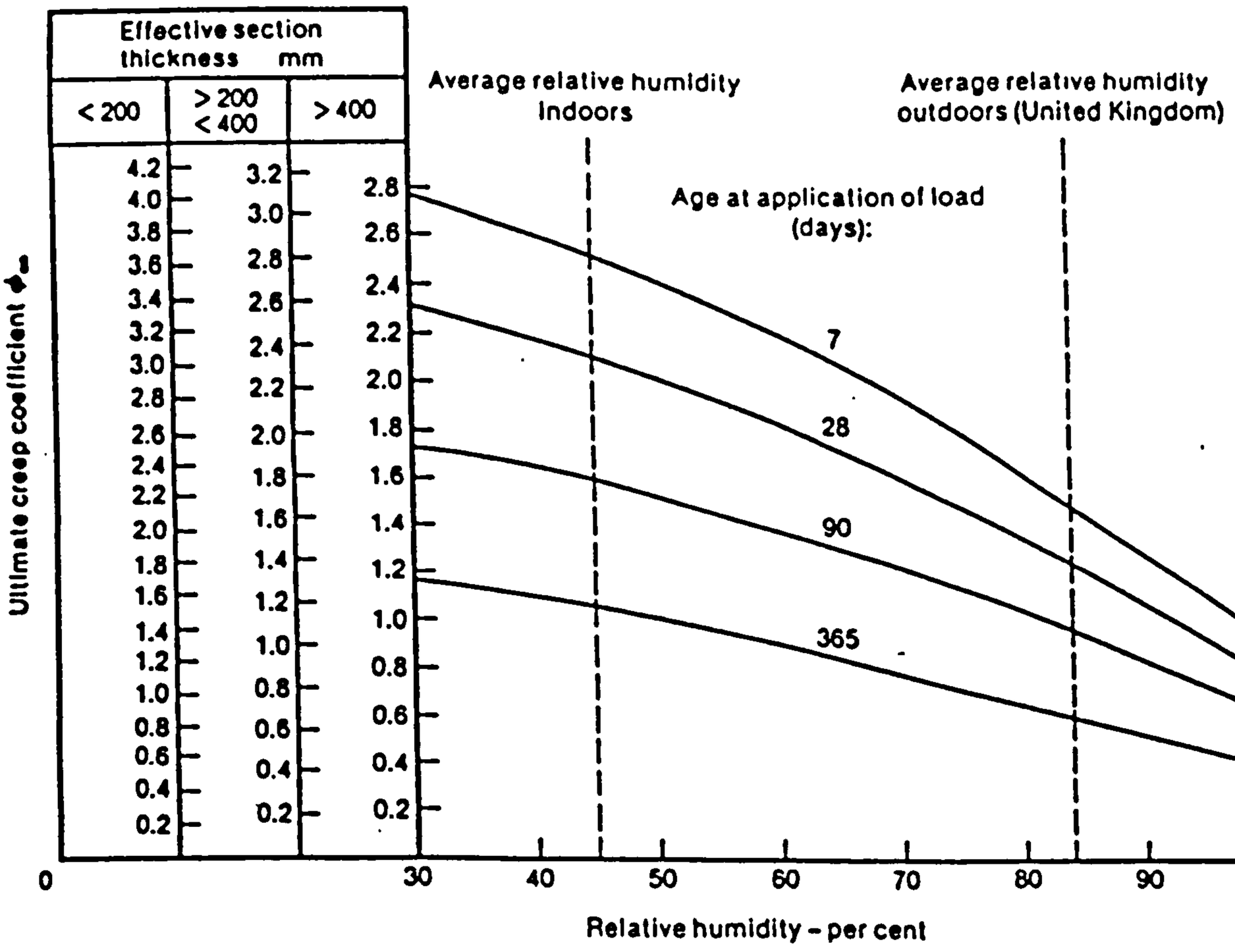

Fig 4.5(a) CS 1978 data for predicting ultimate creep coefficient

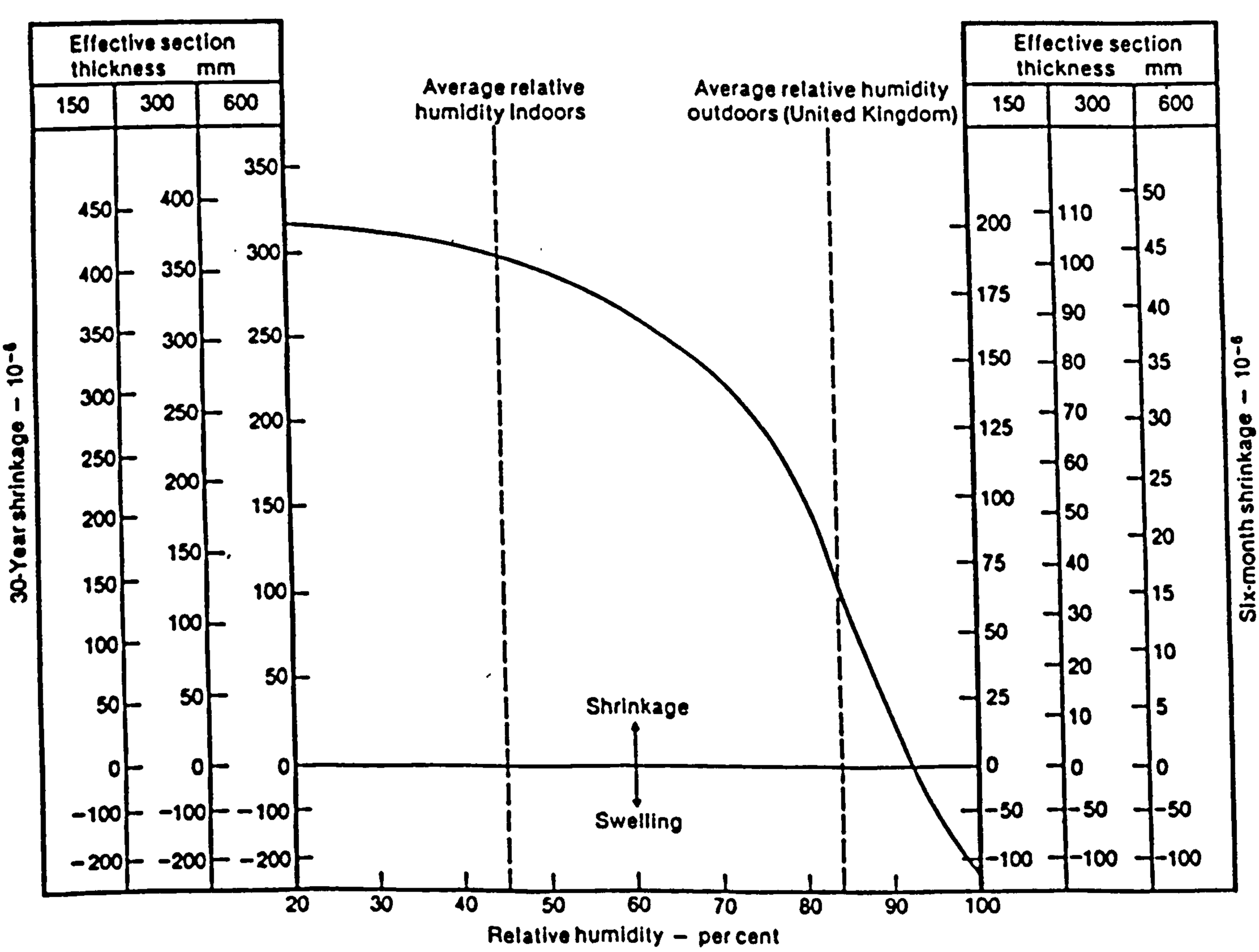

Fig. 4.5(b) Parrott's data for predicting shrinkage and swelling of high quality dense aggregate concrete

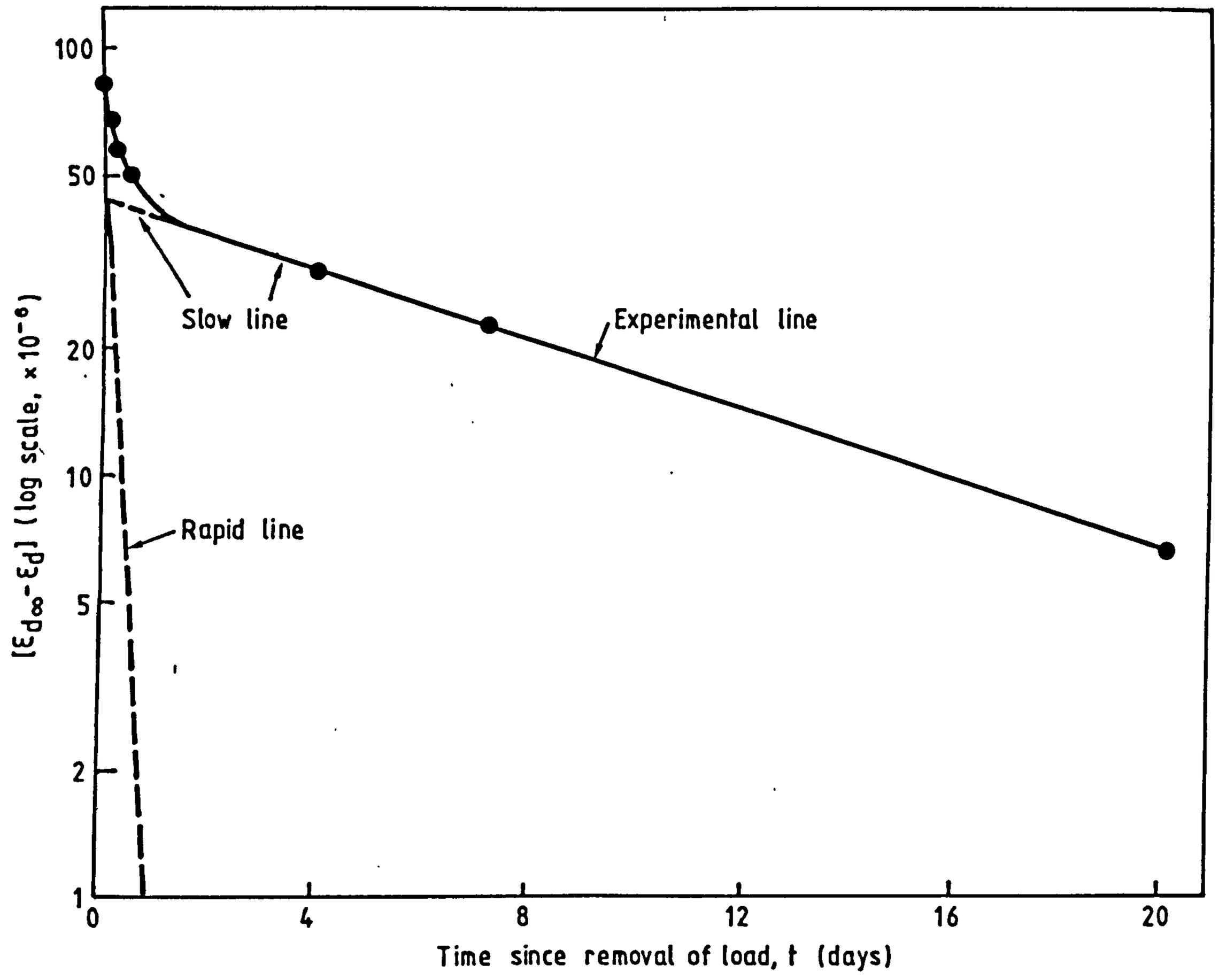

Fig. 4.6 Creep recovery curve plotted to a semi-logrithmic scale to obtain the rate parameters Q_1 and Q_2

$\varepsilon_{d\infty}$ = limiting value of delayed elastic strain or recovery; ε_d = delayed elastic strain or recovery at any time t since removal of load

CHAPTER 5 - AN EXPERIMENTAL INVESTIGATION OF FACTORS AFFECTING THE CREEP AND SHRINKAGE OF PRESTRESS CONCRETE MEMBERS

5.1 Introduction

This chapter investigates the factors affecting the behaviour of instantaneous and time-dependent deformation of various concrete mixes of different shapes and sizes stored in different environmental conditions.

A comprehensive study was conducted on the comparison between current prediction methods of creep and shrinkage and experimental results obtained.

5.2 Analysis and Discussion of Test Results

5.2.1 Compressive Strength

The development of compressive strength for various mixes are shown in Figures 5.1 and 5.2 and Table 5.1 which, in addition, shows mean cube density at various ages of testing. All concrete mixes had a similar workability and cement content of 5-12 mm slump and 420 kg/m^3, respectively, except for OPC mix which had a slightly higher workability of 30 mm slump and lower cement content of 340 kg/m^3. Fig.5.1 shows that large differences in strength are obtained at early ages for all concrete mixes but, as indicated in Fig. 5.2, the strengths tend to approach the same value at later ages, except for OPC mix strength which remained lower than the other mixes. The percentage increase in cube strength over

prestressing transfer strength is shown in Table 5.2. It is clear that the OPC mix stored in constant humidity condition has the lowest percentage increase of strength over a period of one year, while the OPC mix stored in the variable humidity condition has more or less the same values as the other concrete mixes at later ages. OPC concrete exposed to constant humidity is about 78 percent as strong at 12 months as OPC concrete continuously kept in variable humidity of drying and wetting. A similar pattern of behaviour is apparent when comparing the two humidity conditions of a RHPC concrete, whereas the concrete stored in constant humidity is about 95 percent as strong at 12 months as variable humidity one. It seems to be that drying and wetting cycles may lead to a higher strength in various concrete mixes, the extent of which probably depends on the degree of hydration at first exposure, because such an increase is minor with concrete having RHPC. These trends are more or less similar to those obtained by Price (84) for early age drying concrete ranging from 3-7 days.

The results of early compressive strength (Fig.5.1) show that, for age of 28 days, the compressive strength of RHPC/Admixture concrete (cured for 1 day) is greater than that of the plain RHPC concrete (cured for 2 days) by approximately 6 percent for constant humidity. Since the admixture concrete has a lower water-cement ratio, this concrete has a higher strength than the plain RHPC concrete when stored in constant humidity of 65 percent; after 365 days, the average difference is 3 percent and the percentage increase in compressive strength is nearly the same; a similar observation has been reported by Brooks et al. (38).

In comparison with RHPC concrete of similar workability, the effect of a combined influence of replacement of cement by PFA and reduced water content is a considerable decrease in strength at early ages but, after approximately 365 days, the strength between the two concretes is almost the same. This behaviour concurs with that known for mixtures of Portland cement and pozzolanic materials (85). As indicated in Table 5.2, the percentage increase of strength of RHPC/PFA concrete at 28 days is the lowest among all RHPC mixes, but is the highest after a period of one year; whereas this is attributed to a slower rate of hydration and, hence, a slower gain of strength over a long period of time.

A similar pattern of behaviour is apparent when comparing the two concretes containing PFA (RHPC/PFA and RHPC/Admixture & PFA) except that, because of a lower mixing water content, the level of strength of RHPC/Admixture & PFA is higher than the RHPC/PFA concrete. Compared with the plain RHPC and RHPC/Admixture mixes of similar workability, the addition of PFA as a part-replacement of cement produces lower early strength but, after approximately 180 days, the strength is higher than that of plain RHPC concrete and almost the same as that of RHPC/Admixture concrete; a similar observation has been reported by Brooks et al. (42). It can be seen from Table 5.1 and 5.2 that the addition of a superplasticiser to a RHPC/PFA mix is a compromise between the beneficial effect of the high-early strength RHPC/Admixture concrete and the low-early strength feature of RHPC/PFA concrete, as well as a compromise between the 28 to 365 days increase in strength of the RHPC/admixture and the RHPC/PFA concretes.

The comparison between the strength of 100 mm cubes and the strength of 76 x 267 mm cylinders is shown in Fig.5.3. The level of cube strength is greater than the level of 76 x 267 mm cylinder strength, an observation which is in accordance with previous observations (85, 86); the greater cube strength is caused by the restraining effect of the test machine platens whereas a part of the 76 x 267 mm cylinders is free from the restraining effect of the test machine platens due to the greater length-diameter ratio. Previous investigators report a slightly non-linear relation between cube and cylinder strength which is independent of storage environment and slightly dependent upon level of strength (85). Moreover, it should be noted that the general tendency is for strength to decrease with an increase in specimen size as the likelihood of an element of extremely low strength is greater in a larger specimen (85). However, the difference in volume of the cubes and the cylinders was small.

5.2.2 Static Modulus of Elasticity

The variation of static modulus of elasticity with age, using prisms stored under the same environmental conditions as the strength specimens, for early-age and one year age are shown in Figures 5.4 and 5.5, respectively. It can be seen that the early-age and one year age development have a similar pattern of behaviour to the develpment of compressive strength. Also, when comparing the effect of wetting and drying on the elastic modulus, it seems to be that the variable humidity increases the static modulus throughout the one year testing period. This point is pursued in Table 5.1 and

5.3, from which it is determined that, at 365 days, the modulus of elasticity of variable humidity is 10 and 8 percent higher than modulus of elasticity at constant humidity for OPC and RHPC mixes, respectively. These trends are similar to those obtained by Davis and Troxell (87) and Ghali et al. (1) for concrete stored in wet and dry environments.

Figure 5.5 presents the one year relation between all concrete mixes stored in constant humidity. It can be seen that the OPC mix seen to give the lowest static modulus, while the mixes containing PFA show a higher increase in elastic modulus with age than plain RHPC and OPC mixes, especially when a superplasticizer is used. As it is shown in Fig.5.5, the RHPC/Admixture & PFA mix gives the highest static modulus after a period of one year. Thus, it appears that part-replacement of cement by PFA, with or without a superplasticizer, influences static modulus of elasticity in the same manner as compressive strength. The explanation of the PFA mixes behaviour probably lies in retardation of the slow pozzolanic activity because water is removed in the process of drying, an effect which would impair the development of static modulus of elasticity (42).

The relation between the static modulus of elasticity and cube compressive strength for various concrete mixes stored in constant environment is shown in Fig. 5.6. It can be seen that at later ages the modulus of elasticity increases more rapidly than strength, especially with concrete mix having OPC. In Fig. 5.7, the relation between modulus of elasticity and strength for OPC and RHPC

mixes exposed to different environmental conditions indicates that the wetting and drying cycle has slightly higher rate of increase of elastic modulus to strength than constant humidity condition. A comparison between measured and predicted elastic modulus values is fully discussed in Section 5.3.1.

5.2.3 Creep and Shrinkage

5.2.3.1 Influence of Concrete Mix and Characteristics of Materials on Creep and Shrinkage

The shrinkage and creep characteristics of the cylinder specimens of the five types of concrete, and stored in constant environment are shown in Fig. 5.8 and 5.9. In addition, the creep slope coefficients for all concrete mixes are presented in Table 5.4. It can be seen that OPC concrete mix exhibits a higher creep and shrinkage deformations than RHPC concrete mix in spite of the lower cement paste content of the OPC mix. This behaviour is thought to be associated with the water/cement ratio of the OPC concrete mix which is higher than one of RHPC concrete mix. Also it has been observed by many investigators that mixes having OPC always exhibit a higher creep and shrinkage than mixes having RHPC (34, 33).

As for RHPC concrete mixes, the admixture concrete has a slightly greater creep and shrinkage in spite of having a lower water-cement ratio than the plain RHPC concrete. These trends are similar to those obtained by Brooks et al. (38). In admixture-free mixes, a decrease in the water-cement ratio leads to less creep and

shrinkage but when admixtures are used to produce water-reduced concrete and flowing concrete an increase in creep and shrinkage sometimes occurs (88, 89, 90). Compared with RHPC concrete mix with and without admixture, creep and shrinkage are reduced by the use of PFA and, more so, by a combination of admixture and PFA. Figure 5.8 shows that after 365 days, the shrinkage of RHPC/PFA concrete mix was 6% and 18% lower than mixes having plain RHPC and RHPC/Admixture concrete mixes, respectively. Moreover, with the RHPC/Admixture & PFA concrete mix, the shrinkage deformation was reduced to a greater extent, i.e. the shrinkage was 14% and 27% lower than the shrinkage of plain RHPC and RHPC/Admixture concretes, respectively. Consequently, the observations on shrinkage are generally as expected and confirm those observed previously using fly ash (91, 92, 42). Figure 5.9 shows that the creep of the RHPC/PFA and RHPC/Admixture & PFA concretes is almost the same, and about 27% and 43% lower than plain RHPC and RHPC/Admixture concretes, respectively. Furthermore, the total deformations (elastic plus creep plus shrinkage) of all concrete mixes are shown in Fig. 5.10. It seems to be that the combination of PFA and superplasticizing admixture with RHPC appears to give a beneficial effect of high long-term strength, coupled with low shrinkage and creep.

5.2.3.2 Influence of Environmental Condition and Size and Shape of Members on Creep and Shrinkage

A comparison is made in Fig. 5.11 of the shrinkage of the cylindrical specimens and that of the I-shaped beam specimens stored

in constant environment for a period of one year after loading. For specimens of equal volume/surface ratio, the shrinkage values after one year for I-shaped specimens having OPC, RHPC, RHPC/Admixture, RHPC/PFA and RHPC/Admixture & PFA are 15, 11, 16, 11 and 3 percent less than the shrinkage values of the cylinders. In the case of shrinkage values of rectangular shaped beam in comparison with cylinder of the same volume/surface ratio, a similar trends were obtained as previously described for the I-beam and cylinder specimens relation. These trends are similar to those obtained by many investigators (35, 24). According to Hansen and Mattock (24) findings, the rate and the final values of shrinkage and creep decrease as the member becomes larger. In view of this, the volume/surface ratio does not account perfectly for variation of both size and shape (24).

Table 5.5 and Figures 5.12 to 5.16 show the variation of shrinkage and swelling deformations of different concrete mixes, shapes and environmental conditions. It can be seen from Table 5.5 that the shrinkage of an I-shaped beam of a 21.8 mm volume/surface ratio is always higher than the shrinkage of rectangular beam of a 31.4 mm volume/surface ratio for different mixes and environmental conditions, which is in accordance to previous findings of size effects (22, 24, 93). As illustrated in Fig. 5.12, the effect of wetting and drying for different concrete mixes and shapes using cylindrical specimens has decreased the shrinkage deformation to a slightly greater than half the shrinkage of the constant environment. These trends are similar to those obtained by Bryant (94) and El-Shafey (93). Bryant (94) in his findings indicated that

the average shrinkage values of specimens kept in the outdoor environment of 80% average relative humidity are 50 to 35 percent lower than the shrinkage of specimens stored in constant environment of 67% relative humidity, while Gamble (19) presented a much lower shrinkage value for outdoor environment than constant environment. Figure 5.12 also indicates that, after one year since loading, the differences between the shrinkage values of the cylindrical specimens having different volume/surface ratios and different mix properties for the variable environmental condition are insignificant, while the swelling values of the RHPC concrete mix is twice as high as the OPC concrete mix.

The effects of shape and size and environmental condition upon creep are shown in Table 5.6 and Figures 5.17 and 5.18. From Table 5.6, it is clear that the creep for the I-shaped beams exhibits a higher value of creep than rectangular shaped beams kept in different environmental conditions. Furthermore, the difference in creep between the rectangular and I-shaped beams kept in variable environment is approximately twice the difference in creep of beams kept in constant environment (approximately 31 percent for variable environment and 16 percent for constant environment). Moreover, it should be noted that the creep of specimens stored in variable environmental conditions are 28 and 40 percent lower than creep of constant environment for an I and rectangular shapes respectively. In view of this, it can be seen that for different environmental conditions, the behaviour of creep and shrinkage is effected by the shape and size of members, this effect influencing creep more than shrinkage.

5.3 Comparison between Experimental Results and Current Prediction Methods

Various standard methods of predicting instantaneous and time-dependent concrete strains are compared with each other and with experimental data obtained from this investigation in Table 5.7 to 5.12 and Figures 5.19 to 5.27. Details of the five standard methods used are given in Chapter 4. In their basic forms, these methods only require a knowledge of strength, mix composition and physical operating conditions in order to predict time-dependent strains. It can be seen from Table 5.7 to 5.10, that two kinds of estimating procedures are adopted, i.e. using strength and mix composition, and using a known modulus of elasticity. However, the comparisons between predicted and experimental data are mainly based on the known strength and mix composition procedure, as shown in Figures 5.19 to 5.27 and Tables 5.7 to 5.12. For practical purposes it should be noted that the one-year shrinkage and creep values of the Concrete Society and BS8110 method were obtained from an assumed log-log linear relationship between shrinkage or creep and times of 180 days and 30 years, whilst the early-age values of the shrinkage and creep were obtained from the slope line between the 180 and 365 days experimental and Concrete Society values.

In the following sections, the comparison between the experimental and predicted instantaneous and time-dependent strains are presented for different shapes and sizes of members, environmental conditions and concrete mixes. Furthermore, an attempt was made to relate time-dependent deformations between

predicted and experimental values, based on the slope coefficient of regression line of predicted-to-measured ratio. The correlations were obtained in terms of the coefficient of variance which is shown in parenthesis in Tables 5.11 and 5.12. It should be noted that the comparison between predicted and experimental results is limited for concrete mixes of plain ordinary and rapid hardening Portland cement, since the current prediction methods do not consider concrete mixes having PFA and admixtures.

5.3.1 Elastic Strain

The experimental and predicted elastic strains at loading for ordinary and rapid hardening Portland cement mixes are illustrated in Tables 5.7-5.10. It is evident that the predicted instantaneous elastic strains of the ACI and the CS & BS8110 prediction methods are very close to the experimental elastic strain at loading, whereas the predicted elastic strains of the other prediction methods lie within 25 percent of the experimental elastic strain. It can be concluded that all prediction methods give a good estimation of the elastic strains at loading.

5.3.2 Shrinkage and Swelling

The comparison between the experimental and predicted shrinkage of concrete specimens having different volume/surface ratios and concrete mixes and stored in different environmental conditions are shown in Figures 5.19-5.26 and Tables 5.7-5.12 as indicated previously. It can be seen that the predicted shrinkage

strains of the ACI method gives more or less the same values of the experimental shrinkage of specimens stored in constant environment, having a slope coefficients ranging from 1.09-0.85 as shown in Tables 5.11 and 5.12, these observations essentially agree with those of Bryant (94). On the other hand, all other prediction methods considerably underestimate the experimental shrinkage by 41-68 percent, the CS & BS8110 method exhibiting the highest underestimations of 68 percent.

For the case of predicted shrinkage strains of variable environment of a wetting and drying cycle, all prediction methods generally underestimate the experimental values by 10 to 63 percent of the experimental shrinkage, while the ACI method overestimates shrinkage up to a limit up to 82 percent. These trends are similar to those obtained by EL-Shafey (93) and Bryant (94) for concrete specimens stored in variable environment. In view of this, it can be seen that none of the current prediction methods estimates shrinkage of variable environment properly.

Of the five methods available, the CEB70 and ACI methods give no consideration for prediction of swelling. According to Tables 5.7 and 5.9, for RHPC concrete mix, the CS & BS8110 exhibits the best swelling estimation which is within 8 percent of the experimental swelling, whereas for OPC concrete mix the CS & BS8110 method considerably overestimates the swelling. In the case of OPC concrete mix, the BaP method seems to give similar values as the experimental swelling as shown in Tables 5.8 and 5.10, but for RHPC concrete mix, the BaP method underestimates the swelling by 40

percent. It may also be noted that the CEB78 method always underestimates the swelling for both OPC and RHPC concrete mixes.

5.3.3 Basic and Total Creep

The comparison of basic creep and total creep between the experimental and prediction methods of concrete specimens having different volume/surface ratios and concrete mixes and stored in different environmental conditions are illustrated in Figures 5.19 to 5.27 and Tables 5.7 to 5.12.

In the case of basic creep, it can be seen that the CEB78 method exhibits a very close estimate to the measured basic creep, whereas the other prediction methods overestimate basic creep considerably, especially the BaP, Concrete Society and ACI prediction methods. Furthermore, when estimation is based on the known elastic modulus, the overestimations of basic creep are slightly lower than the estimation based on the strength and mix composition.

Considering predicted total creep of concrete specimens stored in constant environment, it is evident that the ACI and CEB78 methods give the best results which lie within 23 percent of the measured total creep, with a slope coefficients ranging from 0.77 to 1.12 as shown in Tables 5.11 and 5.12. Figure 5.27 illustrates a typical linear relation between measured creep and predicted creep. It can be seen that all the other prediction methods generally overestimate the total measured creep by up to 121 percent. It

should also be noted that the BaP and CS methods exhibited the highest overestimation of 121 percent for RHPC concrete and 31 percent for OPC concrete, whereas for OPC concrete of an I-shape volume/surface ratio the values of both methods are very close to the experimental values obtained. In view of this, it can be seen that for both the BaP and CS methods, the degree of overestimation is considerably lower for OPC concrete specimens loaded at the age of 7 days than that of RHPC concrete specimens loaded at the age of 2 days.

The predicted total creep of concrete specimens stored in variable environment of wetting and drying cycle seem to exhibit more or less the same trends of the predicted total creep stored in constant environment. Therefore, the ACI and CEB78 methods give the best predictions which lie within 24 percent of the measured total creep; these observations essentially agree with those observed by Bryant (94) for concrete specimens stored in variable environment. However, it should be noted that both methods slightly overestimate the measured total creep of RHPC concrete specimens having the volume/surface ratio of the rectangular beam. Furthermore, all the other prediction methods generally overestimate total creep by up to 213 percent.

Finally, it should be mentioned that the use of known elastic modulus seem to be slightly beneficial for the prediction methods with the exception of the CEB70 and CEB78 methods. However, such a small difference between the estimated values using a known elastic modulus and those using a known strength and mix composition is not significant.

5.3.4 Total Time-Dependent Deformations

The predicted total time-dependent deformations of concrete specimens of various concrete mixes and beam shapes and sizes stored in constant environment are shown in Tables 5.7 to 5.12 and Figures 5.19 to 5.26. It is evident that the ACI, CEB70 and BaP methods give a very close estimates when compared with the experimental values in spite of the low shrinkage and high creep values obtained by the CEB70 and BaP methods. Whilst the CEB78 and CS & BS8110 methods generally underestimate the time-dependent strains of OPC concrete with a percentage variation up to 50 percent, it must be pointed out that the CS & BS8110 gives a very close estimated result for RHPC concrete specimens.

In the case of predicted values of concrete specimens stored in a variable environment of a wetting and drying cycle, all prediction methods give reasonable estimates, with slope coefficients ranging from 0.608 to 1.32; however, it should be noted that, for RHPC concrete specimens, both the ACI and BaP methods overestimate measured values by 47 to 72 percent. It should be remarked that in spite of the substantial differences in creep and shrinkage estimates of most prediction methods, the same methods seem to give a fair estimation of the total time-dependent deformations of specimens stored in variable environment.

Generally speaking, it can be concluded that for both environmental conditions adopted in this investigation, the CEB70 followed by the ACI and BaP methods give more or less the best predictions.

5.4 Conclusions

The factors affecting the strength, static modulus of elasticity, creep and shrinkage of various concrete mixes stored in different environments have been described in this chapter.

The concrete mixes having RHPC exhibit a large difference in strength at early ages which tend to approach the same values at later ages, whereas the OPC concrete mix tends to give a lower concrete strength. The addition of the superplasticising admixture to concrete provides an excellent means of increasing the early-age strength. However at later ages the percentage increase in cube compressive strength over transfer strength is the same as the plain RHPC concrete of a similar workability, this confirms observations reported by Brooks et al. (38). The effect of a combined influence of 30 percent replacement of RHPC by PFA and reduced water content decreased the strength at early ages considerably compared with the RHPC concrete. Whereas the strength after one year is the same for both concrete mixes, this generally concurring with that obtained by previous investigators (85). Moreover, the combination of PFA and superplasticizing admixture produces a concrete strength higher than all concretes after a period of one year. Therefore, it was concluded that the addition of a superplasticizer to a RHPC/PFA mix is a compromise between beneficial effect of the high-early strength of admixture concrete and low-early strength feature of PFA concrete.

For concrete mixes stored in different environmental

conditions, the wetting and drying cycle tends to exhibit a higher development of strength with time than concrete stored in constant environment, especially with OPC concrete. On the other hand, the difference in RHPC concrete strength for different environments seem to be insignificant.

The variation of static modulus of elasticity of various concrete mixes with age, stored under the same conditions as strength shows a similar pattern of behaviour to the development of compressive strength; at later ages the modulus of elasticity increases more rapidly than compressive strength of concrete.

The composition of concrete and the characteristics of materials greatly influence the behaviour of creep and shrinkage. The OPC concrete exhibits a higher creep and shrinkage than RHPC concrete in spite of the lower cement paste content of the OPC concrete, these observations are similar to those found by previous investigators (33, 34, 35). The use of a superplasticizing admixture increases the creep and shrinkage in spite of high early age strength and lower water/cement ratio than RHPC control concrete. Compared with RHPC concrete with and without admixture, creep and shrinkage are reduced by the use of PFA and, more so, by a combination of admixture and PFA. The one year values of shrinkage of RHPC/PFA concrete were 6% and 18% lower than plain RHPC and RHPC/Admixture concrete, respectively. Moreover, when using the RHPC/Admixture & PFA concrete, the shrinkage was reduced to a greater extent, i.e. the shrinkage was 14% and 27% lower than the shrinkage of plain RHPC and RHPC/Admixture concrete, respectively.

Similar, but bigger trends were observed for creep of PFA concrete when compared with RHPC and RHPC/Admixture concretes. The creep of both PFA concrete mixes is almost the same, and about 27 and 43 percent lower than plain RHPC and RHPC/Admixture concretes, respectively. It can be concluded that the combination of PFA and superplasticizing admixture with RHPC give beneficial effects of high early-age and long-term strength, coupled with low shrinkage and creep, such behaviour being of benefit in prestressed concrete applications.

The environmental conditions and size and shape of members are considerable in influencing the creep and shrinkage behaviour of prestressed concrete elements. When comparing the shrinkage development for all concrete mixes of full size rectangular and I-shaped beams with cylindrical specimens of the same volume/surface ratio stored in different environmental conditions, the shrinkage of full size beams seem to exhibit lower shrinkage values than cylindrical specimens by up to 16 percent. Moreover, when comparing the shrinkage of different shapes of beam having different volume/surface ratios, the I-shaped beam of a lower volume/surface ratio always exhibit a higher shrinkage value than the rectangular beam of a higher volume/surface ratio as found by previous investigators (24, 22, 93).

For different concrete mixes and beam shapes, the effect of variable humidity decreases shrinkage by slightly greater than half the shrinkage of the constant environment. Moreover, after one year since loading, the difference between shrinkage of the

cylindrical specimens in the variable environment condition seem to be insignificant, whilst in a saturated state swelling of the RHPC concrete is twice as high as the OPC concrete.

A similar pattern of behaviour has been observed for creep of specimens stored in the variable environment, which is 28 and 40 percent lower than creep in a constant environment for cylindrical specimen having volume/surface ratios equivalent to the I and rectangular sections, respectively. Moreover, creep of an equivalent I-section cylinder is greater than creep of equivalent rectangular section cylinders kept in constant and variable environmental conditions. Furthermore, the differences in creep between cylinders having equivalent volume/surface ratios of both shapes of beam kept in variable environment is approximately twice the difference of the creep values of cylinders kept in constant environment.

A substantial difference has been found between predicted and measured creep and shrinkage of specimens stored in different environments, although some methods give better predictions than others.

For the instantaneous elastic strain, the ACI and CS & BS8110 methods give a very close result to the experimental value, whereas the other prediction methods give a conservative estimation within 25 percent of the experimental results.

For shrinkage specimens of different volume/surface ratios stored in a constant environment, the predicted shrinkage by the ACI

method is more or less the same as the experimental shrinkage with a slope coefficient ranging from 1.09-0.85. Other prediction methods can considerably underestimate shrinkage by 41-68 percent, especially the CS & BS8110 method which underestimates shrinkage by 68 percent.

For a variable environment, assuming an average relative humidity, most prediction methods underestimate the experimental values by 10 to 63 percent. However, the ACI method overestimates shrinkage by 82 percent; these observations confirm findings obtained by previous investigators (93, 94). It is therefore concluded that no current prediction method can precisely give a conservative estimation of shrinkage deformation of a variable environmental cycle.

For swelling, CS & BS8110 and BaP methods give the best estimation for RHPC and OPC concrete, respectively, whilst the CEB-78 method underestimates swelling for both concrete mixes.

In the case of prediction of basic creep, the CEB-78 method gives the best estimation, whereas the other methods overestimate basic creep considerably. For a known elastic modulus, the overestimations are slightly lower than those using strength and mix composition.

For total creep in a constant environment, it is evident that the ACI method followed by CEB-78 method give the best predictions, viz. within 23 percent of the measured total creep with

a slope coefficient ranging from 0.77 to 1.12. All the other prediction methods generally overestimate total creep. Similar trends have been observed for specimens stored in the variable environment, in which the ACI and CEB-78 methods give the best predicted results (within 24 percent). With all methods, a constant average relative humidity is assumed, except that of BaP II. Other prediction methods generally overestimate the total creep by up to 213 percent. Furthermore, the recent method of Bazant et al. (67) which is considered to be the only method that can deal with cyclic humidity effect seems to overestimate the creep considerably. Using a known elastic modulus, predictions are improved for most methods, the exceptions being the CEB-70 and CEB-78 methods.

When the total strains are considered in a constant environment, the ACI, CEB-70 and BaP methods give the best values, in spite of the low shrinkage and high creep values obtained by the CEB-70 and BaP methods, whilst the CEB-78 and CS & BS8110 methods generally underestimate measured values by 50 percent. In the case of specimens stored in variable environment, it is surprising to find that all prediction methods give a very close estimate, with a slope coefficient ranging from 0.608 to 1.32.

However, while a method may be regarded as satisfactory if the total strain is predicted accurately there remains some doubt with that method if the components of total strain, i.e. elastic creep and shrinkage are <u>not</u> predicted accurately.

Generally speaking, it can be concluded that for both

environmental conditions used in this investigation, the ACI method gives the best overall estimation of time-dependent deformations.

Table 5.1 - Development of compressive strength and static modulus of elasticity

Mix Reference	Type of Humidity	Age (days)	Cube Compressive Strength (MPa)	Cube Density (kg/m^3)	Cylinder Compressive Strength (MPa)	Static Modulus of Elasticity (GPa)
OPC	Constant	At Transfer(7)	46.5	2416	34.2	31.3
		28	56.2	2405	41.4	34.8
		90	58.6	2381	-	36.6
		180	59.7	2388	-	37.2
		365	61.2	2380	46.3	37.6
	Variable	28	59.2	2413	41.9	36.8
		90	68.2	2396	-	38.5
		180	72.2	2408	-	40.5
		365	78.4	2395	53.6	41.2
RHPC	Constant	At Transfer(2)	49.4	2423	34.0	34.2
		28	75.1	2416	45.2	40.2
		90	80.2	2407	-	41.5
		180	82.3	2422	-	42.2
		365	84.9	2416	55.9	42.6
	Variable	28	78.1	2436	53.9	41.9
		90	82.4	2516	-	42.3
		180	86.5	2425	-	45.3
		365	89.3	2412	61.8	45.9
RHPC/Admx.	Constant	At Transfer(1)	49.9	2386	31.2	35.8
		28	80.1	2397	-	40.5
		90	82.0	2396	-	42.4
		180	84.8	2391	55.6	42.7
		365	87.1	2382	58.2	43.1
RHPC/PFA	Constant	At Transfer(8)	44.7	2365	32.1	34.8
		28	61.3	2362	-	37.7
		90	67.1	2354	-	38.7
		180	75.5	2350	51.4	40.6
		365	84.1	2352	55.3	41.8
RHPC/PFA ,Admx.	Constant	At Transfer(6)	48.7	2299	35.1	34.4
		28	69.0	2281	-	38.4
		90	76.3	2282	-	39.3
		180	84.1	2278	53.0	42.1
		365	88.3	2272	59.3	43.9

Table 5.2 - Percentage increase in cube compressive strength over prestressing transfer strength

Mix Reference	Type of Humidity	Percentage increase in strength			
		28 days	90 days	180 days	365 days
OPC	Constant	20.8	26.0	28.4	31.6
	Variable	27.3	46.7	55.3	68.6
RHPC	Constant	52.0	62.3	66.6	71.9
	Variable	58.1	66.8	75.1	80.8
RHPC/Admx.	Constant	60.5	64.3	70.0	74.6
RHPC/PFA	Constant	37.1	50.1	68.9	88.1
RHPC/Admx. and PFA	Constant	41.7	56.7	72.7	81.3

Table 5.3 - Percentage increase in static modulus of elasticity over prestressing transfer elastic modulus

Mix Reference	Type of Humidity	% increase in Modulus			
		28 days	90 days	180 days	365 days
OPC	Constant	10.0	16.9	18.9	20.1
	Variable	17.6	23.0	29.4	31.6
RHPC	Constant	17.5	21.3	23.4	24.6
	Variable	22.5	23.7	32.5	34.2
RHPC/Admx.	Constant	13.1	18.4	19.3	20.4
RHPC/PFA	Constant	8.3	11.2	16.7	20.1
RHPC/Admx. and PFA	Constant	11.6	14.2	22.4	27.5

Table 5.4 - Slope coefficient for creep values of different mixes representing the same volume/surface ratio of I-shaped beam and stored in constant environment

Y	Coefficient	X				
		OPC	RHPC	RHPC/ Admixture	RHPC/ PFA	RHPC/Admx. & PFA
OPC	S.C.	1	1.306	1.161	1.667	1.634
	RC.C	1	0.998	0.992	0.988	0.991
RHPC	S.C.	0.765	1	0.887	1.271	1.247
	RC.C	0.998	1	0.997	0.995	0.996
RHPC/Admx	S.C.	0.861	1.128	1	1.433	1.407
	RC.C	0.992	0.997	1	0.999	0.999
RHPC/PFA	S.C.	0.600	0.787	0.698	1	0.982
	RC.C	0.988	0.995	0.999	1	0.999
RHPC/Admx & PFA	S.C.	0.612	0.802	0.711	1.018	1
	RC.C.	0.991	0.996	0.999	0.999	1

Note:

S.C. represents the slope coefficient of regression line between two mixes and equal to Y/X

RC.C. represents the square root of the correlation coefficient between two mixes

Table 5.5 - Values of shrinkage and swelling after 365 days, as measured by cylinder and beam control specimens

Concrete type	Shape of Beam	Shrinkage (10^{-6}) Constant Humidity		Shrinkage (10^{-6}) Variable Humidity		Swelling (10^{-6})
		Cylinder	Beam	Cylinder	Beam	Cylinder
OPC	I	593	514	310	288	-66
	R	568	493	304	278	-66
RHPC	I	564	510	292	279	-134
	R	540	486	278	219	-134
RHPC/Admixture	I	632	546	-	-	-
RHPC/PFA	I	534	479	-	-	-
RHPC/Admixture and PFA	I	496	482	-	-	-

Note: I represents the volume/surface ratio of I-Beam

R represents the volume/surface ratio of rectangular Beam

Table 5.6 - The effect of relative humidity upon creep for various ages, as measured by cylindrical specimens

Time since application of load (days)	Volume to Surface Ratio (mm)	Creep (10^{-6})					
		OPC Mix			RHPC Mix		
		Relative Humidity (%)			Relative Humidity (%)		
		65%	77%	100%	65%	77%	100%
7	21.8(I)	120	115	61	113	103	57
	31.4(R)	101	80	61	70	69	57
30	21.8(I)	227	191	82	195	183	73
	31.4(R)	173	142	82	150	111	73
90	21.8(I)	341	240	115	255	203	109
	31.4(R)	276	165	115	212	134	109
180	21.8(I)	382	276	127	284	212	122
	31.4(R)	320	184	127	232	141	122
365	21.8(I)	390	281	133	302	219	128
	31.4(R)	329	196	133	251	150	128

Note:

(1) Relative Humidity of 77% represent the average time relative humidity of a week wetting of 100% and two weeks drying of 65%

(2) Volume-to-Surface ratio of 21.8mm represent an I-shaped prestress concrete beam

(3) Volume-to-Surface ratio of 31.4 mm represent a Rectangular shaped prestress concrete beam

Table 5.7 - Comparison between measured and prediction methods deformations for cylinders having RHPC mix and representing an I-beam shape

Type of deformation	Time since application of load (days)	DEFORMATION IN (10^{-6}) USING STRENGTH AND MIX COMPOSITION						DEFORMATION IN (10^{-6}) USING KNOWN MODULI OF ELASTICITY				
		Measured	CEB70	CEB78	ACI82	BaP78	CS78	CEB70	CEB78	ACI82	BaP78	CS78
Elastic Strain	0	175	145	155	168	139	175	175	175	175	175	175
Basic Creep	7	57	53	88	75	98	104	59	101	66	93	84
	30	65	98	97	131	164	118	107	111	114	155	96
	180	122	153	134	214	263	223	168	154	188	248	181
	365	128	166	146	240	319	232	184	168	210	301	188
Total Creep (65% R.H.)	7	113	133	122	101	254	214	146	140	88	245	156
	30	177	244	167	173	353	362	269	191	151	346	244
	180	284	381	275	283	545	489	420	316	248	537	396
	365	302	416	314	315	600	508	459	360	276	592	411
Total Creep (77% R.H.)	7	108	106	109	90	183	192	117	125	79	175	173
	30	183	195	140	156	284	300	215	161	137	225	293
	180	212	305	222	256	439	419	336	255	225	432	339
	365	219	333	249	286	510	435	367	286	251	502	352
Shrinkage (65% R.H.)	7	170	91	58	113	141	55	91	58	113	141	55
	30	341	166	146	312	227	110	166	146	312	227	110
	180	502	260	271	566	295	161	260	271	566	295	161
	365	564	284	300	616	306	184	284	300	616	306	184
Shrinkage (77% R.H.)	7	129	69	34	95	106	61	69	34	95	106	61
	30	158	125	79	263	170	74	125	79	263	170	74
	180	236	196	166	476	221	115	196	166	476	221	115
	365	292	214	193	518	230	133	214	193	518	230	133
Swelling	7	-75	-	0	-	-39	-65	-	0	-	-39	-65
	30	-107	-	-2	-	-63	-94	-	-2	-	-63	-94
	180	-133	-	-8	-	-81	-110	-	-8	-	-81	-110
	365	-134	-	-12	-	-84	-123	-	-12	-	-84	-123
Total long term Strain (65% R.H.)	7	283	224	180	214	395	275	237	193	201	386	211
	30	518	410	313	485	511	472	435	337	463	573	354
	180	786	641	546	849	840	650	680	587	814	832	557
	365	866	700	614	931	906	692	743	660	892	898	595
Total long term Strain (77% R.H.)	7	237	175	143	185	289	247	186	159	174	281	234
	30	341	320	219	419	454	374	340	240	400	395	367
	180	448	501	388	732	660	534	532	415	701	653	454
	365	511	547	442	804	740	568	581	479	769	732	485

Table 5.8 - Comparison between measured and prediction methods deformations for cylinders having an OPC mix and representing an I-beam shape

Type of deformation	Time since application of load (days)	DEFORMATION IN (10^{-6}) USING STRENGTH AND MIX COMPOSITION						DEFORMATION IN (10^{-6}) USING KNOWN MODULI OF ELASTICITY				
		Measured	CEB70	CEB78	ACI82	BaP78	CS78	CEB70	CEB78	ACI82	BaP78	CS78
Elastic Strain	0	165	140	149	161	124	173	165	165	165	165	165
Basic Creep	7	61	65	76	69	67	90	74	80	66	53	80
	30	82	119	92	124	106	120	135	97	119	84	108
	180	127	187	133	197	165	188	212	140	189	131	168
	365	133	204	147	219	199	195	232	155	210	158	175
Total Creep (65% R.H.)	7	163	163	87	90	155	175	185	92	87	122	157
	30	227	298	146	161	244	244	339	154	155	211	218
	180	392	467	276	258	365	415	531	291	247	333	371
	365	286	510	321	290	434	431	580	339	278	402	385
Total Creep (77% R.H.)	7	125	130	82	82	131	155	148	86	79	99	138
	30	191	238	125	147	199	236	271	131	141	163	212
	180	276	374	220	235	302	342	425	232	226	269	306
	365	396	408	256	263	351	355	464	269	252	319	318
Shrinkage (65% R.H.)	7	157	112	8	98	112	49	112	8	98	112	49
	30	391	206	96	270	195	122	206	96	270	195	122
	180	512	322	221	486	285	161	322	221	486	285	161
	365	593	352	250	533	304	184	352	250	533	304	184
Shrinkage (77% R.H.)	7	121	84	3	82	84	54	84	3	82	84	54
	30	184	155	50	226	146	82	155	50	226	146	82
	180	243	243	137	408	214	115	243	137	408	214	115
	365	310	265	164	448	228	133	265	164	448	228	133
Swelling	7	-30	-	0	-	-31	-56	-	0	-	-31	-56
	30	-34	-	-2	-	-54	-64	-	-2	-	-54	-64
	180	-58	-	-8	-	-79	-110	-	-8	-	-79	-110
	365	-66	-	-12	-	-84	-123	-	-12	-	-84	-123
Total long term Strain (65% R.H.)	7	320	275	95	188	267	224	297	100	185	234	206
	30	618	504	242	431	439	366	545	250	425	406	340
	180	904	789	497	744	650	576	853	512	733	618	532
	365	989	862	571	823	738	615	932	589	811	706	569
Total long term Strain (77% R.H.)	7	246	214	85	164	215	209	232	89	161	183	192
	30	375	393	175	373	345	318	426	181	367	309	294
	180	519	617	357	643	516	457	668	369	634	483	421
	365	596	673	420	711	579	488	729	433	700	547	451

Table 5.9 - Comparison between measured and prediction methods deformations for cylinders having RHPC mix and representing a rectangular beam shape

Type of deformation	Time since application of load (days)	DEFORMATION IN (10^{-6}) USING STRENGTH AND MIX COMPOSITION						DEFORMATION IN (10^{-6}) USING KNOWN MODULI OF ELASTICITY				
		Measured	CEB70	CEB78	ACI82	BAP78	CS78	CEB70	CEB78	ACI82	BaP78	CS78
Elastic Strain	0	162	145	155	168	139	175	162	162	162	162	162
Basic Creep	7	57	45	88	70	98	104	49	101	61	93	84
	30	65	85	100	122	164	118	93	115	107	155	96
	180	122	140	130	198	263	223	154	150	173	248	181
	365	128	154	143	221	319	232	169	164	193	301	188
Total Creep (65% R.H.)	7	70	111	114	92	193	144	122	131	81	185	117
	30	135	212	162	159	313	278	233	186	139	305	225
	180	232	349	260	261	504	489	385	299	229	496	396
	365	251	384	296	292	585	508	423	340	256	577	411
Total Creep (77% R.H.)	7	69	89	105	84	168	202	98	120	73	160	164
	30	111	170	136	144	269	325	186	156	126	260	263
	180	141	279	210	236	414	419	308	241	207	407	339
	365	150	307	237	265	493	435	338	272	232	484	352
Shrinkage (65% R.H.)	7	160	76	42	103	103	54	76	42	103	103	54
	30	299	145	121	299	184	100	145	121	299	184	100
	180	490	241	246	541	275	161	241	246	541	275	161
	365	540	264	284	590	294	183	264	284	590	294	183
Shrinkage (77% R.H.)	7	97	57	26	91	77	47	57	26	91	77	47
	30	144	109	59	251	138	70	109	59	251	138	70
	180	230	182	123	454	206	115	182	123	454	206	115
	365	278	199	156	496	220	133	199	156	496	220	133
Swelling	7	-74	-	0	-	-28	-65	-	0	-	-28	-65
	30	-107	-	0	-	-51	-93	-	0	-	-51	-93
	180	-133	-	-5	-	-76	-110	-	-5	-	-76	-110
	365	-134	-	-7	-	-81	-123	-	-7	-	-81	-123
Total long term Strain (65% R.H.)	7	230	187	156	195	296	198	198	173	184	288	171
	30	434	357	283	458	497	378	378	307	438	489	325
	180	722	590	506	802	779	650	626	545	770	771	457
	365	791	648	580	882	879	691	687	624	846	871	594
Total long term Strain (77% R.H.)	7	166	146	131	175	245	249	155	146	164	237	211
	30	255	279	195	395	407	395	295	215	377	398	333
	180	371	461	333	690	620	534	490	364	661	613	454
	365	428	506	393	761	713	568	537	428	728	704	485

Table 5.10 - Comparison between measured and predicted methods déformations for cylinders having an OPC mix and representing a rectangular beam shape

Type of deformation	Time since application of load (days)	DEFORMATION IN (10^{-6}) USING STRENGTH AND MIX COMPOSITION						DEFORMATION IN (10^{-6}) USING KNOWN MODULI OF ELASTICITY				
		Measured	CEB70	CEB78	ACI82	BaP78	CS78	CEB70	CEB78	ACI82	BaP78	CE78
Elastic Strain	0	155	140	149	161	124	173	155	155	155	155	155
Basic Creep	7	61	54	75	65	67	90	62	79	62	53	81
	30	82	103	91	116	106	121	117	96	111	84	108
	180	127	171	129	184	165	188	194	136	176	131	168
	365	133	188	143	206	199	195	213	151	198	158	175
Total Creep (65% R.H.)	7	101	135	79	84	136	132	154	83	80	103	117
	30	173	257	139	150	219	225	292	147	144	186	201
	180	320	427	261	239	366	415	486	275	229	333	371
	365	329	469	303	268	415	431	534	319	257	382	385
Total Creep (77% R.H.)	7	80	108	78	76	121	146	123	81	73	88	131
	30	142	206	119	137	179	260	234	126	132	147	233
	180	184	342	209	216	282	342	389	220	207	250	306
	365	196	375	242	244	337	355	427	256	234	304	318
Shrinkage (65% R.H.)	7	148	94	19	94	79	49	94	19	94	79	49
	30	343	179	76	258	151	111	179	76	258	151	111
	180	500	298	200	465	254	161	298	200	465	254	161
	365	568	327	238	510	284	184	327	238	510	284	184
Shrinkage (77% R.H.)	7	87	71	17	79	59	39	71	17	79	59	39
	30	177	135	40	216	113	80	135	40	216	113	80
	180	242	225	104	390	190	115	225	104	390	190	115
	365	304	246	137	428	213	133	246	137	428	213	133
Swelling	7	-30	-	0	-	-22	-56	-	0	-	-22	-56
	30	-34	-	0	-	-42	-64	-	0	-	-64	-64
	180	-58	-	-5	-	-70	-110	-	-5	-	-110	-110
	365	-66	-	-7	-	-78	-123	-	-7	-	-123	-123
Total long term Strain (65% R.H.)	7	249	229	100	178	215	181	248	102	174	182	166
	30	516	436	215	408	370	336	471	223	402	337	312
	180	820	725	461	704	620	579	784	475	694	587	532
	365	897	796	541	778	699	615	861	557	767	666	569
Total long term Strain (77% R.H.)	7	167	179	95	155	180	185	194	98	152	147	170
	30	319	341	159	353	292	340	369	166	348	260	313
	180	426	567	313	606	472	457	614	324	597	440	421
	365	500	621	379	672	550	488	673	393	662	517	451

Table 5.11 - Slope coefficients between measured and predicted values for an I-shaped beam

Type of Deformation and Environment			Rapid Hardening Portland Cement Mix					Ordinary Portland Cement Mix				
			CEB70	CEB78	ACI82	BaP78	CS78	CEB70	CEB78	ACI82	BaP78	CS78
Average constant Relative Humidity of 65%	SHRINKAGE	S.C.	0.519	0.508	1.075	0.53	0.324	0.590	0.359	0.847	0.50	0.310
		C.V.	(4.890)	(14.14)	(13.33)	(11.45)	(2.000)	(5.900)	(29.82)	(12.86)	(6.310)	(1.320)
	TOTAL CREEP	S.C.	1.323	0.957	0.973	1.92	1.745	1.246	0.806	0.782	1.02	1.088
		C.V.	(4.470)	(7.650)	(5.810)	(7.170)	(9.094)	(5.780)	(10.35)	(7.380)	(9.440)	(8.160)
	TOTAL DEFORMATION	S.C.	0.822	0.68	1.05	1.01	0.853	0.895	0.497	0.781	0.72	0.625
		C.V.	(4.450)	(7.240)	(9.730)	(6.610)	(7.300)	(2.270)	(17.88)	(8.630)	(3.270)	(3.300)
Average variable Relative Humidity of 77% (65-100%)	SHRINKAGE	S.C.	0.793	0.619	1.824	0.83	0.466	0.912	0.448	1.449	0.80	0.450
		C.V.	(14.58)	(25.74)	(23.77)	(14.85)	(4.030)	(12.07)	(36.50)	(21.03)	(10.96)	(2.660)
	TOTAL CREEP	S.C.	1.297	0.956	1.080	2.13	1.895	1.326	0.760	0.824	1.17	1.240
		C.V.	(16.35)	(14.27)	(17.59)	(14.39)	(9.900)	(9.510)	(13.62)	(10.47)	(8.830)	(0.170)
	TOTAL DEFORMATION	S.C.	1.038	0.786	1.468	1.47	1.165	1.127	0.608	1.110	0.99	0.855
		C.V.	(12.57)	(15.22)	(19.74)	(6.970)	(8.030)	(9.750)	(21.14)	(17.23)	(6.400)	(2.930)

Remarks: Predicted values are based on strength and composition of concrete

S.C. Slope coefficients of regression line of Predicted/measured ratio; a value >1.0 indicates overestimation

C.V. Coefficient of Variance

Table 5.12 - Slope coefficients between measured and predicted values for a rectangular shaped beam

Type of Deformation and Environment			Rapid Hardening Portland Cement Mix					Ordinary Portland Cement Mix				
			CEB70	CEB78	ACI82	BaP70	CS78	CEB70	CEB78	ACI82	BaP78	CS78
Average variable Relative Humidity of 65%	SHRINKAGE	S.C.	0.501	0.484	1.094	0.54	0.332	0.573	0.347	0.867	0.50	0.324
		C.V.	(4.080)	(14.13)	(10.28)	(6.810)	(1.610)	(4.390)	(27.36)	(9.370)	(4.720)	(0.520)
	TOTAL CREEP	S.C.	1.479	1.118	1.113	2.21	2.059	1.366	0.821	0.768	1.20	1.305
		C.V.	(4.870)	(10.75)	(6.423)	(9.115)	(1.567)	(5.250)	(11.00)	(8.220)	(9.780)	(0.450)
	TOTAL DEFORMATION	S.C.	0.825	0.695	1.102	1.08	0.901	0.875	0.527	0.831	0.76	0.693
		C.V.	(2.060)	(4.830)	(5.340)	(4.580)	(3.280)	(2.180)	(13.47)	(4.720)	(5.490)	(2.910)
Average variable Relative Humidity of 77% (65-100%)	SHRINKAGE	S.C.	0.759	0.490	1.840	0.83	0.488	0.863	0.372	1.447	0.73	0.445
		C.V.	(8.515)	(19.22)	(15.09)	(9.360)	(1.760)	(9.290)	(26.39)	(14.35)	(8.360)	(3.770)
	TOTAL CREEP	S.C.	1.793	1.398	1.534	3.13	2.929	1.750	1.062	1.118	1.60	1.815
		C.V.	(15.44)	(10.05)	(13.67)	(15.06)	(0.840)	(11.80)	(13.25)	(9.840)	(10.57)	(1.840)
	TOTAL DEFORMATION	S.C.	1.171	0.849	1.724	1.70	1.32	1.246	0.668	1.307	1.09	1.032
		C.V.	(9.210)	(8.270)	(13.27)	(5.040)	(6.180)	(9.050)	(14.58)	(11.79)	(6.300)	(4.120)

Remarks: Predicted values are based on strength and composition of concrete

S.C. Slope coefficient of regression line of Predicted/measured ratio

C.V. Coefficient of Variance

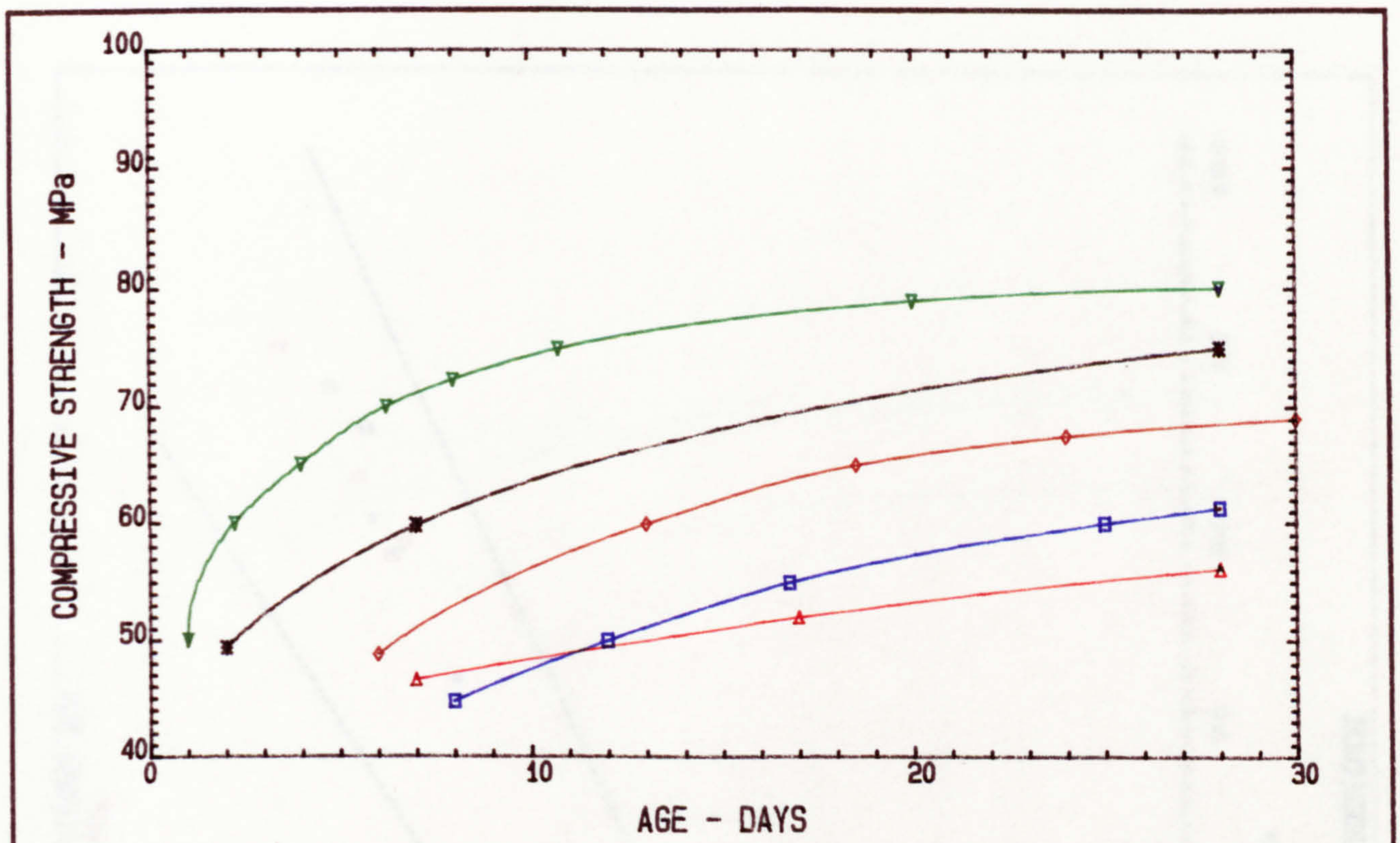

FIG. 5.1 EARLY-AGE CUBE COMPRESSIVE STRENGTH FOR VARIOUS CONCRETE MIXES

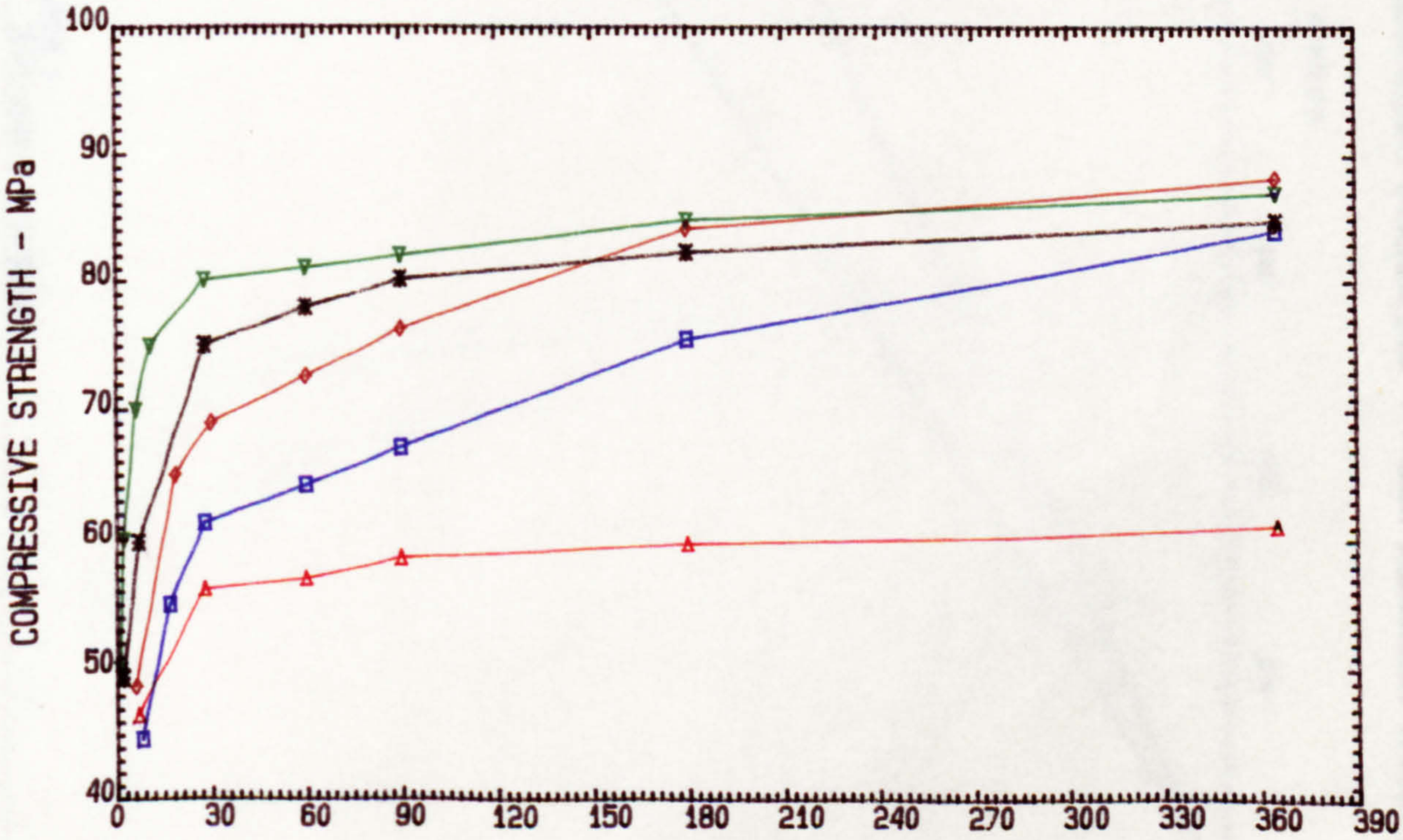

FIG. 5.2 ONE YEAR DEVELOPMENT OF CUBE COMPRESSIVE STRENGTH FOR VARIOUS CONCRETE MIXES

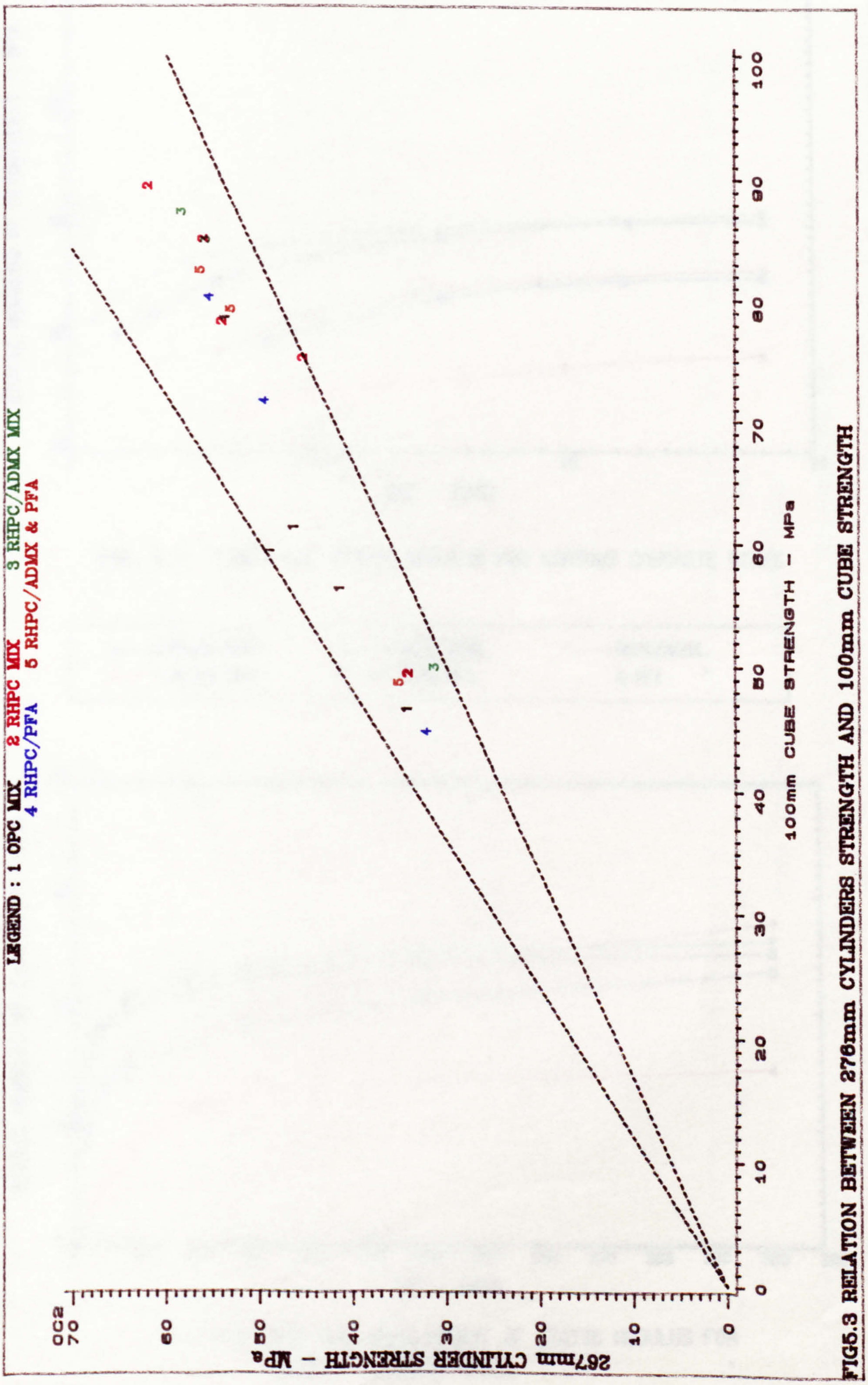

FIG5.3 RELATION BETWEEN 267mm CYLINDERS STRENGTH AND 100mm CUBE STRENGTH

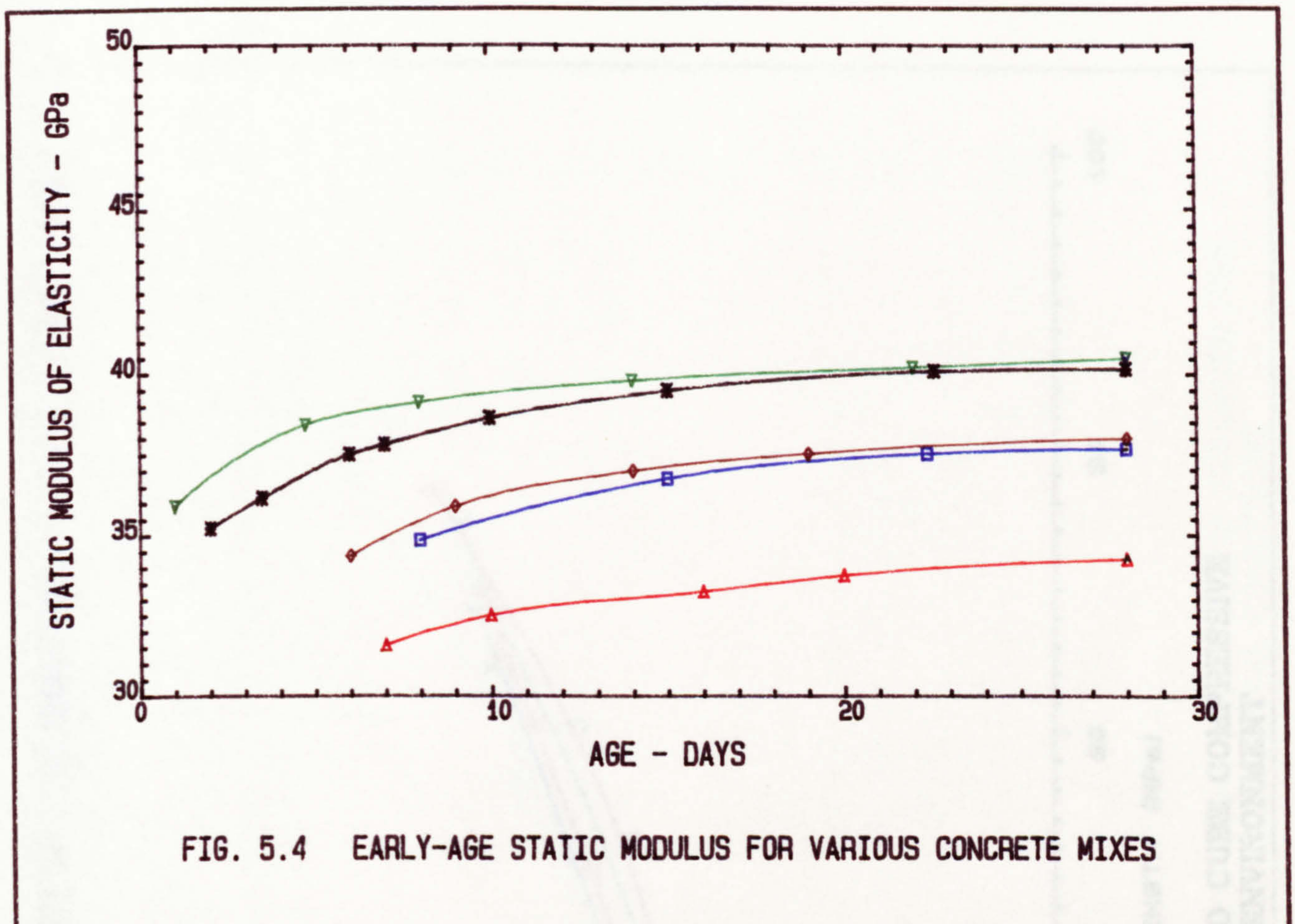

FIG. 5.4 EARLY-AGE STATIC MODULUS FOR VARIOUS CONCRETE MIXES

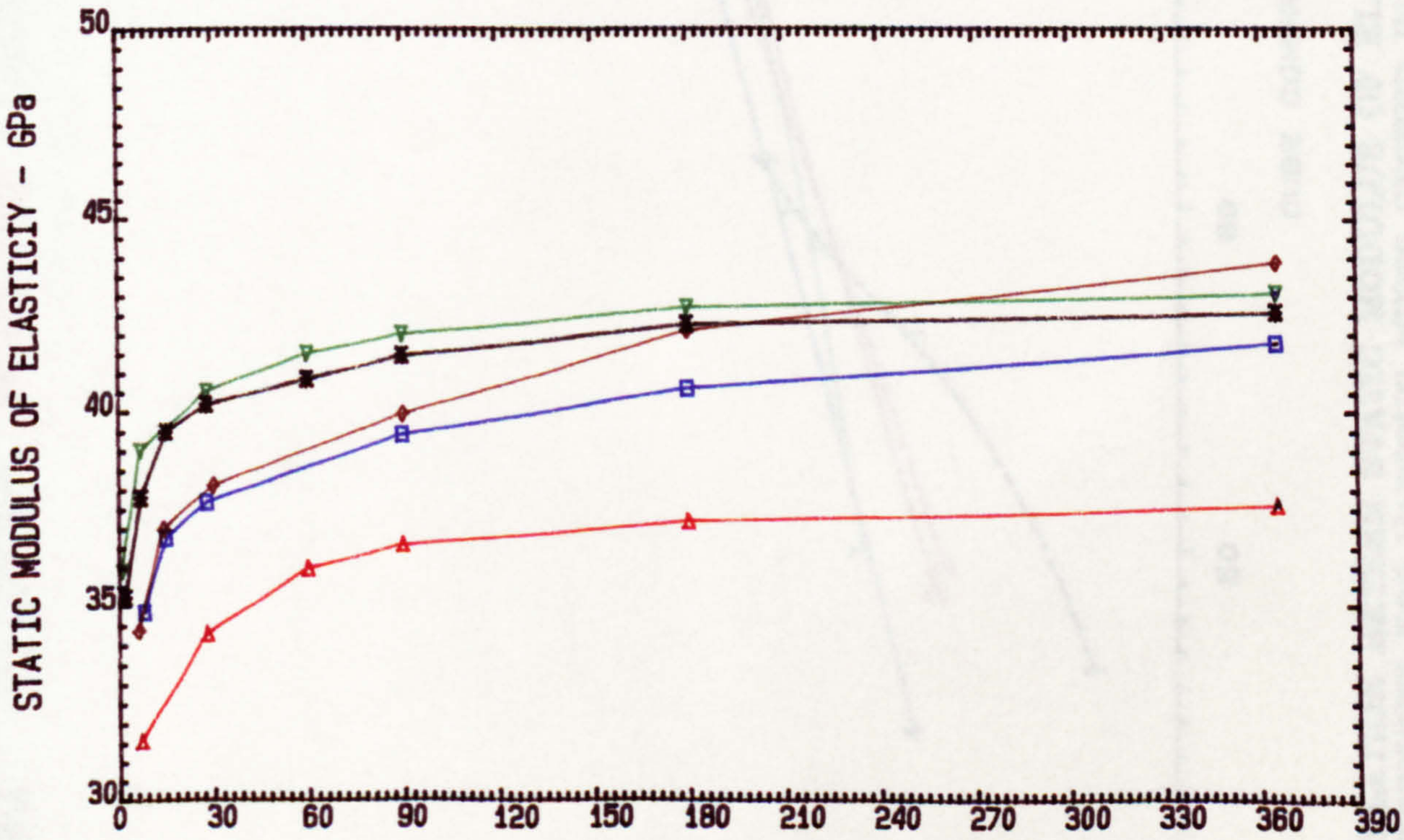

FIG. 5.5 ONE YEAR DEVELOPMENT OF STATIC MODULUS FOR VARIOUS CONCRETE MIXES

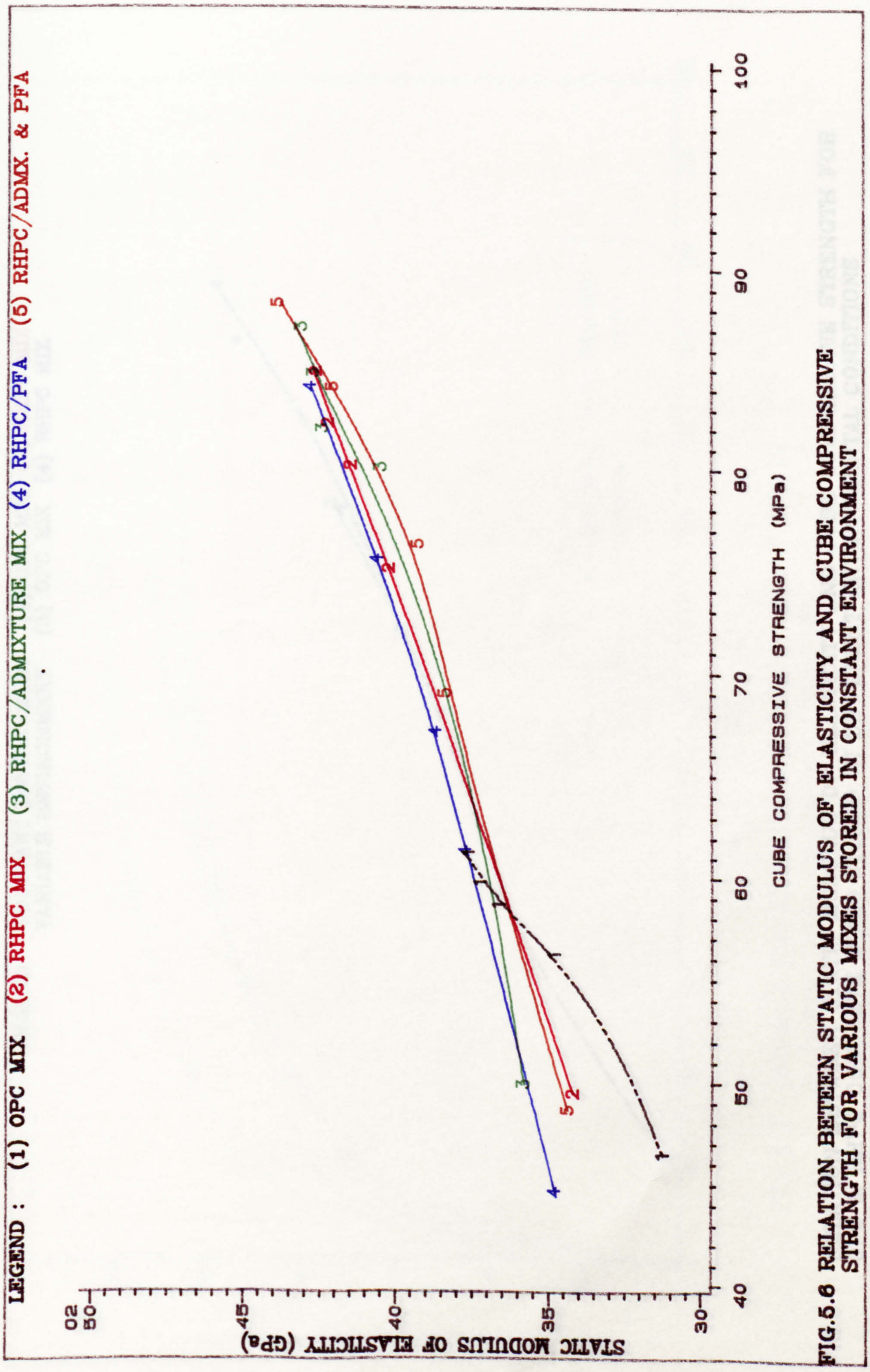

FIG.5.6 RELATION BETEEN STATIC MODULUS OF ELASTICITY AND CUBE COMPRESSIVE STRENGTH FOR VARIOUS MIXES STORED IN CONSTANT ENVIRONMENT

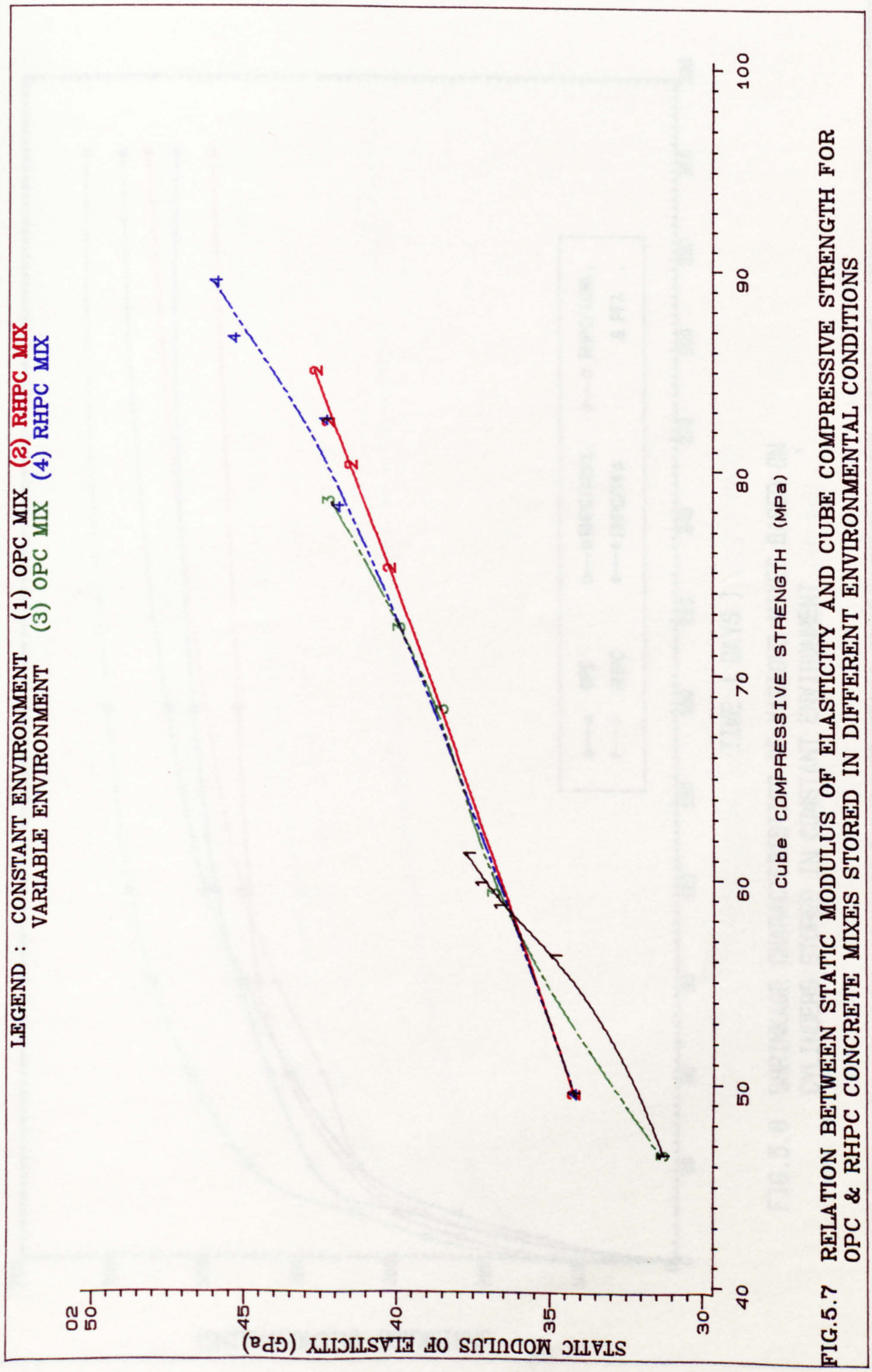

FIG.5.7 RELATION BETWEEN STATIC MODULUS OF ELASTICITY AND CUBE COMPRESSIVE STRENGTH FOR OPC & RHPC CONCRETE MIXES STORED IN DIFFERENT ENVIRONMENTAL CONDITIONS

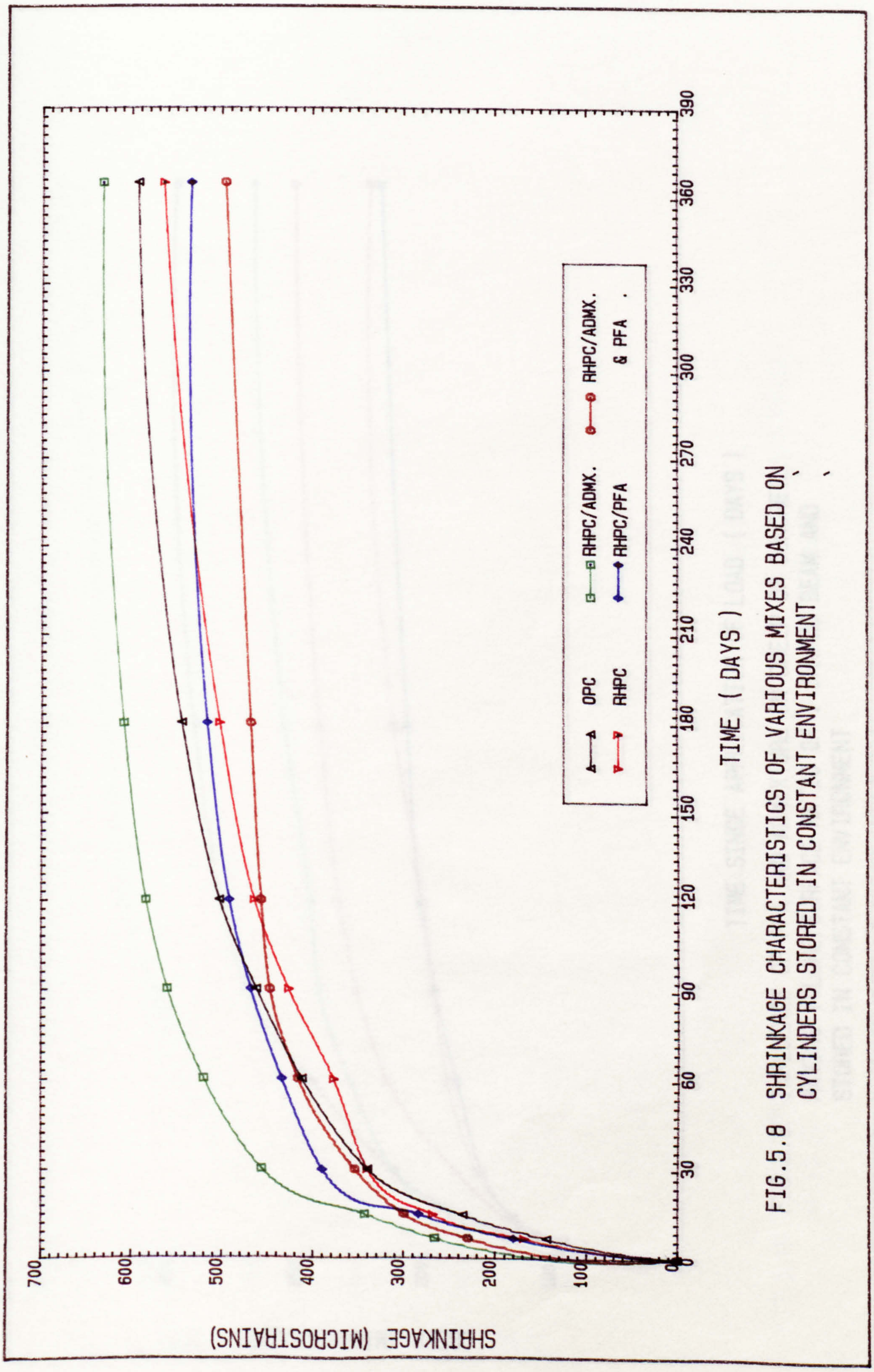

FIG.5.8 SHRINKAGE CHARACTERISTICS OF VARIOUS MIXES BASED ON CYLINDERS STORED IN CONSTANT ENVIRONMENT

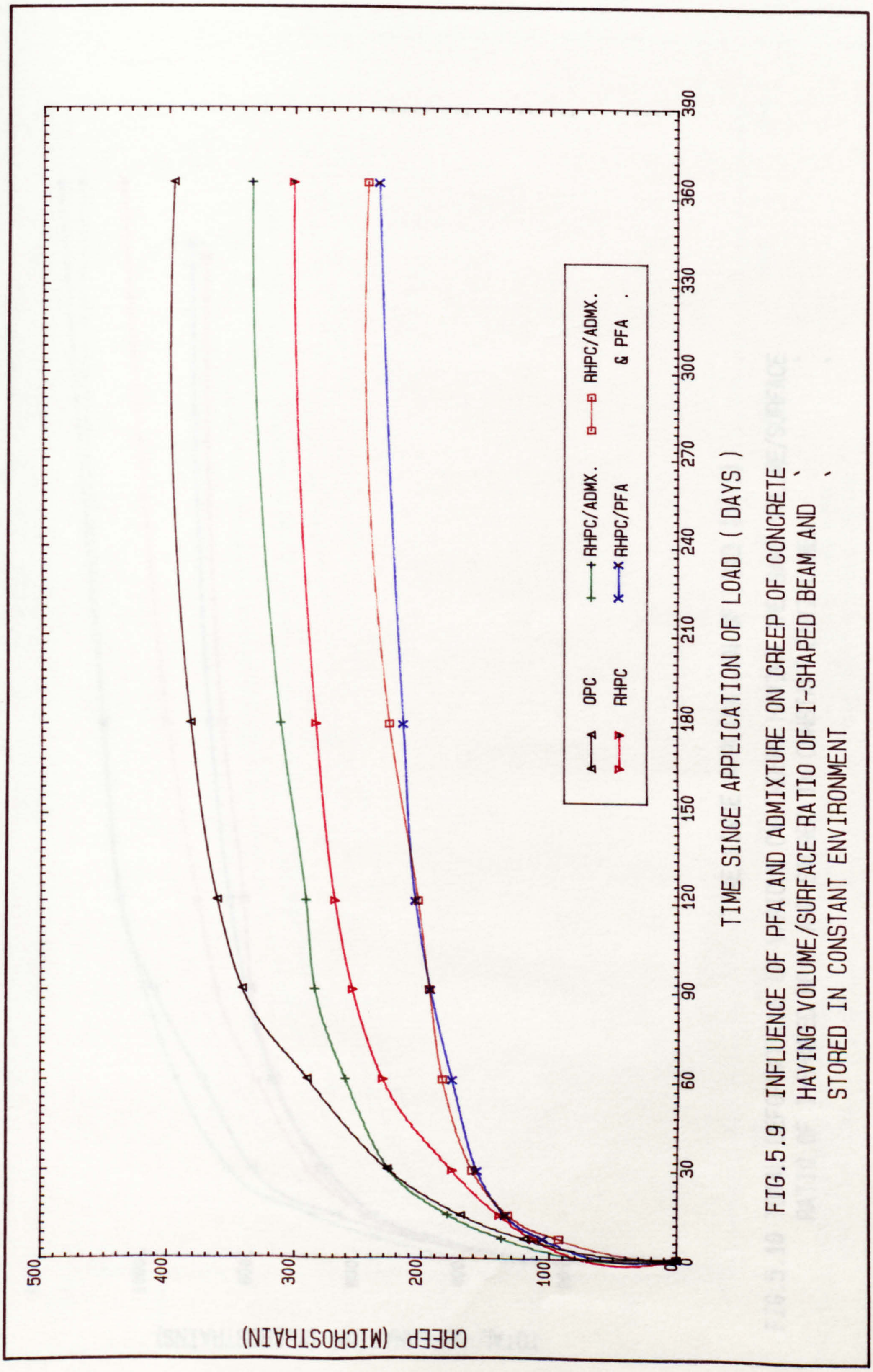

FIG.5.9 INFLUENCE OF PFA AND ADMIXTURE ON CREEP OF CONCRETE HAVING VOLUME/SURFACE RATIO OF I-SHAPED BEAM AND STORED IN CONSTANT ENVIRONMENT

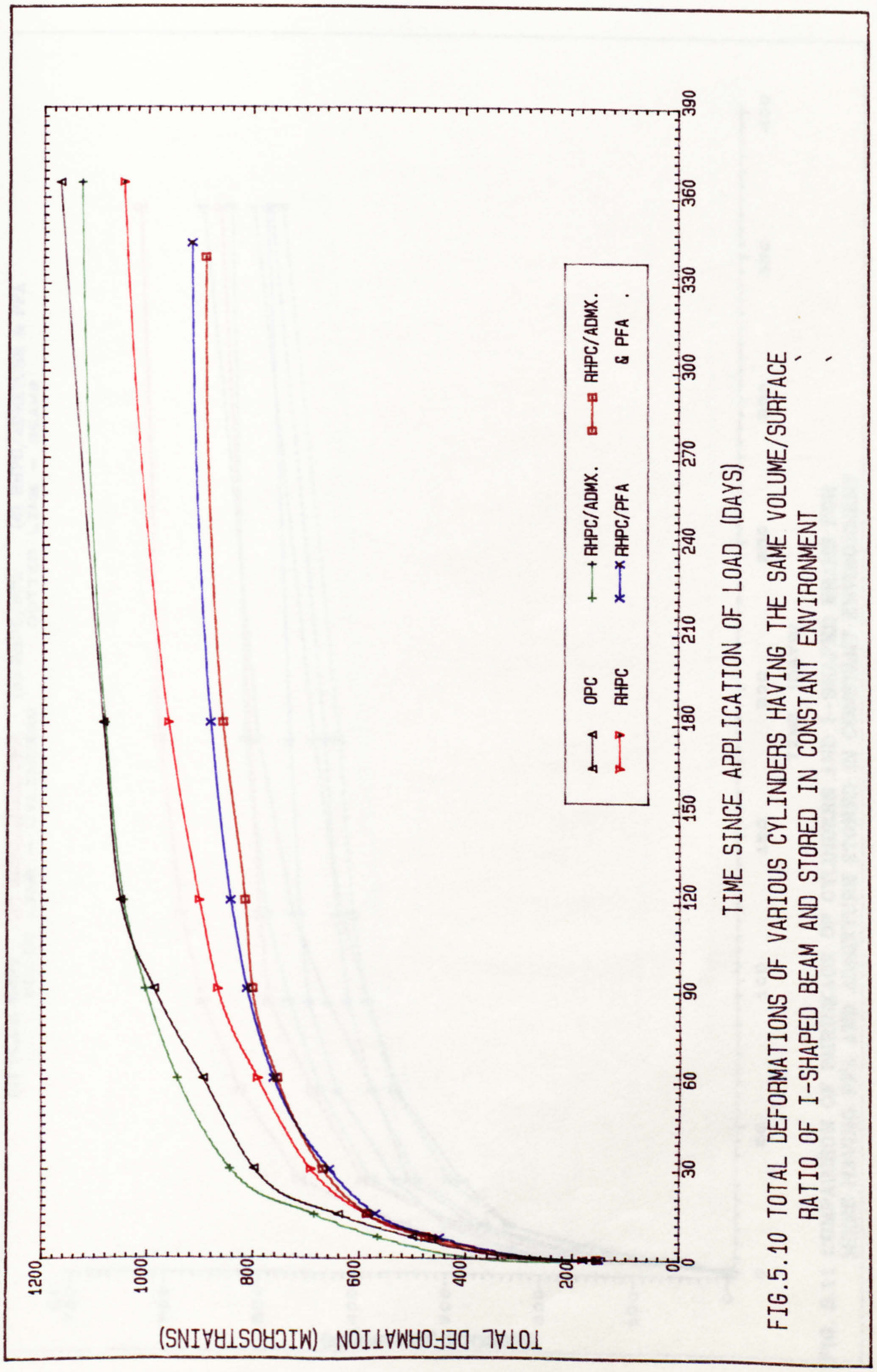

FIG.5.10 TOTAL DEFORMATIONS OF VARIOUS CYLINDERS HAVING THE SAME VOLUME/SURFACE RATIO OF I-SHAPED BEAM AND STORED IN CONSTANT ENVIRONMENT

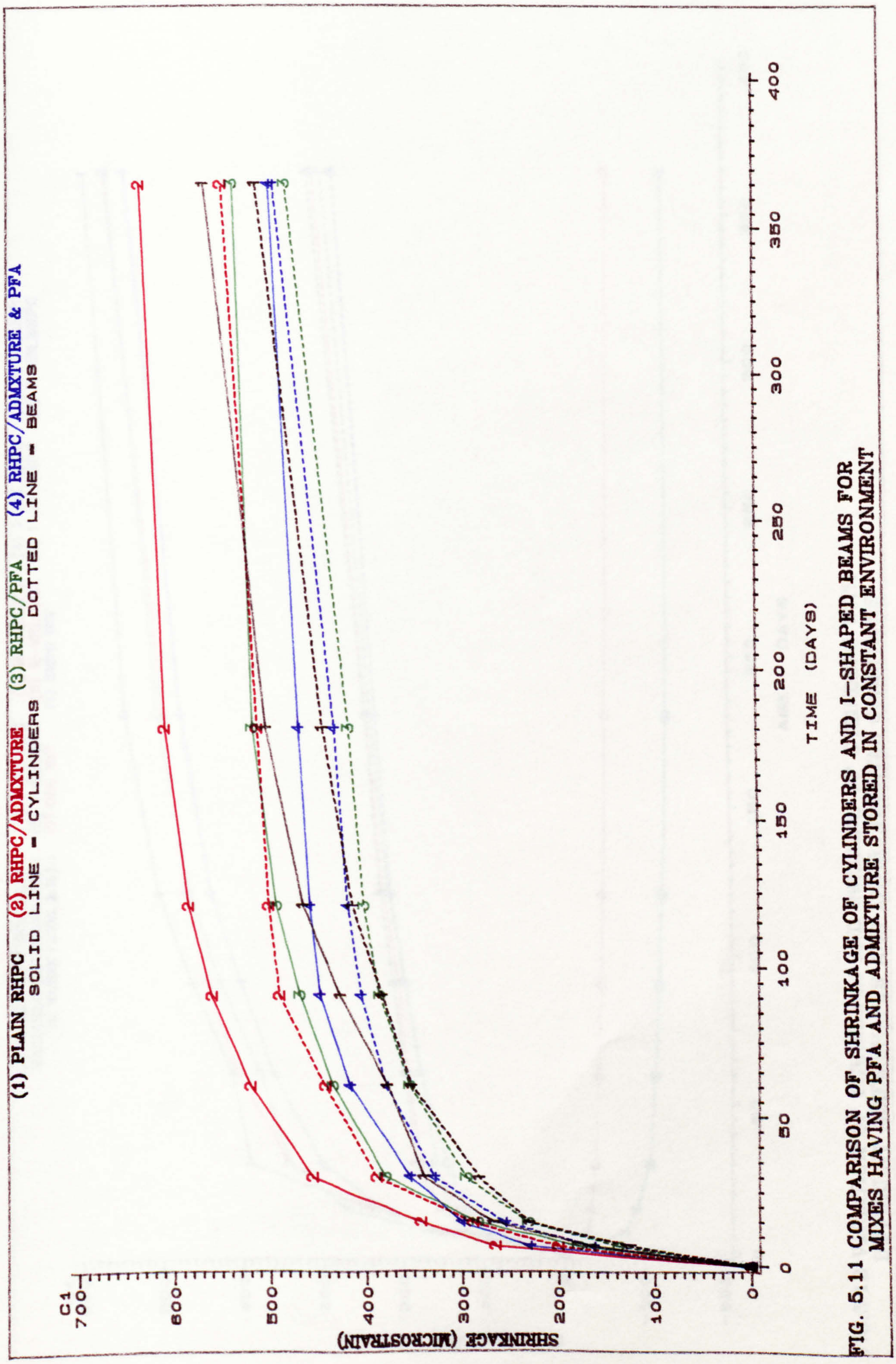

FIG. 5.11 COMPARISON OF SHRINKAGE OF CYLINDERS AND I-SHAPED BEAMS FOR MIXES HAVING PFA AND ADMIXTURE STORED IN CONSTANT ENVIRONMENT

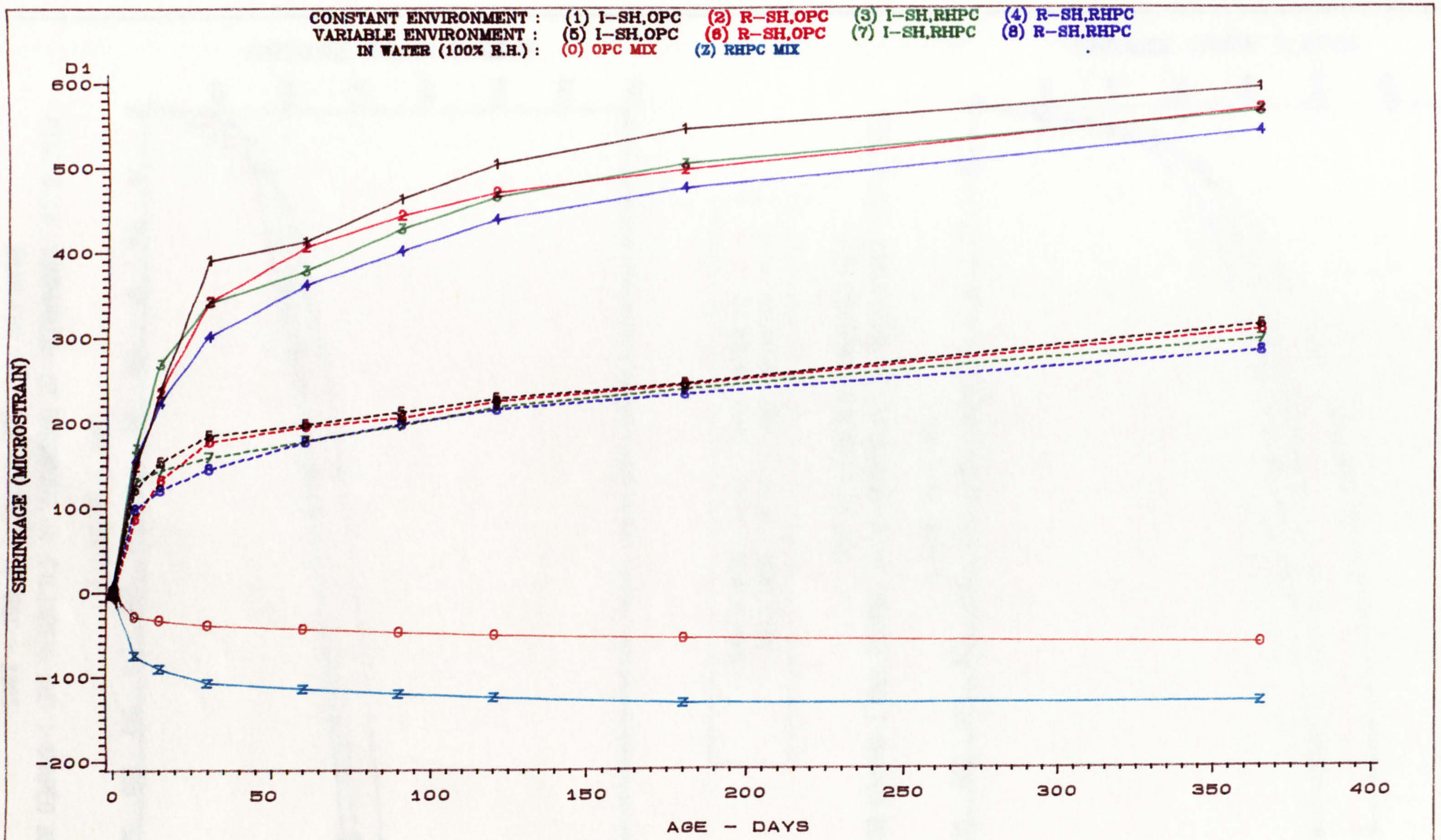

FIG.5.12 VARIATION OF SHRINKAGE AND SWELLING OF CYLINDERS WITH DIFFERENT MIXES,SHAPES AND ENVIRONMENTAL CONDITIONS

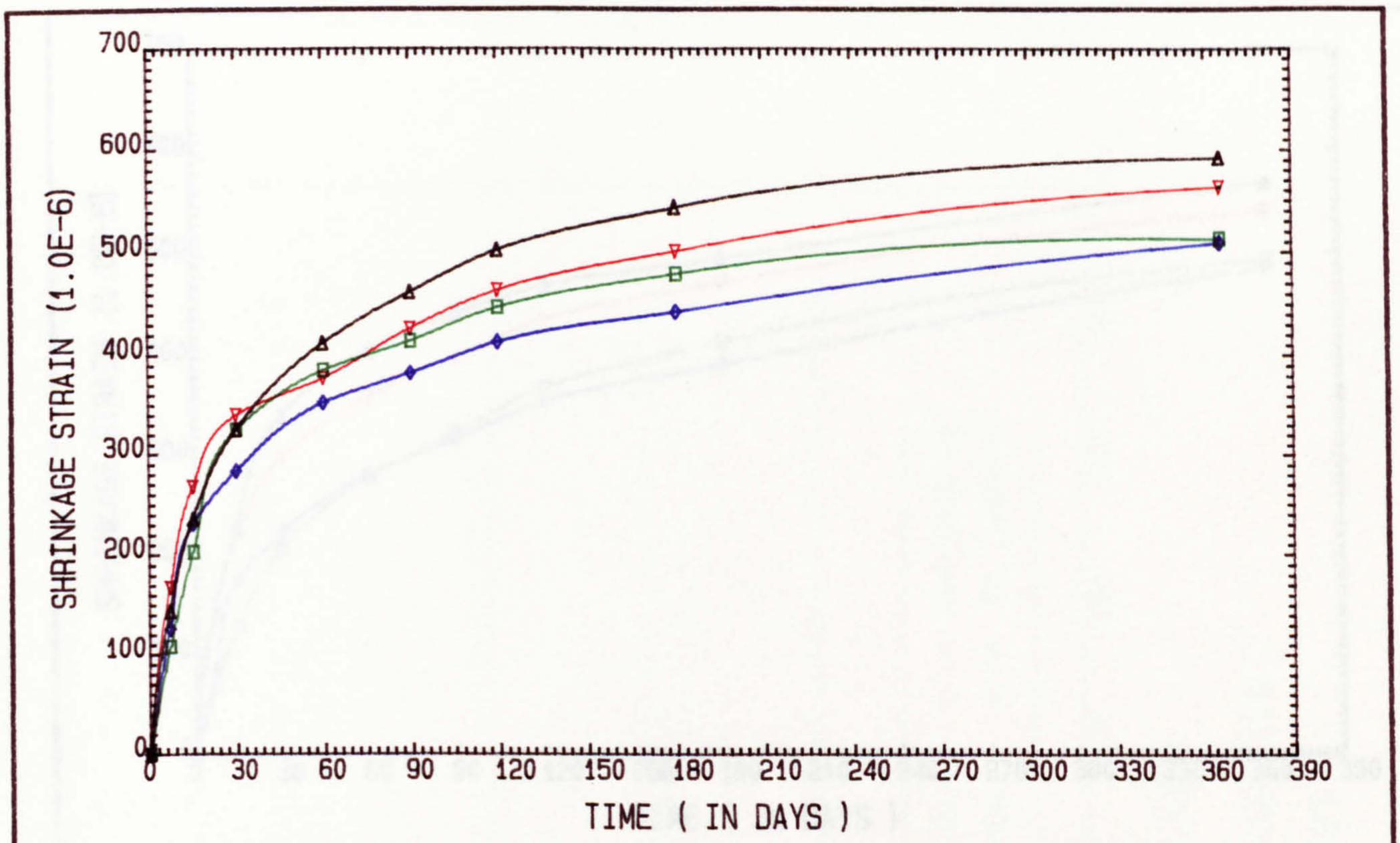

FIG. 5.13 COMPARISON OF SHRINKAGE OF CYLINDERS AND I-SHAPED BEAMS FOR CONSTANT HUMIDITY OF 65%

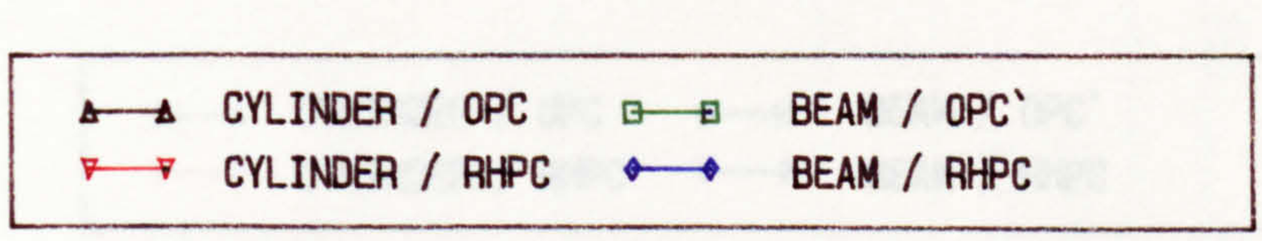

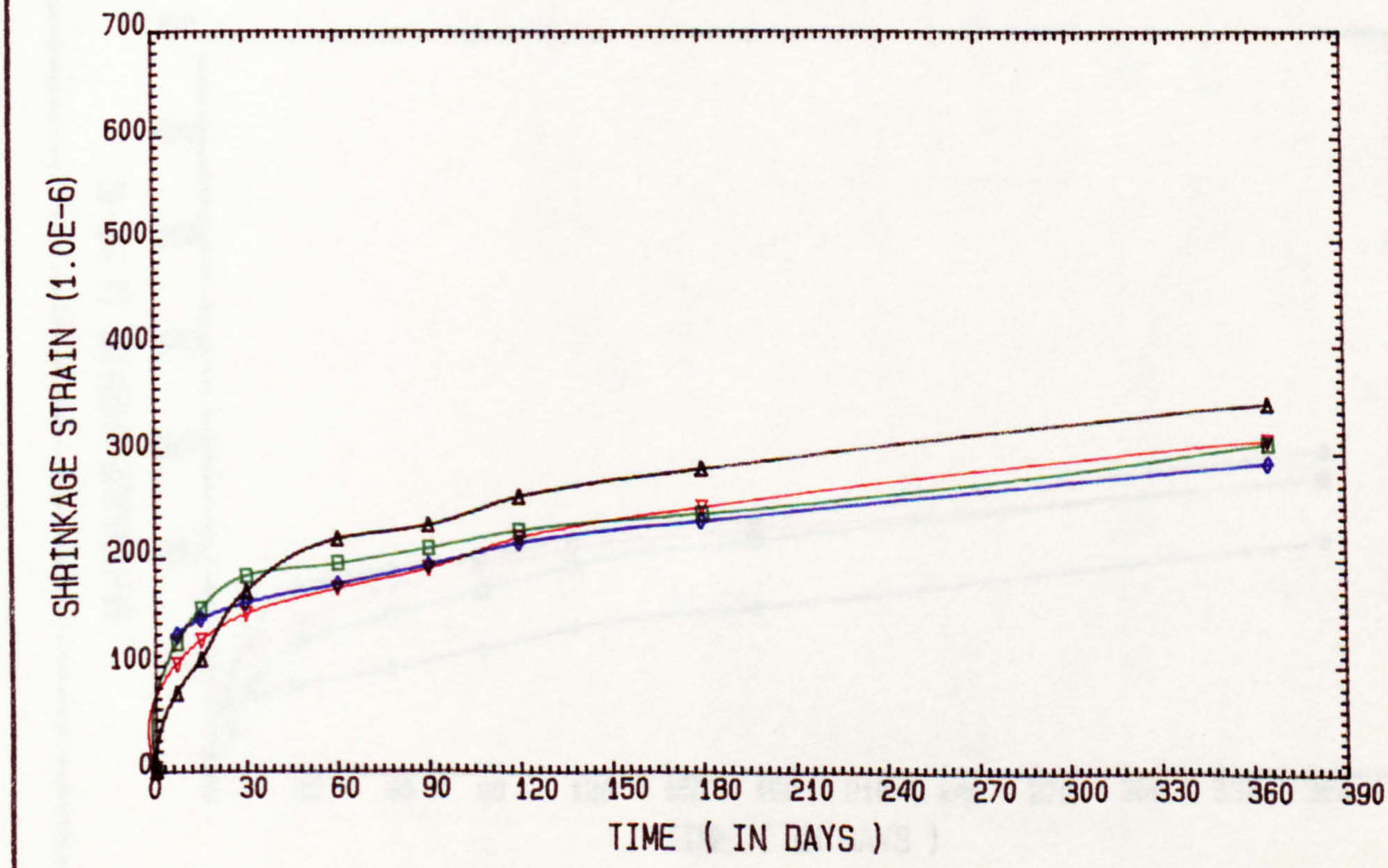

FIG. 5.14 COMPARISON OF SHRINKAGE OF CYLINDERS AND I-SHAPED BEAMS BEAM FOR VARIABLE HUMIDITY OF 65% - 100%

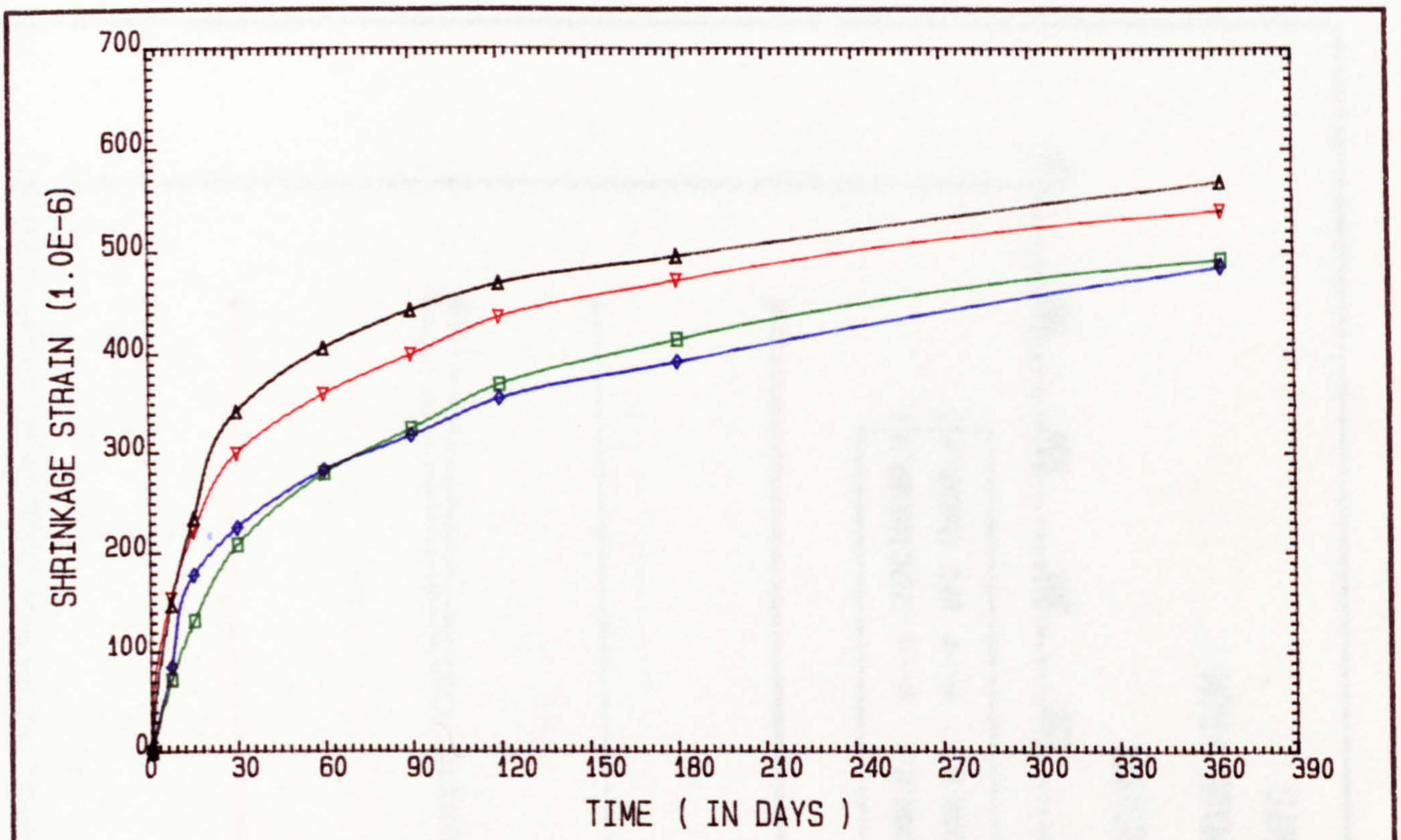

FIG. 5.15 COMPARISON OF SHRINKAGE OF CYLINDERS AND RECTANGULAR SHAPE BEAMS FOR CONSTANT HUMIDITY OF 65%

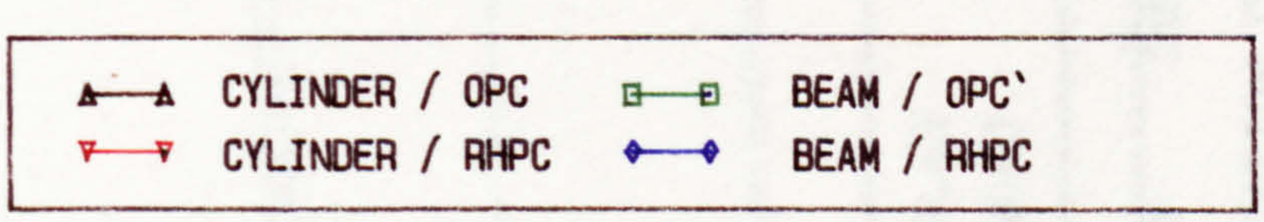

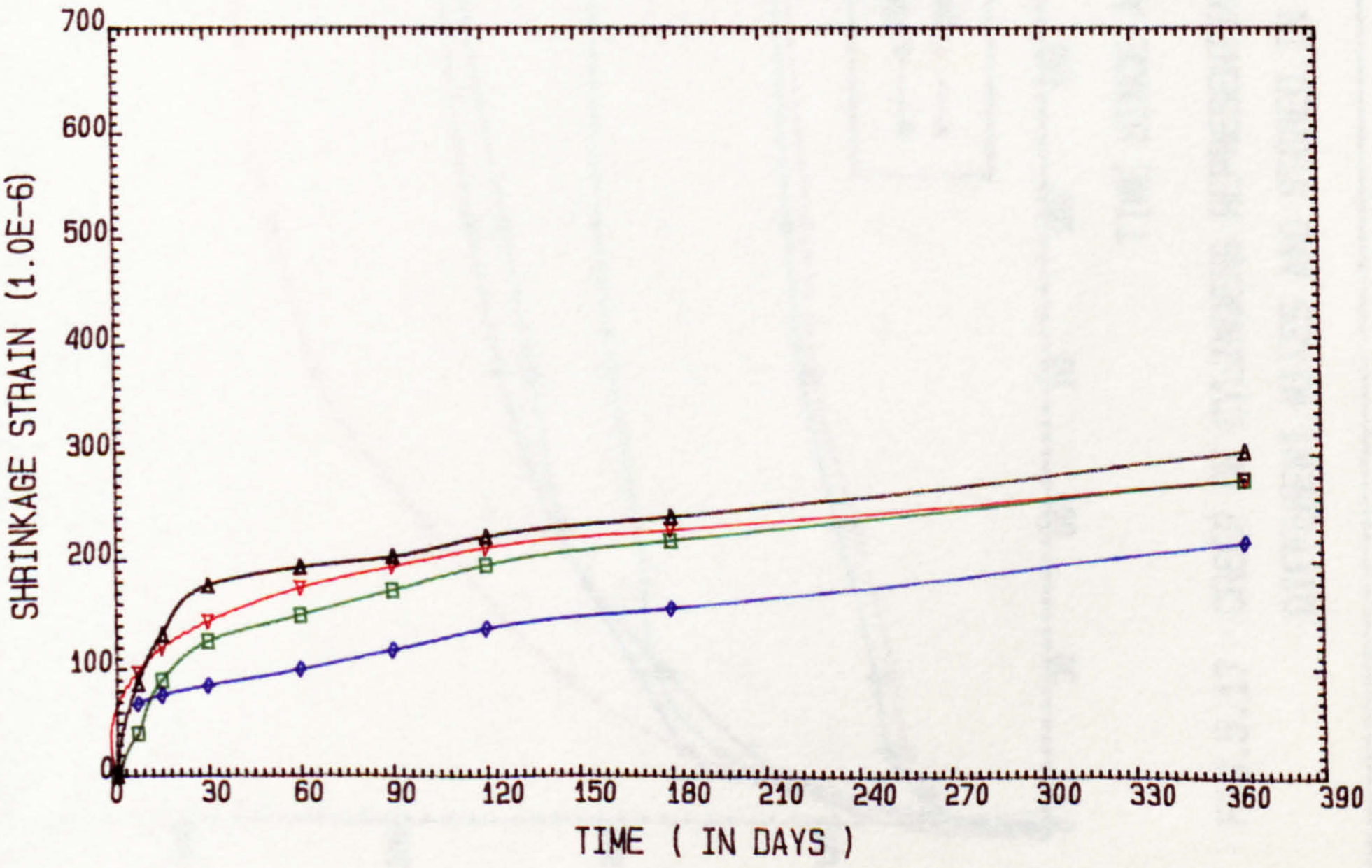

FIG. 5.16 COMPARISON OF SHRINKAGE OF CYLINDERS AND RECTANGULAR SHAPE BEAMS FOR VARIABLE HUMIDITY OF 65% - 100%

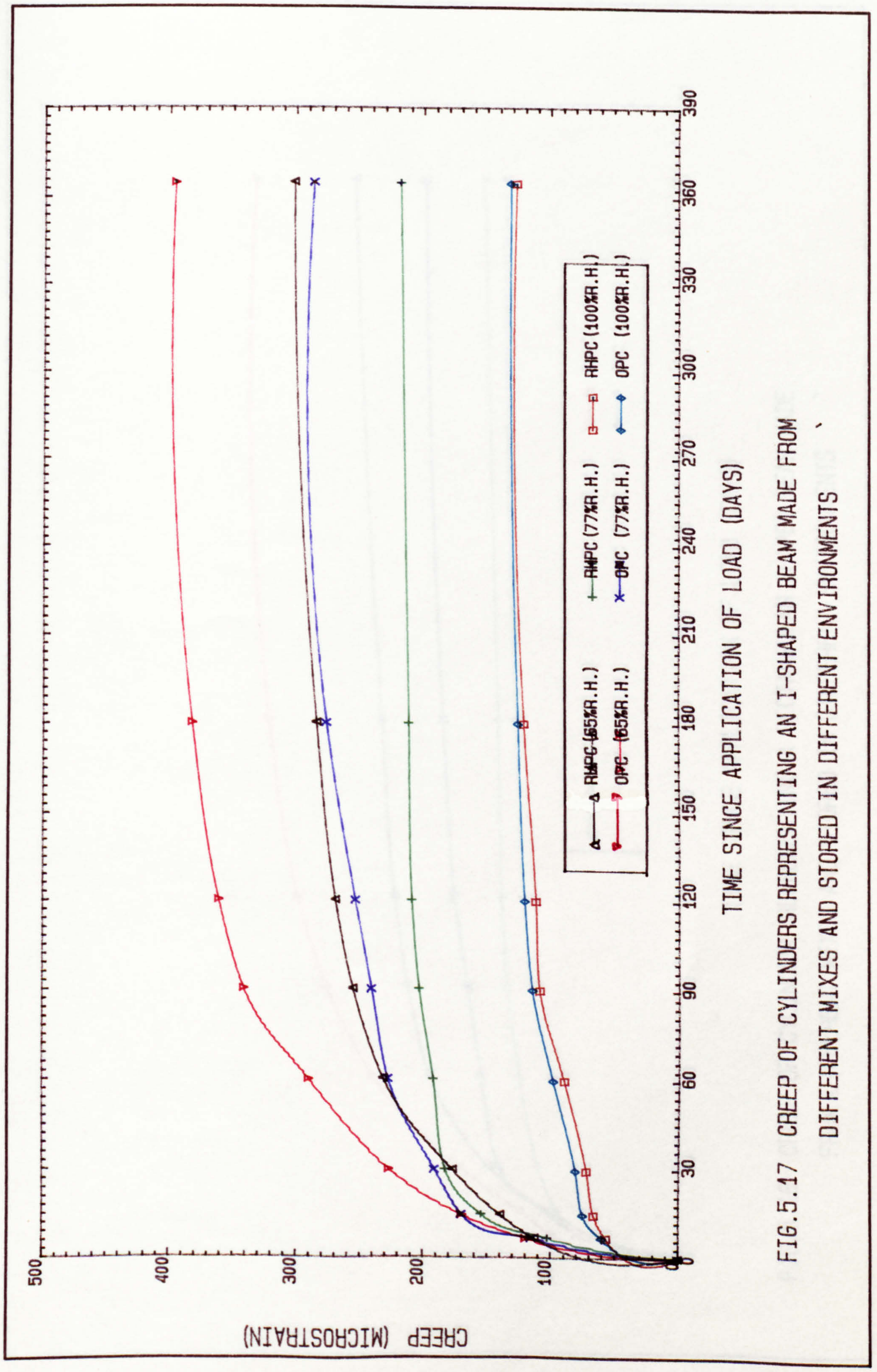

FIG.5.17 CREEP OF CYLINDERS REPRESENTING AN I-SHAPED BEAM MADE FROM DIFFERENT MIXES AND STORED IN DIFFERENT ENVIRONMENTS

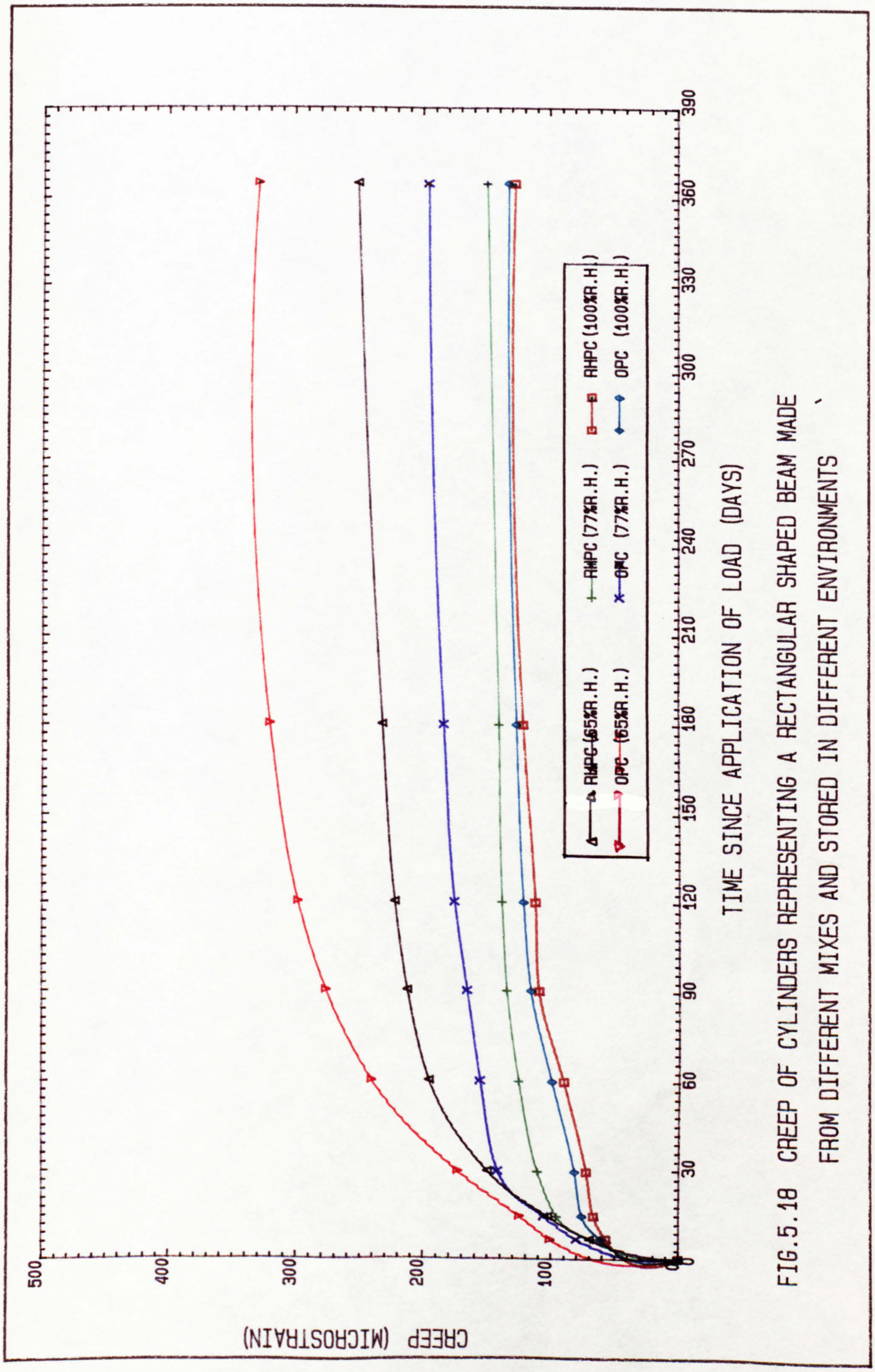

FIG.5.18 CREEP OF CYLINDERS REPRESENTING A RECTANGULAR SHAPED BEAM MADE FROM DIFFERENT MIXES AND STORED IN DIFFERENT ENVIRONMENTS

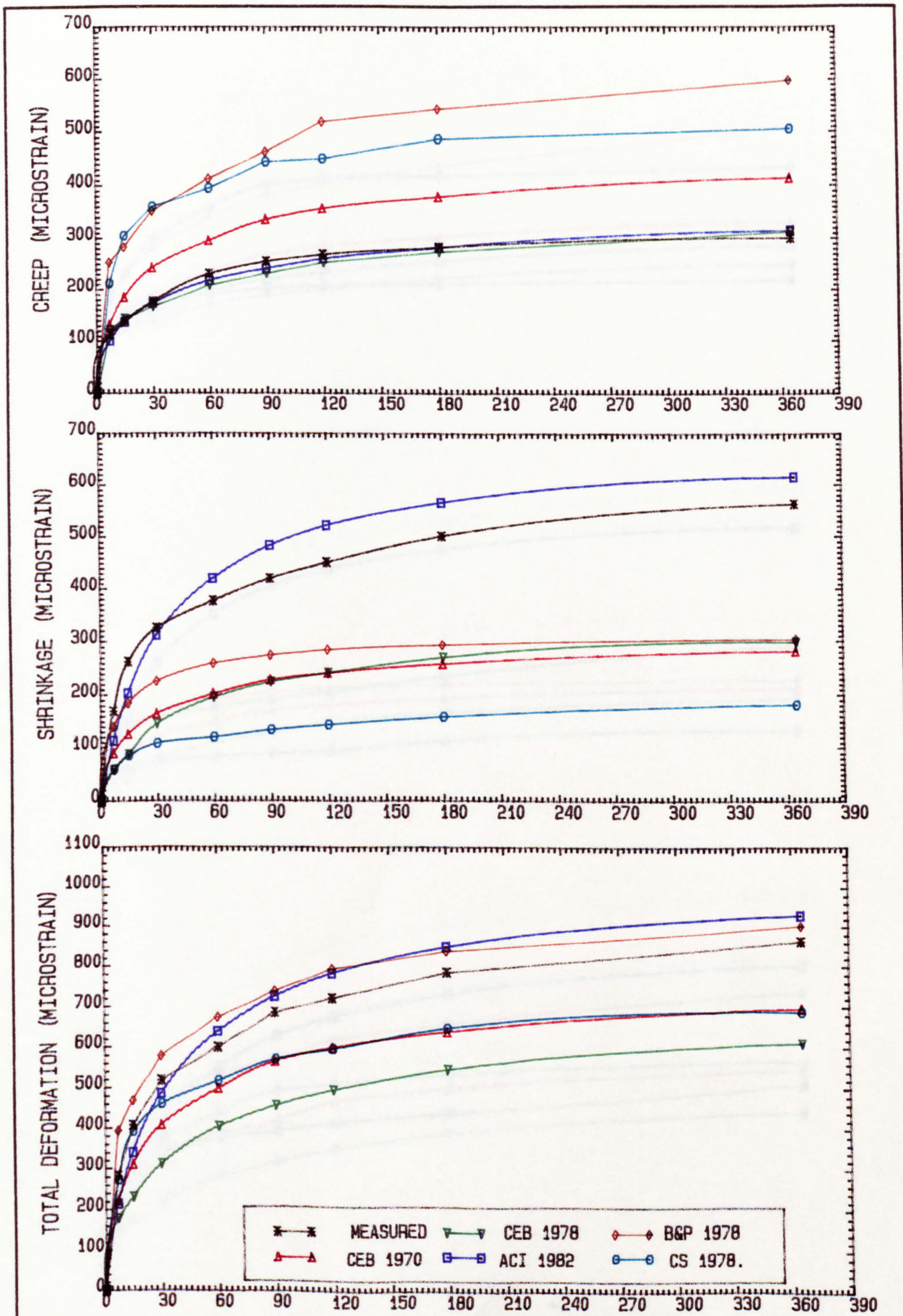

FIG. 5.19 RELATION BETWEEN MEASURED AND PREDICTED VALUES OF LONG-TERM DEFORMATIONS FOR CYLINDERS REPRESENTING AN I-SHAPED BEAM MADE FROM RHPC MIX AND STORED IN A CONSTANT HUMIDITY

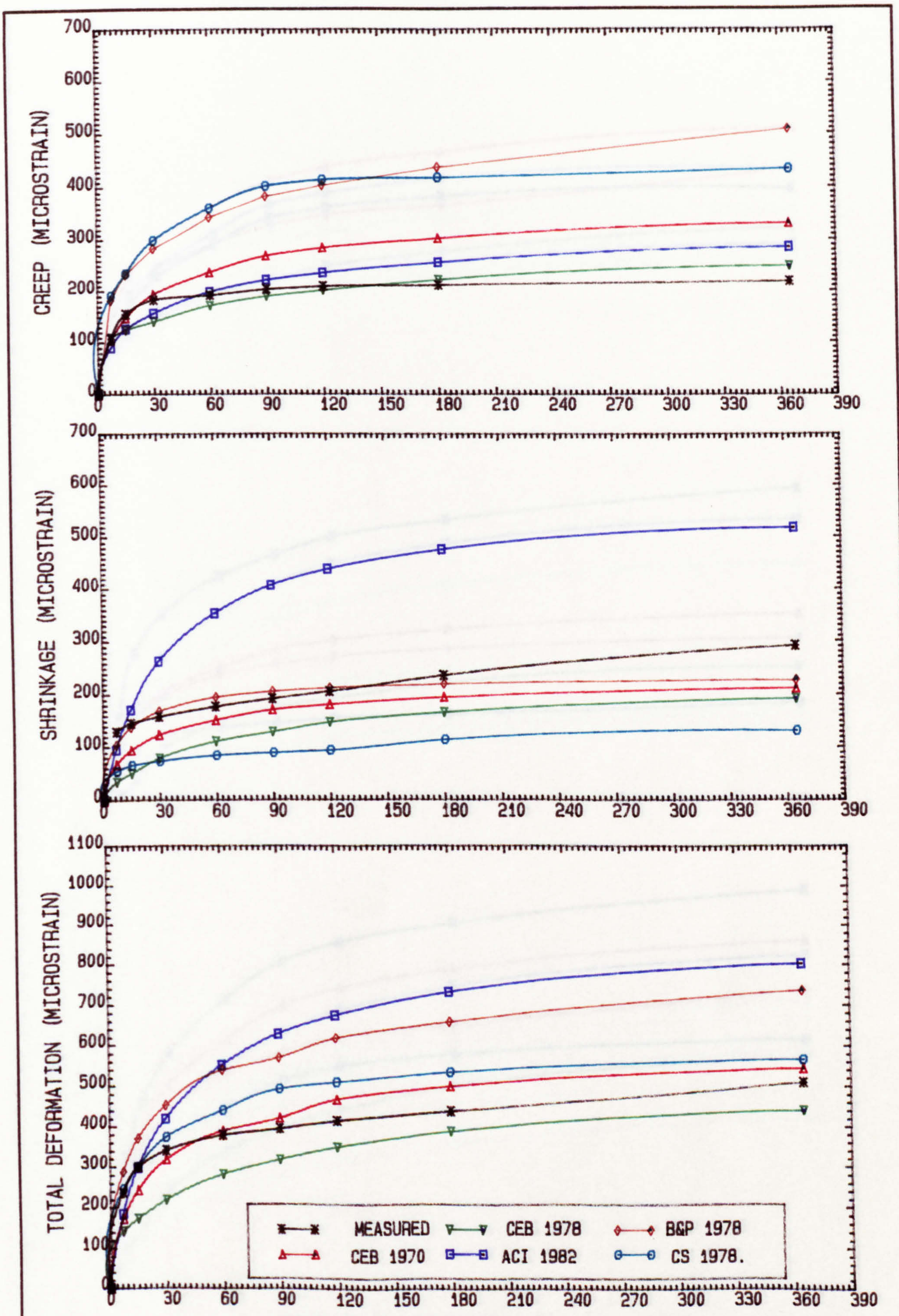

FIG. 5.20 RELATION BETWEEN MEASURED AND PREDICTED VALUES OF LONG-TERM DEFORMATIONS FOR CYLINDERS REPRESENTING AN I-SHAPED BEAM MADE FROM RHPC MIX AND STORED IN A VARIABLE HUMIDITY

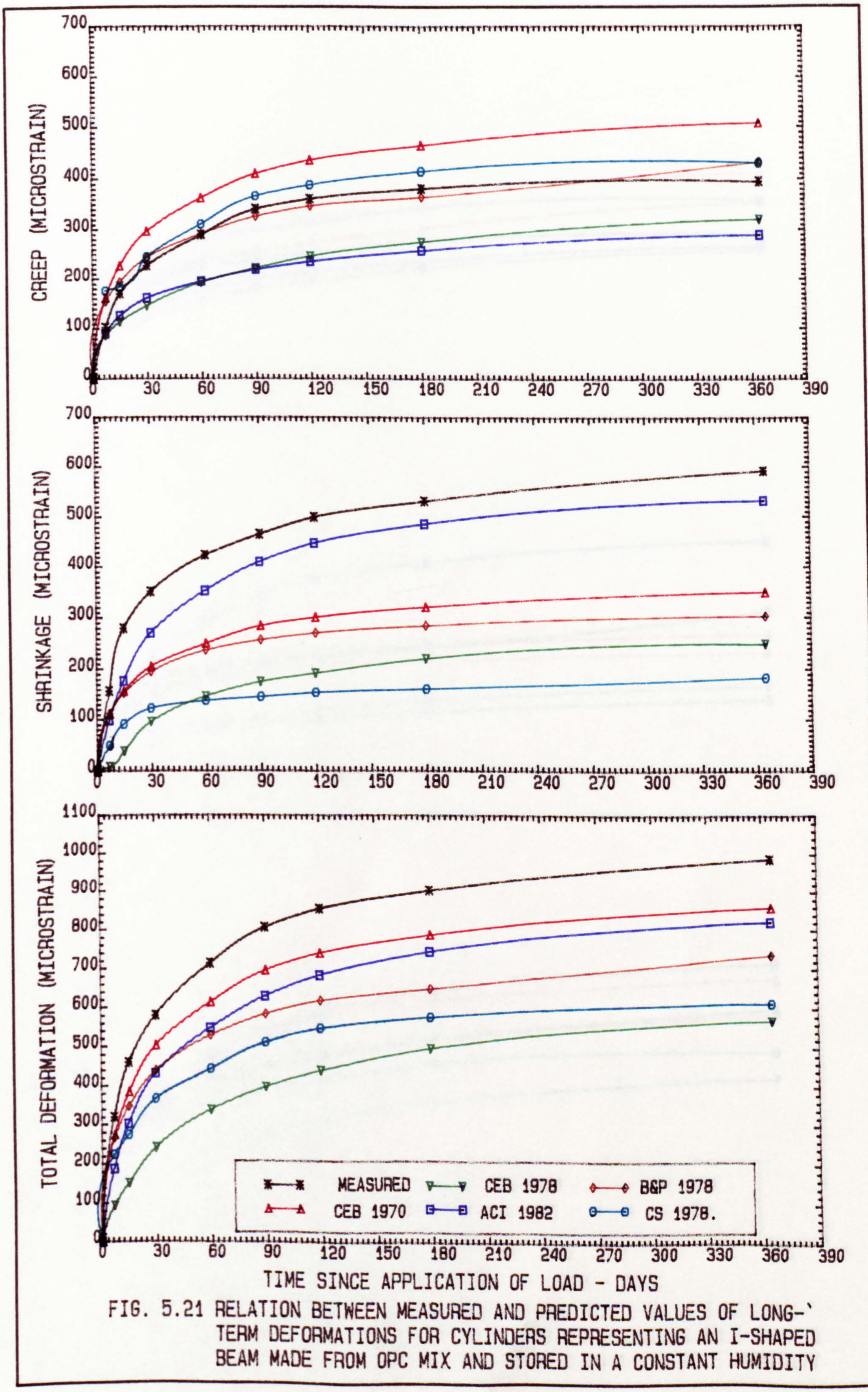

FIG. 5.21 RELATION BETWEEN MEASURED AND PREDICTED VALUES OF LONG-TERM DEFORMATIONS FOR CYLINDERS REPRESENTING AN I-SHAPED BEAM MADE FROM OPC MIX AND STORED IN A CONSTANT HUMIDITY

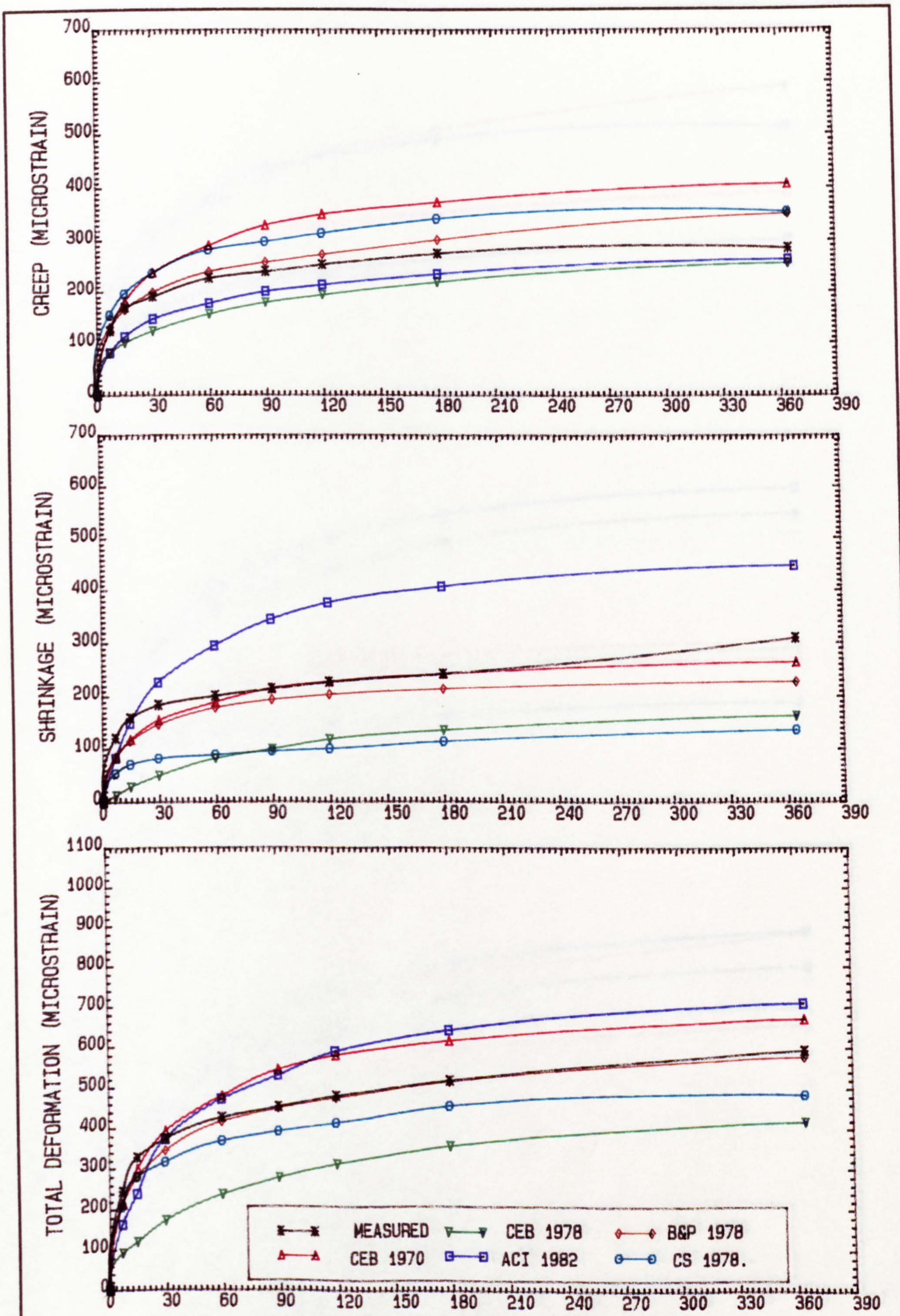

FIG. 5.22 RELATION BETWEEN MEASURED AND PREDICTED VALUES OF LONG-TERM DEFORMATIONS FOR CYLINDERS REPRESENTING AN I-SHAPED BEAM MADE FROM OPC MIX AND STORED IN A VARIABLE HUMIDITY

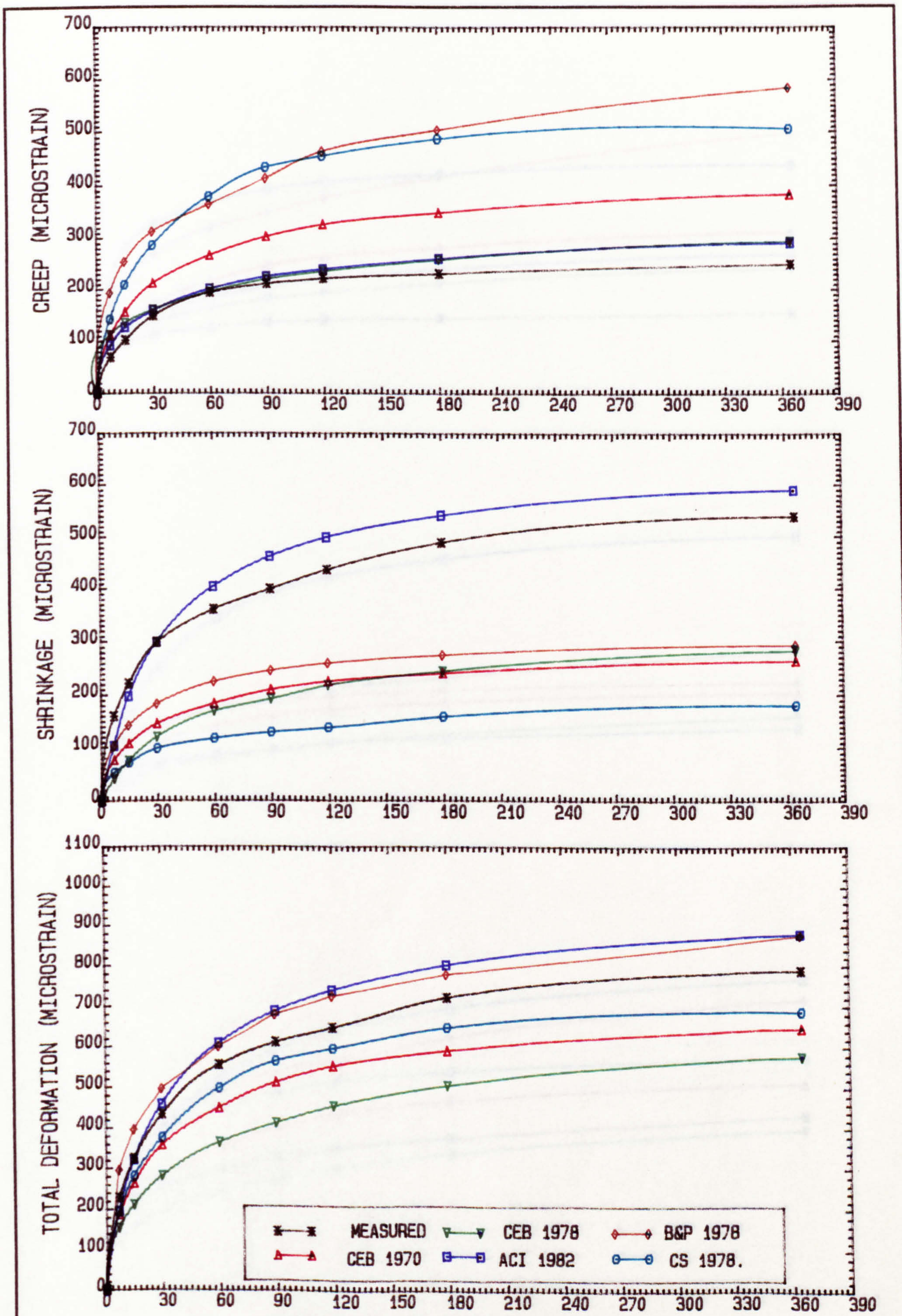

FIG. 5.23 RELATION BETWEEN MEASURED AND PREDICTED VALUES OF LONG-TERM DEFORMATIONS FOR CYLINDERS REPRESENTING A RECTANGULAR-SHAPED BEAM MADE FROM RHPC MIX AND STORED IN A CONSTANT HUMIDITY

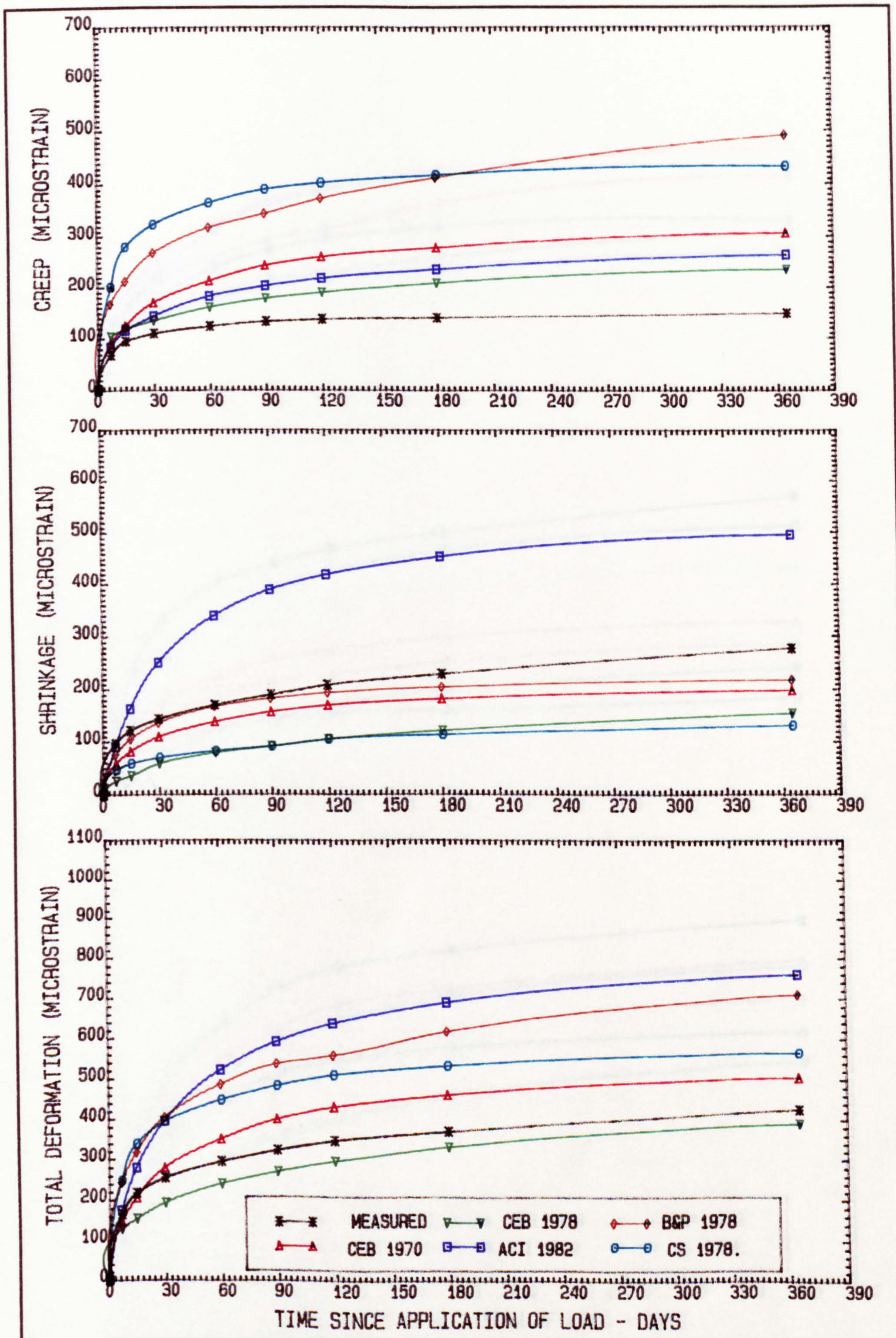

FIG. 5.24 RELATION BETWEEN MEASURED AND PREDICTED VALUES OF LONG-TERM DEFORMATIONS FOR CYLINDERS REPRESENTING A RECTANGULAR-SHAPED BEAM MADE FROM RHPC MIX AND STORED IN A VARIABLE HUMIDITY

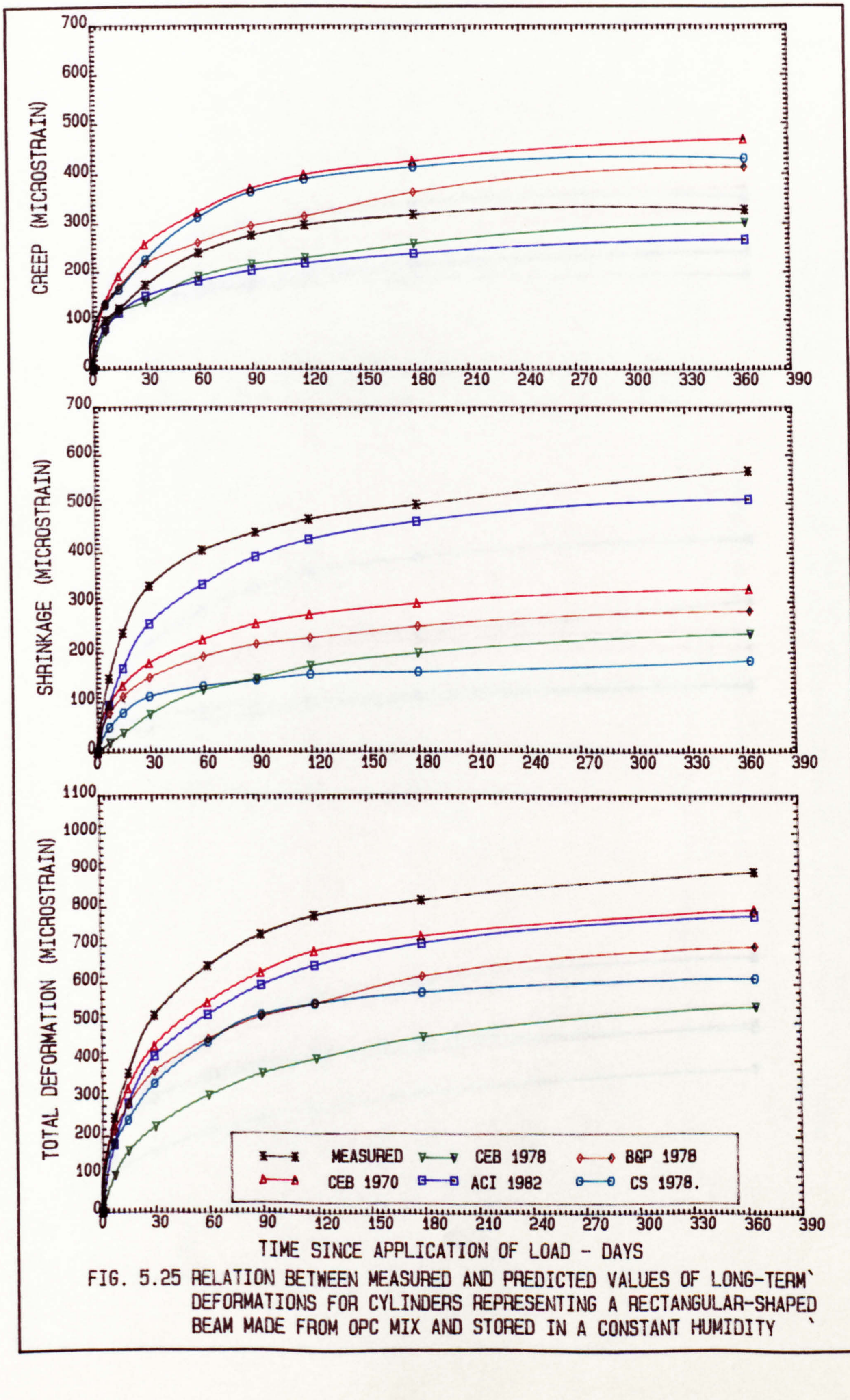

FIG. 5.25 RELATION BETWEEN MEASURED AND PREDICTED VALUES OF LONG-TERM DEFORMATIONS FOR CYLINDERS REPRESENTING A RECTANGULAR-SHAPED BEAM MADE FROM OPC MIX AND STORED IN A CONSTANT HUMIDITY

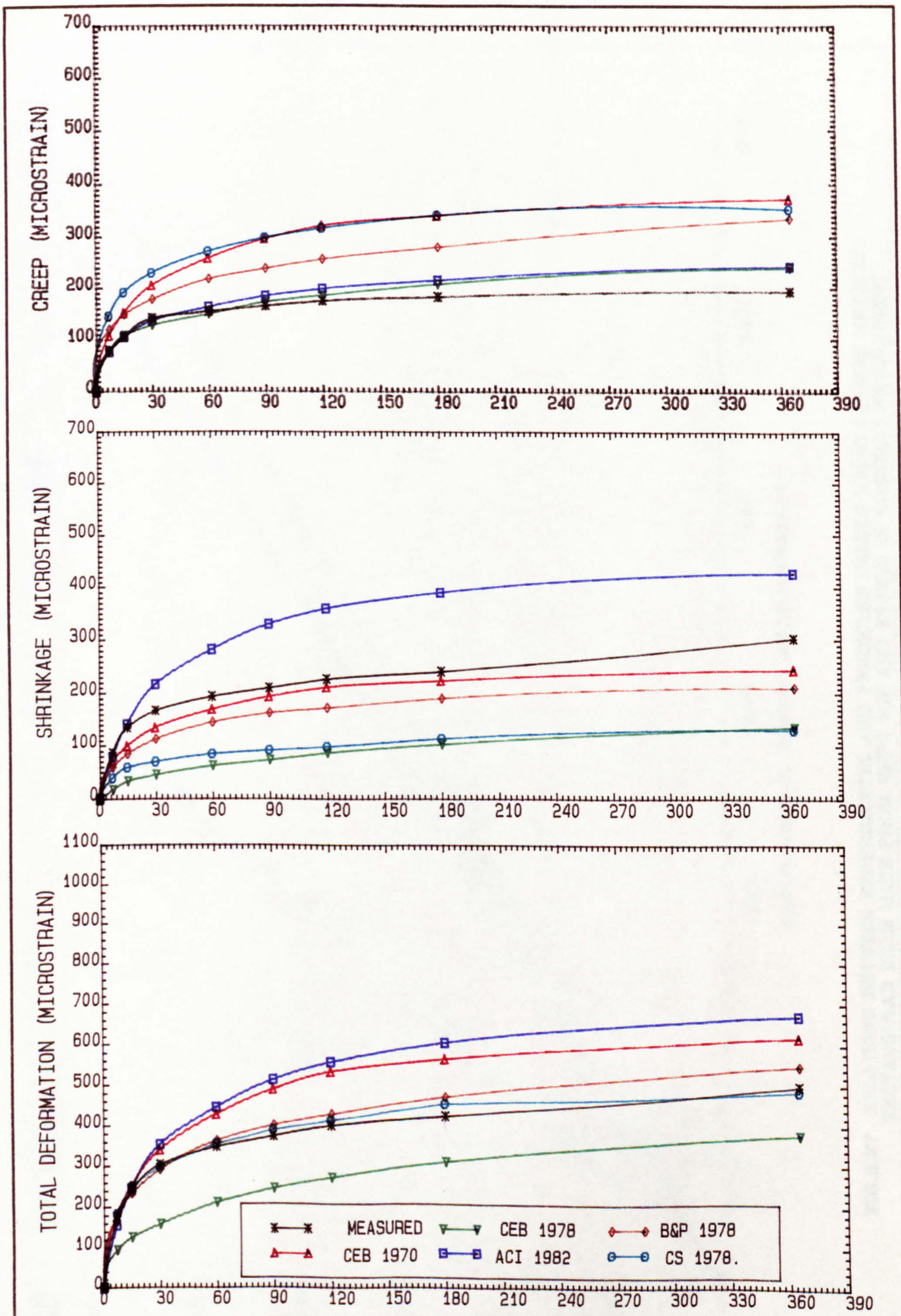

FIG. 5.26 RELATION BETWEEN MEASURED AND PREDICTED VALUES OF LONG-TERM DEFORMATIONS FOR CYLINDERS REPRESENTING A RECTANGULAR-SHAPED BEAM MADE FROM OPC MIX AND STORED IN A VARIABLE HUMIDITY

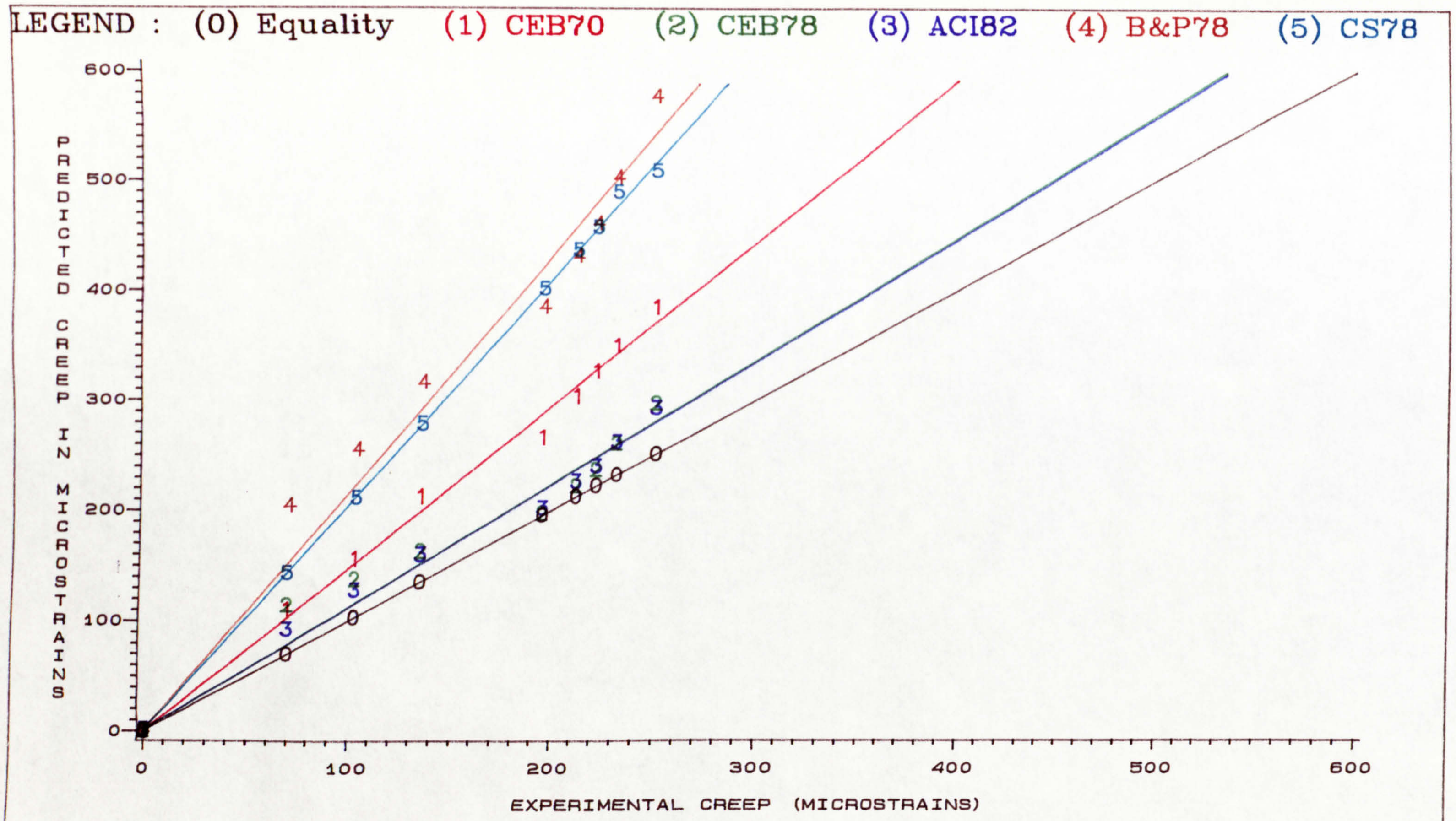

FIG.5.27 RELATIONS BETWEEN EXPERIMENTAL AND PREDICTED VALUES USING VARIOUS METHODS; RECTANGULAR BEAM MADE FROM RHPC MIX AND STORED IN CONSTANT ENVIRONMENT

CHAPTER 6 EXPERIMENTAL OBSERVATIONS OF TIME-DEPENDENT PRESTRESS LOSSES AND A COMPARISON WITH PREDICTION METHODS

6.1 Introduction

This chapter is concerned with the time-dependent prestress losses of Class-1 post-tensioned concrete structures. Several factors influencing prestress losses have been monitored experimentally, analytically examined and are discussed in this chapter.

In order to determine the reliability of various methods of predicting prestress losses, a comprehensive study has also been undertaken on a comparison between major national and international prediction methods of prestress loss with experimental results obtained during this research programme..

6.2 Analysis and Discussion of Test Results

6.2.1 Effect of Environmental Conditions

Despite the fact that there have been many laboratory tests conducted on creep and shrinkage of concrete and long-term behaviour of prestressed concrete members, there have been few attempts to investigate the actual behaviour of members under field storage conditions with companion laboratory and field stored specimens.

Actual prestressed concrete members in the field are subjected to fluctuations in relative humidity and temperature of the surrounding atmosphere. Therefore, effects of variable humidity on time-dependent deformations of prestressed concrete members are important phenomena for design consideration. In applying results of constant humidity tests to site exposure it is necessary to know the correlation between the results of analyses based on material properties of constant humidity stored specimens, and the actual behaviour of the structure under fluctuating humidity conditions.

Diagrams showing measured concrete strain distribution for all concrete beams stored in different environmental conditions are shown in Figures 6.1 to 6.27. It can be seen that in nearly all cases the mean total concrete strain curves are actually straight lines. Although some variation from a straight line was found in individual rows of gauges, the average strain distribution was linear throughout the depth of the cross-section. If the shrinkage strains are accepted as being constant across the depth of the beam, then this also leads to the conclusion that creep strains are linearly proportional to stress.

From the measured strains across the depth of the beam, the strain at the centre of gravity of the prestressing steel can be interpolated. Prestress loss is then computed from this strain knowing the modulus of elasticity and area of prestressing steel, and by finally including the steel relaxation loss based on the proposed expression (44) of Eq. (2.4) described earlier in Section 2.1.3.2, (which produces values close to the 1000 hour relaxation

value supplied by the wire manufacturer for the wire used in the present study).

Figures 6.1 to 6.27 show the mid-span loss of prestress and the average concrete strain at the steel level. It should be noted that the measured prestress losses used in this chapter are mainly based on the wire strain gauge reading obtained which seems to give slightly higher loss values than those based on the measured concrete strain at the steel level, and a more sensitive reading than that obtained from the load cell.

Figures 6.1 to 6.24 indicate that when beams are stored in a variable humidity environment, the total time-dependent deformation and prestress losses were reduced. Figures 6.28 to 6.31 and Tables 6.1 and 6.2 give a comparison of experimental prestress losses for various prestressed concrete beams stored in different environmental conditions. It has been observed that the variable humidity condition has caused an average of 20 percent reduction in prestress losses over a one year period of monitoring. Values of variable/constant environment ratio range from 0.886 to 0.732 for different prestressed concrete beams as shown in Tables 6.1 and 6.2. Similar findings have been observed by previous investigators (31, 35, 48) for different constant relative humidities. The principal reason that total prestress losses in beams in a variable environment are less than the total prestress losses of the companion constant environment beams lies mainly in the amount of shrinkage that has taken place, although the effect of concrete creep also contributes to this difference. For the variable

environmental condition, variation in relative humidity produced variation of concrete strains, which was not the case for the constant humidity condition, where strains increased continuously at a low rate because of continuous drying maintaining creep and shrinkage deformations in the structural members.

6.2.2 Effect of Loading Conditions

The measured concrete strain distribution diagrams are presented in Figs. 6.1 to 6.24. It can be seen that when the service load is applied there are instantaneous elastic and time-dependent changes in strains at the top and bottom fibres of the beam, with a general tendency to place the top fibres in compression and the bottom fibres of the member under low compression. On the other hand the cyclic service load imposed on beams tended to exhibit similar values for compressive strains at the top and bottom of prestressed beam fibres. This point is pursued in Table 6.1 and 6.2, from which it is determined that, at 365 days after prestressing, the total time-dependent deformation at steel wire level seems to be greater for non-loaded beams than cyclic and sustained loaded beams, whereas the deformtion of the cyclic loaded beam seems to give values which lie between the strain deformation values of the non-loaded and sustained loaded beams. Consequently, it can be seen that the development of prestress losses has occurred in a manner similar to the time-dependent deformation.

Figures 6.28 and 6.29 show the influence of loading conditions on time-dependent prestress losses for I-shaped and

rectangular shaped beams, respectively. It is clear that for the constant sustained service load, the average prestress loss for different shaped beams was between 19 and 13 percent lower than the non-loaded beams for constant and variable humidity conditions respectively. These trends are similar to those obtained by previous investigators (30, 31, 32, 48, 95). It is thought that the reduction in prestress losses for loaded beams is probably caused by the reduction of creep at steel level. For loaded beams, the loss of prestress due to creep was approximately 28 and 48 percent of the creep loss of prestress of the non-loaded beams for constant and variable environments, respectively. Furthermore, the creep loss in loaded beams stored in variable humidity seems to be higher than beams stored in a constant humidity. This is thought to be caused by the cyclic variation in prestressing force due to the drying and wetting cycle increasing the contraction of the beam.

For cyclic loaded beams, the average prestress losses for different shaped sections were between 11 and 2 percent lower than the non-loaded beams for constant and variable environments, respectively. The reduction is mainly caused by the loss of prestress due to creep which is approximately 47 and 94 percent of the creep loss of the non-loaded beams for constant and variable environments, respectively. Therefore, it was found that values of prestress loss were equal to the average prestress losses of non-loaded and loaded beams stored in constant environment. Whilst for variable environment, the effect of cyclic loading seems to be negligible and it's prestress losses can be considered equal to prestress losses of the non-loaded beams.

The results obtained for the sustained service load and cyclic load conditions serve generally to point out the relatively beneficial effect of loading prestressed concrete beams as early as possible (since imposed loading decreases creep at tendon level).

6.2.3 Effect of Shape and Size of Members

The effect of cross-sectional shape on time-dependent deformations and prestress losses is shown in Table 6.3. It is clear that the I-shaped beams with a volume/surface ratio of a 21.8 mm exhibit higher concrete deformations and prestress losses than the rectangular beams of 31.4 mm volume/surface ratio, i.e. the lower the volume/surface ratio the higher the concrete deformations and hence the higher prestress losses. These observations support findings of previous workers (35, 96).

Referring to Table 6.3, it can be seen that for beams stored in constant environment, the mean prestress loss of the rectangular shaped beams is 7 percent lower than the I-shaped beams with a percentage variation range of 3 to 9 percent. This loss is associated with the percentage variation of total concrete deformation at the tendon level which ranged from 4 to 13 percent. Similar trends were obtained for beams maintained in variable environment in which the mean prestress loss of the rectangular shaped beams is 10 percent lower than the I-shaped beam with a percentage variation ranging from 8 to 16 percent, corresponding to total concrete deformation of a percentage variation ranging from 15 to 27 percent.

In view of this, it is interesting to notice that the percentage loss variation between the rectangular and the I-shaped beams stored in a variable environment seems to be greater than that for beams stored in constant environment. This is thought to be mainly associated with the high shrinkage variation between the two shapes (as presented in Table 5.5) causing a bigger difference in shrinkage loss of prestress. The general results were in agreement with test results obtained by Hanson (96).

6.2.4 Effect of Concrete Mix Composition

The effect of mix composition on time-dependent deformation and prestress loss at an age of one year is illustrated in Table 6.4. The test results show that the RHPC concrete beams always exhibit lower prestress losses than the OPC concrete beams maintained in constant and variable humidity conditions. The variation in prestress losses is mainly caused by creep and shrinkage behaviour of each concrete mix as discussed earlier in Section 5.2.3.1. For the grouted non-loaded I-beam, the prestress loss at one year for the RHPC beams is about 3 percent lower than the OPC beams for both constant and variable environmental conditions. It is also clear that there is little difference in the percentage loss of prestress between beams of the two mixes when storage conditions are the same, these observations essentially agree with those obtained by Peterson (35) for grouted prestressed concrete members stored in different constant environments. In the case of non-loaded I-beam with non-grouted tendon, the average prestress losses of the RHPC beams are 9 percent lower than the OPC

beams for constant and variable humidity conditions. This may be due to the shortening of the non-grouted tendon towards it's initial length which tend to alter the behaviour of creep deformation at steel level and prestressing force for both concrete mixes.

The effect of concrete mixes on prestress losses of cyclic and sustained loaded beams stored in constant and variable environment are presented in Fig. 6.31 and Table 6.4. It was observed from the rectangular section beams which had been stored in a constant humidity condition that prestress losses for the RHPC beams were 6.5 and 8.3 percent lower than the OPC beams of cyclic and constant loading conditions, respectively. However, it is interesting to note that when the loaded beams are maintained in a cyclic drying and wetting environment, the prestress losses of beams having RHPC and OPC concrete mixes seem to be more or less the same. This behaviour may be associated with the fluctuation of creep deformation at steel level caused by the drying and wetting environment and loading conditions which in turn tend to alter the prestress losses of both concrete mixes.

The influence of superplasticizing admixture and PFA on time-dependent prestress losses has been studied and compared with the RHPC control beam as presented in Fig.6.32 and Table 6.4. It can be seen from the test results of the I-shaped beams stored in constant environment, that the superplasticizing admixture beam (NI/C3) exhibited the largest prestress loss, the percentage loss of prestress being about 14 percent higher than the RHPC control beam. This may be explained by the fact that the admixture concrete

exhibited the highest creep and shrinkage deformation as mentioned earlier in Section 5.2.3.1; also this can be deduced from Fig. 6.25 which it shows a high rate of total strain deformation at steel level.

In the case of PFA concrete beam (NI/C4), the 30 percent replacement of cement by PFA seems to reduce the prestress losses at one year by 7.4 percent when compared with the prestress loss of RHPC control beam. A similar trend was observed for admixture & PFA concrete beam (NI/C5) which seems to exhibit an 11.5 percent reduction in prestress loss when compared with the RHPC control beam values. The reduction of prestress losses when using PFA on the one hand, and admixture & PFA on the other is believed to be associated with the lower rate of creep and shrinkage deformation of the two concrete mixes when compared with the deformation of plain RHPC concrete mix, as described earlier in Section 5.2.3.1. In view of this, it should be pointed out that the PFA concrete beam (NI/C4) and the admixture & PFA beam (NI/C5) have a delayed age at prestressing transfer of 8 and 5 days, respectively, when compared with the 2 days age of transfer for the RHPC concrete beam (NI/C1). This reduction in prestressing losses seems to be beneficial and promising for concrete structural application especially when using the combination of PFA and a superplasticizing admixture with RHPC.

6.3 Comparison between Experimental Results and Current Prediction Methods

6.3.1 Major Prediction Methods of Prestress Losses

In the following sections, the methods used in several specifications and codes of practice for time-dependent prestress loss prediction in post-tensioned members will be presented. These methods deal specifically with the loss of prestress at any time, with the exception of the ACI-ASCE Joint Committee (100) and ASSHTO specifications (60) in which only the ultimate loss of prestress is taken into consideration.

6.3.1.1 Comite Europeen du Beton, CEB-1970 (15)

The total loss due to shrinkage and creep of the concrete and due to relaxation of the steel tendons is as follows:

$$\text{Total loss} = \Delta\sigma_{ap,r+f} + \Delta\sigma_{ap} \times \sigma_{ap,o} \qquad \text{Eq.6.1}$$

in which $\Delta\sigma_{ap,r+f}$: loss in tension in the steel due to deferred shortening caused by shrinkage and creep

$\Delta\sigma_{ap}$: the apparent relaxation

$$\Delta\sigma_{ap} = \Delta\sigma_{ap,t}\left[1 - \frac{3\Delta\sigma_{ap,r+f}}{\sigma_{ap,o}}\right] \qquad \text{Eq.6.2}$$

where $\sigma_{ap,o}$ represents the initial tension in the steel

$\Delta\sigma_{ap,t}$ is the pure relaxation of the steel at time t

The relaxation of steel is evaluated from test results, given by the supplier, for a temperature of $20^{o}C$ and for the following values of

the initial stress, expressed as a function of the characteristic strength; 0.6 f_{pu}, 0.7 f_{pu}, 0.8 f_{pu}.

In the absence of long-term tests, it is advisable to take values not less than those given in Table (A.1) - Appendix A which corresponds to an initial stress equal to 0.8 f_{pu} and are given as a percentage of this stress.

It has been shown that relaxation varies with time according to a straight-line law of the logarithmic type

$$\log\left(\frac{\Delta\sigma_{ap,t}}{\sigma_{ap,o}}\right) = K_1 + K_2 \log t$$

where $\Delta\sigma_{ap,t}$ represents the relaxation loss at time t and the coefficients K_1 and K_2 depend on the type of prestressing steel. The long-term relaxation is assumed to be double the value at 1000 hours.

Prestress loss due to shrinkage and creep is given by:

$$\Delta\sigma_{ap,r+f} = E_s(\varepsilon_{CR}(t,t_o) + \Sigma_{sh}(t,t_o))$$

in which $\varepsilon_{CR}(t,t_o)$ creep strain (see Section 4.2.1.1)

and $\Sigma_{SH}(t,t_o)$ shrinkage strain (see Section 4.2.1.2)

6.3.1.2 Comite Europeen du Beton, CEB-1978 (16)

The evaluation of time-dependent losses due to shrinkage and

creep of the concrete and relaxation of the steel should take account of the interdependence of these phenomena. An approximate value for the time-dependent losses at time t is given by the following empirical formula:

$$\Delta\sigma_{p,t} = \Delta\sigma_{p,c+s,t} + \Delta\sigma_{p,rel,t}\left[1 - 2\,\frac{\Delta\sigma_{p,c+s,t}}{\sigma_{po}}\right] \qquad \text{Eq.6.3}$$

$$\Delta\sigma_{p,c+s,t} = Es\left(\varepsilon_{CR}(t,t_o) + \Sigma_{Sh}(t,t_o)\right) \qquad \text{Eq.6.4}$$

where $\Delta\sigma_{p,c+s,t}$ denotes the loss of prestress in steel due to shortening of the concrete as a result of creep and shrinkage,

$\varepsilon_{CR}(t,t_o)$ denotes the shortening of the concrete as a result of creep (from the age t_o, the time of prestressing) under a constant stress equal to the final stress at the level of steel tendons under the effect of the prestress, the permanent actions and the variable actions at their quasi-permanent value,

$\Sigma_{sh}(t,t_o)$ shrinkage strain (section 4.2.2.2.)

and $\Delta\sigma_{p,rel,t}$ denotes the pure relaxation of the steel under a stress equal to the initial stress in the prestressing steel σ_{po} due to prestress alone.

6.3.1.3 American Concrete Institute, ACI-1982 (8)

Loss of prestress in non-loaded prestressed beams at any time (λ_t), as a percentage of the initial tensioning stress, is

given by:

$$\lambda_t = \underbrace{[(nf_c)}_{(1)} + \underbrace{(nf_c) \times \phi(t,t_o)(1 - \frac{F_t}{2F_o}) + \frac{\Sigma_{sh}(t,t_{sh,o})}{(1+n\rho\xi_s)} + (f_{sr})_t]}_{(2)} \underbrace{\frac{100}{f_{si}}}_{(3)} \quad \text{Eq.6.5}$$

where:

Term (1) is the prestress loss due to elastic shortening, in

which $f_c = \frac{F_i}{A_t} + \frac{F_i e^2}{I_t} - \frac{M_D e}{I_t}$, and n is the modular ratio

(E_s/E_c) at the time of prestressing. Frequently F_o, A_g and I_g are used as an approximation instead of F_i, A_t and I_t,

where M_D is the bending moment due to dead load

F_i,F_o represent the initial prestress force and prestress force at transfer, after elastic loss, respectively, being

$F_o = F_i (1-n\rho)$; ρ denote reinforcement ratio.

A_t, A_g denote the area of transformed section and area of gross section, respectively.

I_t, I_g denote by the moment of inertia of transformed section and gross section, respectively.

Term (2) is the prestress loss due to the concrete creep and $\phi(t, t_o)$ represents the creep coefficient (Section 4.2.3.1). Approximate values of F_t/F_o are given in Table (A.2) - Appendix A.

Term (3) is the prestress loss due to shrinkage

where $\Sigma_{sh}(t,t_{sh,o})$ represents the shrinkage strain (Sec.4.2.3.2), and ξ_s denotes by the cross section shape coefficent (1 + e^2/r^2)

Term (4) is the prestress loss due to steel relaxation. Values of $(f_{sr})_t$ for wire and strand are given in Table (A.3) - Appendix A, where t is the time after initial stressing in hours and f_y is the 0.1 percent offset yield stress.

Loss of prestress in prestressed beams under the effect of sustained loads at any time ($\lambda_{t,1}$), as a percentage of the initial tensioning stress (98), is given by:

$$\lambda_{t,1} = \underbrace{\lambda_t}_{(1,2,3,4)} + \underbrace{[-(mf_{cs})}_{(5)} \underbrace{- (mf_{cs})(C_{ts})/(1+b)]}_{(6)} \frac{100}{f_{si}} \qquad \text{Eq.6.6}$$

where:

Term (5) is the elastic prestress gain due to the superimposed sustained load. $f_{cs} = M_s\ e/I_g$, and m is the modular ratio at the time of load application, and M_s is the moment due to the superimposed load.

Term (6) is the prestress gain due to concrete creep under the superimposed sustained load. C_{ts} is the creep coefficient, where the age of the beam concrete at the time of load application is taken into account, and b represents the secondary effect of shrinkage and creep parameters as given by:

$$b = n\rho\xi_s[1 + \dot{R}\phi(t,t_o)]$$

where R is the relaxation coefficient due to creep effect.

6.3.1.4 British Code, CP110-1972 (99,100)

According to Clause 4.8.2.2, the relaxation loss of force in the tendon allowed for in the design should be the maximum relaxation after 1000 hour duration, for a jacking force equal to that imposed at transfer. The relaxation loss may be assumed to decrease linearly from 8% for an initial prestress of 70% to 0% for an initial prestress of 50% of the characteristic strength of the tendon.

The loss of prestress in the tendons due to creep of concrete (ΔF_c), as given by Clause 4.8.2.5 is:

$$\Delta F_c = E_s \varepsilon_c f_{co} \qquad \text{Eq.6.7}$$

where ε_c is the creep per unit length, for concrete cube strength at transfer greater than 40.0 MPa, $_c$ values are given for both pre-and post-tensioning as 48×10^{-6} and 36×10^{-6} per MPa, respectively. When the maximum stress at transfer is half the cube strength, the values for creep are 1.25 times the values given above, and f_{co} is the stress in concrete adjacent to the centroid of the tendons and has the same value as used in the calculation of the loss due to elastic shortening.

The loss of prestress in the tendons due to shrinkage of concrete (ΔF_{sh}) is calculated according to Clause 4.8.2.4, as given by:

$$\Delta F_{sh} = E_s A_p \Sigma_{sh} \qquad \text{Eq.6.8}$$

where Σ_{sh} is the shrinkage per unit length obtained from Table (A.4) - Appendix A, and A_p is the area of prestressing steel. The creep and shrinkage values given are related to the ultimate values after a period of years. It may be assumed that half the total creep and shrinkage take place in the first month after transfer and that three-quarters of the total creep takes place in the first six months after transfer.

6.3.1.5 British Code, BS8110-1985 (60)

The long-term relaxation loss of force in the tendon allowed for in the design is obtained by multiplying the appropriate factor given in Table (A.5) - Appendix A by the 1000 hour relaxation test values. The relaxation factors include allowances for the effects of strain reductions due to creep and shrinkage of the concrete. According to BS5896:1980, the final relaxation loss for wire of Class 1 used for post-tensioning is twice the relaxation value of the 1000 hour duration.

The loss of prestress in tendons due to creep of concrete (ΔF_c) is given by:

$$\Delta F_c = E_s A_p \varepsilon_{cc} \qquad \text{Eq.6.9}$$

where ε_{cc} is the creep strain in concrete, as indicated in Clause 7.3, Part 2:

$$\varepsilon_{cc} = \frac{\text{Stress}}{E_t} \times \phi$$

where E_t is the modulus of elasticity of the concrete at the age of loading t, and ϕ is the creep coefficient obtained from Fig. 4.5a (Section 4.2.5.1, chapter 4).

For general design purposes, it can be assumed that about 40%, 60% and 80% of the final creep develops during the first month, 6 months and 30 months under load, respectively, when concrete is exposed to conditions of constant relative humidity.

The loss of prestress in the tendons due to shrinkage of concrete (ΔF_{sh}), as indicated in Clause 4.8.4 is given by:

$$\Delta F_{sh} = E_s A_p \Sigma_{sh} \qquad \text{Eq. 6.10}$$

where Σ_{sh} is the shrinkage per unit length obtained from Fig.4.5b (Section 4.2.5.2); reference should be made to Section seven of BS8110 : Part 2 : 1985.

6.3.1.6 Joint Committee of the American Concrete Institute and American Society of Civil Engineers, ACI-ASCE, 1979 (101)

The final loss of prestress due to creep is computed for bonded members from the following expression (for normal weight concrete)

$$CR = K_{cr} \frac{E_s}{E_c} (f_{cir} - f_{cds}) \qquad \text{Eq.6.11}$$

where K_{cr} = 1.6 for post-tensioned members,

E_c modulus of elasticity of concrete at 28 days,

f_{cir} net compressive stress in concrete at centre of gravity of tendons immediately after the prestressing,

and f_{cds} stress in concrete at centre of gravity of tendons due to all superimposed permanent dead loads that are applied to the member after prestressing.

The final loss of prestress due to shrinkage is given by:

$$SH = 550 \times 10^{-6} K_{sh} E_s (1-0.06 \frac{V}{s})(1.5-0.015\ RH) \qquad \text{Eq.6.12}$$

where 550×10^{-6} is taken as the basic ultimate shrinkage strain value in which:

K_{sh} is factor taken from Table (A.6) for post-tensioned members, and

V/S is the volume to surface area ratio.

The final loss of prestress due to relaxation of tendon is given by:

$$RE = (K_{re} - J(SH + CR + ES))C \qquad \text{Eq. 6.13}$$

This equation has the factor J from Table (A.7) to estimate the effect of reduction of the tendon stress due to elastic

shortening (ES), creep and shrinkage; K_{re} is value taken from Table (A.7); C is value taken from Table (A.8).

6.3.1.7 ASSHTO Standard Specification for Highway Bridges, ASSHTO-1977 (13)

The final loss of prestress due to creep of concrete at steel tendons level is given by:

$$CR_c = 12\ f_{cir} - 7\ f_{cds} \qquad \text{Eq. 6.14}$$

The final loss of prestress due to shrinkage of concrete for post-tensioned member is given by:

$$SH = 0.8\ (117.21 - 1.034\ RH),\ \text{in MPa} \qquad \text{Eq. 6.15}$$

where RH = average ambient relative humidity in percent.

For ultimate tensile strength of steel (f's) ranging from 1724 to 1862 MPa, the final relaxation loss of prestress for post-tensioned members based on an initial stress of 0.7 f's is given by the following equation:

$$CR_s = 137.9 - 0.3\ FR - 0.4\ ES - 0.2\ (SH + CR_c) \qquad \text{Eq. 6.16}$$

where FR represents friction loss

and ES represents elastic shortening loss

6.3.1.8 Prestressed Concrete Institute, PCI-1975 (14)

The PCI method adopts the step-by-step procedure which accounts for creep and shrinkage of concrete and relaxation of steel occurring in successive time intervals. Shrinkage, from the time curing (assumed to cease until the time when the concrete is prestressed), is to be deducted from the total calculated shrinkage for post-tensioned construction. It is recommended that a minimum of four time intervals be used as follows:

Step	Time Interval	
	Beginning, t_1	End, t
1	End of curing	Age at transfer
2	End of Step 1	Age = 30 days or time of loading
3	End of Step 2	Age = 1 year
4	End of Step 3	End of service life

It is recommended that when significant changes in loading are expected, time intervals other than those recommended should be used.

The prestress loss due to creep over each time interval is given by:

$$CR = (UCR)(SCF)(MCF) \times (PCR)(f_c), \text{ psi} \qquad \text{Eq. 6.17}$$

where f_c is the net concrete compressive stress at the centre of gravity of the prestressing force at time t_1 taking into account the loss of prestress force occuring over the preceding time interval,

UCR = ultimate loss of prestress due to creep of concrete (psi per psi of compressive stress in the concrete) and is given by:

$$UCR = 95 - 20\ E_c/10^6 \geq 11$$

for moist curing not exceeding 7 days and for normal weight concrete,

SCF = factor that accounts for the effect of size and shape of a member on creep of concrete as shown in Table (A.9).

MCF = factor that accounts for the effect of age at prestress and length of moist cure on creep of concrete as given by Table (A.10) - Appendix A,

and PCR = amount of creep over time interval t_1 to t as given by the following equation:

$$PCR = (AUC)_t - (AUC)_{t_1}$$

where AUC is portion of the ultimate creep at time after prestress transfer as presented in Table (A.11).

The prestress loss due to shrinkage over each time interval is given by the following equation:

$$SH = (USH)(SSF)(PSH),\ psi \qquad \text{Eq. 6.18}$$

where USH = ultimate loss of prestress due to shrinkage of concrete; for normal weight concrete USH is given by:

$$USH = 27{,}000 - 3{,}000\ E_c/10^6 \geq 12{,}000 \text{ psi},$$

SSF = a factor that account for the effect of size and shape of a member on concrete shrinkage (value found in Table (A.12), Appendix A),

and $$PSH = (AUS)_t - (AUS)_{t_1}$$

where AUS is portion of ultimate shrinkage at time after end of curing as presented in Table (A.13).

In post-tensioning construction, shrinkage from the time when curing is stopped until the time when the concrete is prestressed should be deducted from the total calculated shrinkage.

Loss of prestress due to steel relaxation over the time interval t_1 to t may be estimated using the following equation (for stress-relieved steel):

$$RET = f_{st}\,[(\log 24t - \log 24t_1)/10\,]\ x\ (f_{st}/f_{py} - 0.55) \qquad \text{Eq. 6.19}$$

For $f_{st}/f_{py} - 0.55 \geq 0.05$,

$f_{py} = 0.85\ f_{pu}$

where f_{st} = stress in prestressing steel at time t_1, psi

f_{py} = stress at 1 percent elongation of prestressing steel, psi,

and f_{pu} = guaranteed ultimate tensile strength of prestressing steel, psi.

6.3.2 Comparison Analysis and Discussion

This section contains a comparison of prestress loss values obtained from the current prediction methods and experimental results. In this comparison, the values obtained by using the predicted creep and shrinkage are regarded as values of general material parameters while values using the experimental creep and shrinkage are regarded as values of experimental material parameters. Figures 6.33 to 6.44 present the comparison between the predicted and experimental prestress loss values using the general and experimental material parameters for grouted beams the under self-weight loading condition having different concrete mixes and environmental conditions.

Comparisons have been made for various components of prestress losses obtained by each one of the methods, even though it is more significant to compare only the total prestress losses.

Tabulated values of each of the components of prestress loss as well as total prestress are shown in Tables 6.5 and 6.6 for non-loaded prestressed beams and in Table 6.7 to 6.8 for loaded prestressed beams. The percentage variation between experimental and predicted mid-span loss of prestress at various ages are summarized in Table 6.9.

It should be pointed out that no attempt was made in the present investigation to determine the prestress loss values by prediction methods for the cyclic loaded beams because of the complexity of such an estimation and the lengthy calculations involved. However, it is reasonable to believe that the predicted values of the cyclic loaded beams will lie within the predicted values obtained for the non-loaded and loaded beams as concluded earlier in Section 6.2.2.

Referring to Table 6.5 and 6.7, it is clear that both European model codes CEB-70 (15) and CEB-78 (16) produce similar values for prestress losses which are within -3 to +10% of the measured values for both cases of loaded and unloaded beams of different mixes and maintained in constant relative humidity, and thus lie on the safe side. This finding seems to confirm those obtained by Hernandez (32) and Brikenmair et al. (104). It is evident that both methods give a very conservative estimation of total prestress losses in spite of the underestimation of shrinkage loss (due to low predicted shrinkage, Section 5.3.2) on the one hand and overestimation of relaxation loss and creep loss (due to high predicted creep, Section 5.3.3) on the other, which in turn tends to balance and compensate each other and thus produce values similar to those measured.

According to Table 6.6 and 6.8, the predicted values of both European model codes for the condition of variable relative humidity seem to produce prestress loss values which are 11 to 27% larger than the measured values, although the CEB-78 method apparently

predicts the loss of prestress better than CEB-70 method. In this case, the rather high overestimated values is believed to be associated with the high prestress loss values due to relaxation of steel as illustrated in Table 6.6 and 6.8.

When comparing the percentage variation between measured values and predicted values based on the experimental material parameters (measured creep and shrinkage), the European model codes values seem to overestimate the total prestress losses particularly for the CEB-78 method as indicated in Table 6.9.

In the case of the ACI-82 method (8), the method gives the best and the closest predicted loss values for each individual component for the prestress losses when comapared with the measured values of constant humidity condition, in spite of the tendency of the method to slightly overestimate the total prestress losses (which are 4 to 20% larger than the measured values of both non-loaded and loaded beams) as indicated in Tables 6.5 and 6.7. These findings serve generally to confirm observations obtained by previous investigators (102, 103). However, in the case of the predicted values obtained for variable humidity condition based on the average time-relative humidity, the ACI-82 method considerably overestimates the total prestress loss values which are 18 to 33% larger than the measured values as illustrated in Table 6.9. It is clear that this overestimation in the total prestress losses is mainly caused by the shrinkage losses which are 50 to 122% larger than measured shrinkage prestress loss for different concrete beams. It is obvious that the high shrinkage loss is due to the large

predicted values of shrinkage deformation for beams maintained in the variable humidity condition as mentioned earlier in Section 5.3.2.

It is interesting to notice that when using experimental material parameters to predict the prestress losses by the ACI method, the method seems to give a very good estimation of the actual prestress losses for beams stored in variable environment with a percentage loss variation usually falling between the bounds -5 to +7% of the measured values, whilst the percentage loss variation for the constant environment remained similar to the one obtained for general material parameters.

According to the British Code CP110 (99), clear evidence of a substantial underestimation of total prestress losses can be found by comparing the predicted and observed values in which the percentage loss variation ranged from -28 to -14% of the measured values as shown in Table 6.9. It is obvious that the unconservative estimation of the total prestress losses is due to the considerable underestimation of the predicted shrinkage loss adopted by the CP110 code, whilst the creep and relaxation losses were very close to the experimental values. It should be noted that the relaxation values over 1000 hour were extrapolated by a logarithmic plot (105).

In contrast to the predicted total losses based on the general material parameters, the prestress losses based on the experimental material parameters tend to be very close to the measured values having conservative values of percentage variation

ranging from -2 to +14% for constant environment and -13 to +5% for variable environment.

In the new British Code BS8110 (60), the predicted values of total loss of prestress for the constant humidity condition seem to be reasonably close to the measured values, this point is pursued in Table 6.9, from which it is determined that the overestimated values are 3 to 20% larger than the measured values. Moreover the predicted prestressed losses for the variable humidity condition seem to be significantly greater than the measured values by 19 to 44%. It is evident that the overestimates are significantly influenced by the overestimated relaxation losses which tend to be around two-thirds larger than the measured losses: also the predicted creep losses are overestimtes due to the overestimated creep values mentioned earlier in Section 5.3.3. In contrast, the measured shrinkage losses of prestress were underestimated by more than 50% due to low values of predicted shrinkage, (Section 5.3.2).

According to the relaxation values recommended by BS8110, it is necessary to point out that when the proposed Class 1 relaxation factor of 2.0 is multiplied by the 1000 hour relaxation value in order to obtain the long-term relaxation loss, then the relaxation loss at various ages tend to be very high, whereas the previous British Code CP110 seems to be more reasonable by allowing the 1000 hour relaxation loss to be the maximum long-term relaxation loss of force in tendon. Consequently, when using a relaxation factor of 1.65 to predict the relaxation loss of prestress, better predicted relaxation and total loss of prestress values were obtained, with

values ranging from -2 to +12 percent of measured values. This factor was based on a trial and error calculation (using the creep and shrinkage losses of prestress as given by the Code of Practice) to produce the closest prestress loss estimation between the measured and predicted values. It is therefore felt that a relaxation factor of 1.65 is to be suggested instead of the 2.0 relaxation factor recently adopted by the new British Code BS8110 (for wires of Class 1 relaxation used for post-tensioned members).

In the case of using the experimental material parameters in determining the total losses of prestress according to BS8110, a cosiderable overestimation of losses were observed ranging from 33 to 45% larger than measured values as indicated in Table 6.9. It is certainly apparent that the overestimation of the relaxation prestress loss alone was responsible for the high values of total prestress losses.

According to the ACI-ASCE (101) and AASHTO (13) methods, it is evident that the methods give similar final values of long-term prestress loss since both methods tend to adopt a similar procedure. Unfortunately, the methods give the final values of prestress losses without specifying the age of the final time period or any other period since prestressing. Consequently, in order to establish a relationship between the final pretress losses of the ACI-ASCE and AASHTO methods and the one year experimental values, it was assumed that the one-year prestress loss represents 79 percent of the final time-dependent prestress loss. The assumption is based on the extrapolated one-year creep and shrinkage losses (from 6 months

to final values) of the CP110 code and, from the average creep and shrinkage loss coefficient of the PCI specification as illustrated in Tables A.11 and A.13 (Appendix A). Furthermore, the ACI method assumes that the relaxation loss at one year is equal to 79 percent of the ultimate steel relaxation loss values as obtained from Table A.3 (Appendix A). Thus if such assumption is conceivable, then the predicted one-year losses of the ACI-ASCE and AASHTO methods tend to underestimate the measured values of the constant humidity condition by 7 to 22 percent (due to low shrinkage losses - Tables 6.5 to 6.8), whereas in the case of the variable humidity condition, it can be observed that good agreement was obtained by both methods since the predicted prestress losses were within -7 to +9 percent of the measured losses.

Finally, in the case of the PCI method (14), it is certainly apparent that in spite of the considerable underestimation of shrinkage losses, the predicted total prestress losses are in agreement with measured prestress losses, values being 5 to 18% larger than measured ones and thus on the safe side, especially when 65% relative humidity values were used instead of those specified at 70% relative humidity by PCI method. Moreover, it is interesting to note that the PCI method produces final prestress losses similar to the values obtained by both the ACI and the BS8110 methods despite the variation between each individual component of prestress losses for each method.

6.4 Conclusions

For beams stored in a wetting and drying condition, the variation in relative humidity caused an average of 20 percent reduction in prestress losses when compared with the constant humidity one, having a one-year ratio of variable-to-constant environment values ranging from 0.886 to 0.732 for different concrete beams. The difference in prestress losses is mainly attributed to the shrinkage. Consequently, it must be concluded that the concept of higher relative humidities producing lower shrinkage and creep prestress losses is acceptable.

When concrete beams are subjected to different loading conditions, the test results indicate that the time-dependent concrete deformation at the tendon level tends to be greater for non-loaded than for cyclic and for sustained loaded beams, in which the cyclic loading deformations lie between values of non-loaded and sustained loaded beam. As a consequence, in the case of the sustained loading condition, the prestress loss of various beam sections averaged 16 percent lower than that of the non-loaded beams stored in different humidity conditions. The indicated reduction of total prestress losses due to loading is associated with the lower creep at the tendon level when compared with creep of non-loaded beams.

A smaller variation of loss variation was observed between cyclic and non-loading conditions, and for the variable humidity condition, the effect of cyclic loading being generally negligible

so that its prestress losses can be considered to be equal to the prestress losses of the non-loading condition.

To minimise loss of prestress, the results of the sustained and cyclic loading conditions serve to point out the relatively beneficial effect of loading prestressed concrete beams at early ages. Clearly further loading results at various ages are required to verify this observation.

Test results for different shapes and sizes of concrete beams indicate that I-shaped beams exhibit higher concrete deformations and prestress losses than rectangular shaped beams, which lead to the conclusion that a lower the volume/surface ratio causes higher concrete deformations and prestress losses.

For beams maintained in the constant humidity condition, the mean prestress loss of the rectangular shaped beams was 7 percent lower than the I-shaped beams having a percentage variation ranging from 3 to 9 percent. Similar, but greater percentage loss variations were observed between rectangular and I-shaped beams stored in the variable humidity condition, i.e. the mean prestress loss of the rectangular shaped beams was 10 percent lower than the I-shaped beam having a percentage loss variation ranging from 8 to 16 percent.

Test results for different concrete mix compositions revealed that the RHPC concrete beams exhibit slightly lower prestress losses than OPC concrete beams stored in the various

environmental conditions. In the case of non-loaded I-shaped beams stored, the prestress losses of at year for the RHPC concrete beams were 3% and 9% lower than the OPC beams for grouted and non-grouted beams, respectively.

When rectangular beams were subjected to different loading conditions, the prestress losses for the RHPC beams stored in constant environment were 6.5 and 8.3 percent lower than the OPC beams of cyclic and sustained loading conditions, respectively. On the other hand, when beams were maintained in a variable environment and subjected to cyclic and sustained loadings, the difference between prestress losses of the two concrete mixes was negligible.

The results from the superplasticizing admixture beam when compared with the RHPC control beam showed prestress loss increases of 14 percent at 365 days. On the other hand, the one year results of the PFA concrete beam showed a 7.5 percent reduction in prestress losses when compared with the RHPC control beam. It was observed that the combination of PFA and superplasticizing admixture gave an 11.5 percent reduction in prestress losses when compared with RHPC control beam, so that concrete made from PFA and a superplasticizer appears to be beneficial and promising for prestressed concrete members. Clearly further experimental results are required.

The current national and international prediction methods of predicting time-dependent loss of prestress have been investigated by comparing the estimated values with the experimental results obtained from the present investigation.

For beams maintained in the constant humidity condition, it is concluded that the CEB-70 and CEB-78 methods give the best estimation of total prestress losses, followed by the ACI, BS8110 and PCI methods, respectively.

As in the case of European Codes : CEB-70 and CEB-78, accuracies of prediction were within -3 to +10% of the measured values in spite of the considerable underestimation of shrinkage loss and overestimation of relaxation and creep loss. There is no difference in performance between the two methods, although the CEB-70 method give more conservative estimation of relaxation loss than the CEB-78 method.

In the case of the ACI method, it can be concluded that the method gives the best and the closest predicted losses for each individual component of total prestress, despite the tendency to a slight overestimation of the total prestress losses which are 4 to 20% larger than measured values.

When comparing measured results to the new British Code BS8110, it is concluded that the method gives reasonable results, with an overestimates of 3 to 20%, despite the considerable underestimation of shrinkage loss. Since the relaxation loss gives the largest source of inaccuracy, it is suggested that a relaxation factor of 1.65 be used instead of the 2.0 relaxation factor recently adopted by the BS8110 Code to overcome the inaccuracy. It is indicated that the 1.65 relaxation factor gives marginally the best performance between predicted and measured values, with values ranging from -2 to +12 percent.

In the case of the PCI method, it is indicated that the predicted total prestress losses were in agreement with measured prestress losses despite the considerable underestimation of shrinkage loss; the total loss of prestress which is 5 to 18% larger than the measured values, and thus lies on the safe side.

With regard to the British Code CP110, ACI-ASCE and AASHTO methods, it is concluded that the methods give a substantial underestimation of total prestress losses. On the whole, the greatest source of inaccuracy is the underestimation of shrinkage loss.

For beams maintained in the variable humidity condition, it is concluded that the prediction methods considerably overestimate the final prestress losses, with the exception of the AASHTO, ACI-ASCE and CP110 methods. The AASHTO method has marginally the best performance for the variable humidity condition, followed by the ACI-ASCE method, which predict within -7 to +9% of measured values. On the other hand, the CP110 method tends to give a considerable underestimate of the total prestress losses.

When all standard prediction methods are compared on the basis of experimental material parameters, the ACI method gives the best predictions, followed by the CP110 method which tends to give a slight underestimate for the variable humidity conditions. Other methods tend to overestimate the total prestress loss.

Table 6.1 - Comparison of Experimental Time-Dependent Deformations and Prestresses Losses for Non-Loaded (Self Weight) Prestress Concrete Beams of Various Concrete Mixes, Cross-Sectional Shapes and Stored in Different Environmental Conditions

Beam	Relative Humidity	Cube Compressive Strength at Transfer (MPa)	‡ Total Time-Dependent Deformation (10^{-6})	Ratio: Time-Dependent Deformation/ Elastic Strain	Prestressing Stress Loss (MPa) *					Percentage Loss of Prestress at 365 days	One Year Loss Ratio of Variable-to-Constant Environment Beams
					7 days	30 days	90 days	180 days	365 days		
NGI/C1	65%	47.30	704	4.4	82	137	177	197	227	17.91	0.80
NGI/V1	65-100 %	49.37	490	3.1	80	117	140	161	182	14.32	
NI/C1	65%	44.63	772	4.8	86	149	186	209	243	19.20	0.772
NI/V1	65-100 %	45.83	508	3.2	80	118	142	163	188	14.82	
NGI/C2	65%	48.30	744	4.7	75	144	187	206	235	18.50	0.797
NGI/V2	65-100 %	43.50	518	3.3	70	123	143	163	187	14.75	
NI/C2	65%	49.75	872	5.5	82	160	210	233	264	20.81	0.793
NI/V2	65-100 %	48.91	616	3.9	77	127	154	176	209	16.50	
NI/C3	65%	50.01	988	6.2	130	204	242	267	283	22.29	-
NI/C4	65%	44.67	716	4.5	86	147	189	209	231	18.24	-
NI/C5	65%	48.73	681	4.3	88	145	171	202	224	17.66	-
NGR/C1	65%	47.30	676	5.3	72	125	160	185	221	17.44	0.753
NGR/V1	65-100 %	49.37	416	3.2	67	90	114	140	166	13.13	
NR/C1	65%	44.63	688	5.4	71	121	161	187	222	17.56	0.769
NR/V1	65-100%	45.83	434	3.4	59	96	121	140	171	13.50	

Designation of Beams:

N = No Load/Self Wt.
C = Constant Service Load
CY = Cyclic Service Load
G = Grouted Tendons

I = I-Shape
R = Rectangular Shape
/C = Constant Environment
/V = Variable Environment

1 = RHPC Mix
2 = OPC Mix
3 = RHPC/Admixture Mix
4 = RHPC/PFA MIX
5 = RHPC/Admixture & PFA Mix

* Loss of Prestress Based on Electrical Strain Gauge Wire Reading

‡ Concrete Deformation at Steel Wire Level at 365 Days

Table 6.2 - Comparison of Experimental Time-Dependent Deformations and Prestress Losses for Cyclic and Sustained Loaded Prestress Concrete Beams of Various Concrete Mixes, Cross-Sectional Shapes and Stored in Different Environmental Conditions

Beam	Relative Humidity	Cube Compressive Strength at Transfer (MPa)	ǂ Total Time-Dependent Deformation (10^{-6})	Ratio: Time-Dependent Deformation/ Elastic Strain	Prestressing Stress Loss (MPa) *									Percentage Loss of Prestress at 365 days	One year Loss Ratio of Variable-to-Constant Environment Beams
					1 day		6 days		7 days	30 days	90 days	180 days	365 days		
					No Load	Loading	No Load	Loading							
CYI/C1	65%	49.93	647	4.1	-	-	79	66	72	122	162	184	215	16.98	0.886
CYI/V1	65-100%	47.07	530	3.3	-	-	66	52	58	111	137	159	191	15.04	
CI/C1	65%	48.91	570	3.6	-	-	80	69	75	125	153	170	198	15.61	0.820
CI/V1	65-100%	43.90	398	2.5	-	-	62	47	53	98	116	133	162	12.80	
CYR/C1	65%	48.91	574	4.5	-	-	65	55	62	102	131	163	200	15.77	0.805
CYR/V1	65-100%	43.90	388	3.0	-	-	57	47	52	81	104	128	161	12.70	
CR/C1	65%	49.93	498	3.9	-	-	66	54	59	94	129	151	183	14.44	0.810
CR/V1	65-100%	47.07	330	2.6	-	-	53	43	49	86	104	128	148	11.69	
CYR/C2	65%	45.93	642	5.0	15	7	-	-	50	108	151	184	214	16.86	0.760
CYR/V2	65-100%	49.91	396	3.1	17	4	-	-	60	84	107	133	163	12.82	
CR/C2	65%	44.37	580	4.5	15	7	-	-	42	95	135	169	200	15.75	0.732
CR/V2	65-100%	44.10	302	3.4	15	7	-	-	50	74	92	108	146	11.53	

Note: All beams were loaded at the age of 8 days

* Loss of Prestress Based on Electrical Strain Gauge Wire Reading

ǂ Concrete Deformation at Steel Wire Level at 365 days

Table 6.3 - Effect of Cross-Sectional Shape on Time-Dependent Deformations and Prestress Losses of RHPC Mix after 365 days since prestressing

		Total Concrete Deformation		Prestress Loss	
		Constant Humidity	Variable Humidity	Constant Humidity	Variable Humidity
Range of Variation	R/I Ratio	0.96-0.87	0.85-0.73	0.97-0.91	0.92-0.84
	Percentage Variation	4-13%	15-27%	3-9%	8-16%
Beams mean value	R/I Ratio	0.90	0.82	0.93	0.90
	Percentage Variation	10%	18%	7%	10%
Note: R/I is ratio of Rectangular/I-beam values					

Table 6.4 - Effect of Mix Composition on Time-Dependent Deformations and Prestress Loss after 365 days since prestressing

Type of Loading Condition and Shape of Beam	Ratio of Mixes	Total Deformation Ratio		Loss of Prestress Ratio	
		Constant Humidity	Variable Humidity	Constant Humidity	Variable Humidity
Non-Loaded Grouted I-Beam	Mix1/Mix2	0.946	0.946	0.968	0.971
Non-Loaded I-Beam	Mix1/Mix2	0.885	0.825	0.923	0.90
	Mix1/Mix3	0.781	-	0.861	-
	Mix1/Mix4	1.08	-	1.053	-
	Mix1/Mix5	1.13	-	1.087	-
Cyclic Loaded Rectangular Beam	Mix1/Mix2	0.894	0.98	0.935	0.991
Sustained Loaded Rectangular Beam	Mix1/Mix2	0.859	1.09	0.917	1.014
Note: Mix1 = Plain RHPC, Mix2 = Plain OPC, Mix3 = RHPC/Admixture Mix4 = RHPC/PFA, Mix5 = RHPC/Admixture & PFA					

Table 6.5 - Comparison between Measured and Predicted Methods of Prestress Time-Dependent Losses after 365 Days for Non-Loaded Beams Stored in Constant Environment (using General Material Parameters)

Beam	Deformation Loss		Measured	CEB 1970	CEB 1978	ACI 1982	CP110 1972	BS8110 1985	* ACI-ASCE 1979	* AASHTO 1977	‡ PCI 1975
NGI/C1	Shrinkage Loss	Stress (MPa)	105	59	62	123	57	38	61	40	74
		% Loss	8.28	4.63	4.89	9.73	4.5	2.98	4.77	3.16	5.85
	Creep Loss	Stress (MPa)	43	92	65	65	42	87	52	65	77
		% Loss	3.39	7.23	5.11	5.11	3.33	6.83	4.10	5.10	6.07
	Relaxation Loss	Stress (MPa)	79	87	113	75	74	137	116	117	115
		% Loss	6.19	6.94	8.87	5.91	5.82	10.8	9.18	9.23	9.05
	Total Time-Dependent Loss	Stress (MPa)	227	238	240	263	173	262	229	222	266
		% Loss	17.91	18.80	18.87	20.76	13.65	20.67	18.05	17.49	20.96
	Ratio of Total Computed/Measured Loss Values		-	1.05	1.06	1.16	0.76	1.15	1.01	0.98	1.18
NCI/C2	Shrinkage Loss	Stress (MPa)	106	73	52	107	57	38	61	40	76
		% Loss	8.36	5.73	4.07	8.43	4.5	2.98	4.77	3.16	6.00
	Creep Loss	Stress (MPa)	51	106	66	62	42	73	57	65	66
		% Loss	4.02	8.34	5.23	4.89	3.33	5.78	4.49	5.10	5.17
	Relaxation Loss	Stress (MPa)	78	78	114	75	74	137	116	117	115
		% Loss	6.15	6.22	9.01	5.91	5.82	10.8	9.13	9.23	9.10
	Total Time-Dependent Loss	Stress (MPa)	235	257	232	244	173	248	233	222	257
		% Loss	18.5	20.29	18.31	19.23	13.65	19.57	18.39	17.49	20.27
	Ratio of Total Computed/Measured Loss Values		-	1.10	0.99	1.04	0.74	1.06	0.99	0.94	1.10
NGR/C1	Shrinkage Loss	Stress (MPa)	96	55	59	119	57	38	59	40	73
		% Loss	7.58	4.3	4.63	9.38	4.5	2.98	4.66	3.16	5.73
	Creep Loss	Stress (MPa)	44	63	61	45	32	87	39	49	56
		% Loss	3.39	4.98	4.82	3.58	2.53	6.83	3.08	3.83	4.38
	Relaxation Loss	Stress (MPa)	81	99	116	75	74	137	119	120	116
		% Loss	6.39	7.82	9.20	5.91	5.82	10.8	9.35	9.48	9.18
	Total Time-Dependent Loss	Stress (MPa)	221	217	236	239	163	262	217	209	244
		% Loss	17.44	17.10	18.65	18.88	12.85	20.67	17.09	16.47	19.28
	Ratio of Total Computed/Measured Loss Values		-	0.98	1.07	1.08	0.74	1.19	0.98	0.94	1.11

Note: * Loss values of ACI-ASCE (1979) and AASHTO (1977) are based on Final Time period (end of service life)

‡ PCI values are based on 70% constant relative humidity

Table 6.6 - Comparison Between Measured and Prediction Methods Prestress Time-Dependent Loss after 365 Days for Non-Loaded Beams Stored in Variable Environment (using General Material Parmaeters)

Beam	Deformation Loss		Measured	CEB 1970	CEB 1978	ACI 1982	CP110 1972	BS8110 1985	* ACI-ASCE 1979	* AASHTO 1977	‡ PCI 1975
NGI/V1	Shrinkage Loss	Stress (MPa)	59	44	40	104	37	28	34	30	-
		% Loss	4.65	3.49	3.14	8.19	2,92	2.17	2.64	2.37	-
	Creep Loss	Stress (MPa)	40	73	51	59	42	74	52	65	-
		% Loss	3.16	5.78	4.06	4.65	3.33	5.85	4.10	5.10	-
	Relaxation Loss	Stress (MPa)	83	99	120	75	74	137	120	119	-
		% Loss	6.55	7.76	9.47	5.91	5.82	10.8	9.49	9.39	-
	Total Time-Dependent Loss	Stress (MPa)	182	216	211	238	153	239	206	214	-
		% Loss	14.36	17.03	16.67	18.75	12.07	18.86	16.23	16.86	-
	Ratio of Total Computer/Measured Loss Values		-	1.19	1.16	1.32	0.84	1.31	1.14	1.18	-
NGI/V2	Shrinkage Loss	Stress (MPa)	61	55	34	90	37	28	34	30	-
		% Loss	4.81	4.32	2.67	7.08	2.92	2.17	2.64	2.37	-
	Creep Loss	Stress (MPa)	44	85	53	56	42	60	57	65	-
		% Loss	3.47	6.68	4.17	4.43	3.33	4.74	4.49	5.10	-
	Relaxation Loss	Stress (MPa)	82	91	121	75	74	137	120	119	-
		% Loss	6.47	7.22	9.55	5.91	5.82	10.8	9.44	9.39	-
	Total Time-Dependent Loss	Stress (MPa)	187	231	208	221	153	225	210	214	-
		% Loss	14.75	18.22	16.39	17.42	12.07	17.75	16.57	16.86	-
	Ratio of Total Computed/Measured Loss Values		-	1.24	1.11	1.18	0.82	1.20	1.12	1.14	-
NGR/V1	Shrinkage Loss	Stress (MPa)	46	41	32	100	37	28	33	30	-
		% Loss	3.63	3.24	2.54	7.9	2.92	2.17	2.58	2.37	-
	Creep Loss	Stress (MPa)	36	51	49	41	32	74	39	49	-
		% Loss	2.84	3.99	3.86	3.25	2.53	5.85	3.08	3.83	-
	Relaxation Loss	Stress (MPa)	84	107	122	75	74	137	122	122	-
		% Loss	6.63	8.48	9.6	5.91	5.82	10.8	9.65	9.64	-
	Total Time-Dependent Loss	Stress (MPa)	166	199	203	216	143	239	194	201	-
		% Loss	13.13	15.71	16.00	17.06	11.27	18.86	15.31	15.84	-
	Ratio of Total Computed/Measured Loss Values		-	1.20	1.22	1.30	0.86	1.44	1.16	1.20	-

Note: * Loss values of ACI-ASCE (1979) and AASHTO (1977) are based on Final Time period (end of service life)

Table 6.7 - Comparison Between Measured and Prediction Methods Prestress Time-Dependent Losses after 365 Days for Loaded Beams Stored in Constant Environment (Using general Material Parameters)

Beam	Deformation Loss		Measure	CEB 1970	CEB 1978	ACI 1982	CP110 1972	BS8110 1985	* ACI-ASCE 1979	* AASHTO 1977	ǂ PCI 1975
CI/Cl	Shrinkage Loss	Stress (MPa)	105	59	62	123	57	38	61	40	74
		% Loss	8.28	4.63	4.89	9.73	4.5	2.98	4.78	3.16	5.85
	Creep Loss	Stress (MPa)	12	32	23	35	15	33	32	50	30
		% Loss	0.95	2.52	1.81	2.76	1.18	2.60	2.53	3.96	2.33
	Relaxation Loss	Stress (MPa)	81	107	119	75	74	137	119	120	116
		% Loss	6.39	8.48	9.39	5.91	5.82	10.8	9.42	9.46	9.15
	Total Time-Dependent Loss	Stress (MPa)	198	198	204	233	146	208	212	210	220
		% Loss	15.61	15.61	16.09	18.42	11.50	16.41	16.73	16.58	17.33
	Ratio of total Computed/Measured Loss Values		-	1.0	1.03	1.18	0.74	1.05	1.07	1.06	1.11
CR/Cl	Shrinkage Loss	Stress (MPa)	96	55	59	119	57	38	59	40	73
		% Loss	7.58	4.3	4.63	9.38	4.5	2.98	4.66	3.16	5.73
	Creep Loss	Stress (MPa)	4	24	23	25	12	33	26	38	21
		% Loss	0.32	1.89	1.81	1.98	0.95	2.60	2.05	2.97	1.68
	Relaxation Loss	Stress (MPa)	83	111	119	75	74	137	120	122	117
		% Loss	6.54	8.79	9.39	5.91	5.82	10.8	9.50	9.66	9.21
	Total Time-Dependent Loss	Stress (MPa)	183	190	201	219	143	208	205	200	211
		% Loss	14.44	14.99	15.86	17.31	11.27	16.41	16.21	15.79	16.62
	Ratio of Total Computed/Measured Loss Values		-	1.04	1.10	1.20	0.78	1.14	1.12	1.09	1.15
CR/C2	Shrinkage Loss	Stress (MPa)	100	68	49	103	57	38	59	40	74
		% Loss	7.89	5.36	3.87	8.11	4.5	2.98	4.66	3.16	5.85
	Creep Loss	Stress (MPa)	18	28	24	27	12	28	29	38	18
		% Loss	1.42	2.20	1.89	2.15	0.95	2.21	2.29	2.97	1.43
	Relaxation Loss	Stress (MPa)	82	106	121	75	74	137	120	122	117
		% Loss	6.47	8.36	9.55	5.91	5.82	10.8	9.47	9.66	9.21
	Total Time-Dependent Loss	Stress (MPa)	200	201	194	205	143	203	208	200	209
		% Loss	15.75	15.86	15.31	16.19	11.27	16.02	16.42	15.79	16.49
	Ratio of Total Computed/Measured Loss Values		-	1.01	0.97	1.03	0.72	1.02	1.04	1.00	1.05

Note: * Loss values of ACI-ASCE (1979) and AASHTO (1977) are based on Final Time Period (end of service life)

ǂ PCI values are based on 70% constant relative humidity

Table 6.8 - Comparison Between Measured and Prediction Methods Prestress Time-Dependent Losses after 365 Days for Loaded Beams Stored in Constant Environment (General Material Parameters)

Beam	Deformation Loss		Measured	CEB 1970	CEB 1978	ACI 1982	CP110 1972	BS8110 1985	* ACI-ASCE 1979	* AASHTO 1977	PCI 1975
CI/V1	Shrinkage Loss	Stress (MPa)	59	44	40	104	37	28	34	30	-
		% Loss	4.65	3.49	3.14	8.19	2.92	2.17	2.65	2.37	-
	Creep Loss	Stress (MPa)	19	26	18	30	15	28	32	50	-
		% Loss	1.5C	2.04	1.43	2.37	1.18	2.21	2.53	3.96	-
	Relaxation Loss	Stress (MPa)	84	114	124	75	74	137	123	122	-
		% Loss	6.63	9.0	9.78	5.91	5.82	10.80	9.73	9.61	-
	Total Time-Dependent Loss	Stress (MPa)	162	184	182	209	126	193	189	202	-
		% Loss	12.80	14.53	14.39	16.50	9.92	15.23	14.91	15.94	-
	Ratio of Total Computed/Measured Loss Values		-	1.14	1.12	1.29	0.78	1.19	1.16	1.25	-
CR/V1	Shrinkage Loss	Stress (MPa)	46	41	32	100	37	28	33	30	-
		% Loss	3.63	3.24	2.54	7.9	2.92	2.17	2.58	2.37	-
	Creep Loss	Stress (MPa)	17	20	19	22	12	28	26	38	-
		% Loss	1. 34	1.52	1.50	1.74	0.95	2.21	2.05	2.97	-
	Relaxation Loss	Stress (MPa)	85	117	126	75	74	137	124	124	-
		% Loss	6.71	9.26	9.94	5.91	5.82	10.8	9.80	9.81	-
	Total Time-Dependent Loss	Stress (MPa)	148	178	177	197	123	193	183	192	-
		% Loss	11.69	14.02	13.96	15.54	9.69	15.23	14.43	15.15	-
	Ratio of Total Computed/Measured Loss Values		-	1.20	1.19	1.33	0.83	1.30	1.23	1.30	-
CR/V2	Shrinkage Loss	Stress (MPa)	50	51	28	86	37	28	33	30	-
		% Loss	3.94	4.02	2.21	6.81	2.92	2.17	2.58	2.37	-
	Creep Loss	Stress (MPa)	10	22	20	24	12	23	29	38	-
		% Loss	0.81	1.74	1.58	1.86	0.95	1.82	2.29	2.97	-
	Relaxation Loss	Stress (MPa)	86	113	127	75	74	137	124	124	-
		% Loss	6.79	8.92	10.02	5.91	5.8	10.8	9.77	9.81	-
	Total Time-Dependent Loss	Stress (MPa)	146	186	175	185	123	188	186	192	-
		% Loss	11.53	14.69	13.81	14.6	9.57	14.83	14.64	15.15	-
	Ratio of Total Computed/Measured Loss Values		-	1.27	1.20	1.27	0.84	1.29	1.27	1.31	-

Note: * Loss values of ACI-ASCE (1979) and AASHTO (1977) are based on Final Time period (end of service life).

Table 6.9 - Percentage Variation Between Experimental and Predicted Mid-Span Loss of Prestress at Various Ages for Different Concrete Mixes, Cross-Sectional Shapes, Environmental and Loading Conditions

Method of Prediction	Type of Environment	Percentage Variation Using General Material Parameters		Percentage variation using Experimental Material Parameters
		Loaded Beams	Non-Loaded Beams	Non-Loaded Beams
CEB-1970	Constant	+ 1% to + 4%	- 2% to +10%	+12% to +17%
	Variable	+14% to +27%	+19% to +24%	+15% to +18%
CEB-1978	Constant	- 3% to +10%	- 1% to + 7%	+21% to +28%
	Variable	+12% to +20%	+11% to +22%	+25% to +34%
ACI-1982	Constant	+ 3% to +20%	+ 4% to +16%	+ 3% to +20%
	Variable	+27% to +33%	+18% to +31%	- 5% to + 7%
CP110-1972	Constant	-28% to -22%	-26% to -24%	- 2% to +14%
	Variable	-22% to -16%	-18% to -14%	-13% to + 5%
BS8110-1985	Constant	+ 2% to +14%	+ 6% to +19%	+36% to +45%
	Variable	+19% to +30%	+20% to +44%	+33% to +39%
ACI-ASCE-1979	Constant	-14% to - 7%	-19% to -16%	-
	Variable	- 4% to + 5%	- 7% to - 4%	-
AASHTO-1977	Constant	-17% to -10%	-22% to -19%	-
	Variable	+ 3% to + 9%	- 6% to + 0%	-
PCI-1975	Constant	+ 5% to +15%	+10% to +18%	-

Note: The (-) and (+) signs represent the underestimation and overestimation of total prestress losses, respectively

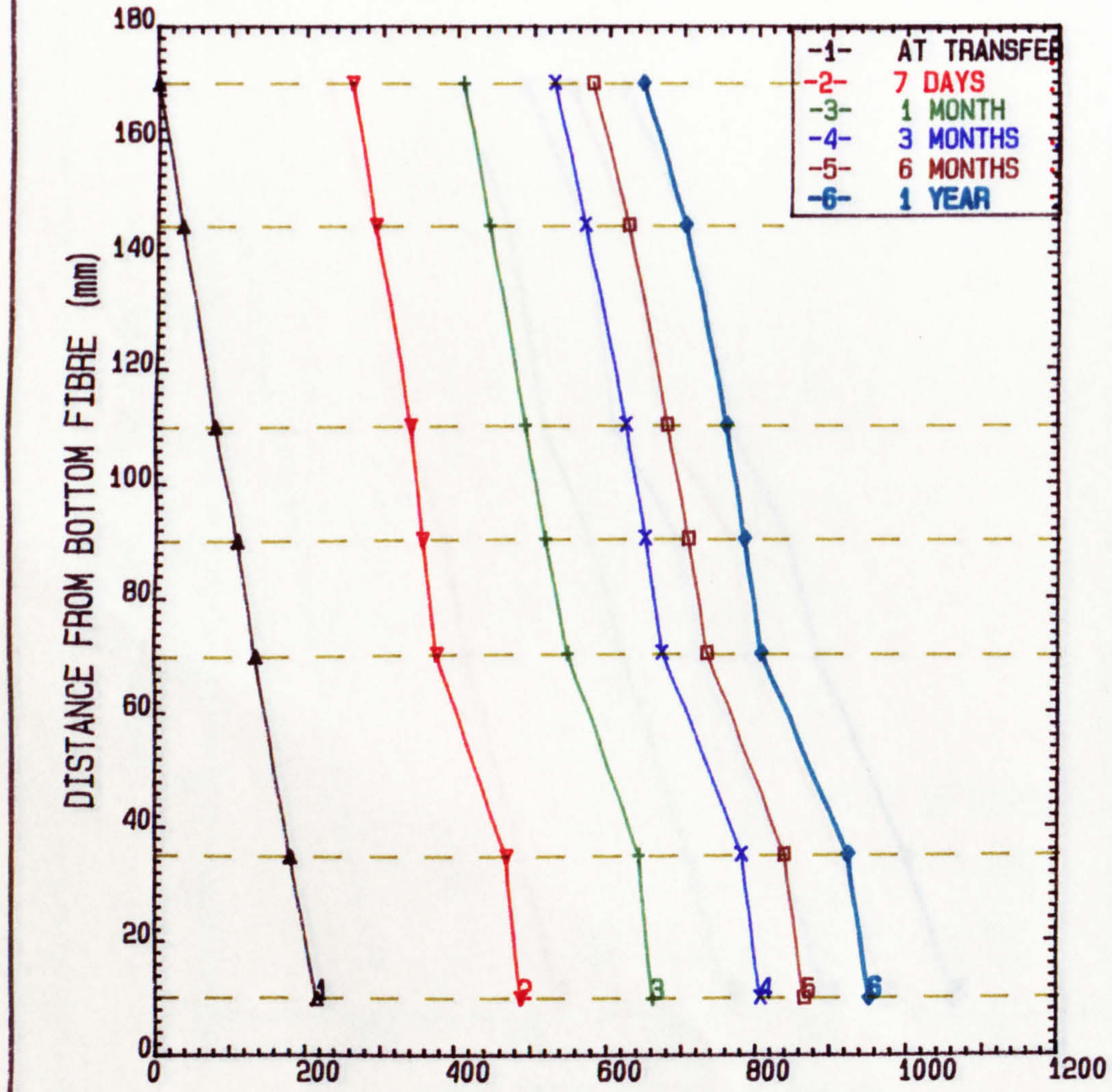

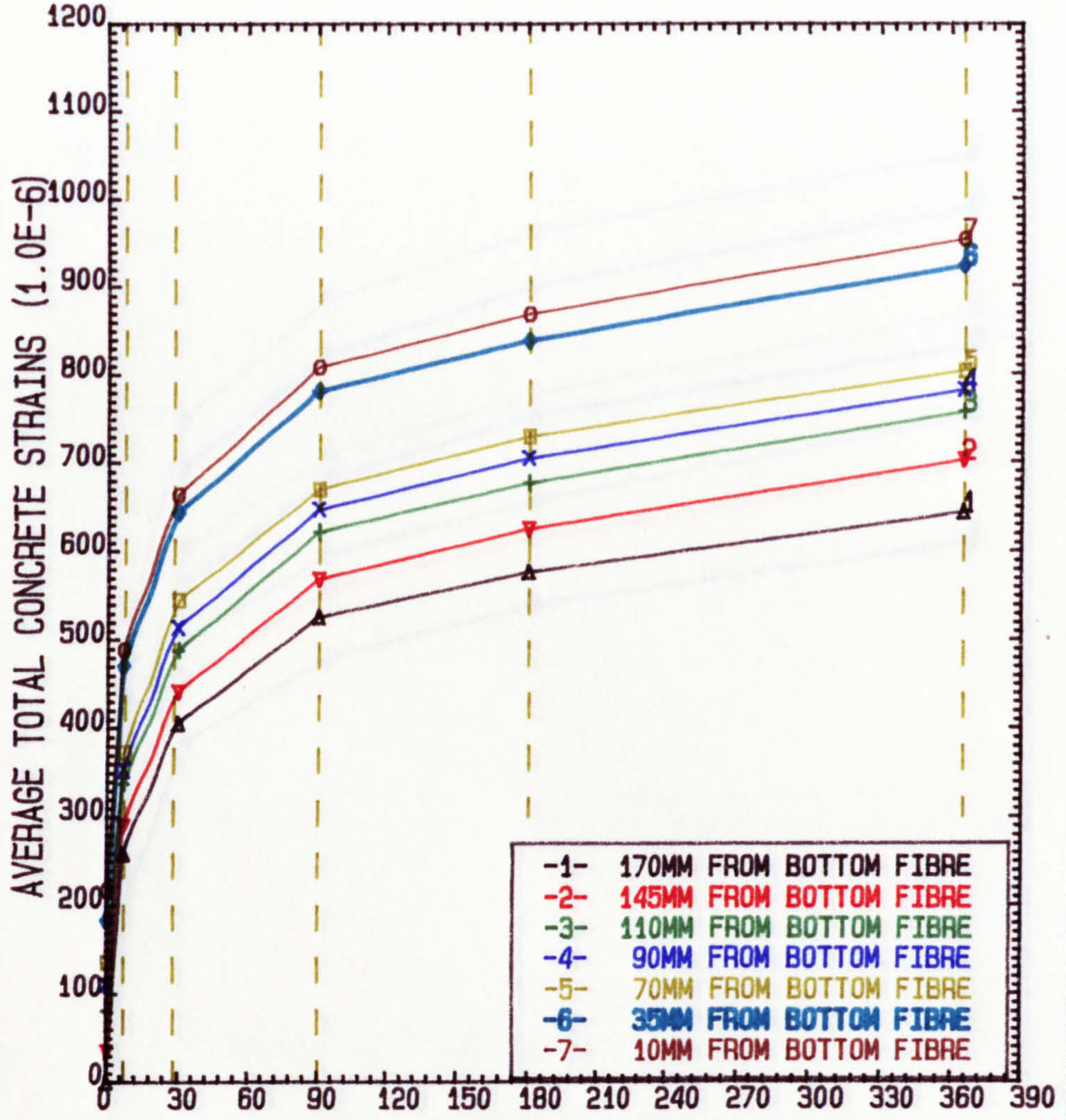

FIG. 6.1 MEASURED CONCRETE STRAIN DISTRIBUTION DIAGRAMS FOR MIDSPAN SECTION OF BEAM NGI/C1

REMARKS: THE EXPERIMENTAL TIME-DEPENDENT PRESTRESS LOSS DETERMINED AT THE STEEL WIRE LEVEL FOR THE MIDSPAN SECTION AT 365 DAYS IS 17.48 % (222.0 MPa)
(THE OBSERVED TIME-DEPENDENT CONCRETE STRAIN AT cgs = 704.0 MICROSTRAINS)

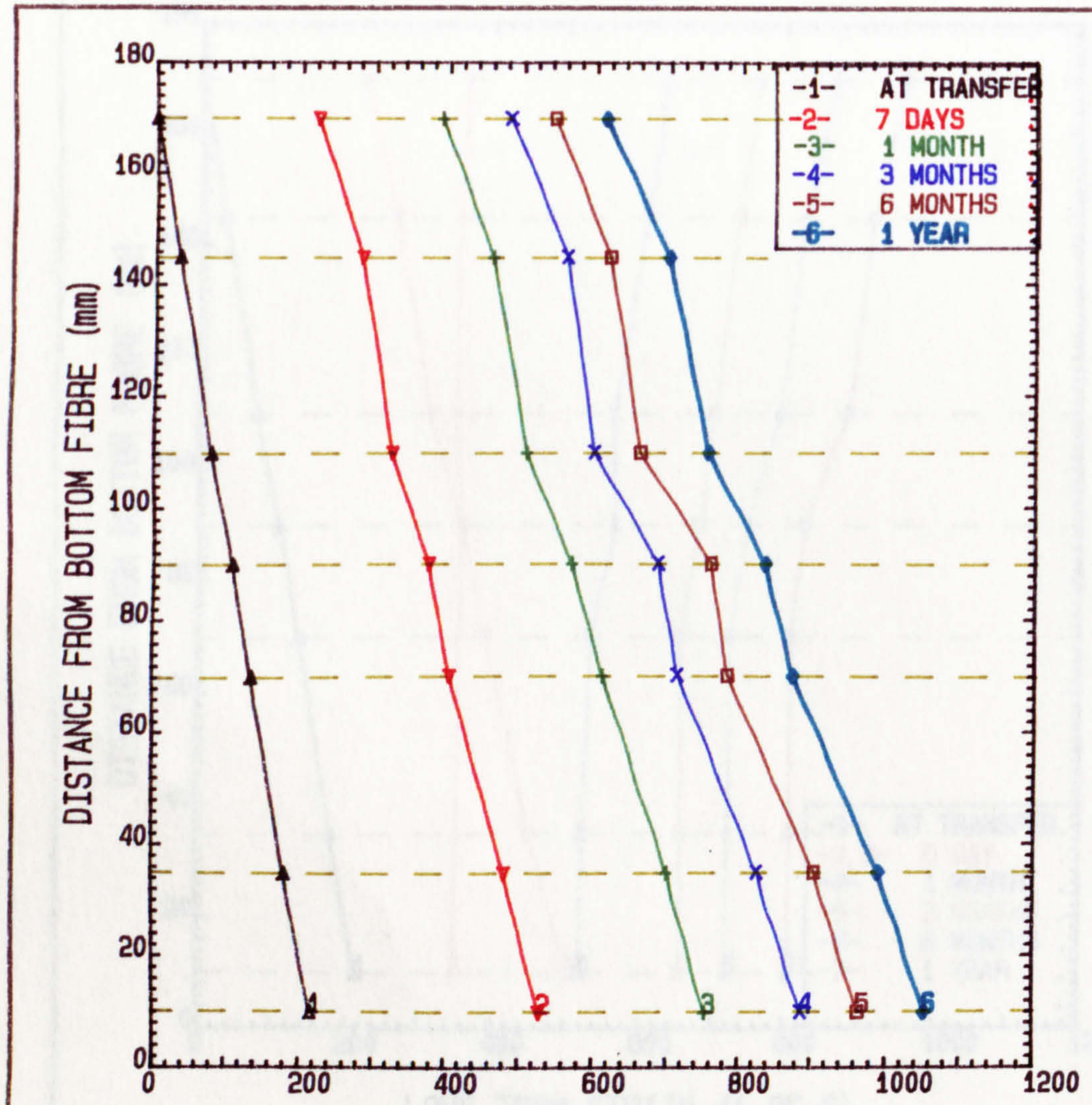

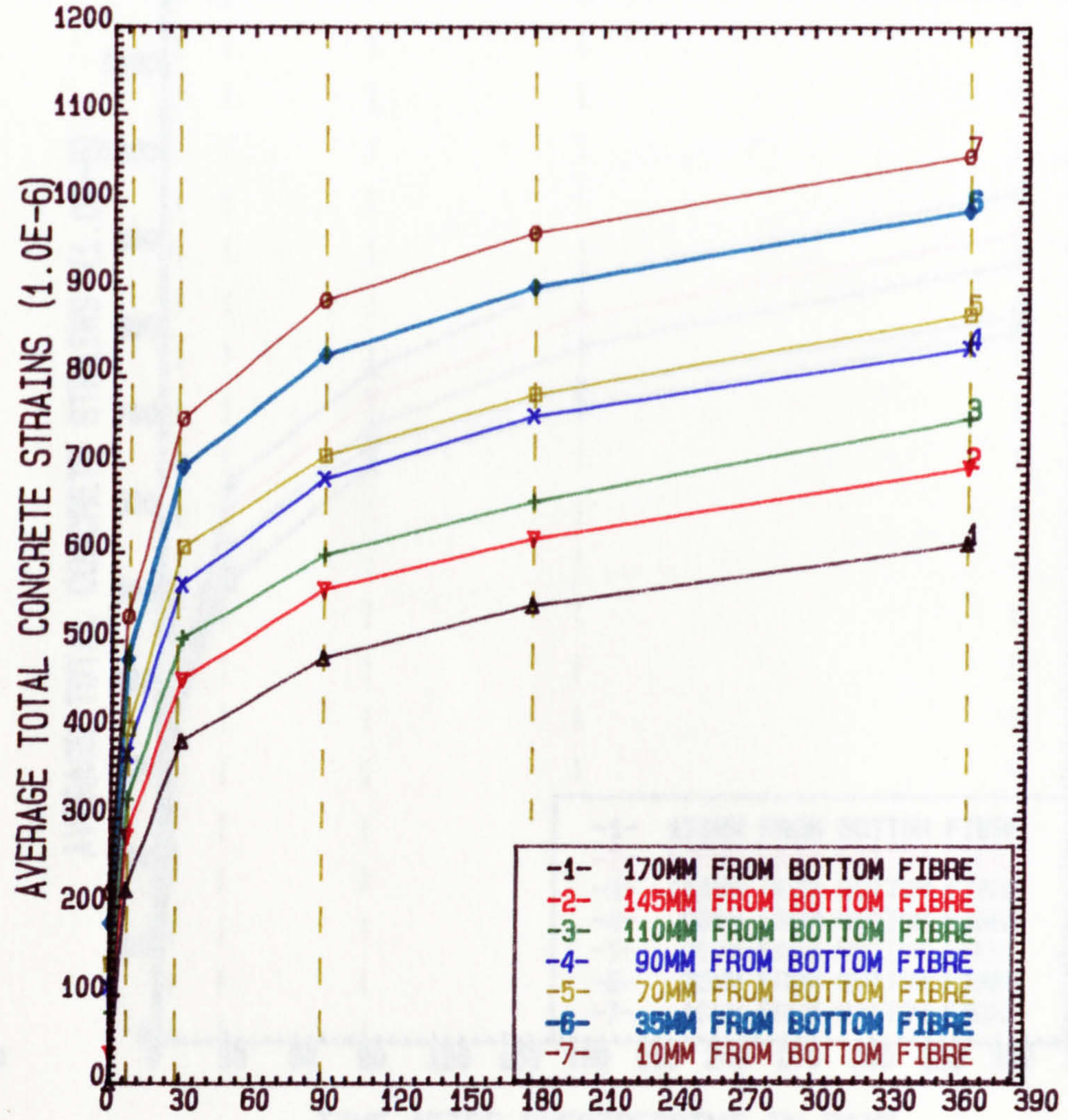

FIG. 6.2 MEASURED CONCRETE STRAIN DISTRIBUTION DIAGRAMS FOR MIDSPAN SECTION OF BEAM NI/C1 .

REMARKS: THE EXPERIMENTAL TIME-DEPENDENT PRESTRESS LOSS DETERMINED AT THE STEEL WIRE LEVEL FOR THE MIDSPAN SECTION AT 365 DAYS IS 18.58 % (236.0 MPa)
(THE OBSERVED TIME-DEPENDENT CONCRETE STRAIN AT cgs = 772.0 MICROSTRAINS)

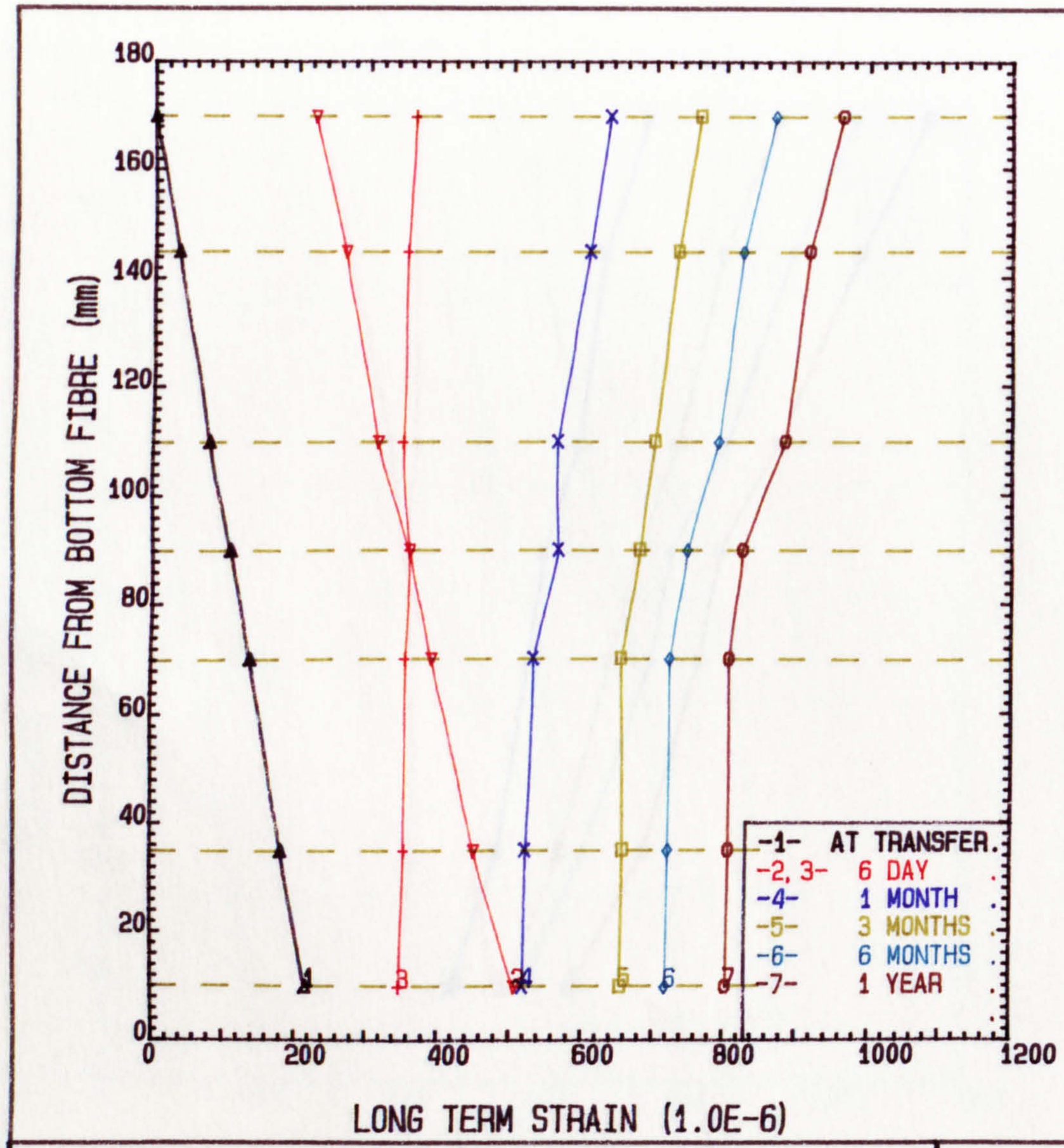

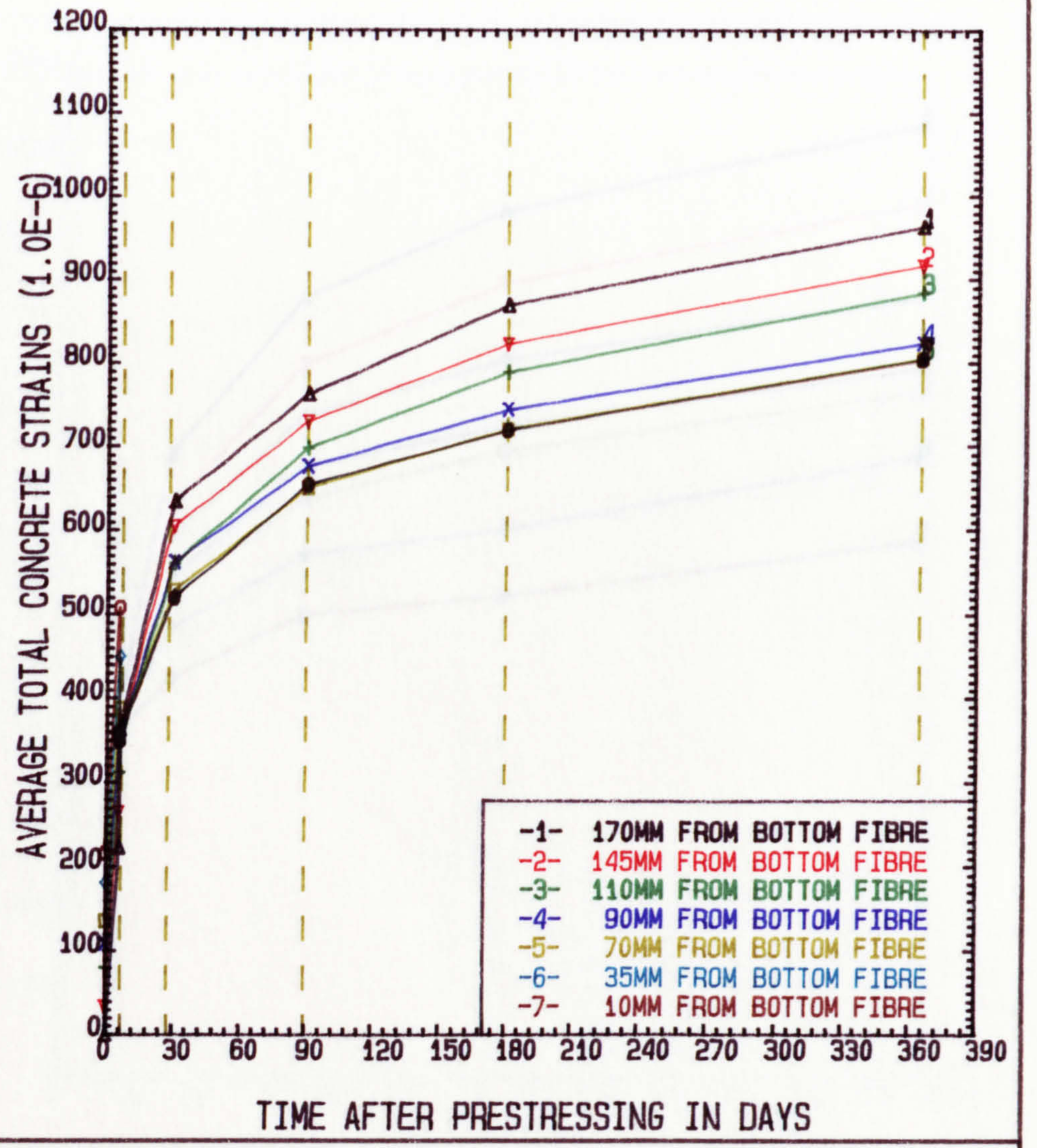

FIG. 6.3 MEASURED CONCRETE STRAIN DISTRIBUTION DIAGRAMS FOR MIDSPAN SECTION OF BEAM CYI/C1 .

REMARKS: THE EXPERIMENTAL TIME-DEPENDENT PRESTRESS LOSS DETERMINED AT STEEL WIRE LEVEL FOR THE MIDSPAN SECTION AT 365 DAYS IS 16.55 % (210.0 MPa) (THE OBSERVED TIME-DEPENDENT CONCRETE STRAIN AT cgs = 647.0 MICROSTRAINS)

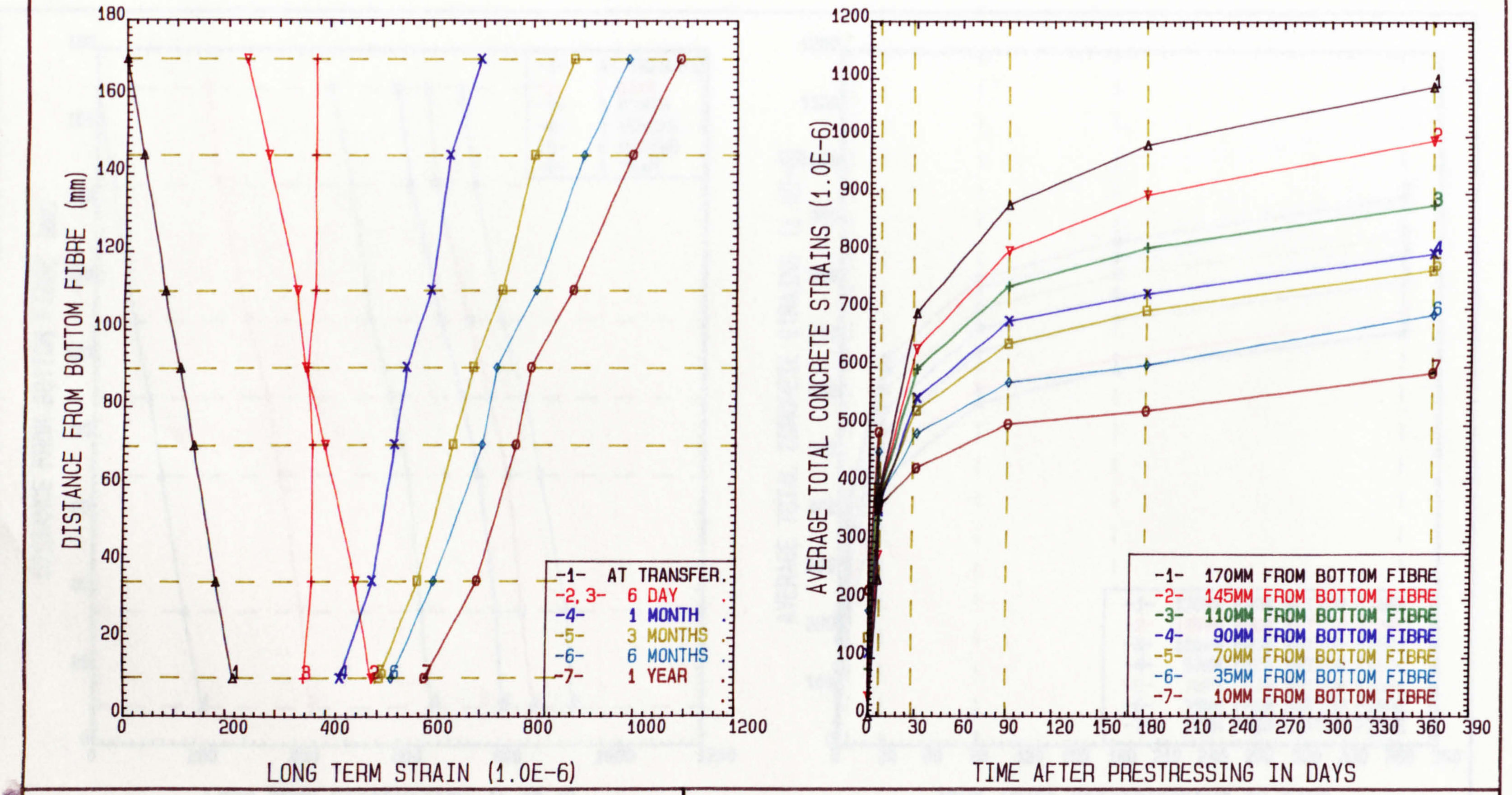

FIG. 6.4 MEASURED CONCRETE STRAIN DISTRIBUTION DIAGRAMS FOR MIDSPAN SECTION OF BEAM CI/C1 .

REMARKS: THE EXPERIMENTAL TIME-DEPENDENT PRESTRESS LOSS DETERMINED AT STEEL WIRE LEVEL FOR THE MIDSPAN SECTION AT 365 DAYS IS 15.30 % (194.0 MPa)
(THE OBSERVED TIME-DEPENDENT CONCRETE STRAIN AT cgs = 570.0 MICROSTRAINS)

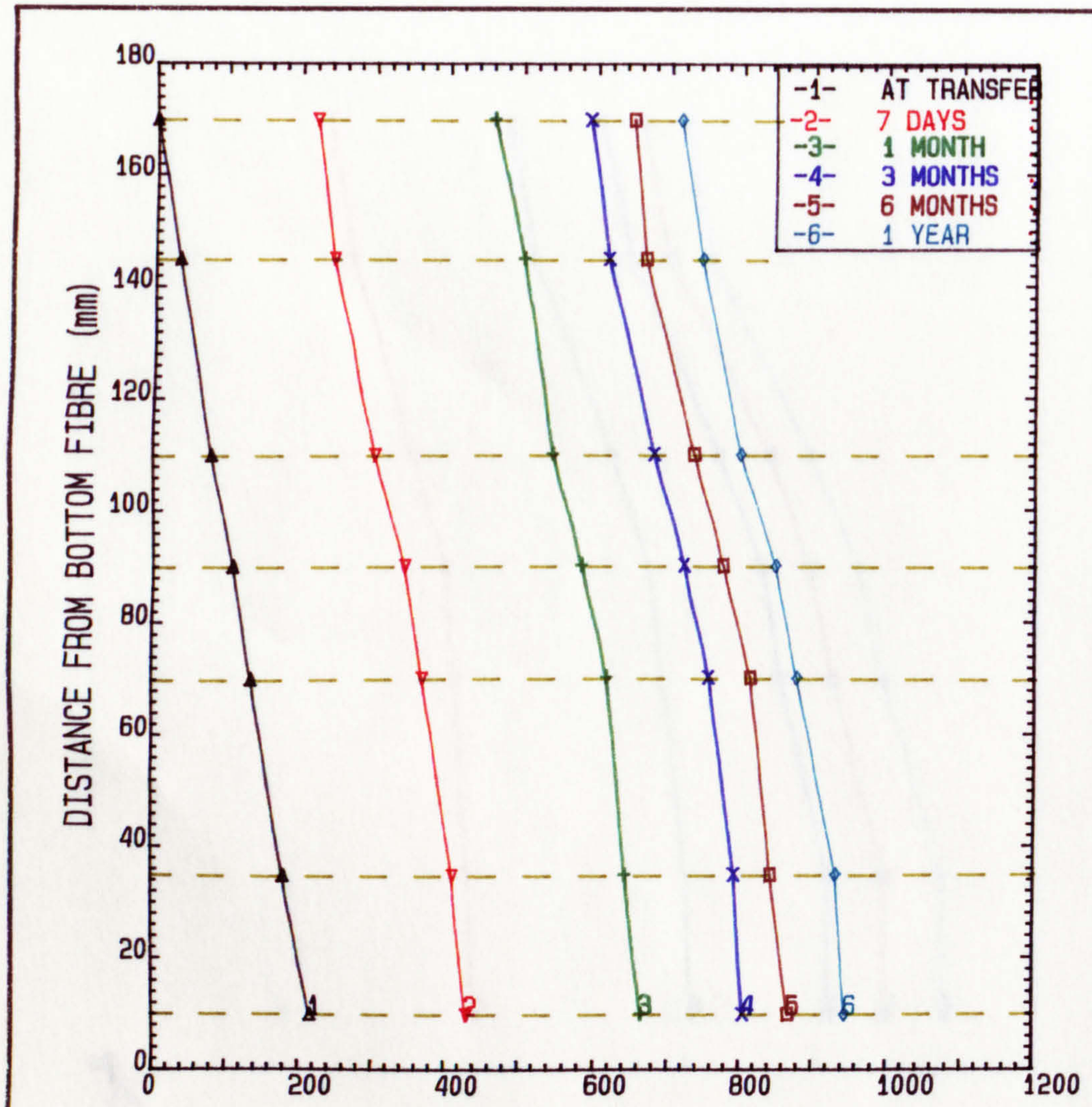

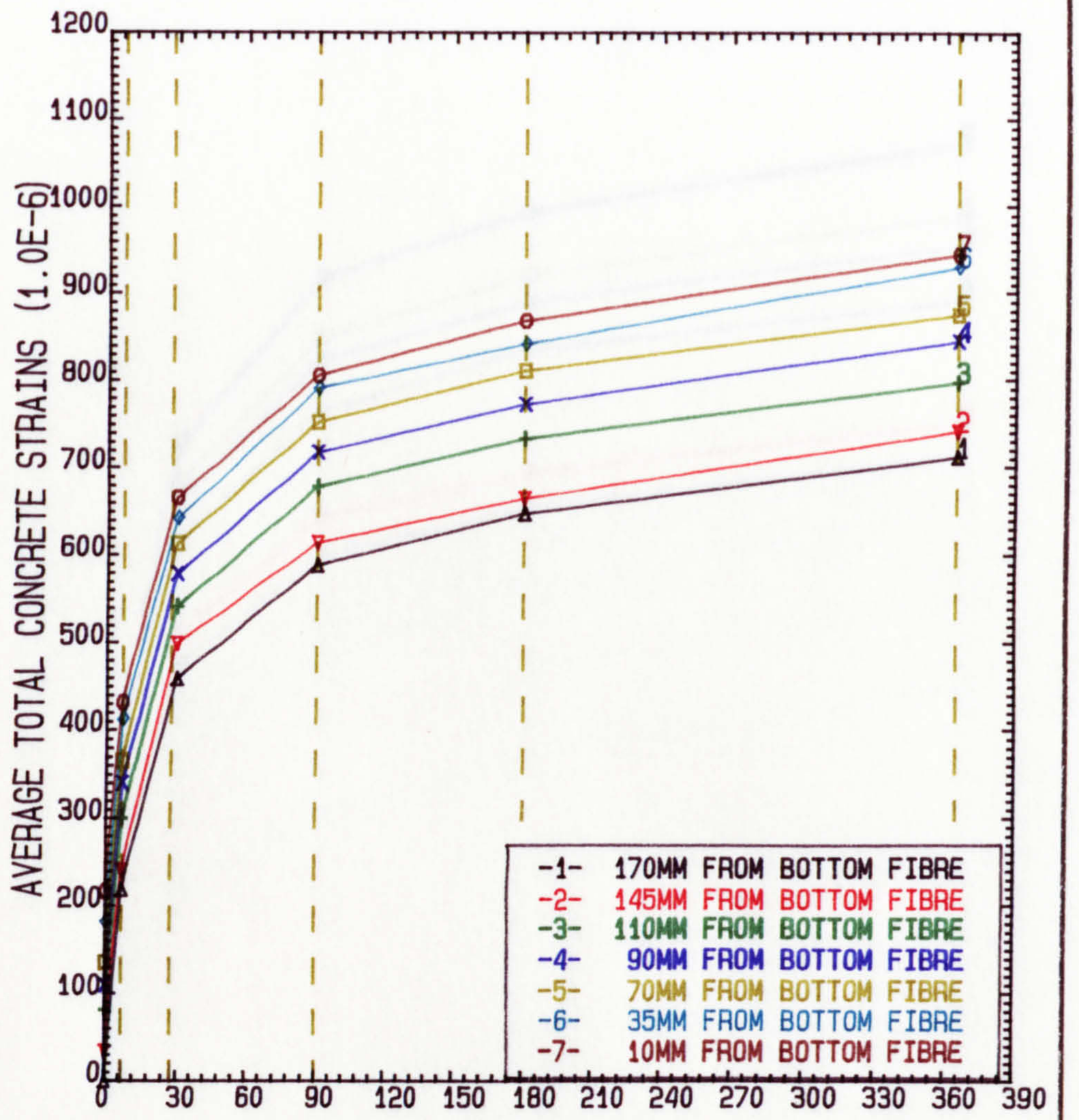

FIG. 6.5 MEASURED CONCRETE STRAIN DISTRIBUTION DIAGRAMS FOR MIDSPAN SECTION OF BEAM NGI/C2

REMARKS: THE EXPERIMENTAL TIME-DEPENDENT PRESTRESS LOSS DETERMINED AT THE STEEL WIRE LEVEL FOR THE MIDSPAN SECTION AT 365 DAYS IS 18.13 % (230.0 MPa)
(THE OBSERVED TIME-DEPENDENT CONCRETE STRAIN AT cgs = 744.0 MICROSTRAINS)

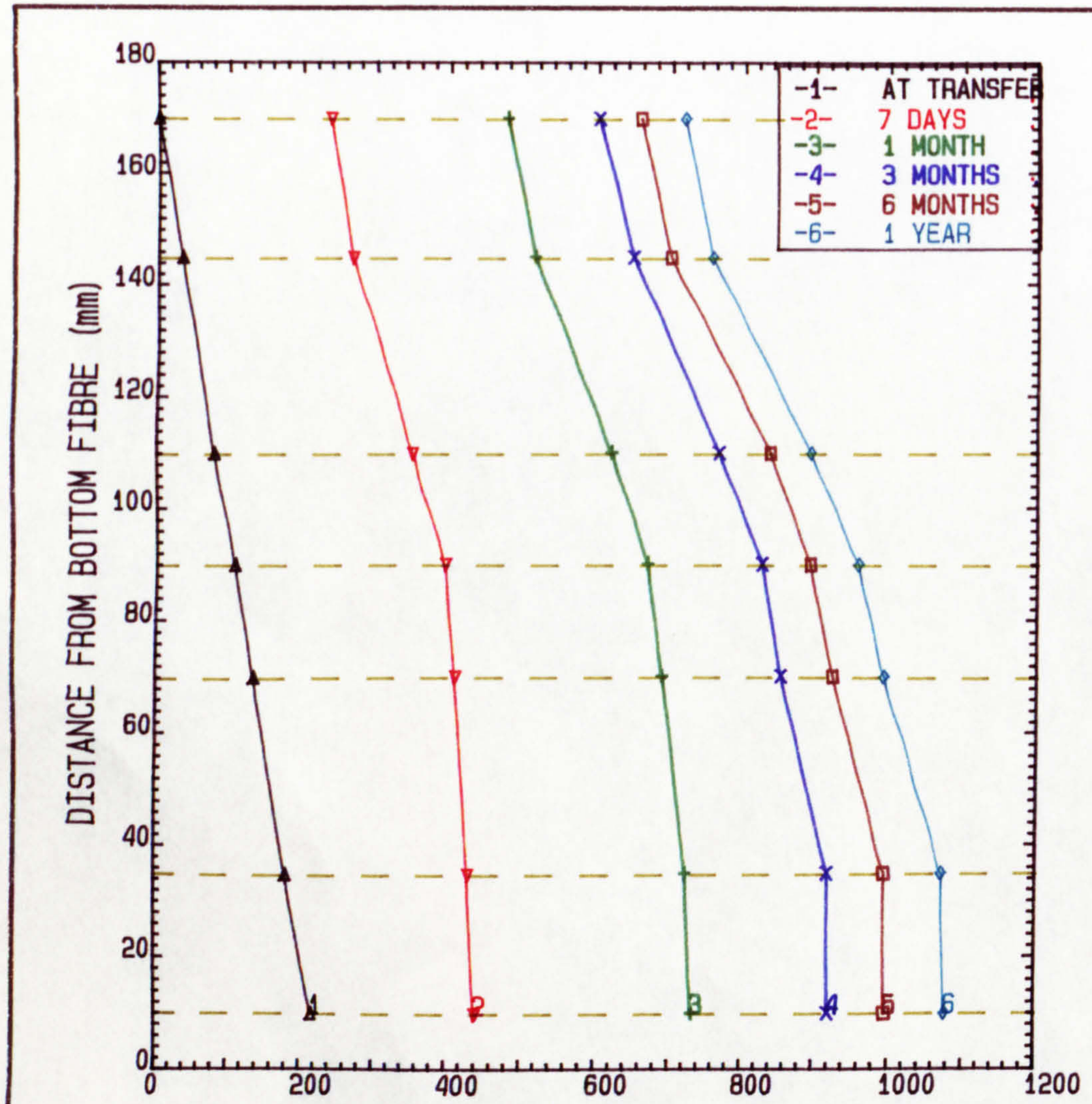

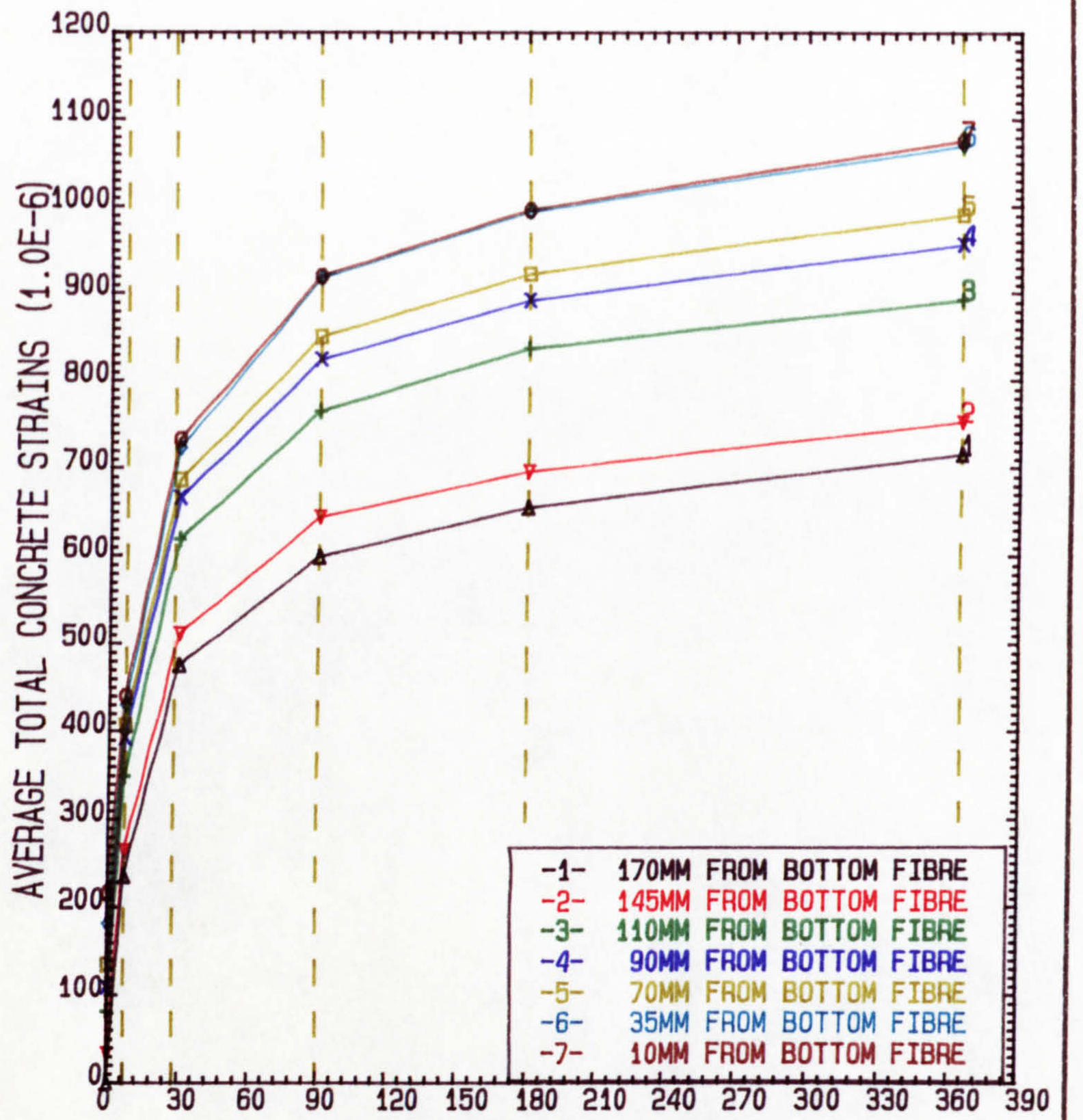

FIG. 6.6 MEASURED CONCRETE STRAIN DISTRIBUTION DIAGRAMS FOR MIDSPAN SECTION OF BEAM NI/C2 .

REMARKS: THE EXPERIMENTAL TIME-DEPENDENT PRESTRESS LOSS DETERMINED AT THE STEEL WIRE LEVEL FOR THE MIDSPAN SECTION AT 365 DAYS IS 20.21 % (256.0 MPa)
(THE OBSERVED TIME-DEPENDENT CONCRETE STRAIN AT cgs = 872.0 MICROSTRAINS)

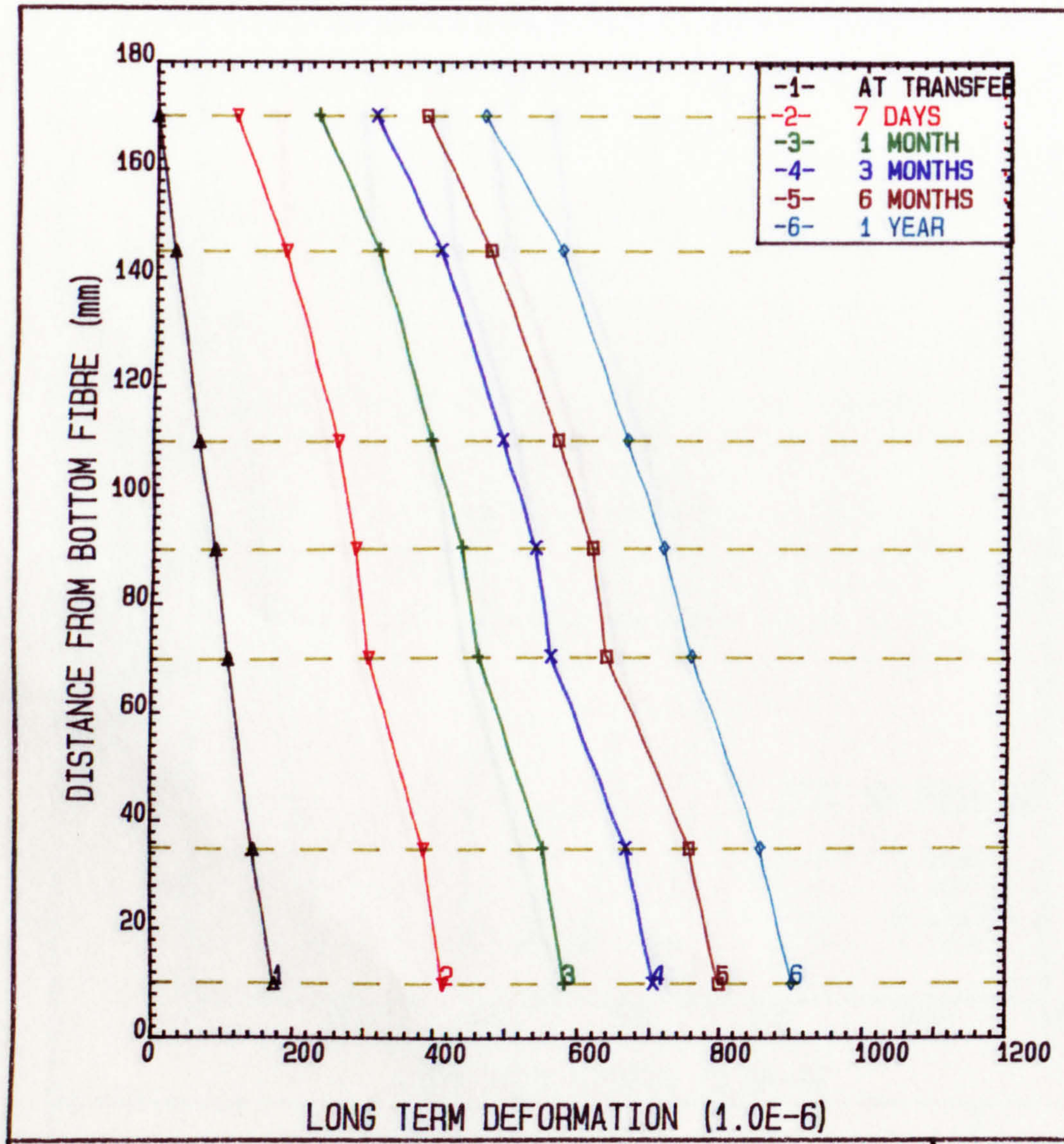

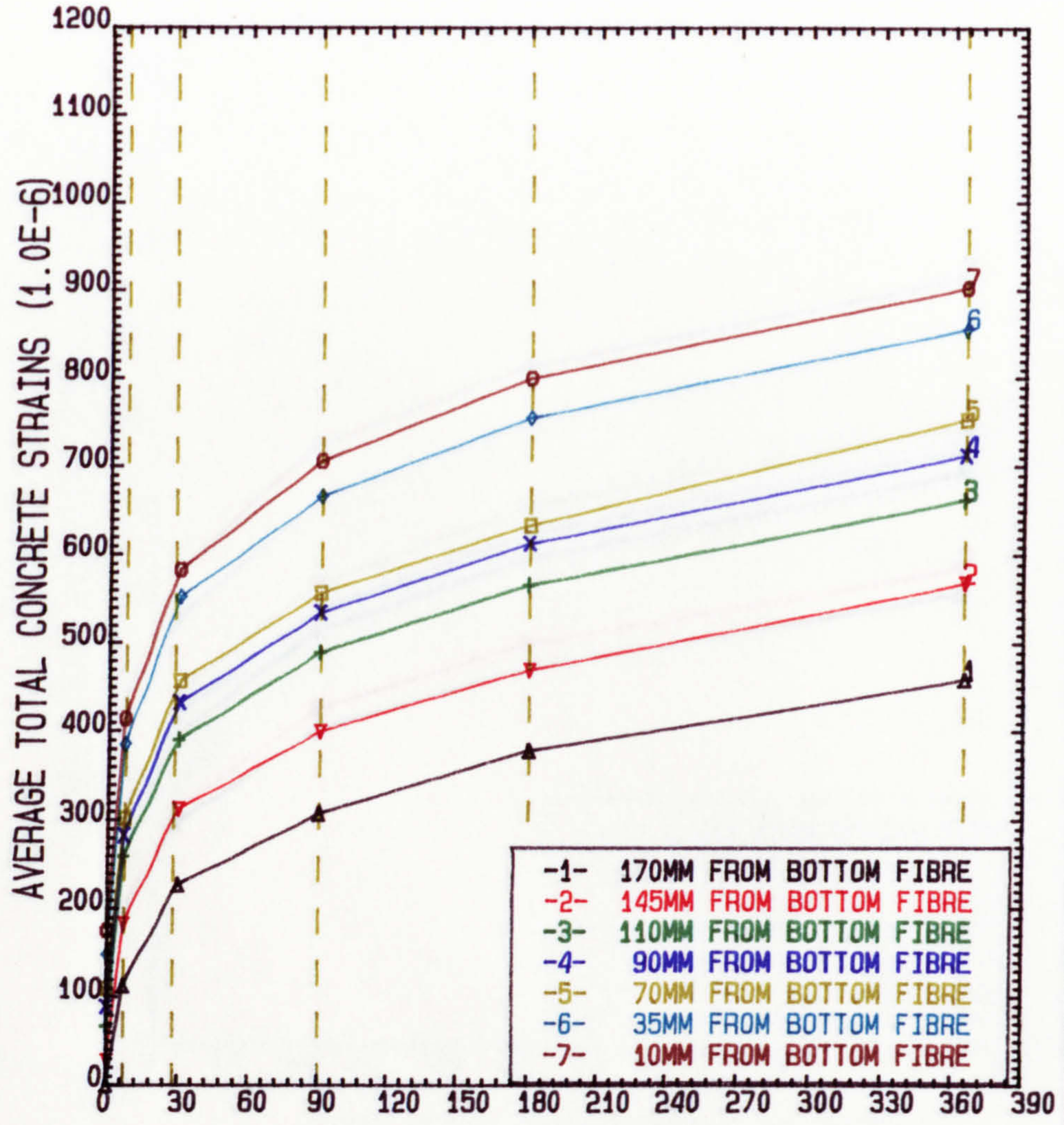

FIG. 6.7 MEASURED CONCRETE STRAIN DISTRIBUTION DIAGRAMS FOR MIDSPAN SECTION OF BEAM NGR/C1 .

REMARKS: THE EXPERIMENTAL TIME-DEPENDENT PRESTRESS LOSS DETERMINED AT THE STEEL WIRE LEVEL FOR THE MIDSPAN SECTION AT 365 DAYS IS 17.02 % (216.0 MPa)
(THE OBSERVED TIME-DEPENDENT CONCRETE STRAIN AT cgs = 676.0 MICROSTRAINS)

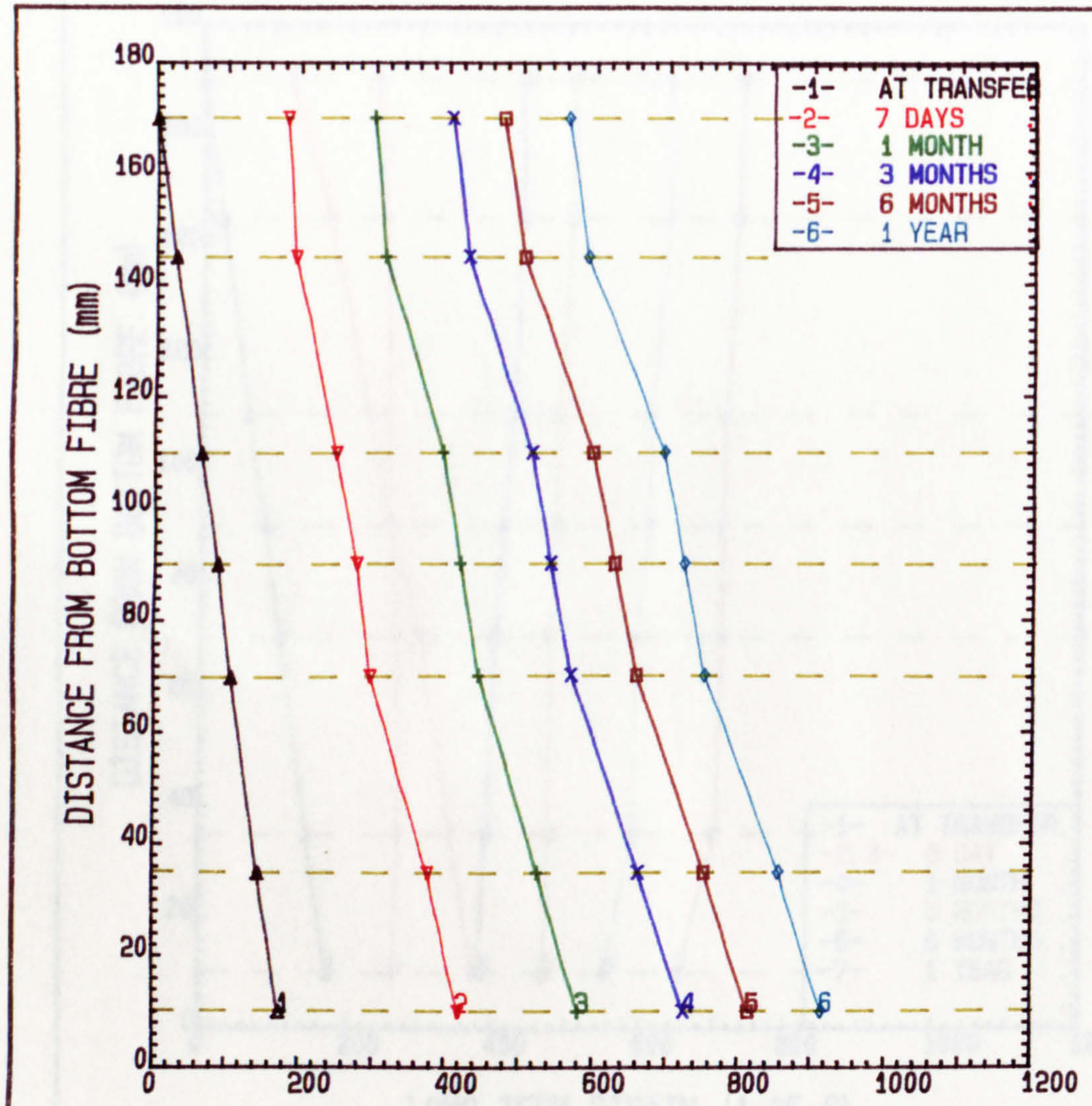

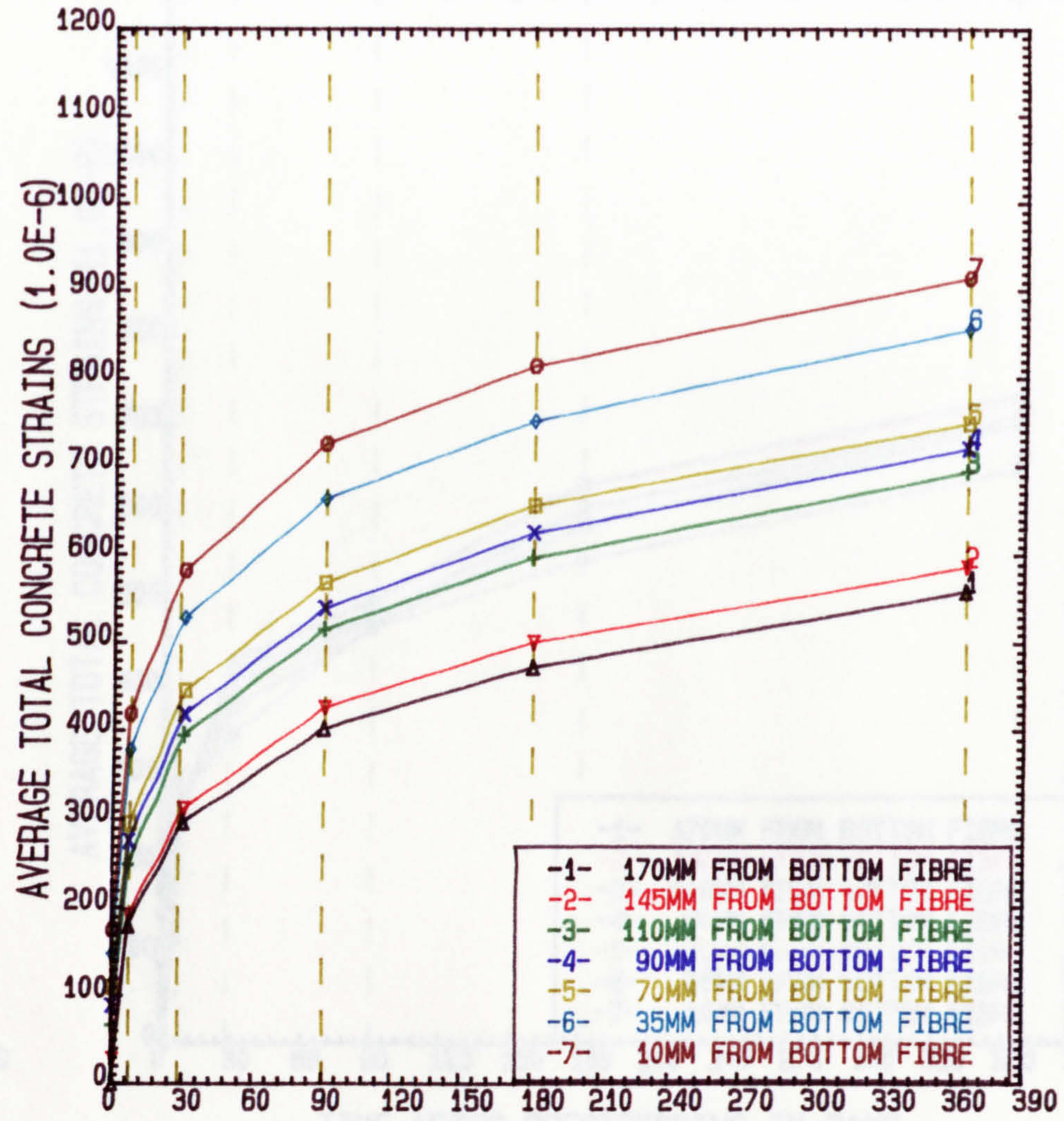

FIG. 6.8 MEASURED CONCRETE STRAIN DISTRIBUTION DIAGRAMS FOR MIDSPAN SECTION OF BEAM NR/C1

REMARKS: THE EXPERIMENTAL TIME-DEPENDENT PRESTRESS LOSS DETERMINED AT THE STEEL WIRE LEVEL FOR THE MIDSPAN SECTION AT 365 DAYS IS 17.23 % (218.0 MPa)
(THE OBSERVED TIME-DEPENDENT CONCRETE STRAIN AT cgs = 688.0 MICROSTRAINS)

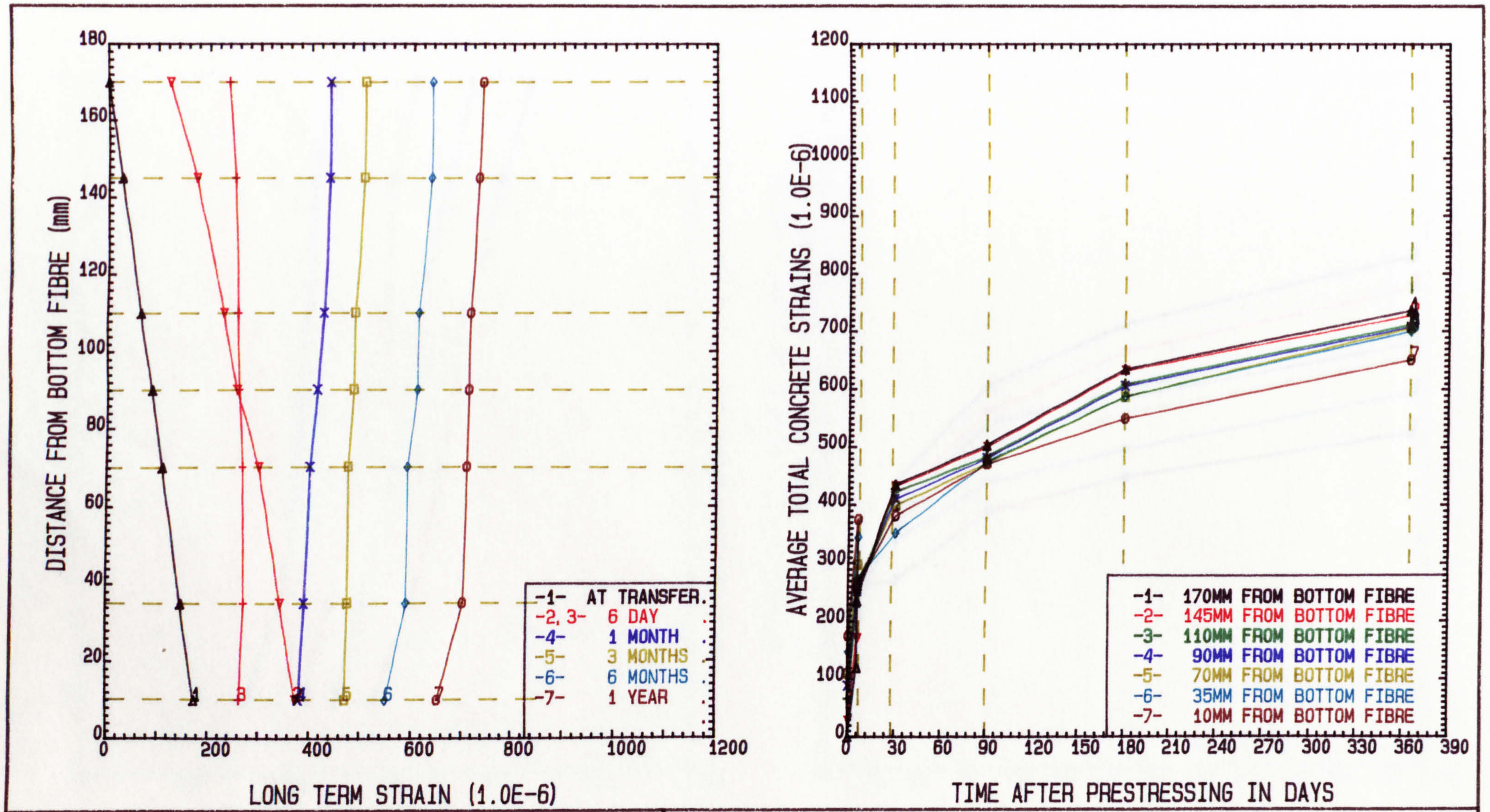

FIG. 6.9 MEASURED CONCRETE STRAIN DISTRIBUTION DIAGRAMS FOR MIDSPAN SECTION OF BEAM CYR/C1 .

REMARKS: THE EXPERIMENTAL TIME-DEPENDENT PRESTRESS LOSS DETERMINED AT STEEL . WIRE LEVEL FOR THE MIDSPAN SECTION AT 365 DAYS IS 15.36 % (195.0 MPa) (THE OBSERVED TIME-DEPENDENT CONCRETE STRAIN AT cgs = 574.0 MICROSTRAINS)

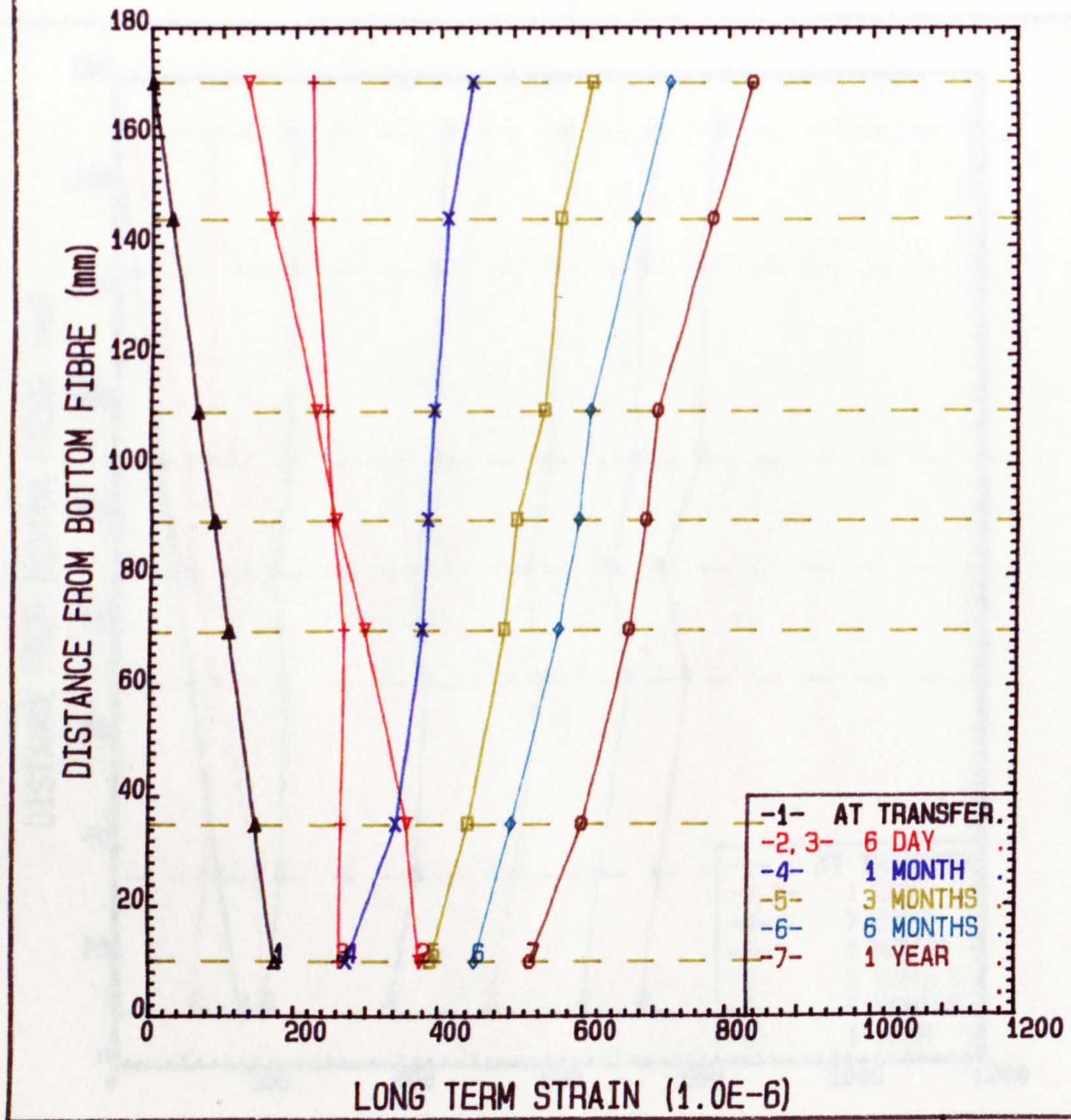

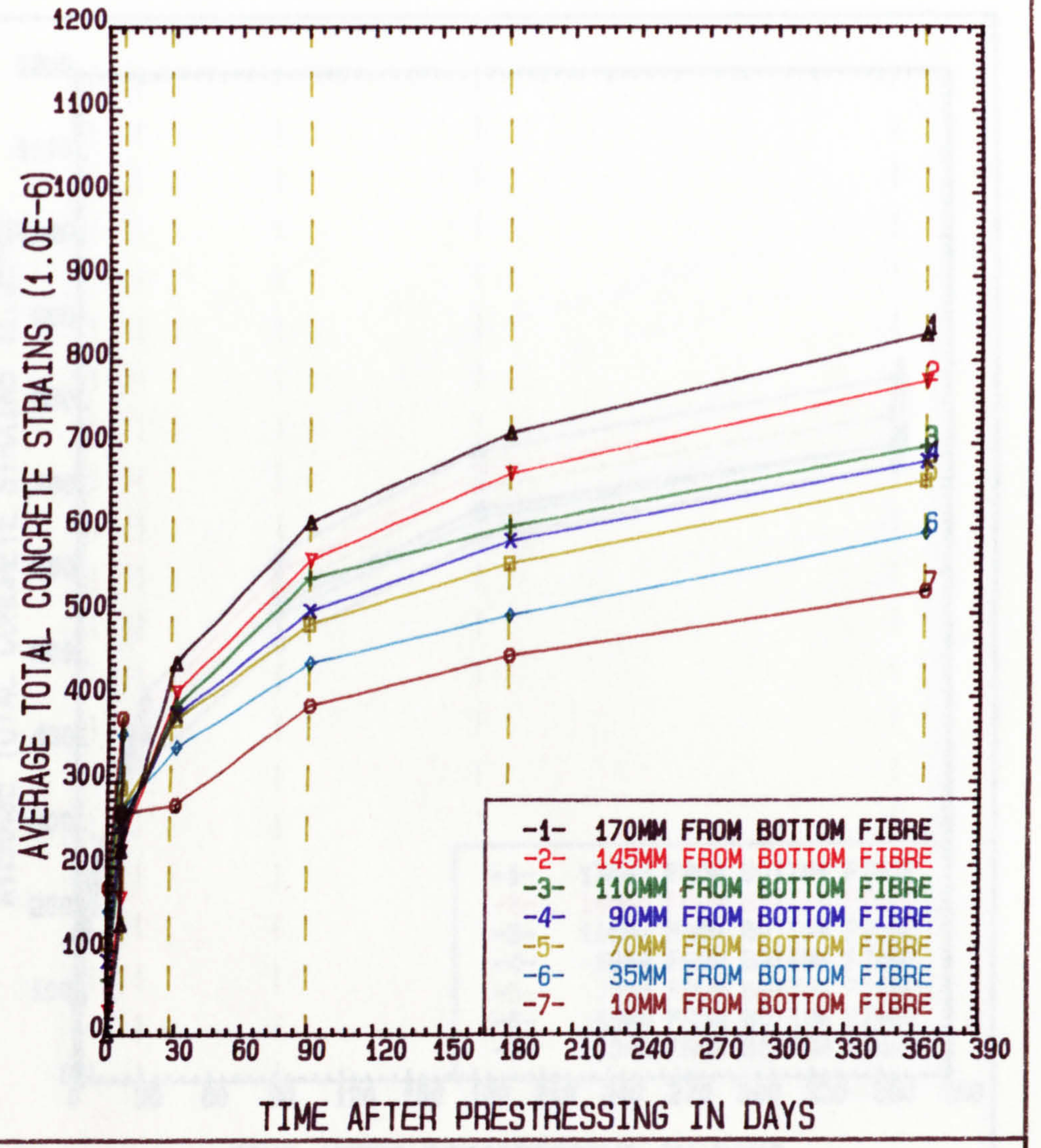

FIG. 6.10 MEASURED CONCRETE STRAIN DISTRIBUTION DIAGRAMS FOR MIDSPAN SECTION OF BEAM CR/C1 .

REMARKS: THE EXPERIMENTAL TIME-DEPENDENT PRESTRESS LOSS DETERMINED AT STEEL WIRE LEVEL FOR THE MIDSPAN SECTION AT 365 DAYS IS 14.12 % (179.0 MPa) (THE OBSERVED TIME-DEPENDENT CONCRETE STRAIN AT cgs = 498.0 MICROSTRAINS)

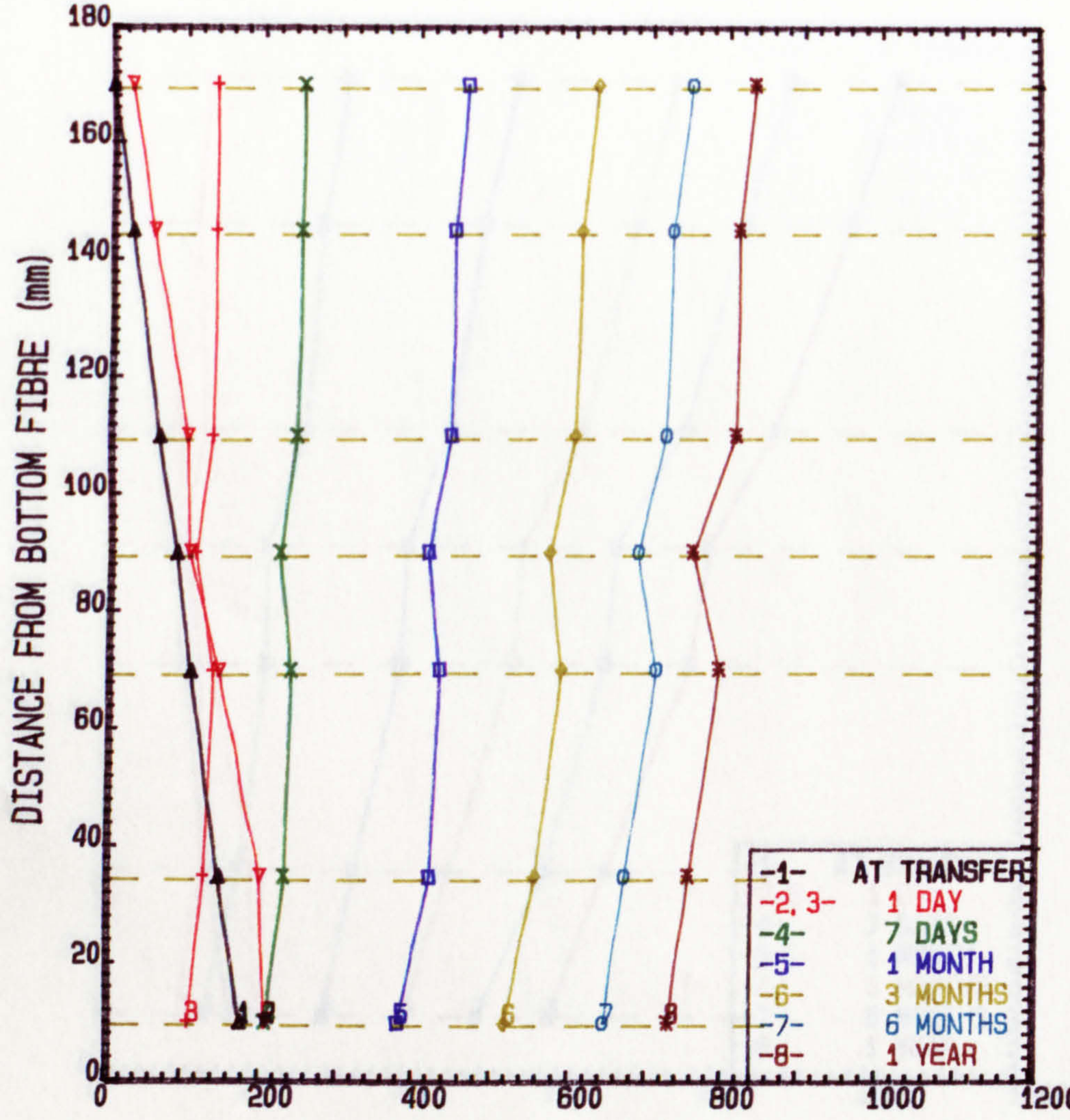

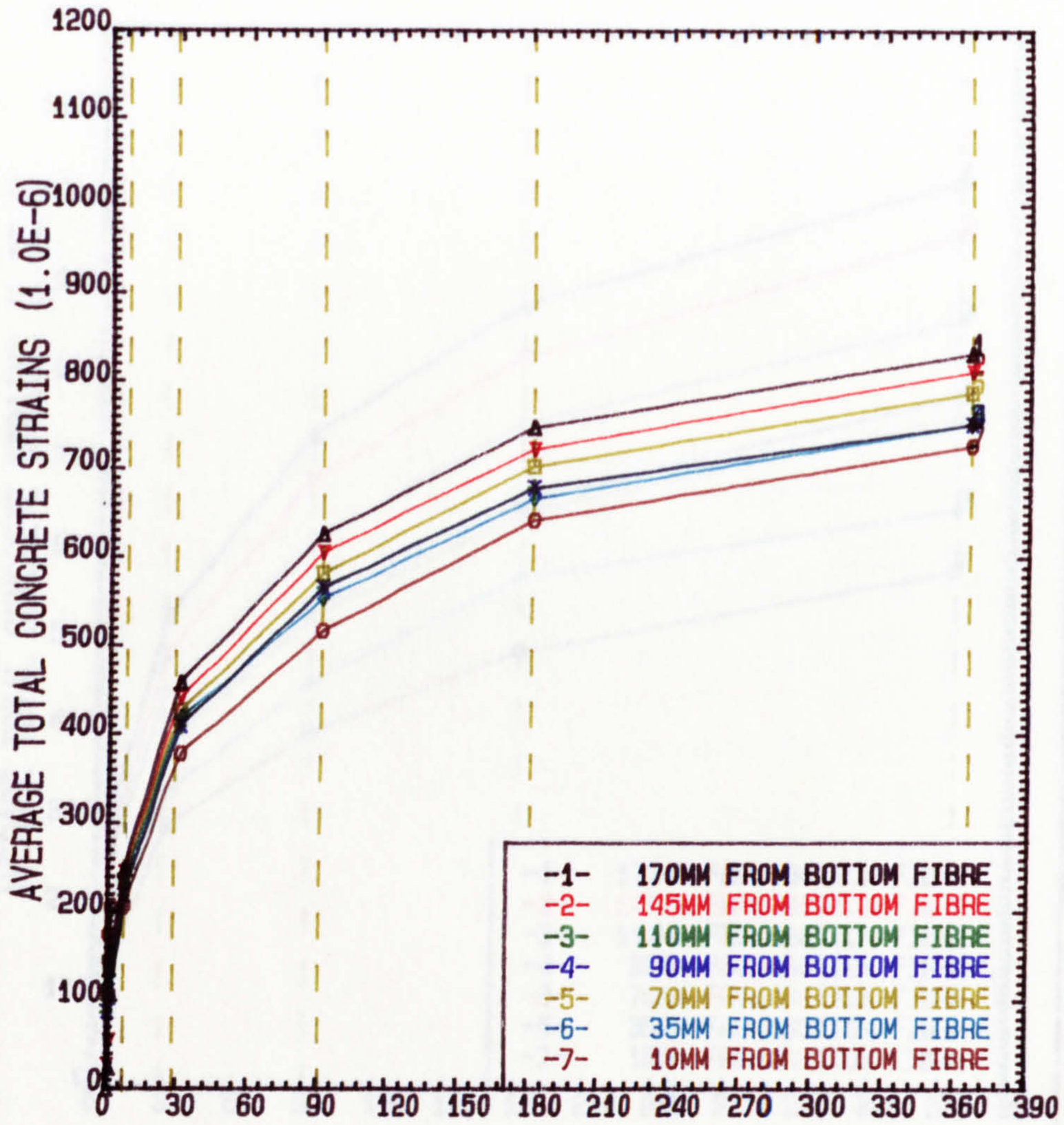

FIG. 6.11 MEASURED CONCRETE STRAIN DISTRIBUTION DIAGRAMS FOR MIDSPAN SECTION OF BEAM CYR/C2 .

REMARKS: THE EXPERIMENTAL TIME-DEPENDENT PRESTRESS LOSS DETERMINED AT STEEL WIRE LEVEL FOR THE MIDSPAN SECTION AT 365 DAYS IS 16.47 % (209.0 MPa) (THE OBSERVED TIME-DEPENDENT CONCRETE STRAIN AT cgs = 642.0 MICROSTRAINS)

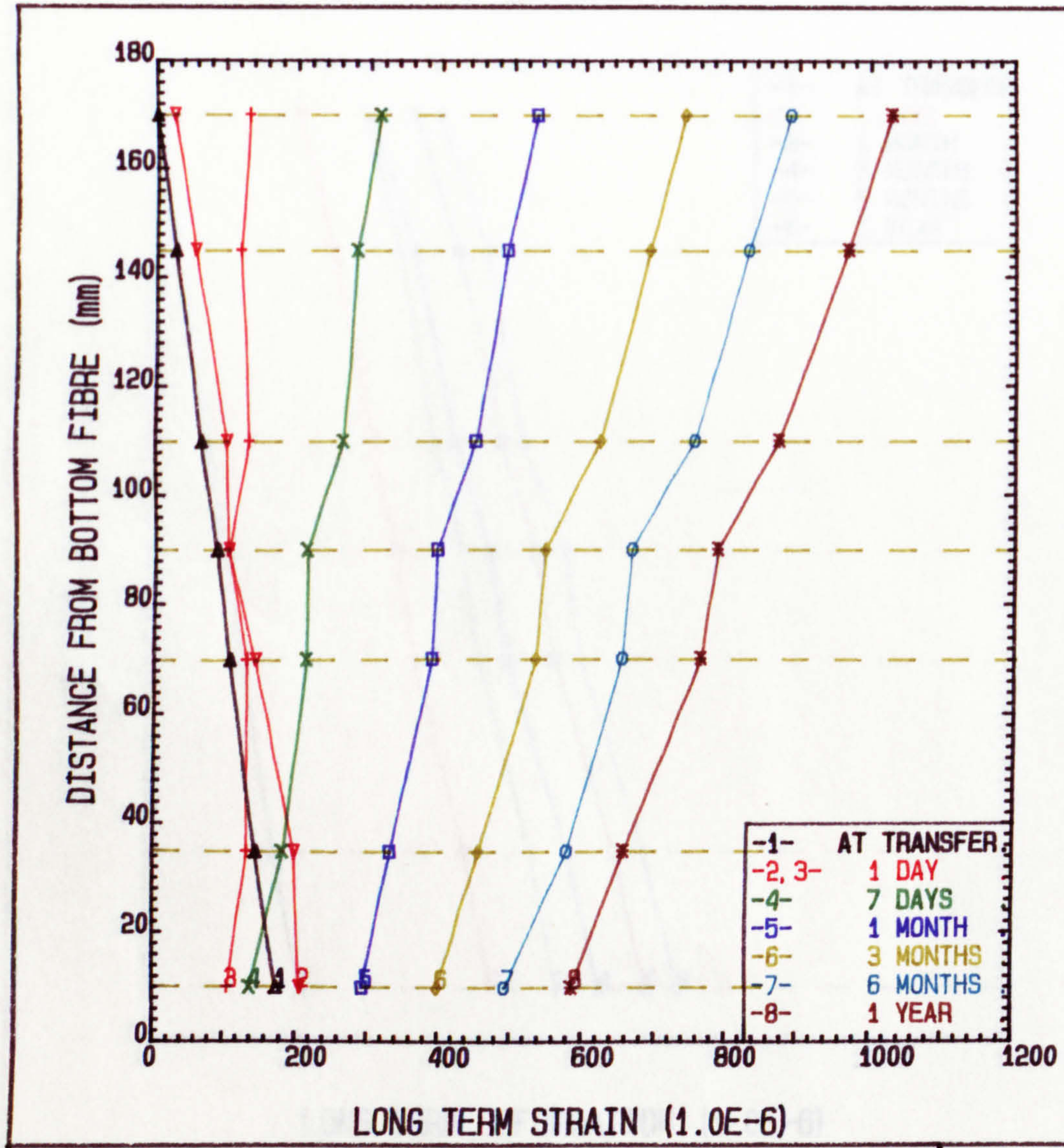

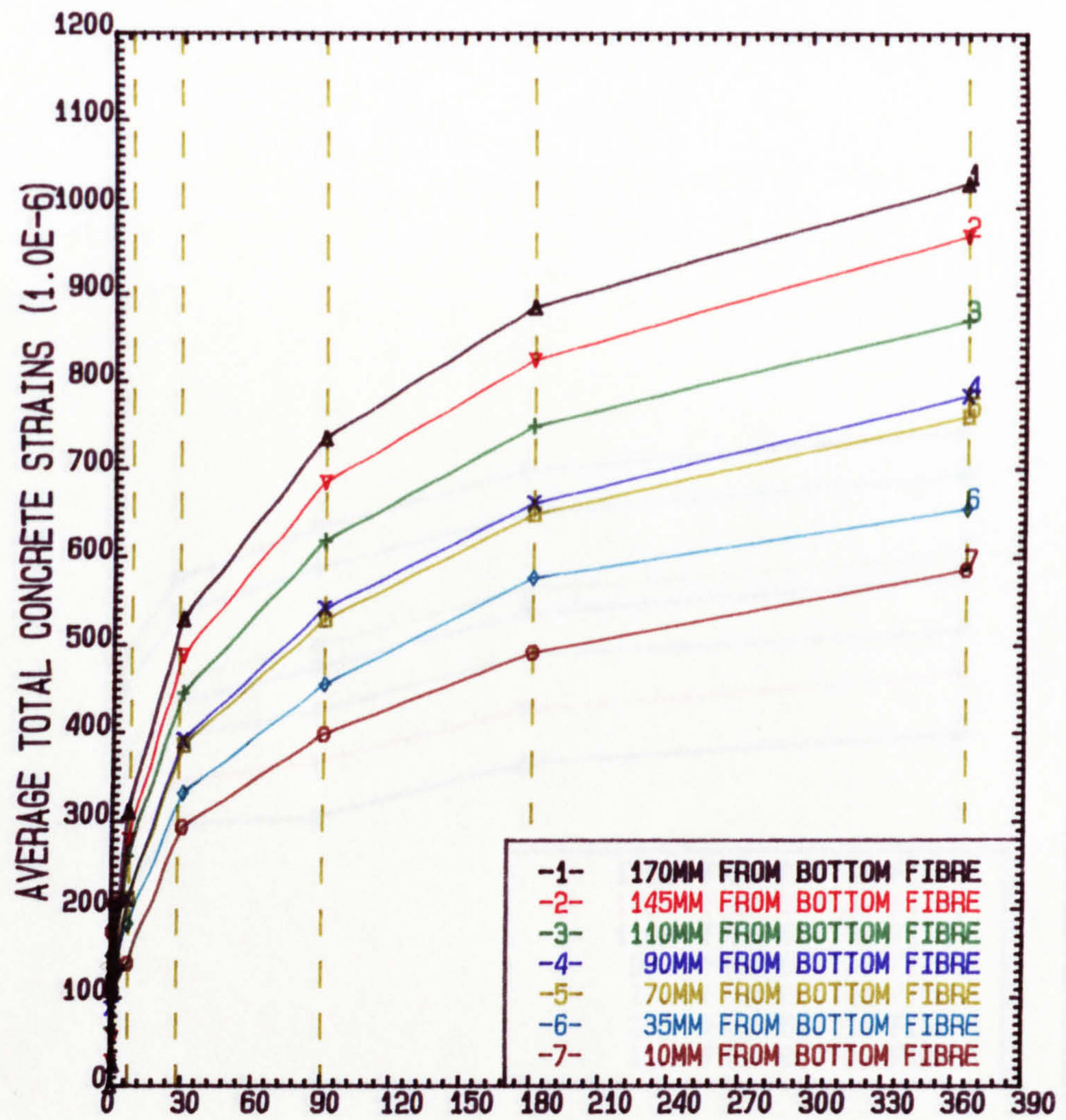

FIG. 6.12 MEASURED CONCRETE STRAIN DISTRIBUTION DIAGRAMS FOR MIDSPAN SECTION OF BEAM CR/C2 .

REMARKS: THE EXPERIMENTAL TIME-DEPENDENT PRESTRESS LOSS DETERMINED AT STEEL WIRE LEVEL FOR THE MIDSPAN SECTION AT 365 DAYS IS 15.47 % (196.0 MPa) (THE OBSERVED TIME-DEPENDENT CONCRETE STRAIN AT cgs = 580.0 MICROSTRAINS)

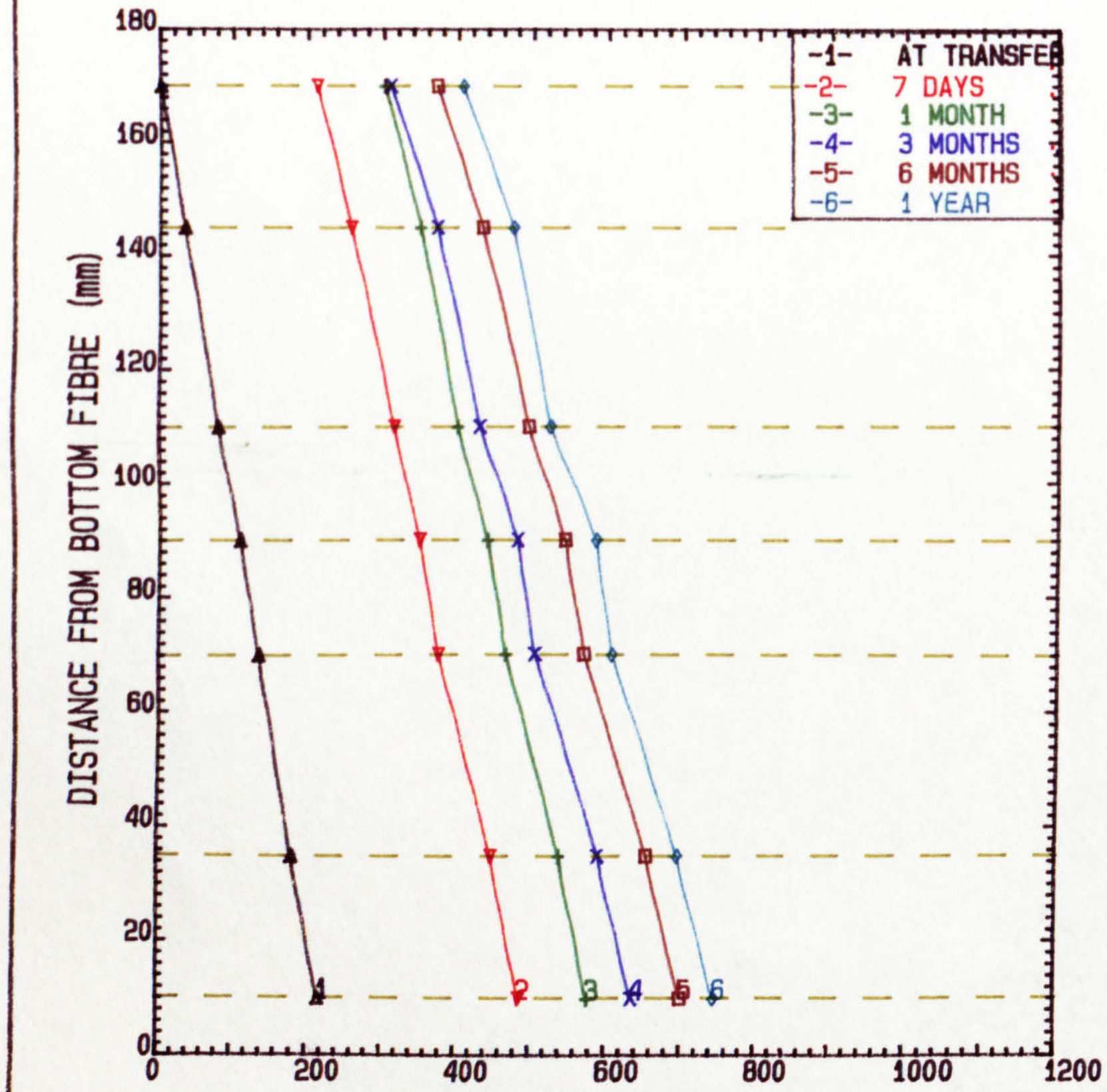

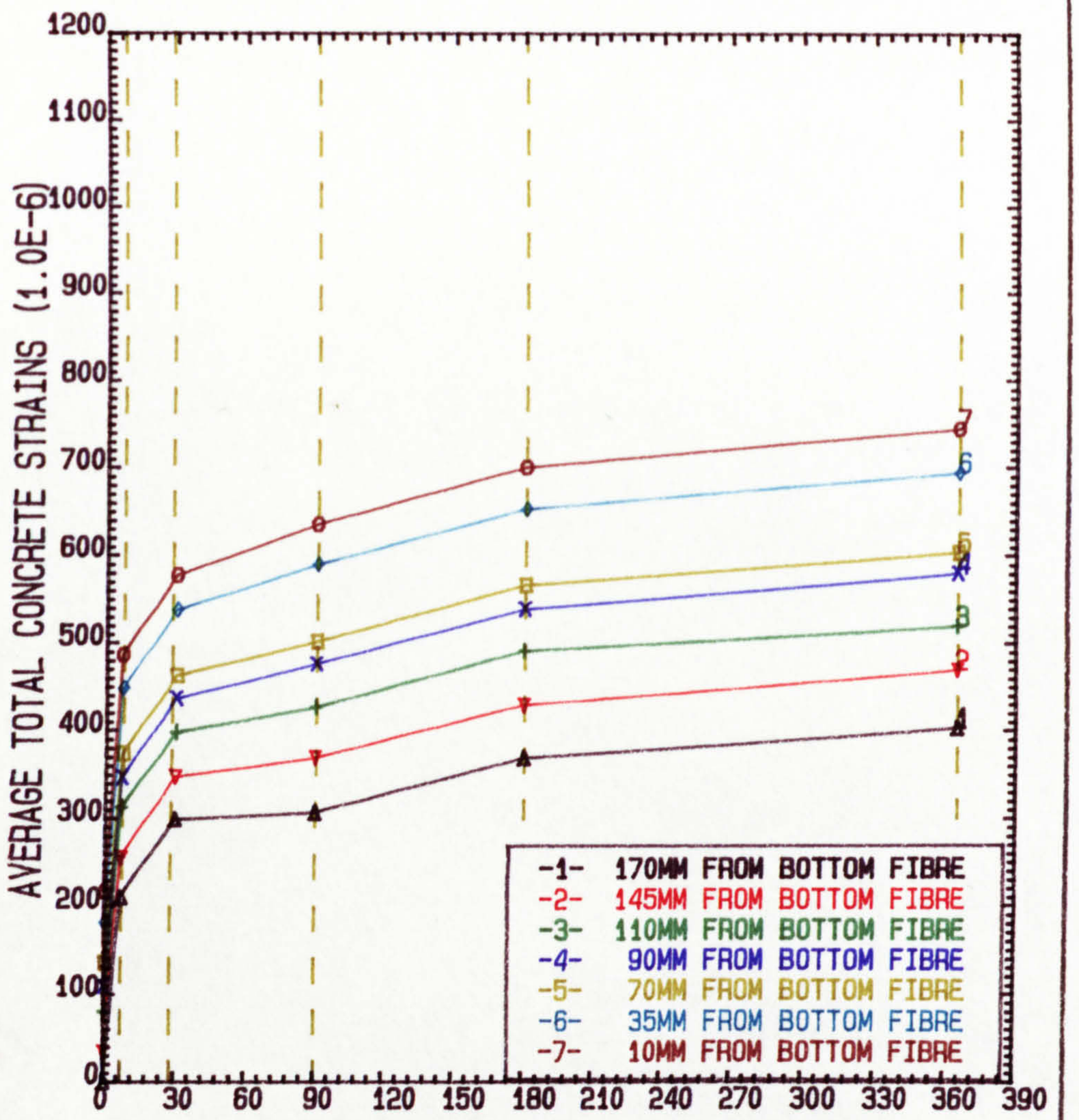

FIG. 6.13 MEASURED CONCRETE STRAIN DISTRIBUTION DIAGRAMS FOR MIDSPAN SECTION OF BEAM NGI/V1 .

REMARKS: THE EXPERIMENTAL TIME-DEPENDENT PRESTRESS LOSS DETERMINED AT THE STEEL WIRE LEVEL FOR THE MIDSPAN SECTION AT 365 DAYS IS 13.99 % (177.0 MPa)
(THE OBSERVED TIME-DEPENDENT CONCRETE STRAIN AT cgs = 490.0 MICROSTRAINS)

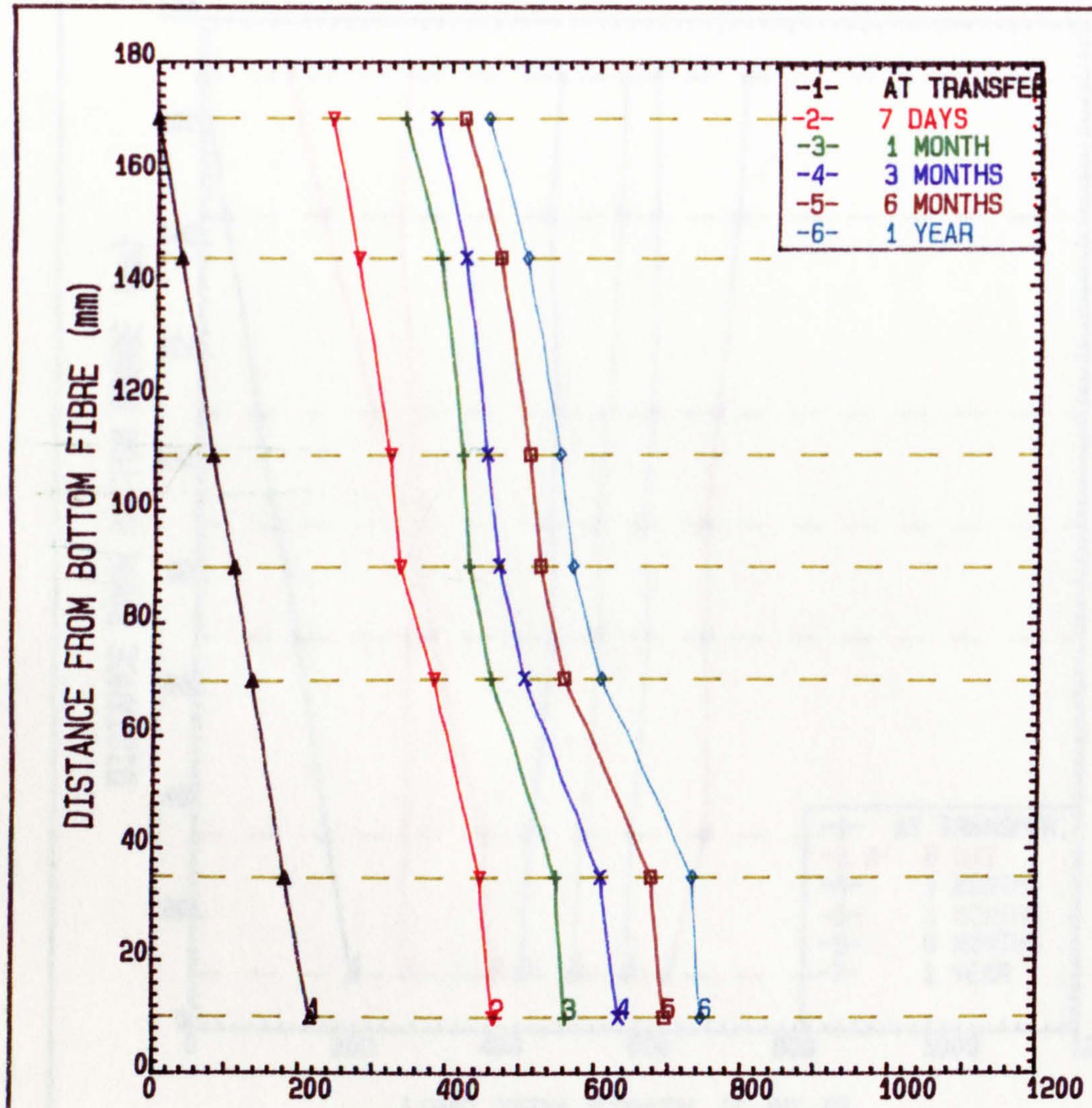

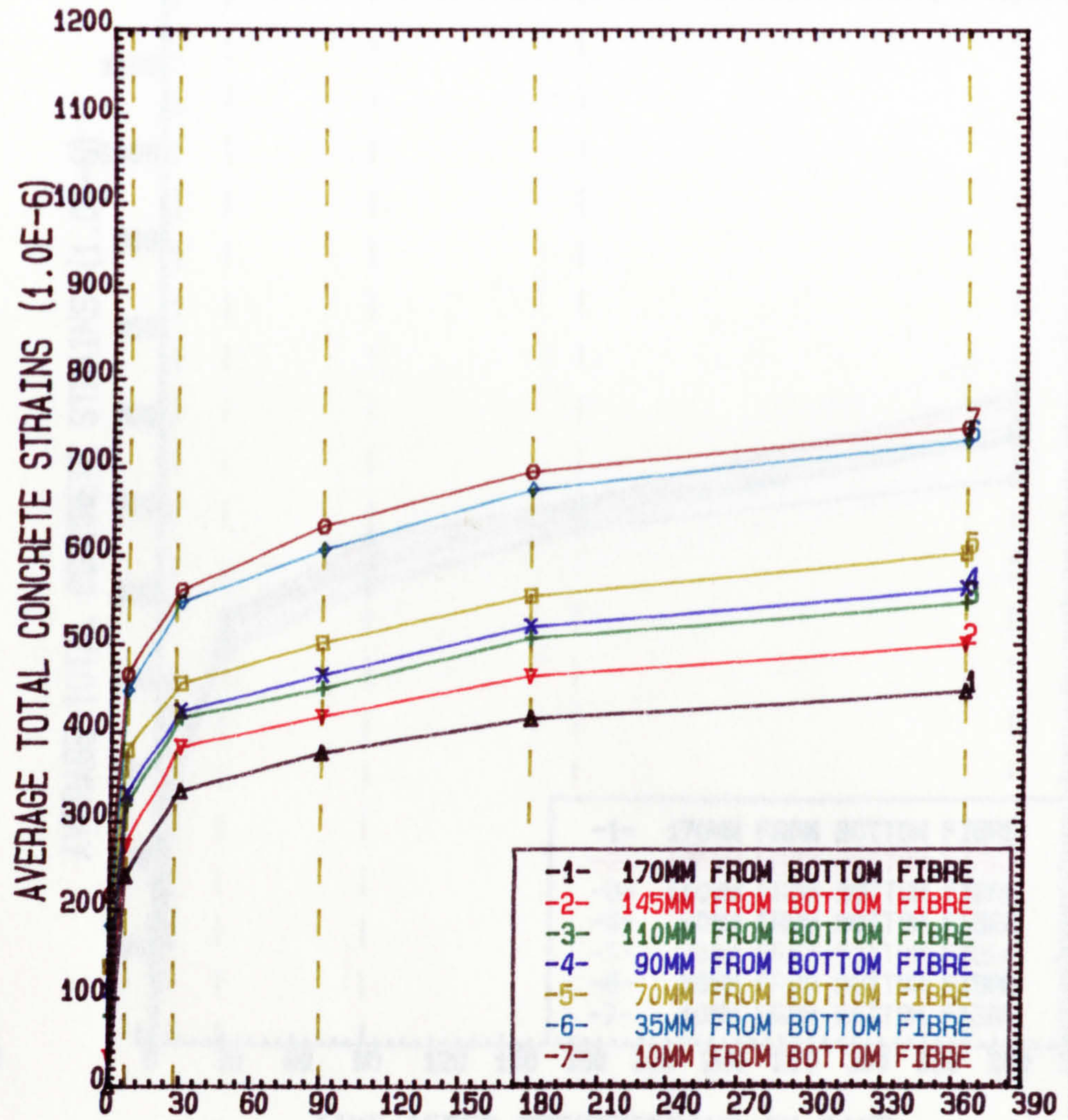

FIG. 6.14 MEASURED CONCRETE STRAIN DISTRIBUTION DIAGRAMS FOR MIDSPAN SECTION OF BEAM NI/V1 .

REMARKS: THE EXPERIMENTAL TIME-DEPENDENT PRESTRESS LOSS DETERMINED AT THE STEEL WIRE LEVEL FOR THE MIDSPAN SECTION AT 365 DAYS IS 14.29 % (181.0 MPa)
(THE OBSERVED TIME-DEPENDENT CONCRETE STRAIN AT cgs = 508.0 MICROSTRAINS)

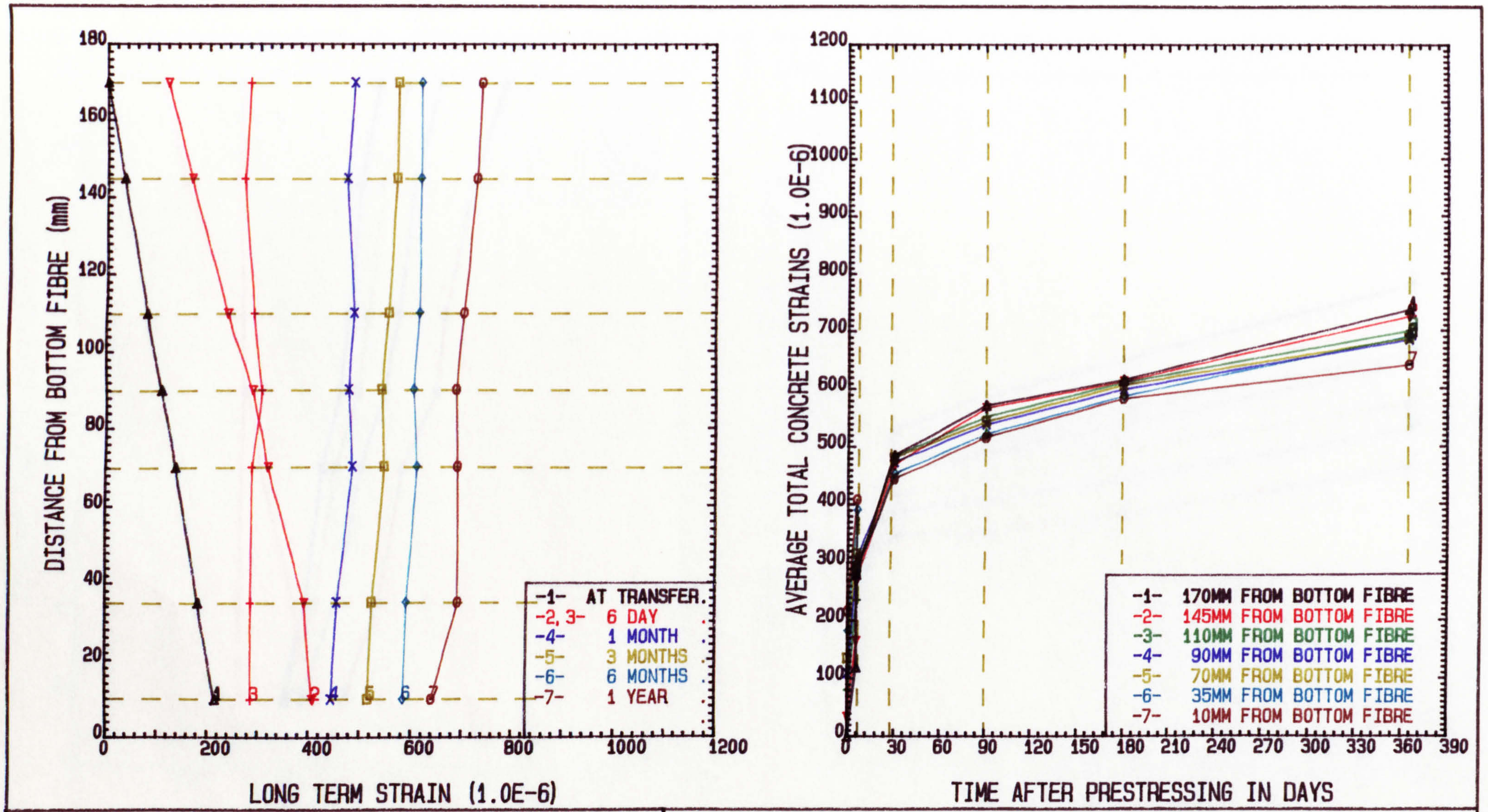

FIG. 6.15 MEASURED CONCRETE STRAIN DISTRIBUTION DIAGRAMS FOR MIDSPAN SECTION OF BEAM CYI/V1 .

REMARKS: THE EXPERIMENTAL TIME-DEPENDENT PRESTRESS LOSS DETERMINED AT STEEL WIRE LEVEL FOR THE MIDSPAN SECTION AT 365 DAYS IS 14.64 % (186.0 MPa) (THE OBSERVED TIME-DEPENDENT CONCRETE STRAIN AT cgs = 530.0 MICROSTRAINS)

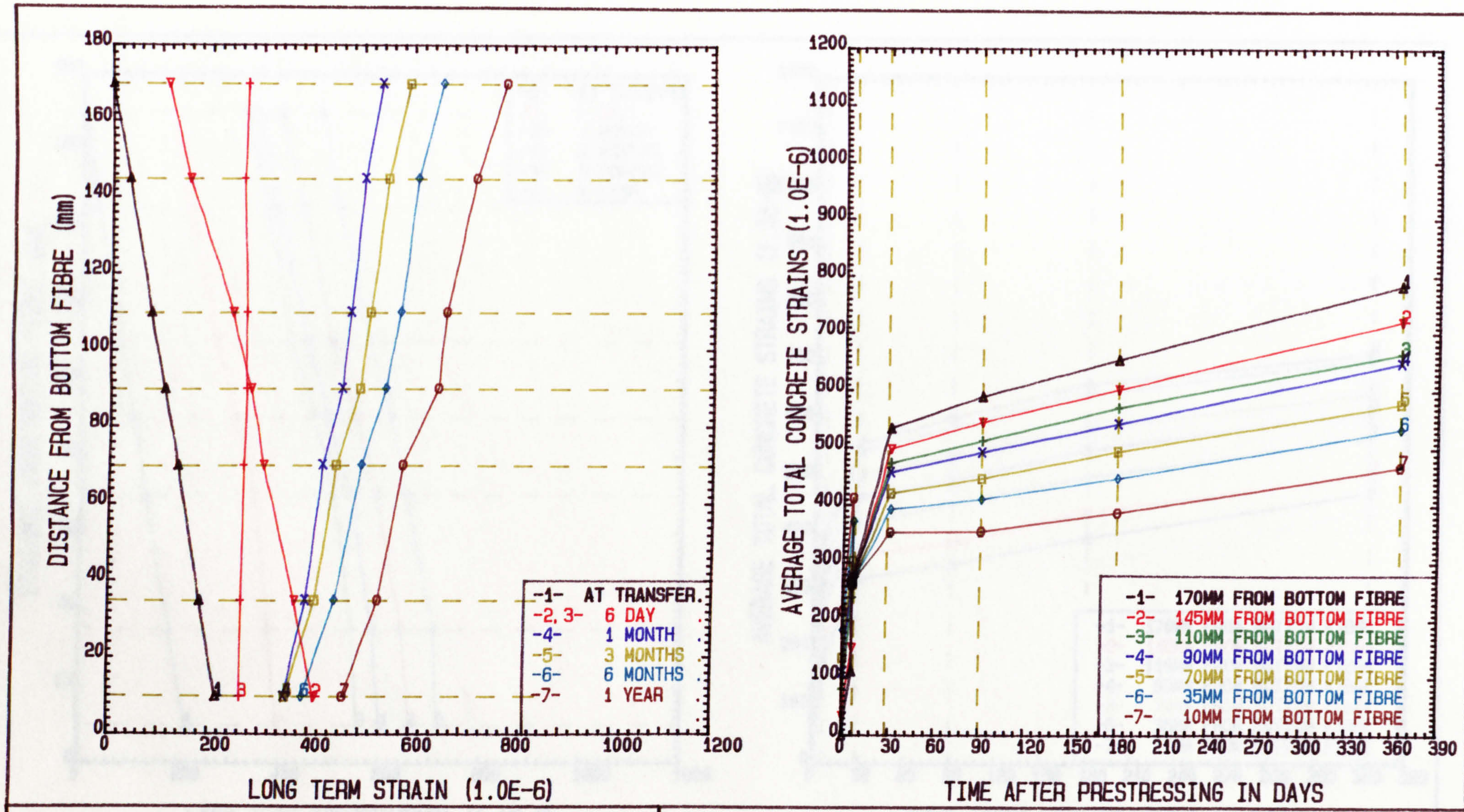

FIG. 6.16 MEASURED CONCRETE STRAIN DISTRIBUTION DIAGRAMS FOR MIDSPAN SECTION OF BEAM CI/V1

REMARKS: THE EXPERIMENTAL TIME-DEPENDENT PRESTRESS LOSS DETERMINED AT STEEL WIRE LEVEL FOR THE MIDSPAN SECTION AT 365 DAYS IS 12.49 % (158.0 MPa)
(THE OBSERVED TIME-DEPENDENT CONCRETE STRAIN AT cgs = 398.0 MICROSTRAINS)

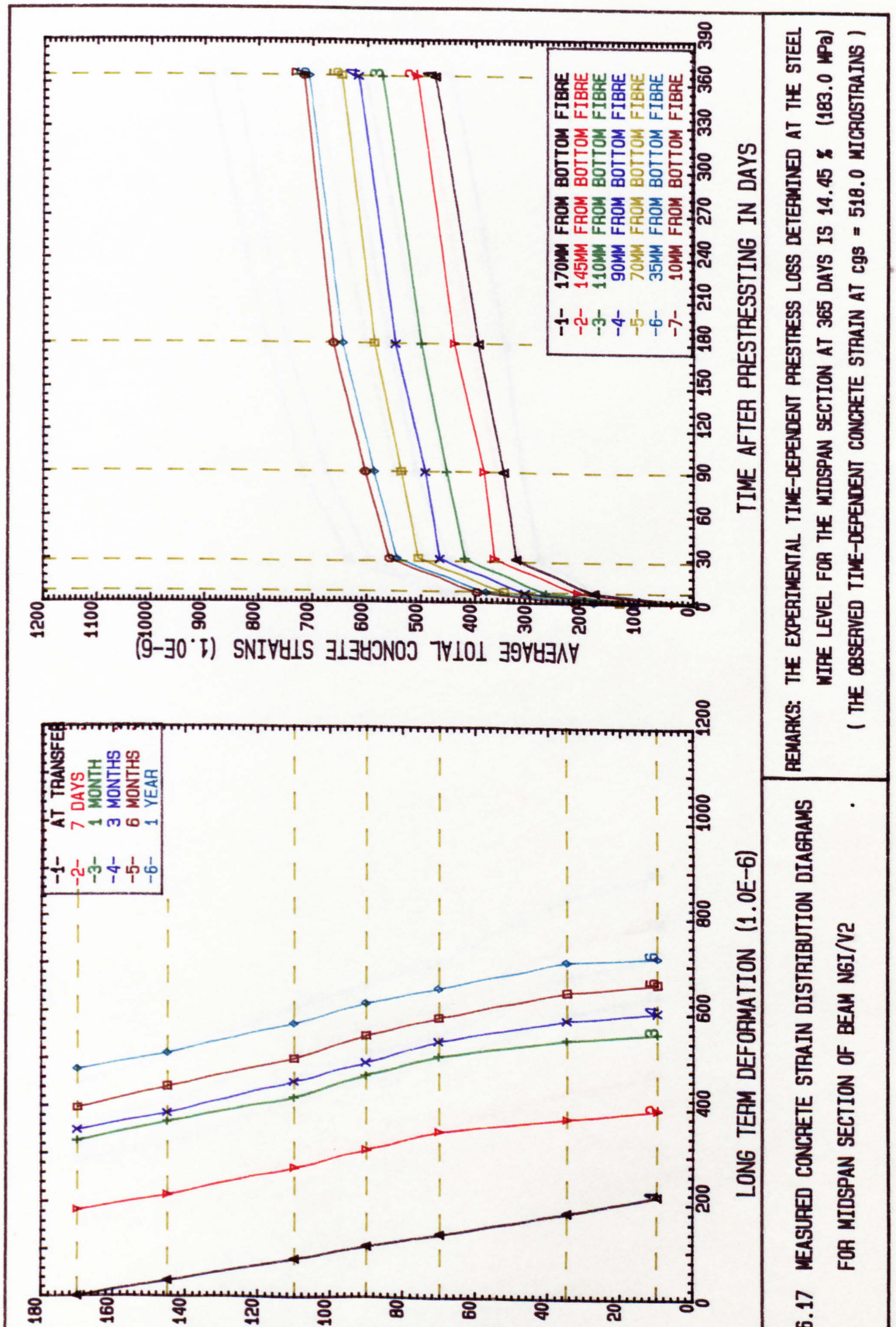

FIG. 6.17 MEASURED CONCRETE STRAIN DISTRIBUTION DIAGRAMS FOR MIDSPAN SECTION OF BEAM N6I/V2

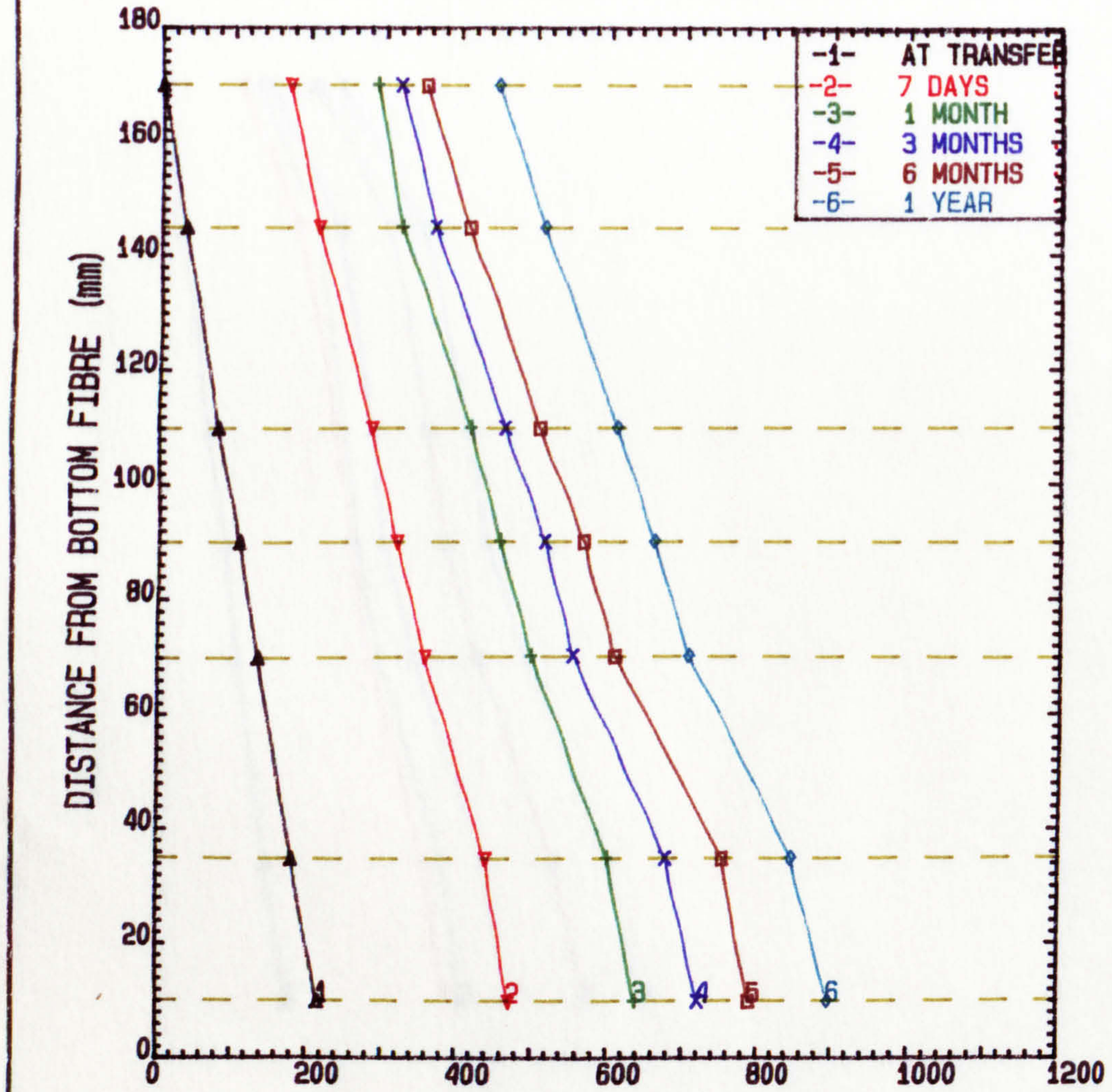

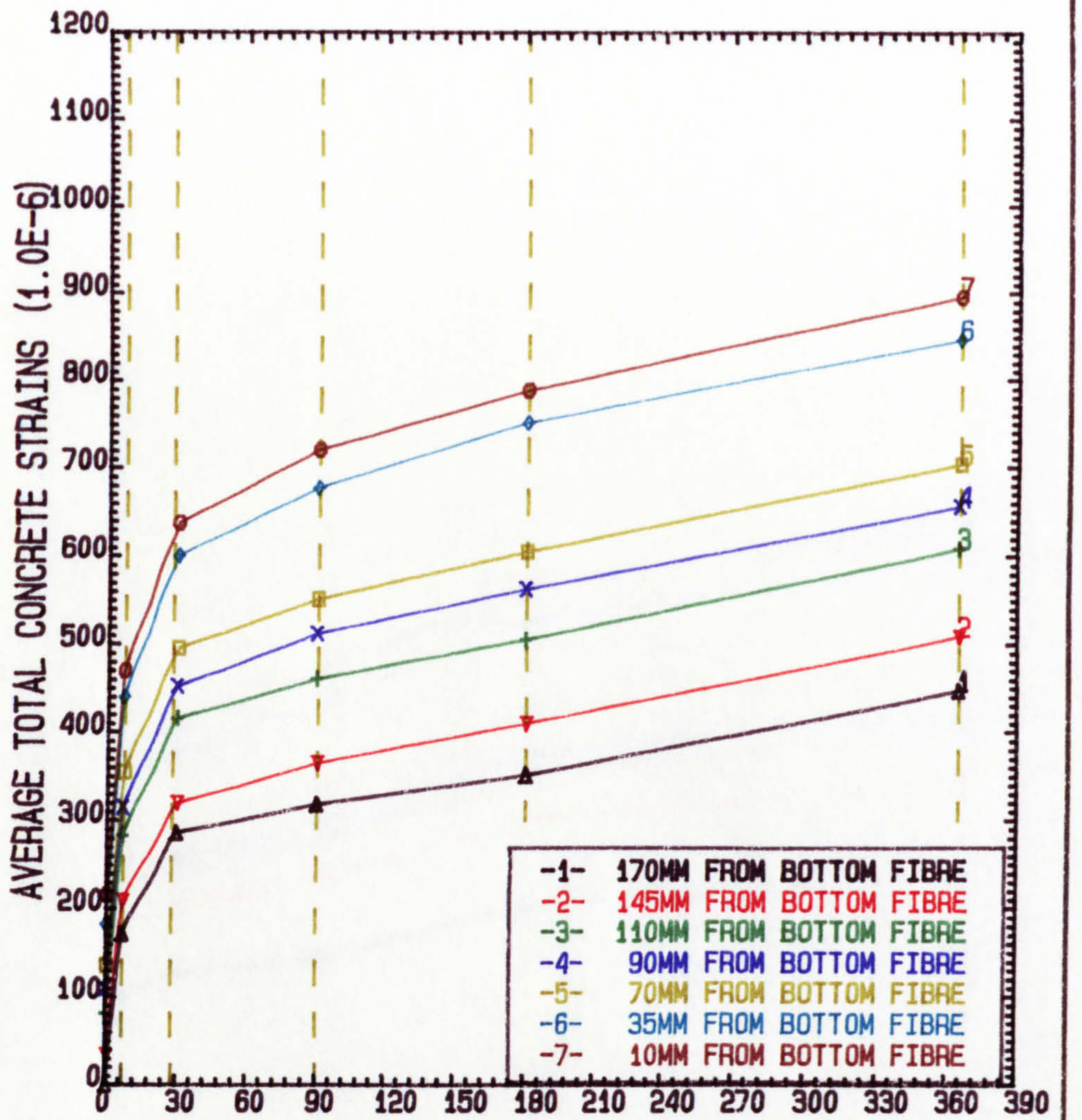

FIG. 6.18 MEASURED CONCRETE STRAIN DISTRIBUTION DIAGRAMS FOR MIDSPAN SECTION OF BEAM NI/V2 .

REMARKS: THE EXPERIMENTAL TIME-DEPENDENT PRESTRESS LOSS DETERMINED AT THE STEEL WIRE LEVEL FOR THE MIDSPAN SECTION AT 365 DAYS IS 16.04 % (203.0 MPa)
(THE OBSERVED TIME-DEPENDENT CONCRETE STRAIN AT cgs = 616.0 MICROSTRAINS)

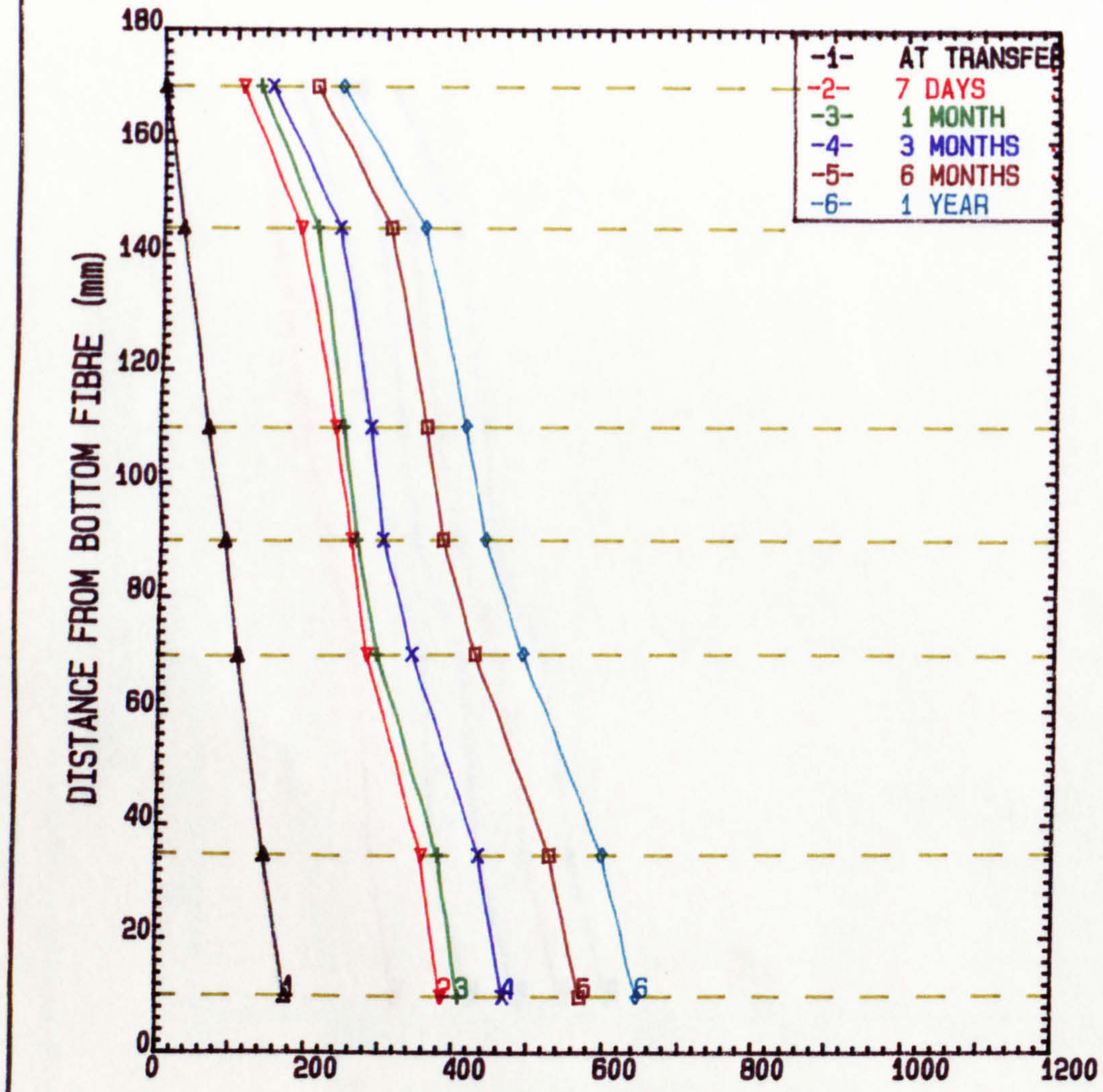

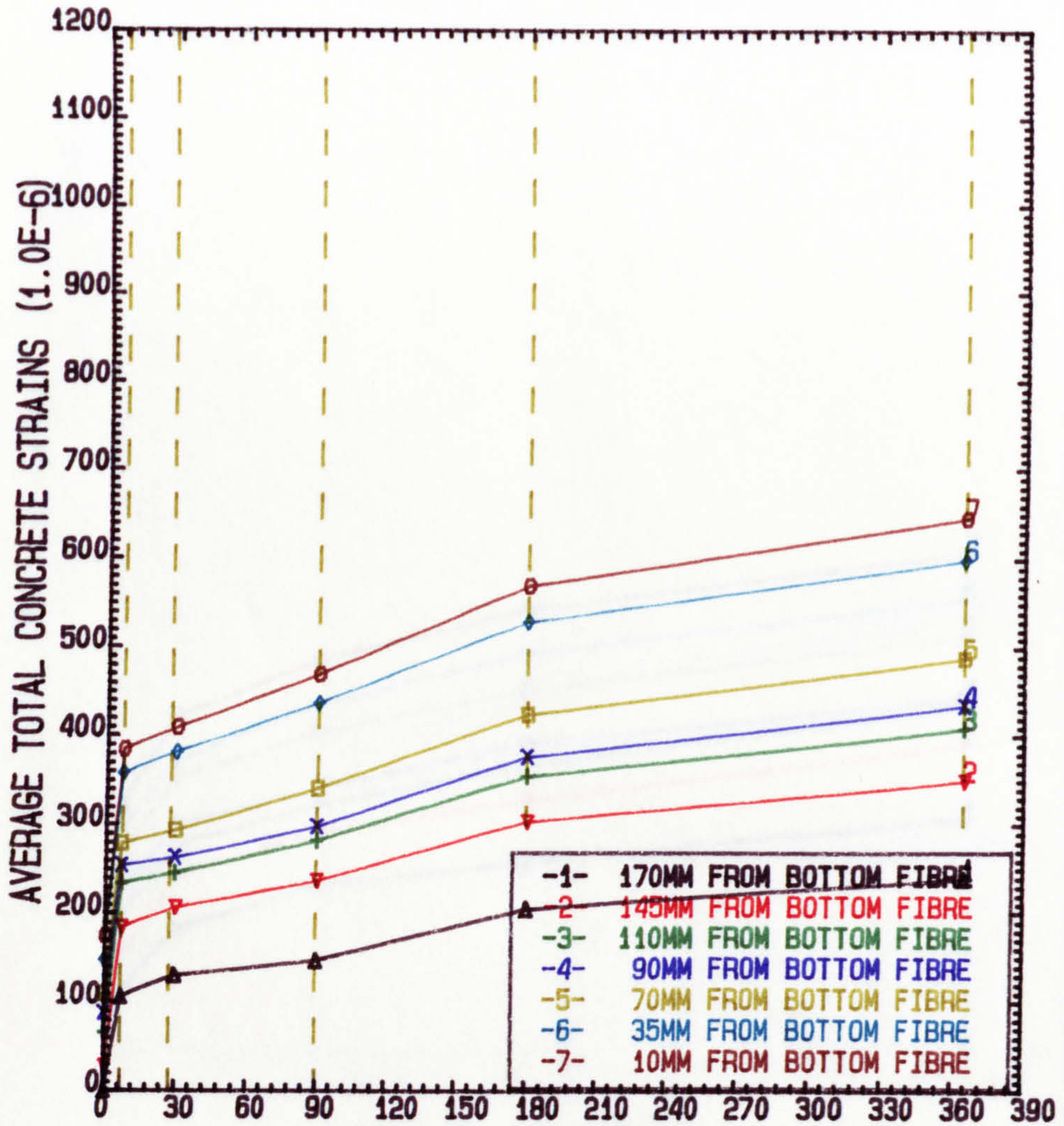

FIG. 6.19 MEASURED CONCRETE STRAIN DISTRIBUTION DIAGRAMS FOR MIDSPAN SECTION OF BEAM NGR/V1

REMARKS: THE EXPERIMENTAL TIME-DEPENDENT PRESTRESS LOSS DETERMINED AT THE STEEL WIRE LEVEL FOR THE MIDSPAN SECTION AT 365 DAYS IS 12.79 % (162.0 MPa)
(THE OBSERVED TIME-DEPENDENT CONCRETE STRAIN AT cgs = 416.0 MICROSTRAINS)

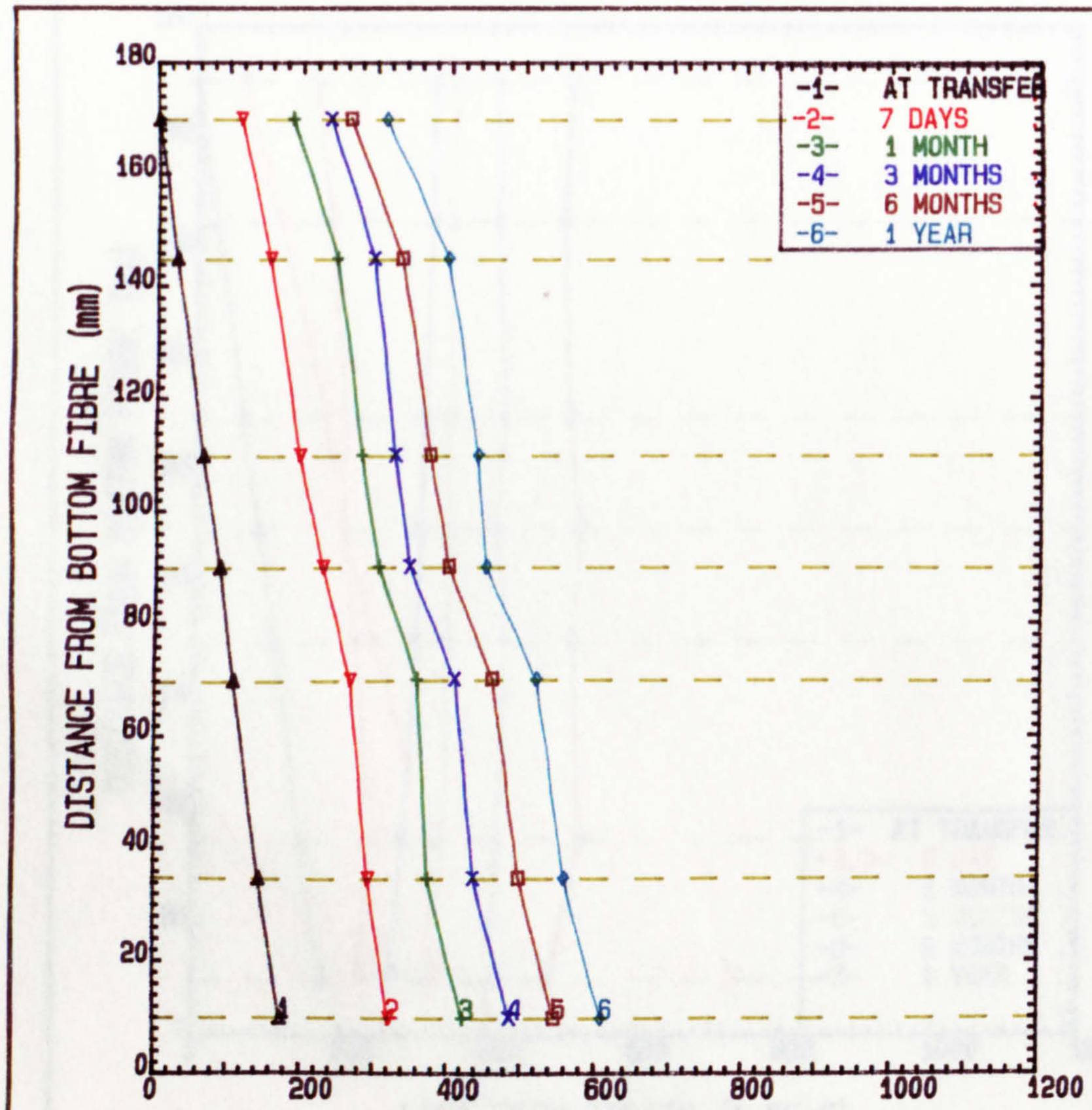

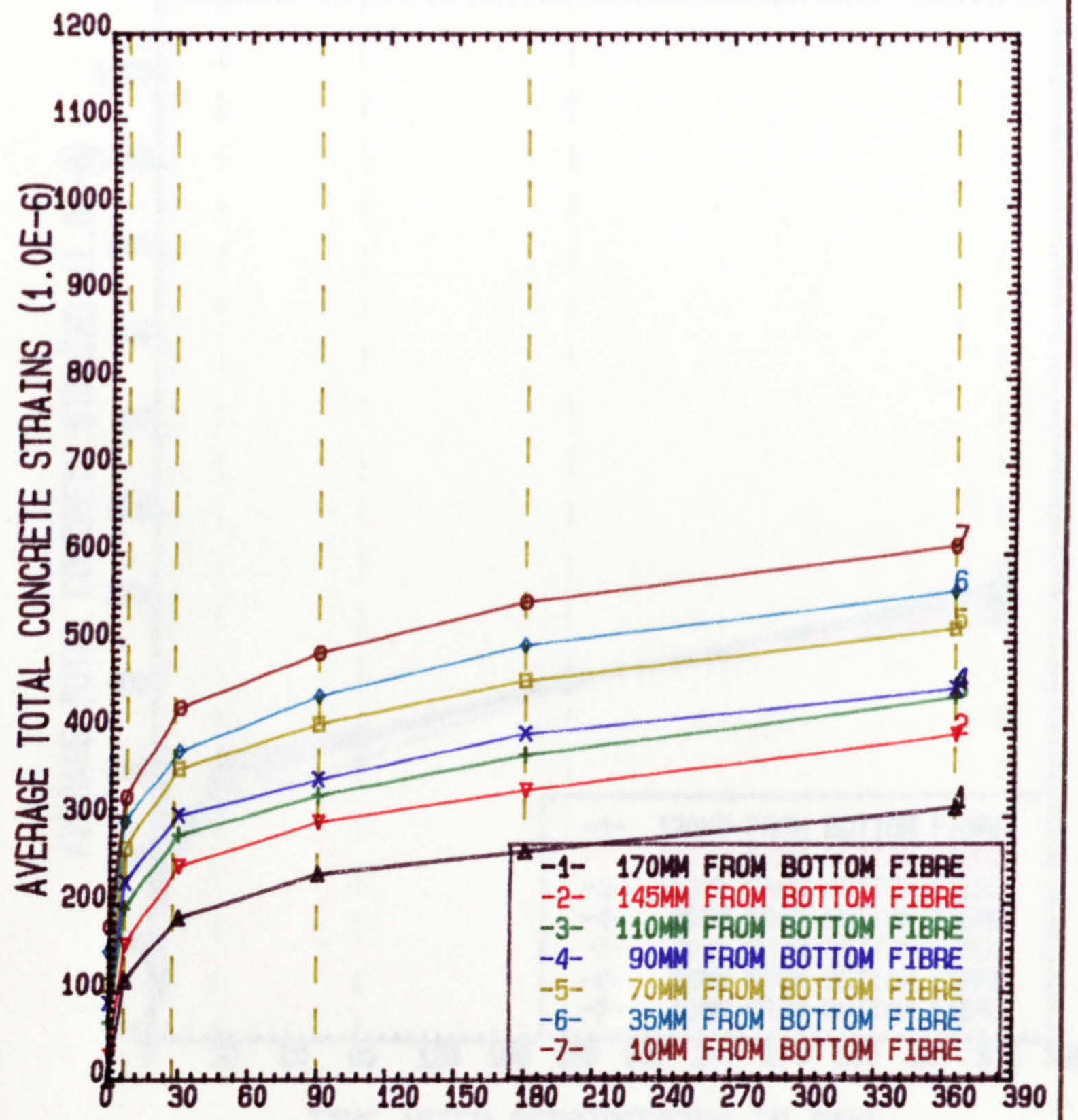

FIG. 6.20 MEASURED CONCRETE STRAIN DISTRIBUTION DIAGRAMS FOR MIDSPAN SECTION OF BEAM NR/V1 .

REMARKS: THE EXPERIMENTAL TIME-DEPENDENT PRESTRESS LOSS DETERMINED AT THE STEEL WIRE LEVEL FOR THE MIDSPAN SECTION AT 365 DAYS IS 13.08 % (166.0 MPa)
(THE OBSERVED TIME-DEPENDENT CONCRETE STRAIN AT cgs = 434.0 MICROSTRAINS)

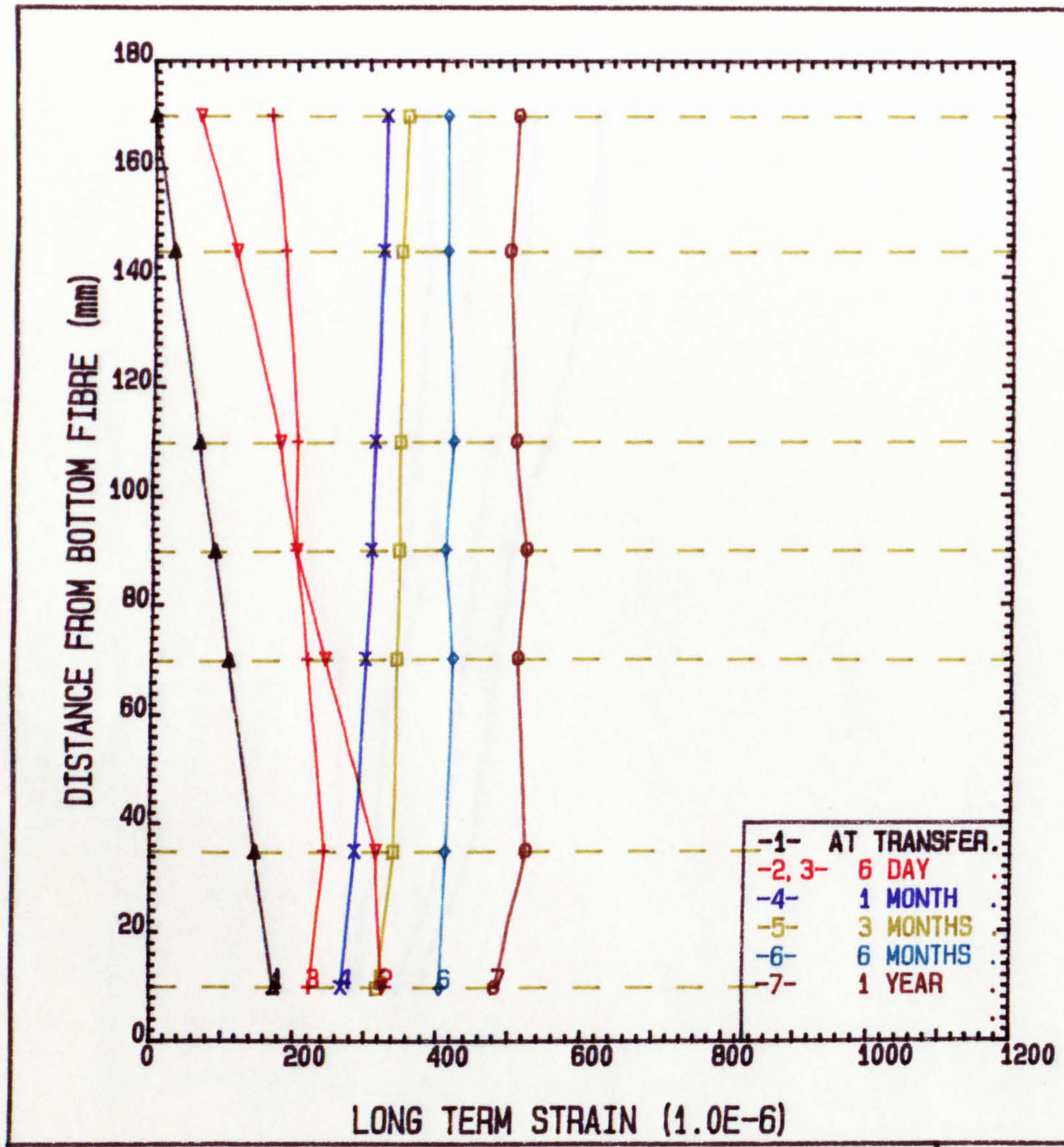

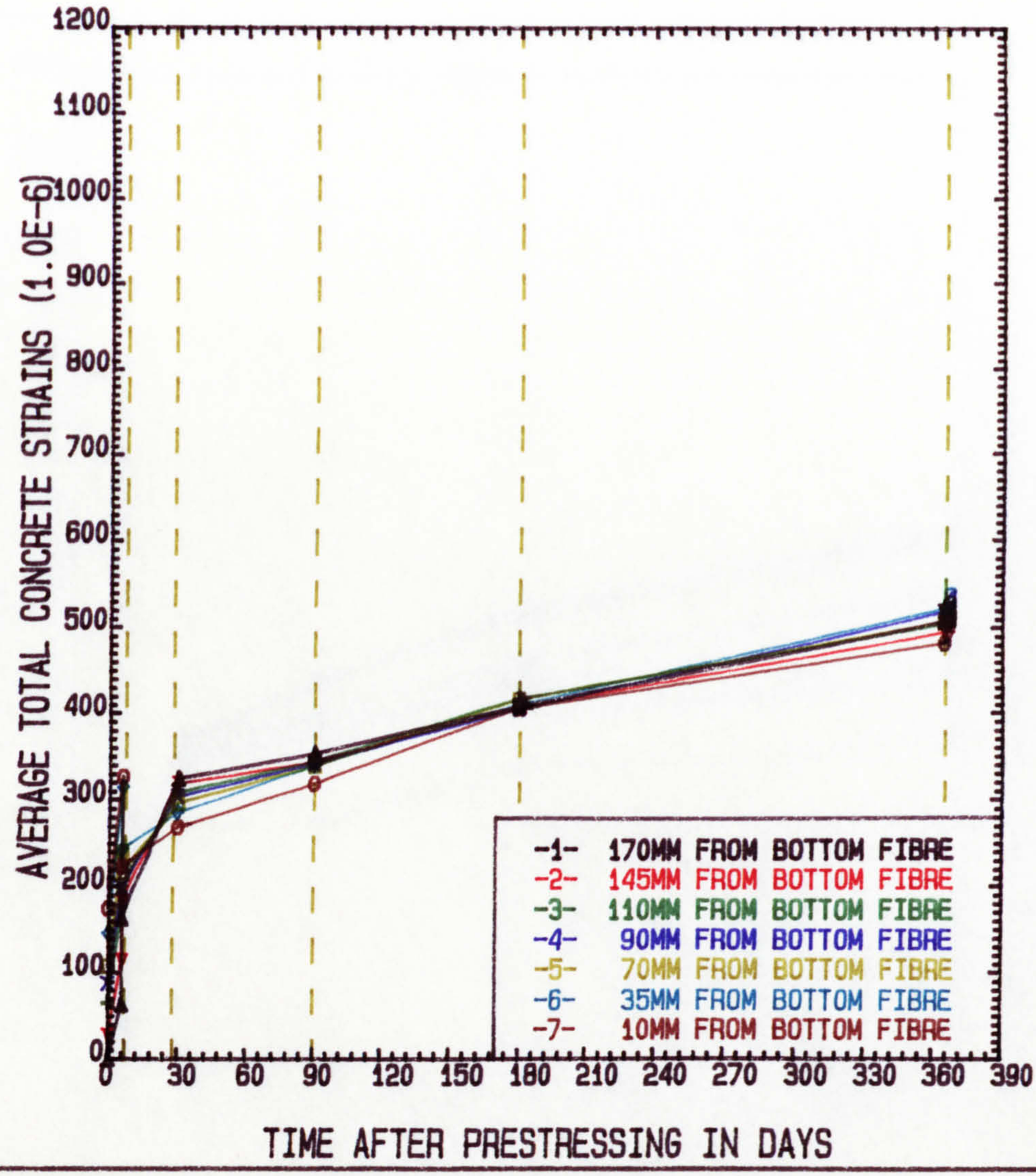

FIG. 6.21 MEASURED CONCRETE STRAIN DISTRIBUTION DIAGRAMS FOR MIDSPAN SECTION OF BEAM CYR/V1 .

REMARKS: THE EXPERIMENTAL TIME-DEPENDENT PRESTRESS LOSS DETERMINED AT STEEL WIRE LEVEL FOR THE MIDSPAN SECTION AT 365 DAYS IS 12.33 % (156.0 MPa) (THE OBSERVED TIME-DEPENDENT CONCRETE STRAIN AT cgs = 388.0 MICROSTRAINS)

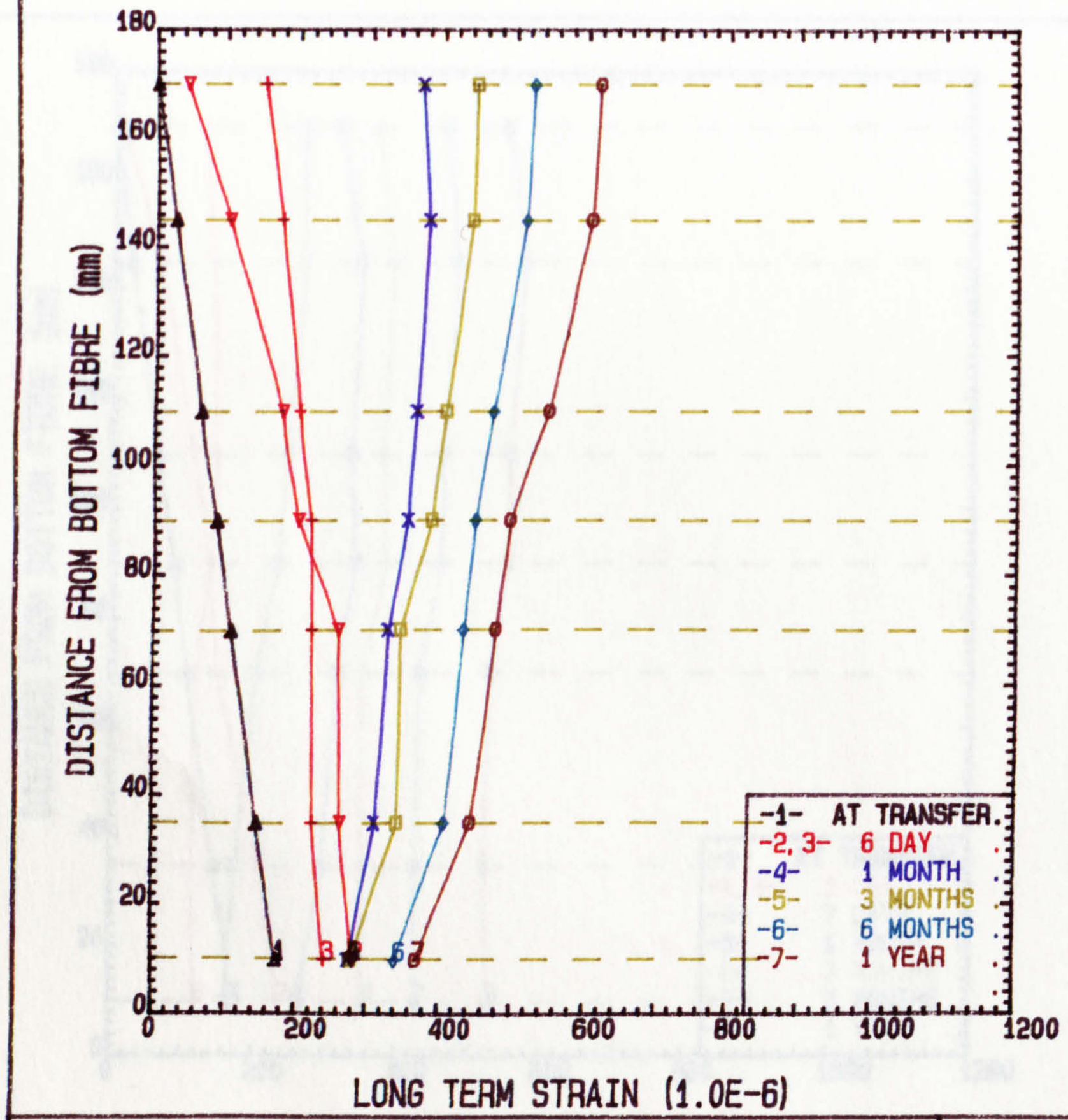

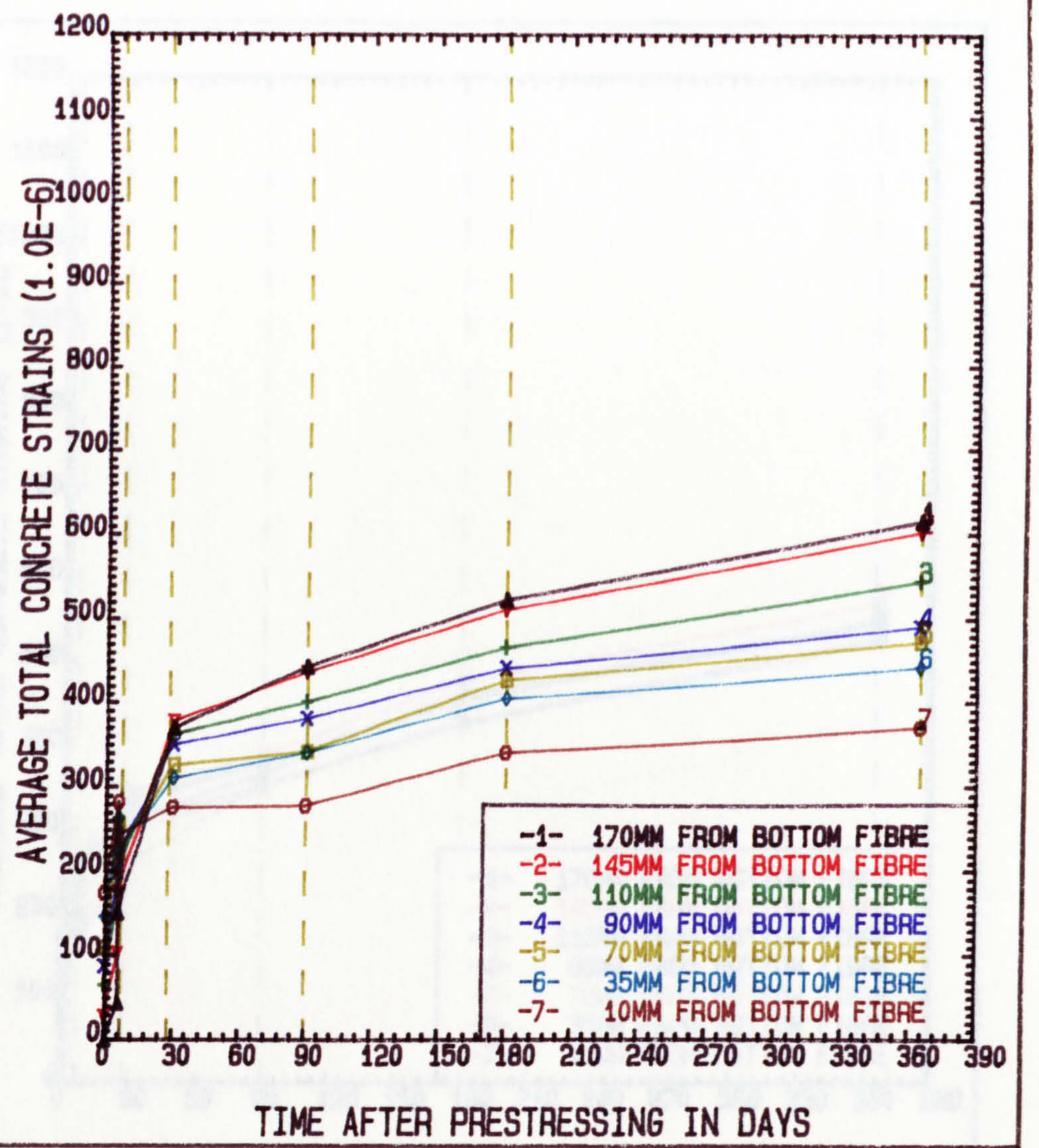

FIG. 6.22 MEASURED CONCRETE STRAIN DISTRIBUTION DIAGRAMS FOR MIDSPAN SECTION OF BEAM CR/V1 .

REMARKS: THE EXPERIMENTAL TIME-DEPENDENT PRESTRESS LOSS DETERMINED AT STEEL WIRE LEVEL FOR THE MIDSPAN SECTION AT 365 DAYS IS 11.39 % (144.0 MPa) (THE OBSERVED TIME-DEPENDENT CONCRETE STRAIN AT cgs = 330.0 MICROSTRAINS)

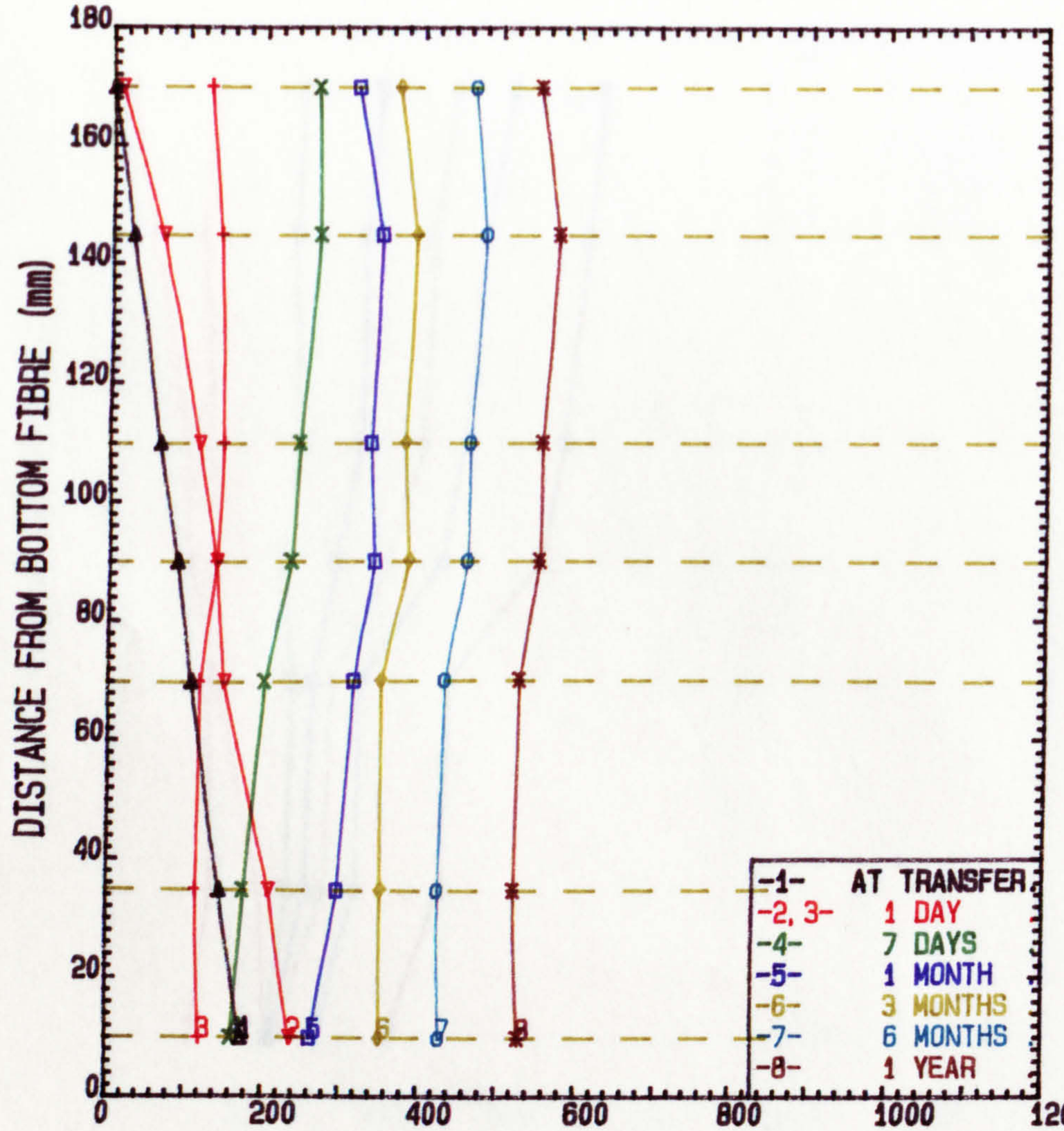

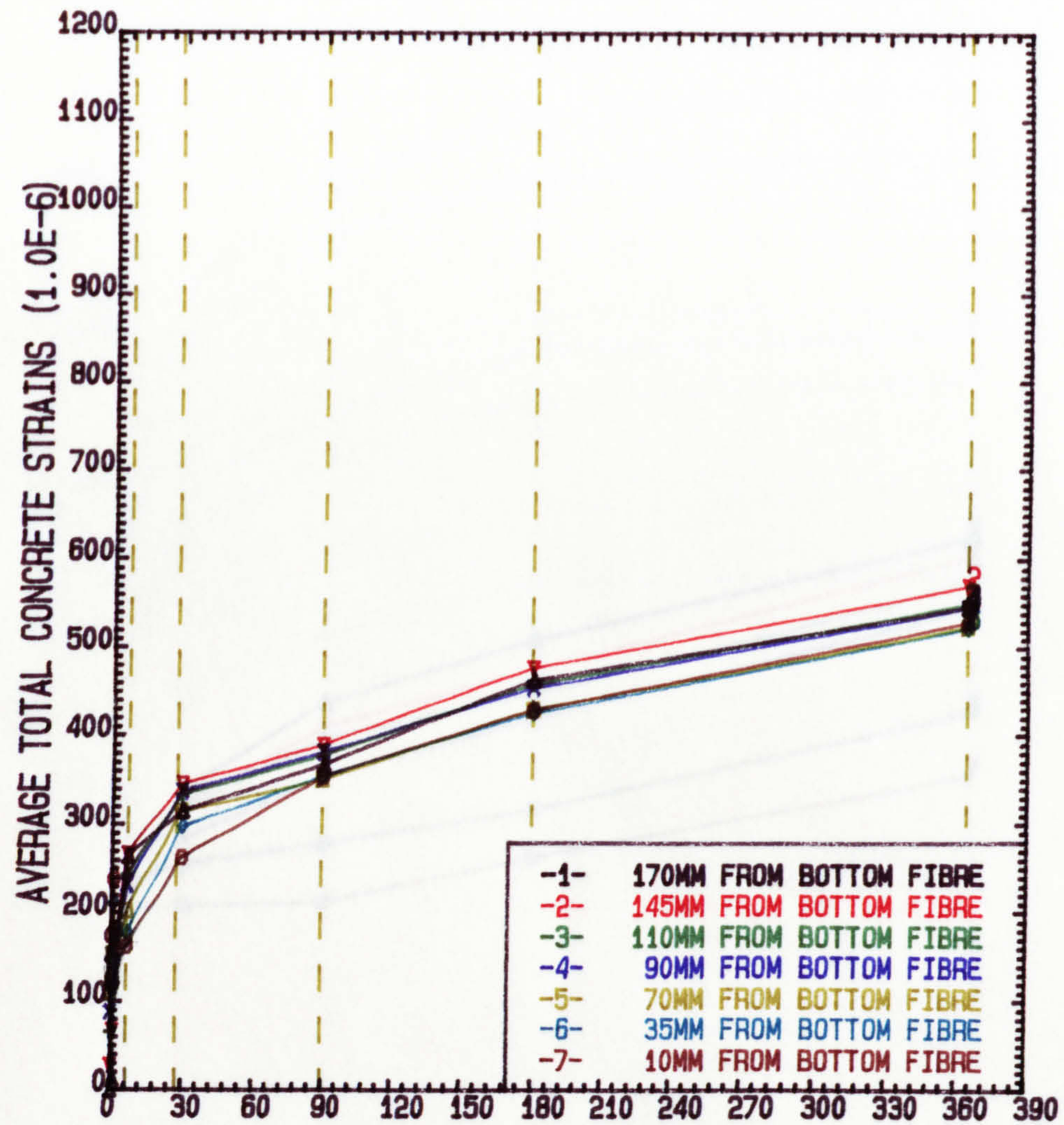

FIG. 6.23 MEASURED CONCRETE STRAIN DISTRIBUTION DIAGRAMS FOR MIDSPAN SECTION OF BEAM CYR/V2 .

REMARKS: THE EXPERIMENTAL TIME-DEPENDENT PRESTRESS LOSS DETERMINED AT STEEL WIRE LEVEL FOR THE MIDSPAN SECTION AT 365 DAYS IS 12.46 % (158.0 MPa)
(THE OBSERVED TIME-DEPENDENT CONCRETE STRAIN AT cgs = 396.0 MICROSTRAINS)

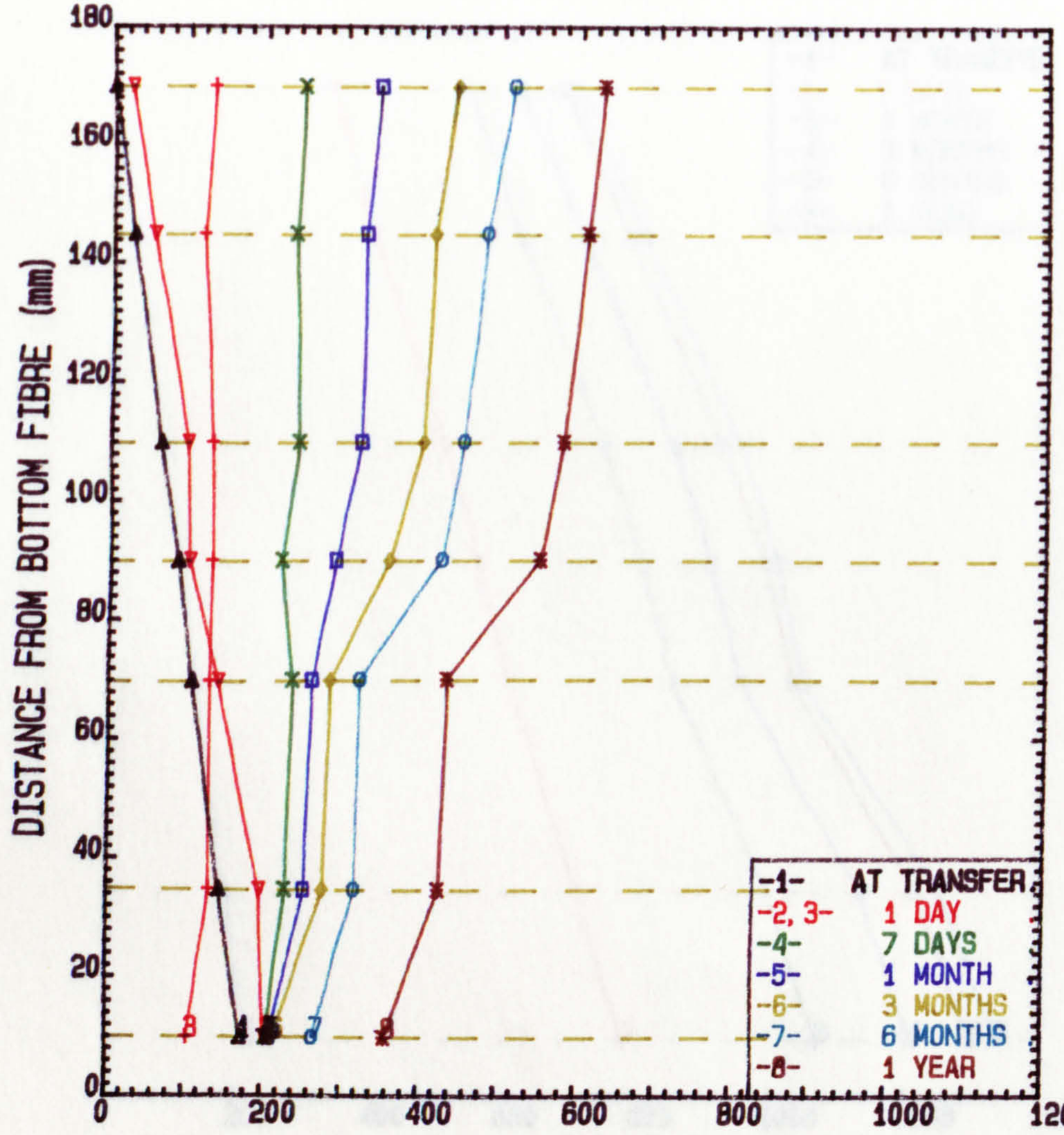

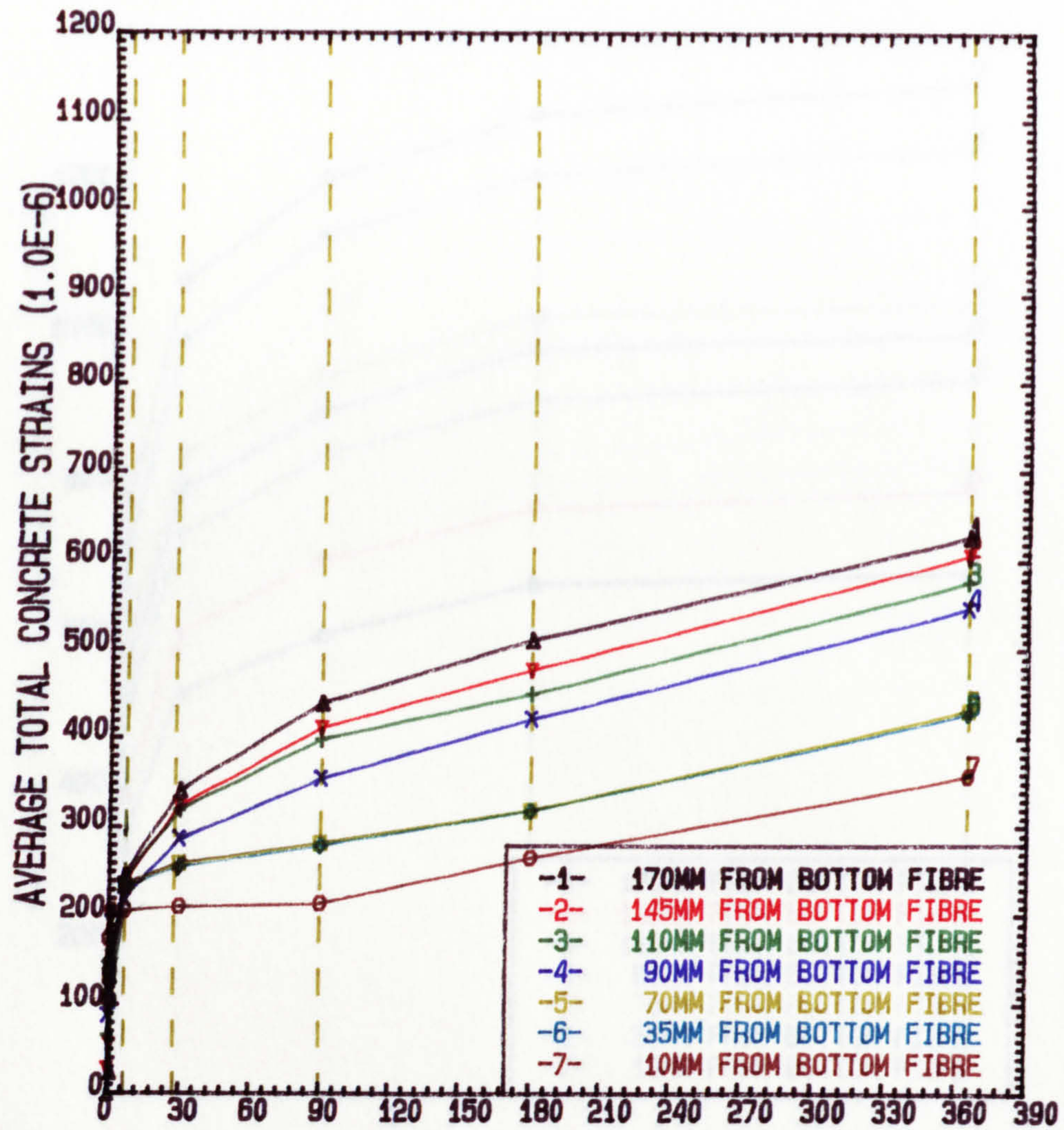

FIG. 6.24 MEASURED CONCRETE STRAIN DISTRIBUTION DIAGRAMS FOR MIDSPAN SECTION OF BEAM CR/V2 .

REMARKS: THE EXPERIMENTAL TIME-DEPENDENT PRESTRESS LOSS DETERMINED AT STEEL WIRE LEVEL FOR THE MIDSPAN SECTION AT 365 DAYS IS 10.93 % (139.0 MPa) (THE OBSERVED TIME-DEPENDENT CONCRETE STRAIN AT cgs = 302.0 MICROSTRAINS)

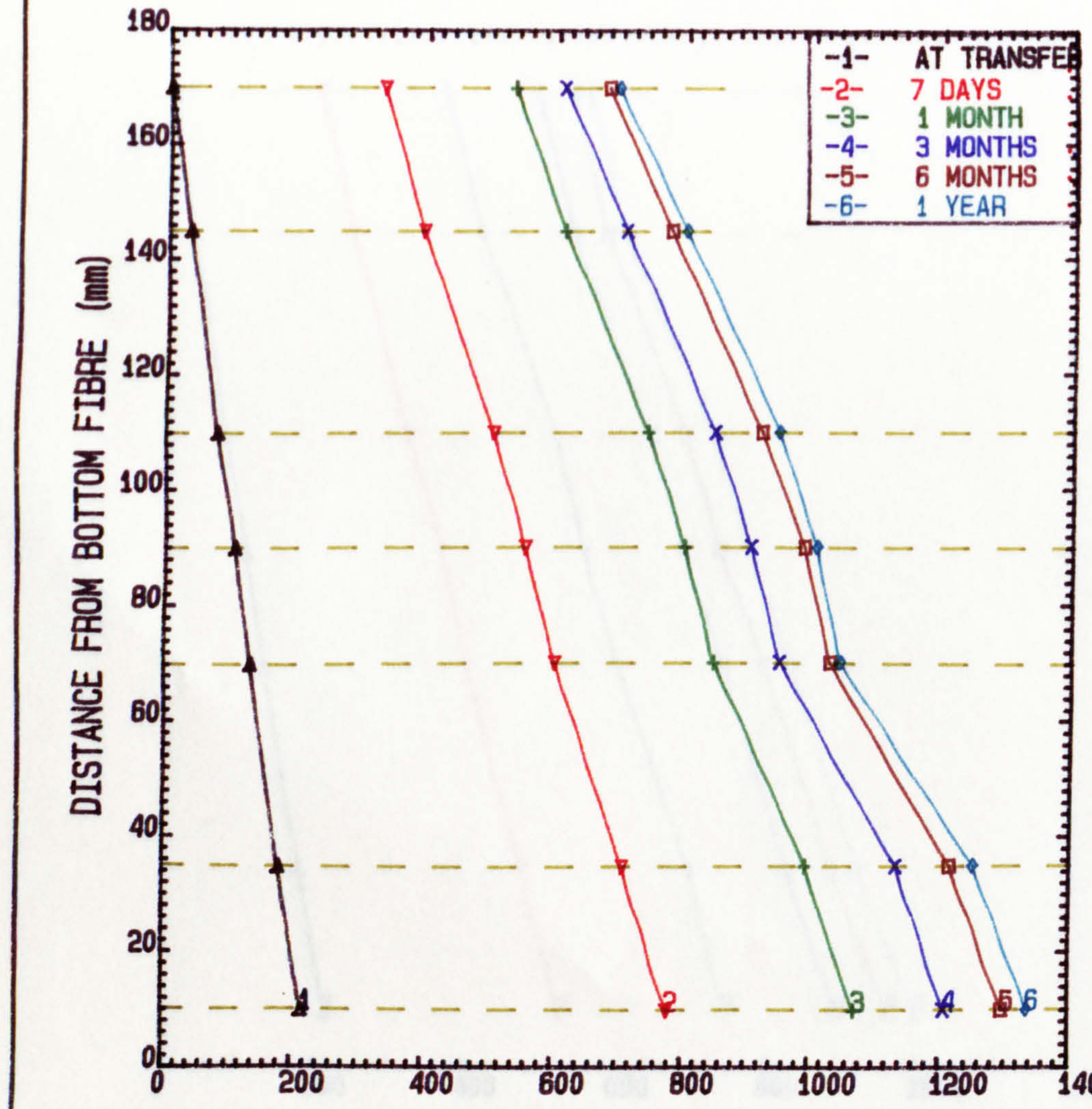

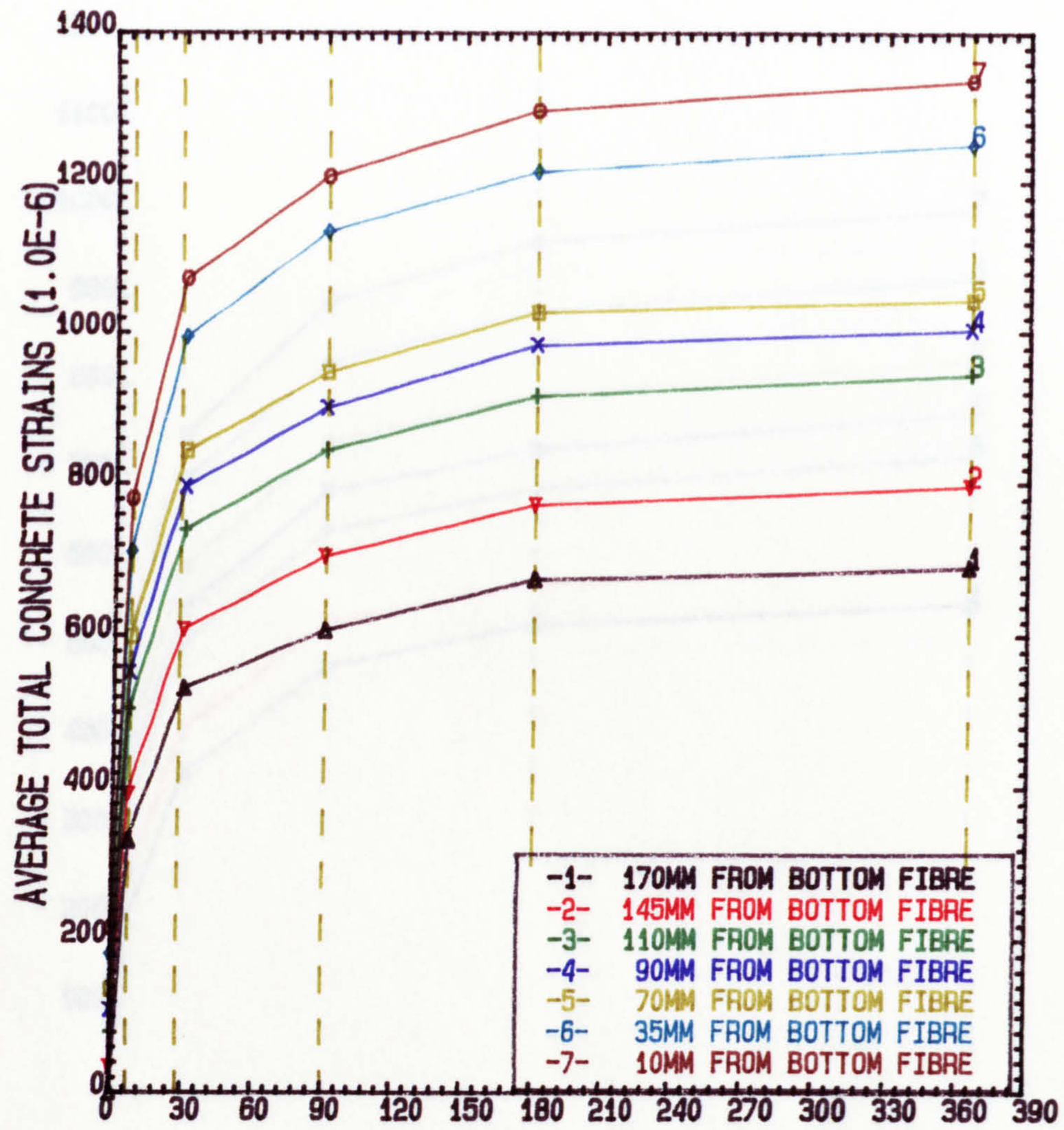

FIG. 6.25 MEASURED CONCRETE STRAIN DISTRIBUTION DIAGRAMS FOR MIDSPAN SECTION OF BEAM NI/C3 .

REMARKS: THE EXPERIMENTAL TIME-DEPENDENT PRESTRESS LOSS DETERMINED AT THE STEEL WIRE LEVEL FOR THE MIDSPAN SECTION AT 365 DAYS IS 22.10 % (280.0 MPa)
(THE OBSERVED TIME-DEPENDENT CONCRETE STRAIN AT cgs = 988.0 MICROSTRAINS)

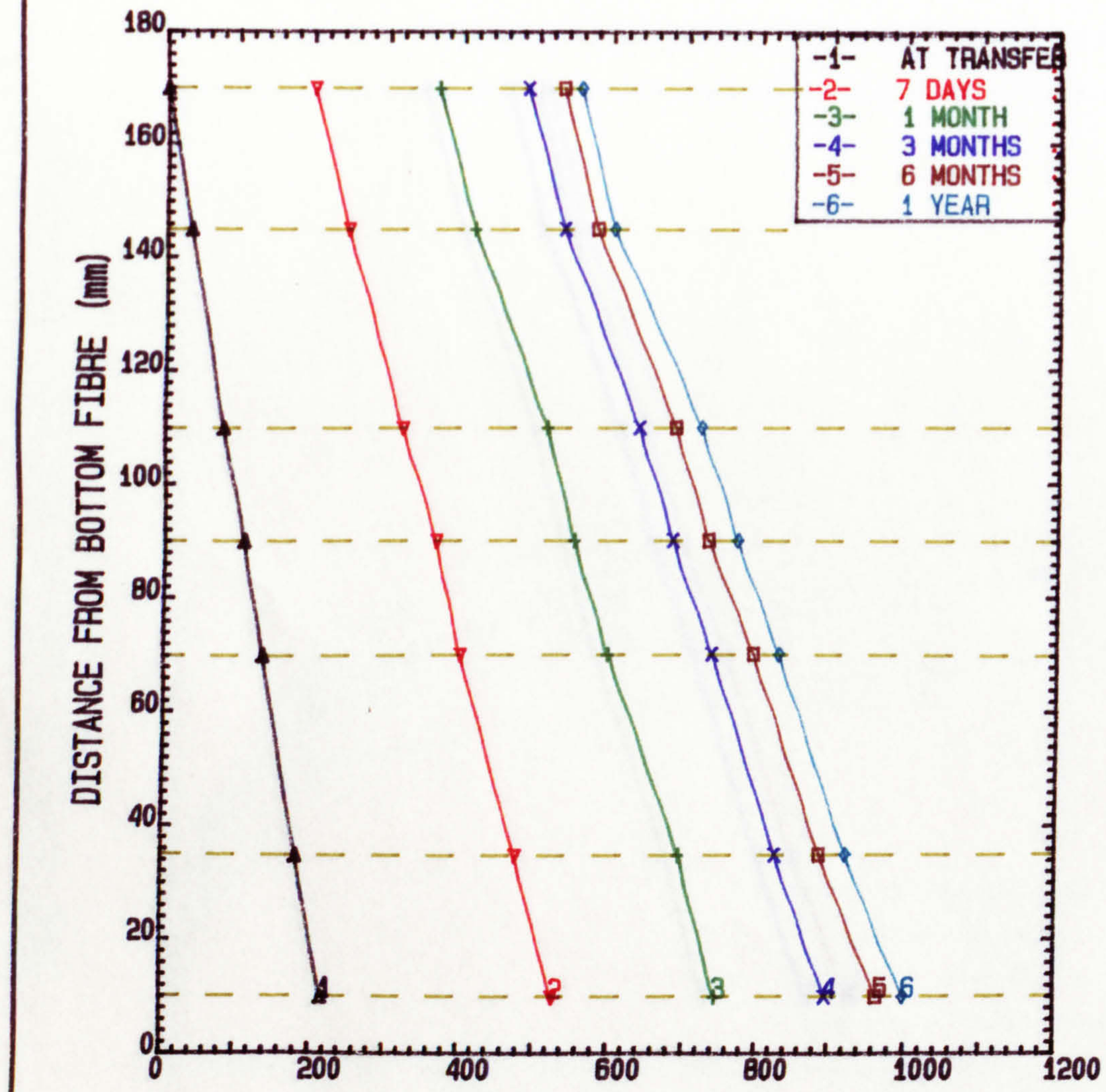

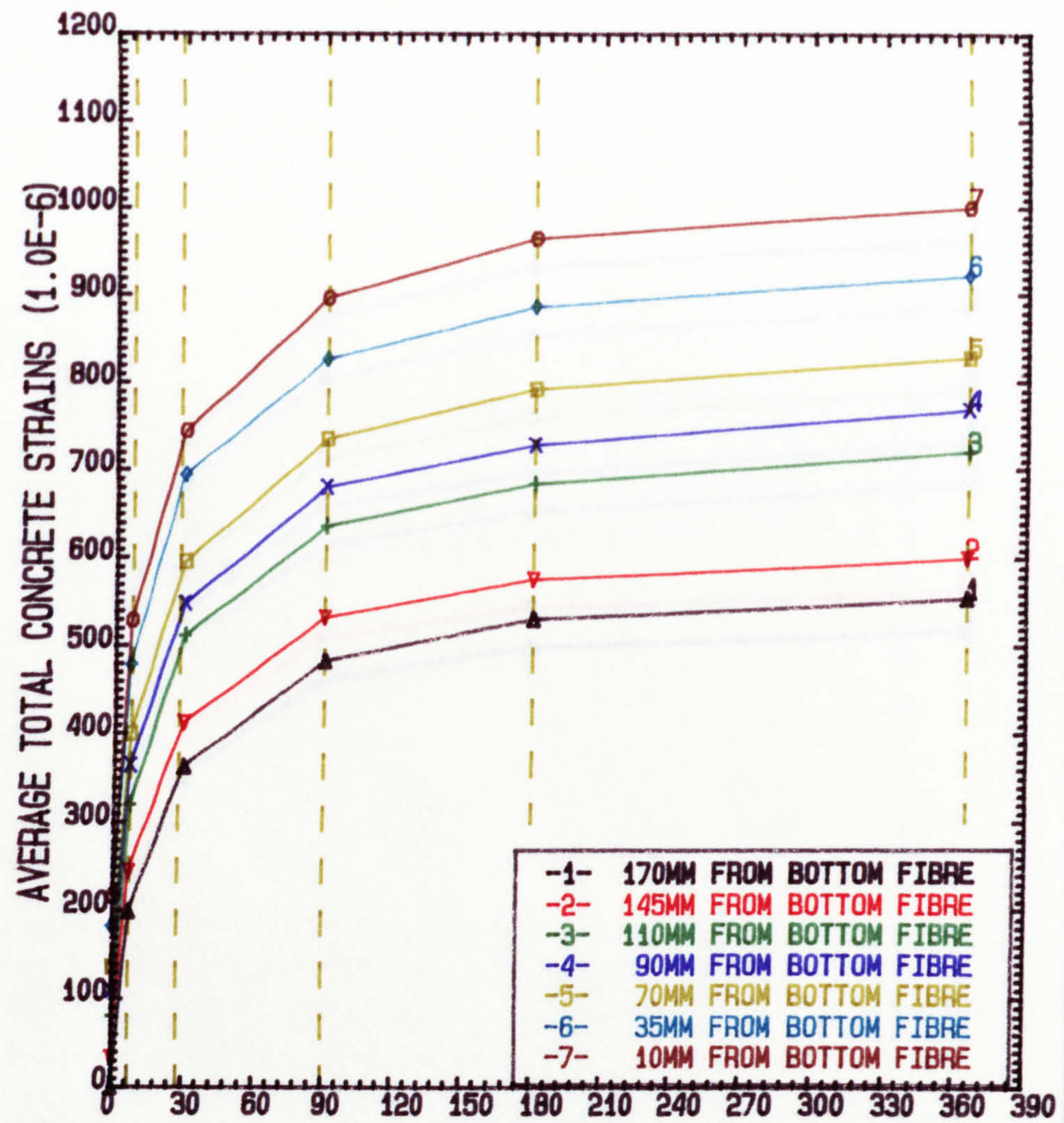

FIG. 6.26 MEASURED CONCRETE STRAIN DISTRIBUTION DIAGRAMS FOR MIDSPAN SECTION OF BEAM NI/C4 .

REMARKS: THE EXPERIMENTAL TIME-DEPENDENT PRESTRESS LOSS DETERMINED AT THE STEEL WIRE LEVEL FOR THE MIDSPAN SECTION AT 365 DAYS IS 17.67 % (224.0 MPa)
(THE OBSERVED TIME-DEPENDENT CONCRETE STRAIN AT cgs = 716.0 MICROSTRAINS)

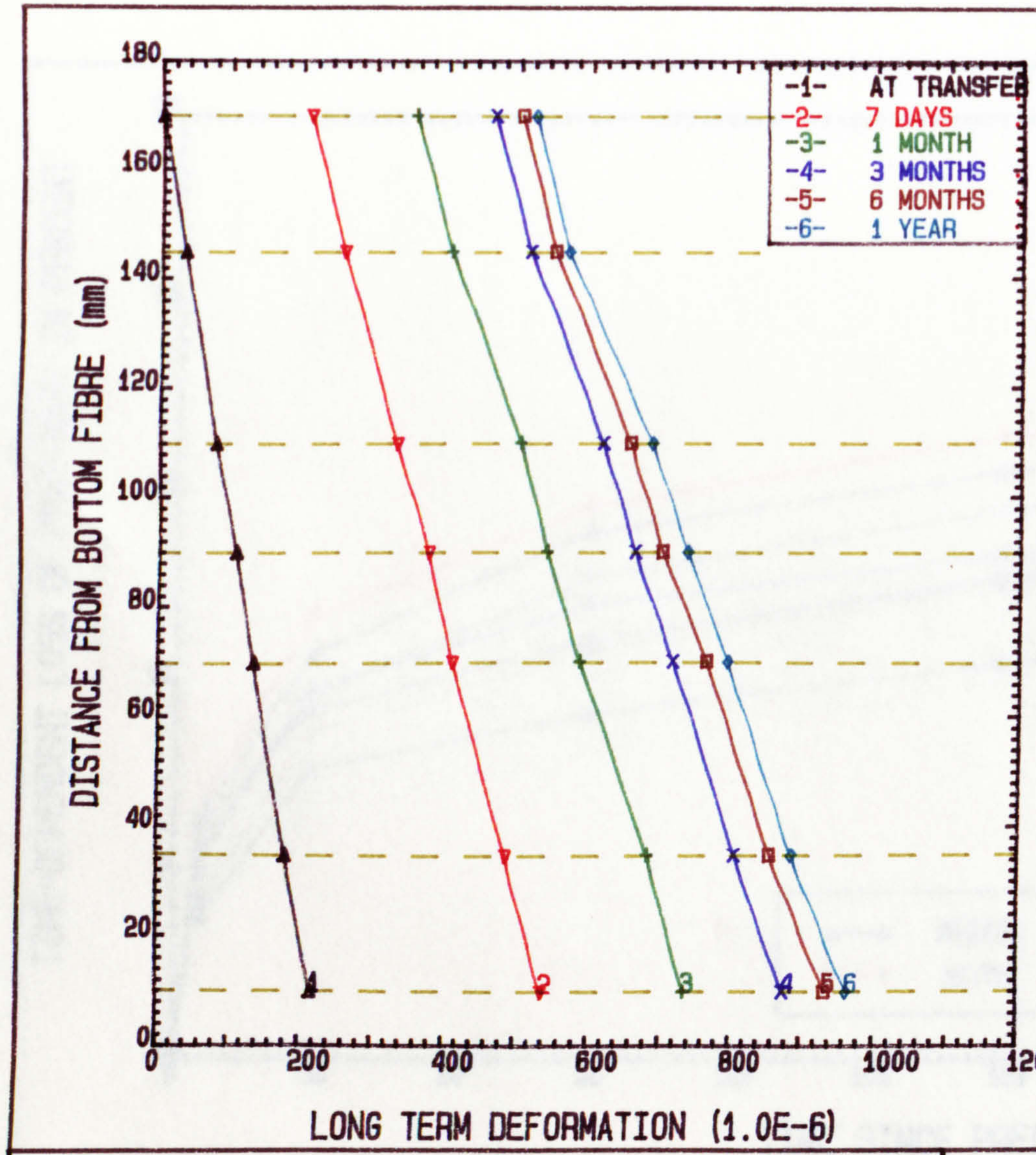

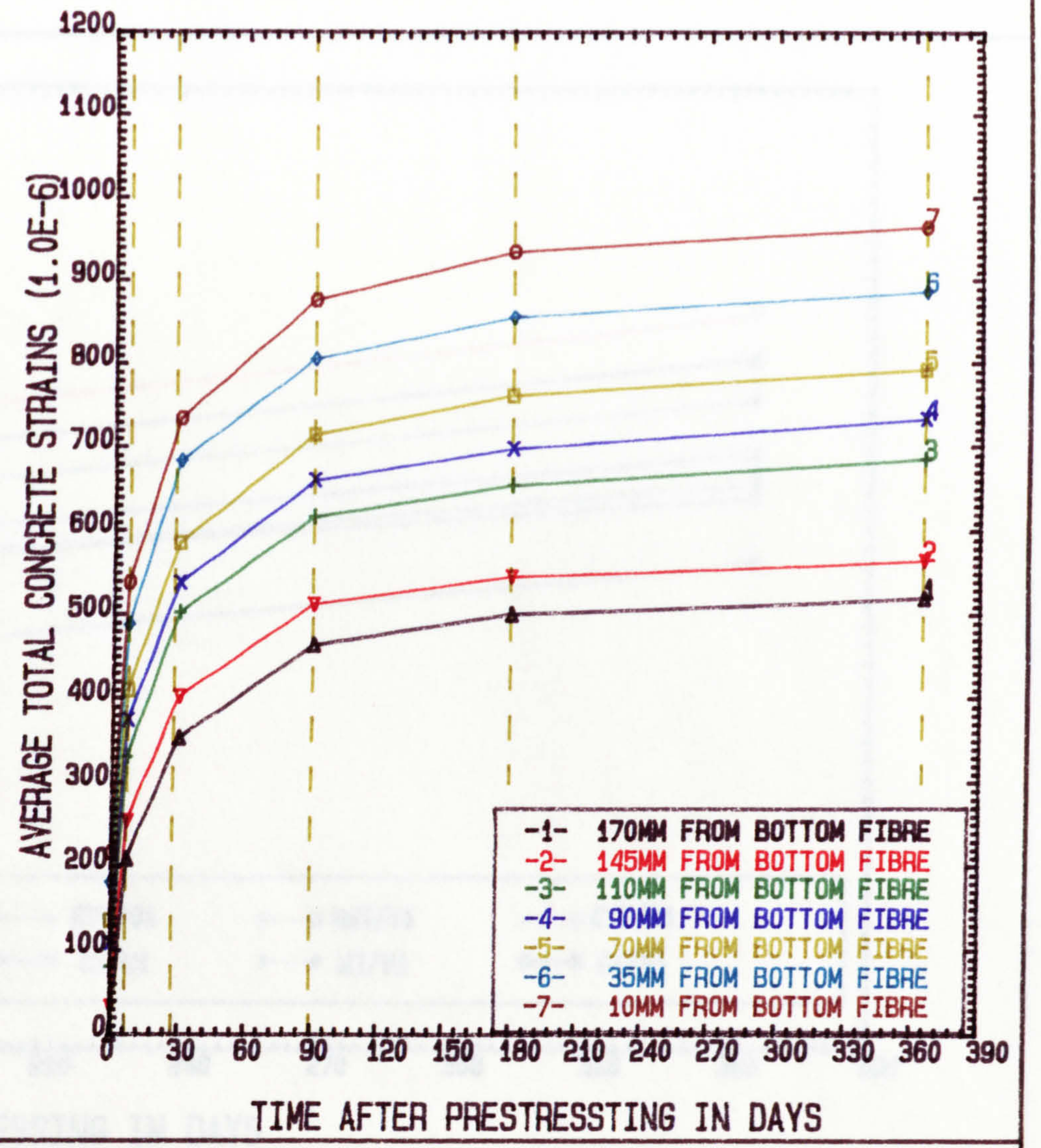

FIG. 6.27 MEASURED CONCRETE STRAIN DISTRIBUTION DIAGRAMS FOR MIDSPAN SECTION OF BEAM NI/C5 .

REMARKS: THE EXPERIMENTAL TIME-DEPENDENT PRESTRESS LOSS DETERMINED AT THE STEEL WIRE LEVEL FOR THE MIDSPAN SECTION AT 365 DAYS IS 17.10 % (217.0 MPa)
(THE OBSERVED TIME-DEPENDENT CONCRETE STRAIN AT cgs = 681.0 MICROSTRAINS)

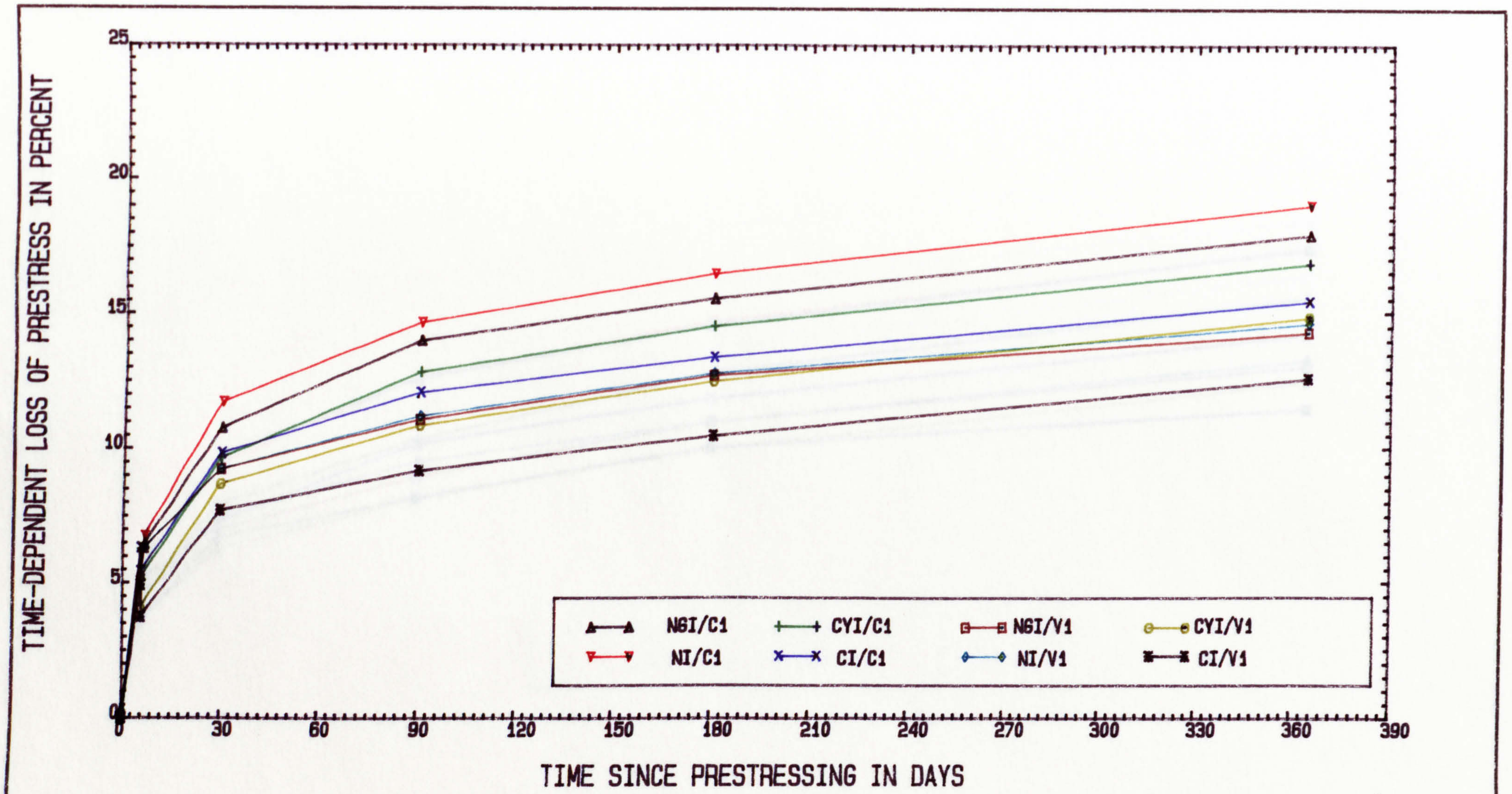

FIG.6.28 INFLUENCE OF LOADING AND ENVIRONMENTAL CONDITIONS ON TIME-DEPENDENT PRESTRESS LOSSES OF I-SHAPED PRESTRESS CONCRETE BEAMS HAVING RHPC CONCRETE MIX

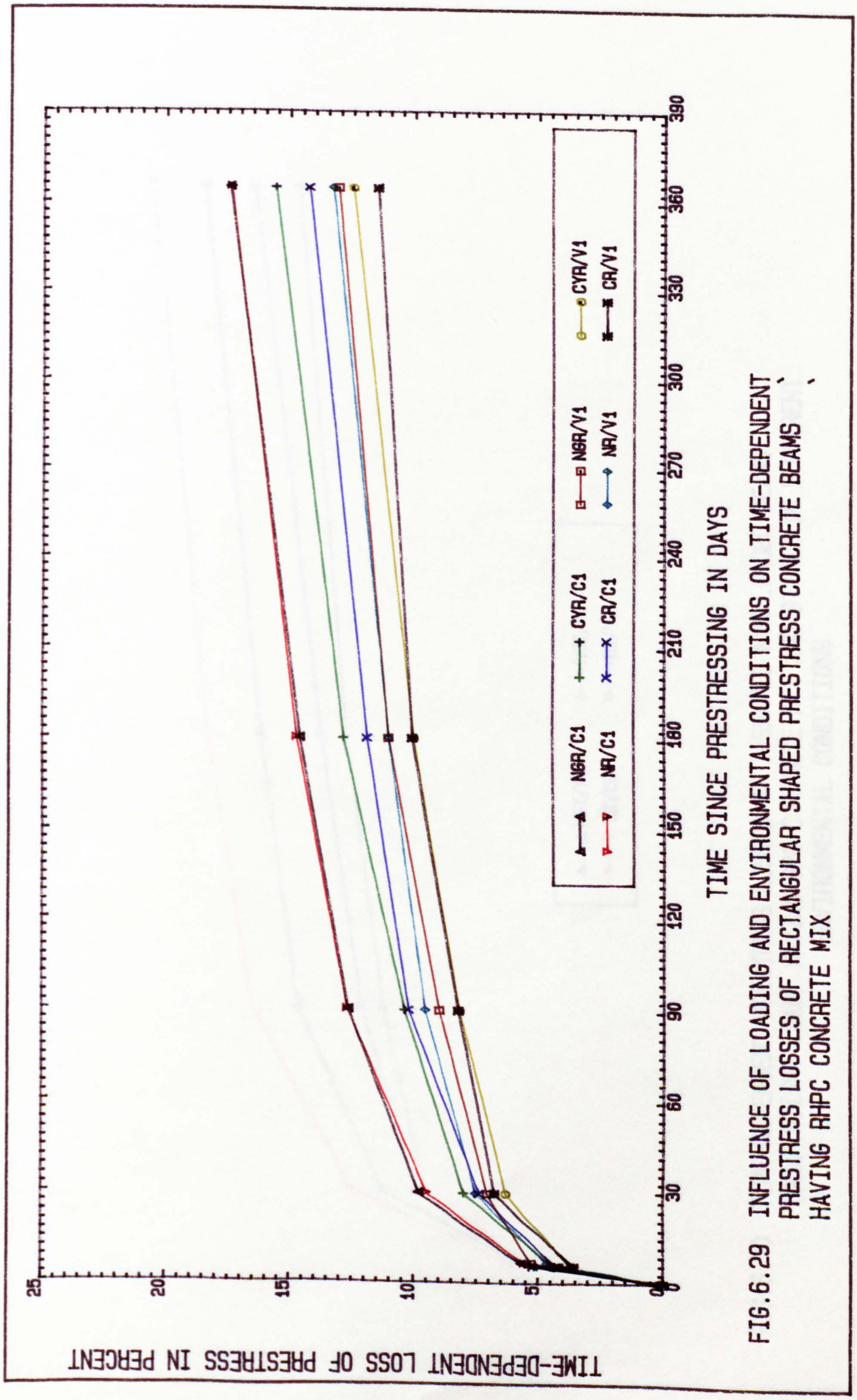

FIG.6.29 INFLUENCE OF LOADING AND ENVIRONMENTAL CONDITIONS ON TIME-DEPENDENT PRESTRESS LOSSES OF RECTANGULAR SHAPED PRESTRESS CONCRETE BEAMS HAVING RHPC CONCRETE MIX

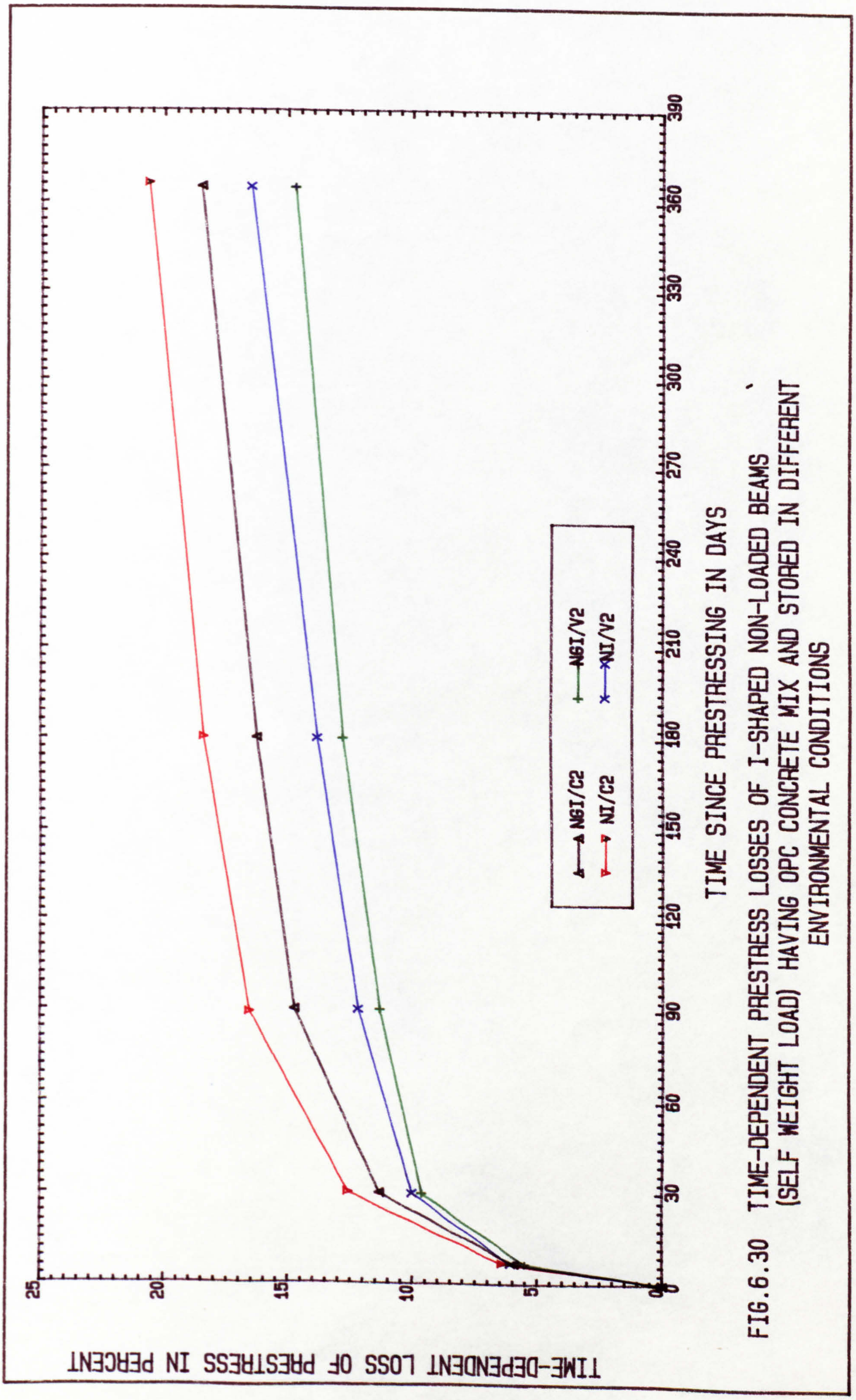

FIG.6.30 TIME-DEPENDENT PRESTRESS LOSSES OF I-SHAPED NON-LOADED BEAMS (SELF WEIGHT LOAD) HAVING OPC CONCRETE MIX AND STORED IN DIFFERENT ENVIRONMENTAL CONDITIONS

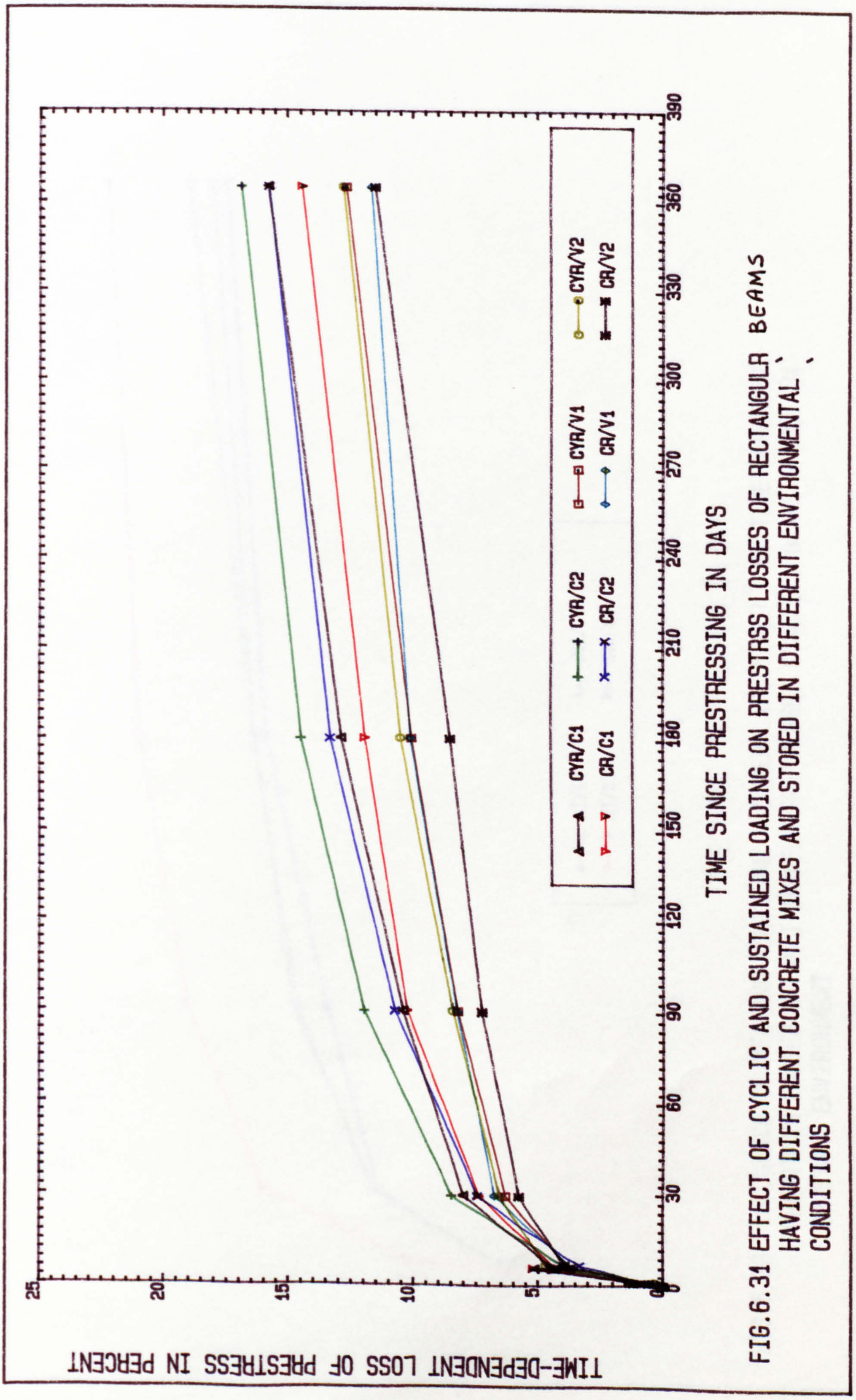

FIG.6.31 EFFECT OF CYCLIC AND SUSTAINED LOADING ON PRESTRSS LOSSES OF RECTANGULAR BEAMS HAVING DIFFERENT CONCRETE MIXES AND STORED IN DIFFERENT ENVIRONMENTAL CONDITIONS

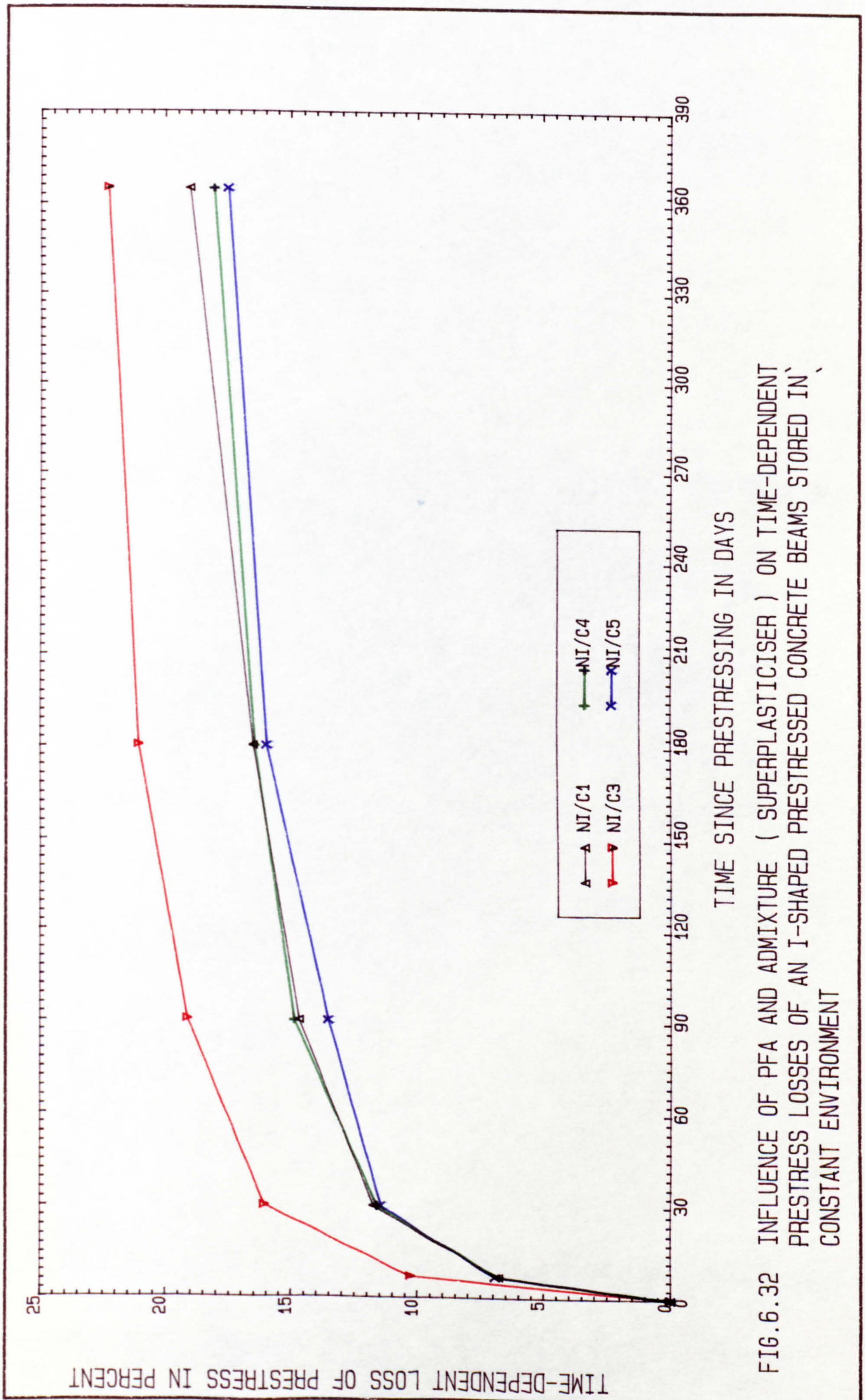

FIG.6.32 INFLUENCE OF PFA AND ADMIXTURE (SUPERPLASTICISER) ON TIME-DEPENDENT PRESTRESS LOSSES OF AN I-SHAPED PRESTRESSED CONCRETE BEAMS STORED IN CONSTANT ENVIRONMENT

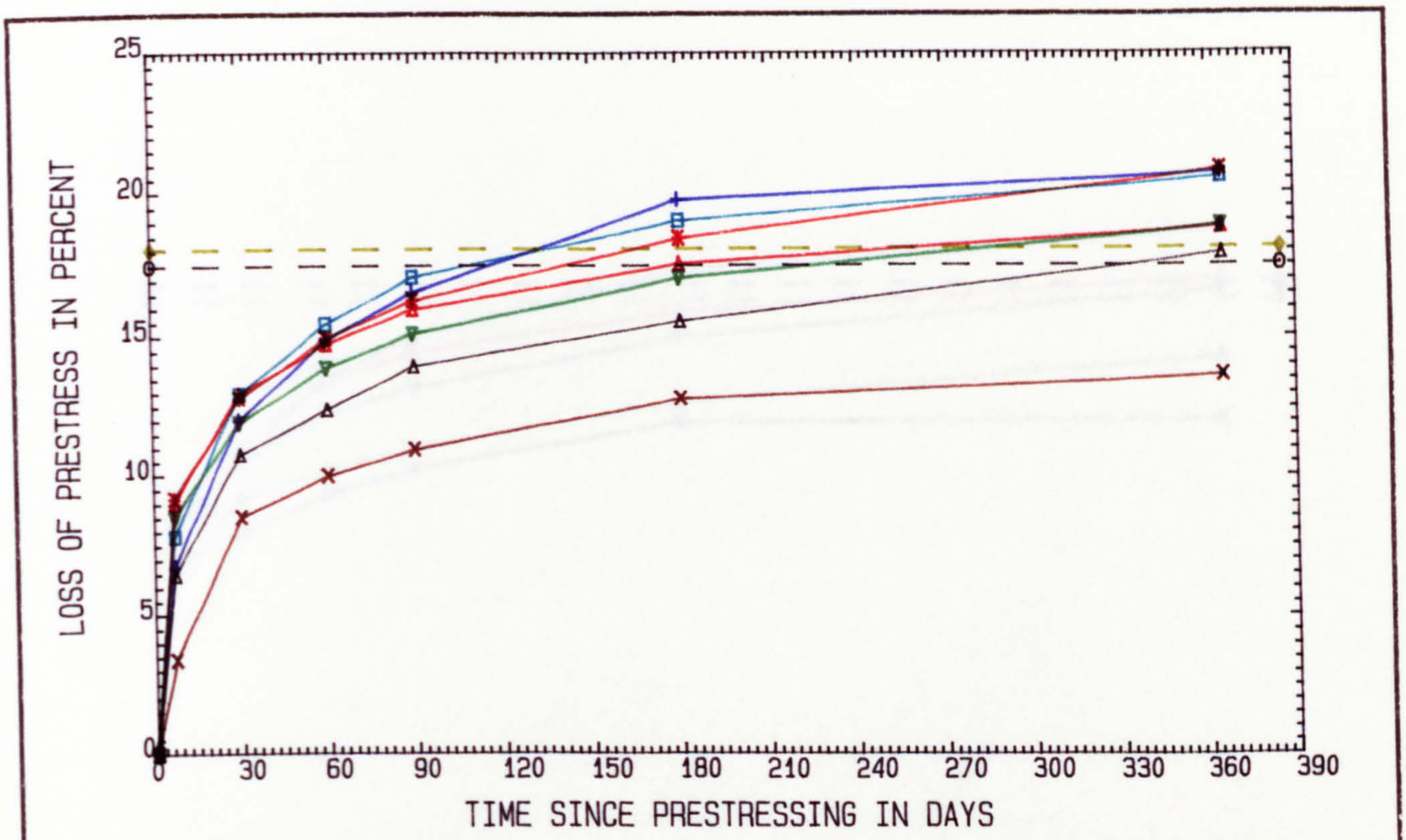

FIG. 6.33 COMPARISON OF EXPERIMENTAL AND PREDICTED TIME-DEPENDENT LOSS OF PRESTRESS BASED ON GENERAL PARAMETERS FOR GROUTED I-BEAM (RHPC MIX) STORED IN CONSTANT ENVIRONMENT

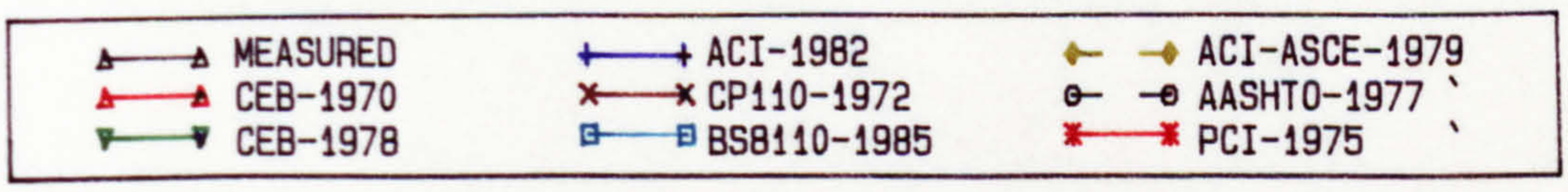

NOTE: PRESENTED VALUES OF ACI-ASCE AND AASHTO ARE FOR END OF SERVICE LIFE

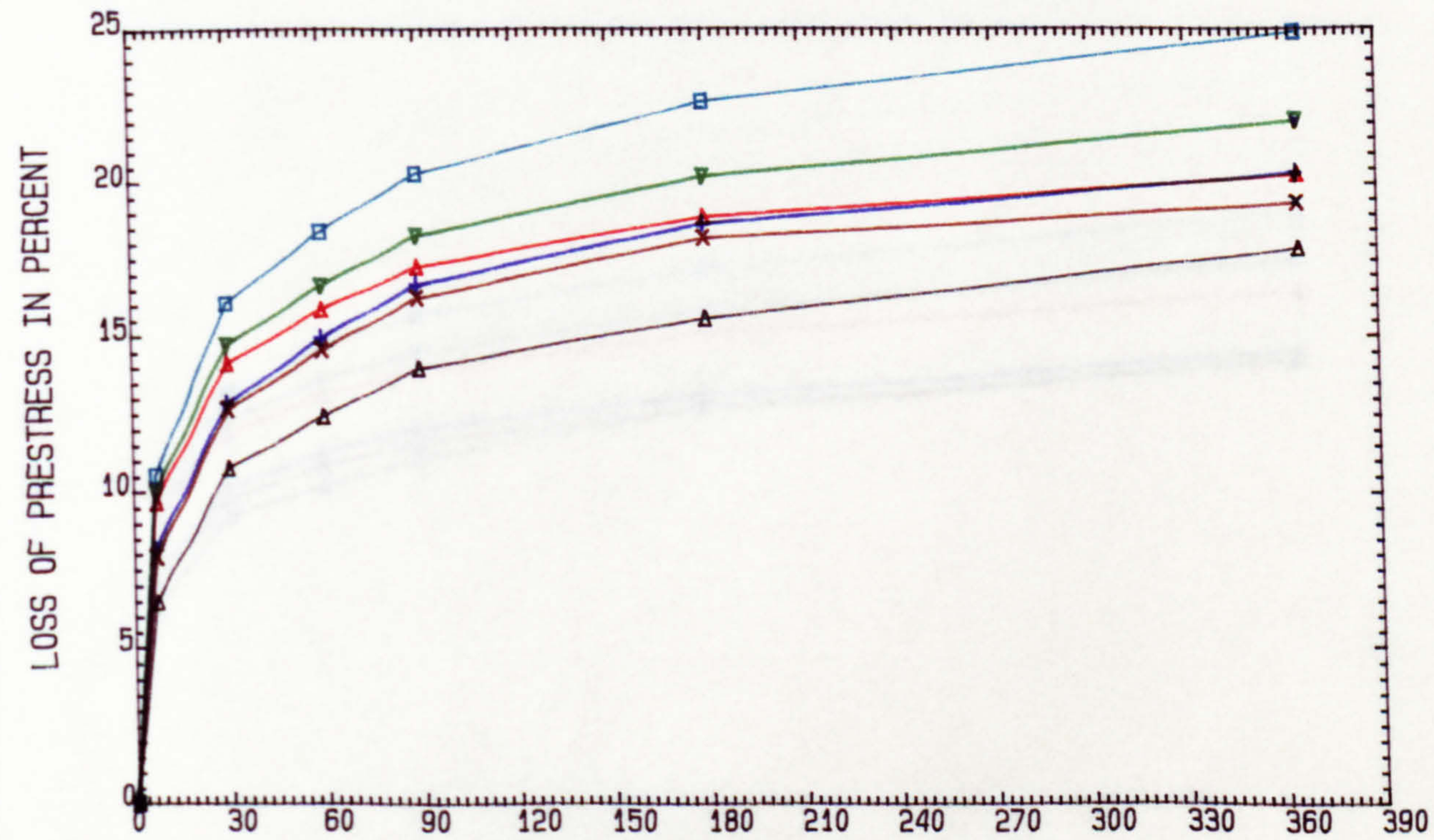

FIG. 6.34 COMPARISON OF EXPERIMENTAL AND PREDICTED TIME-DEPENDENT LOSS OF PRESTRESS BASED ON EXPERIMENTAL PARAMETERS FOR GROUTED I-BEAM (RHPC MIX) STORED IN CONSTANT ENVIRONMENT

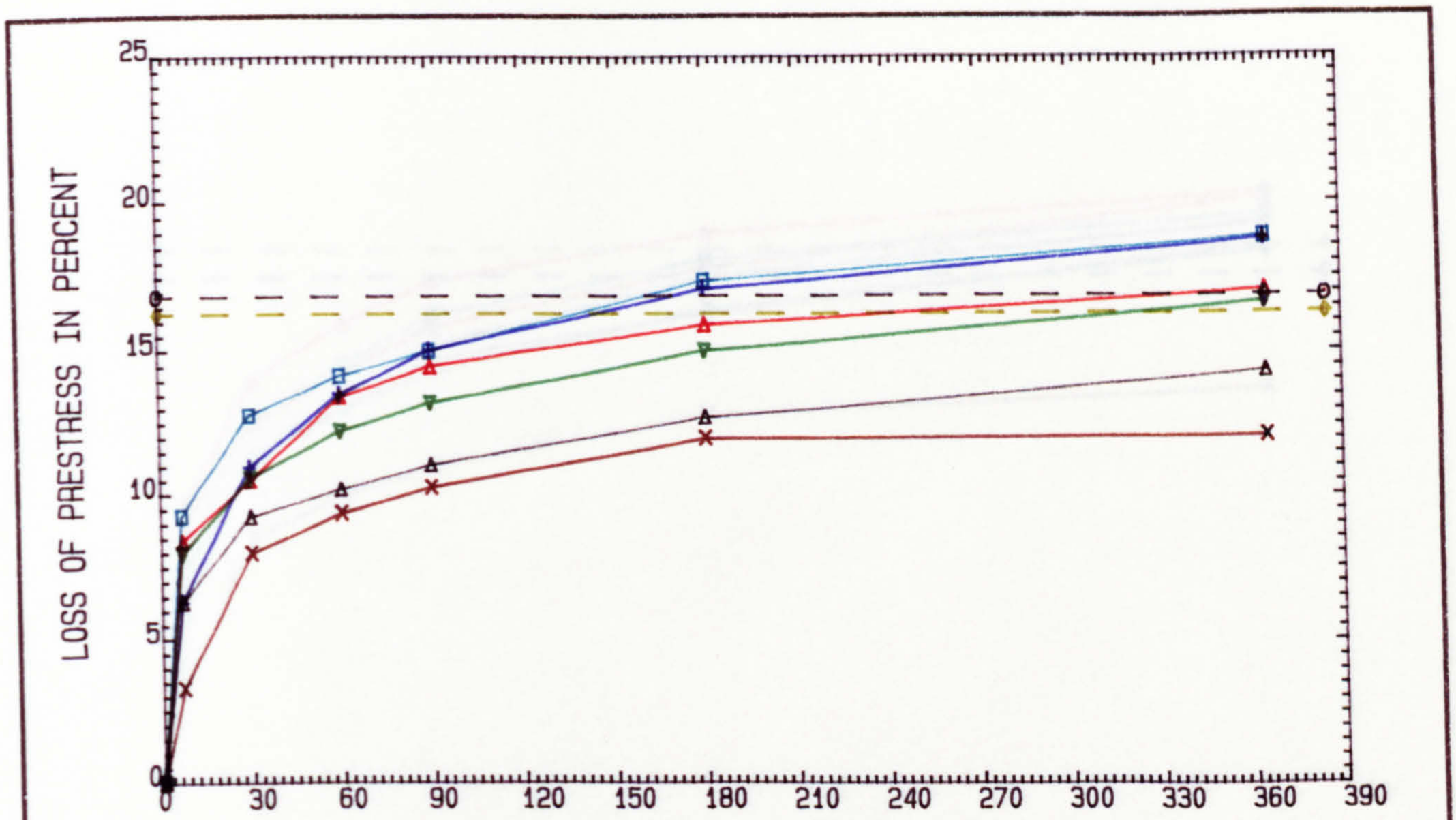

FIG. 6.35 COMPARISON OF EXPERIMENTAL AND PREDICTED TIME-DEPENDENT LOSS OF PRESTRESS BASED ON GENERAL PARAMETERS FOR GROUTED I-BEAM (RHPC MIX) STORED IN VARIABLE ENVIRONMENT

NOTE: PRESENTED VALUES OF ACI-ASCE AND AASHTO ARE FOR END OF SERVICE LIFE

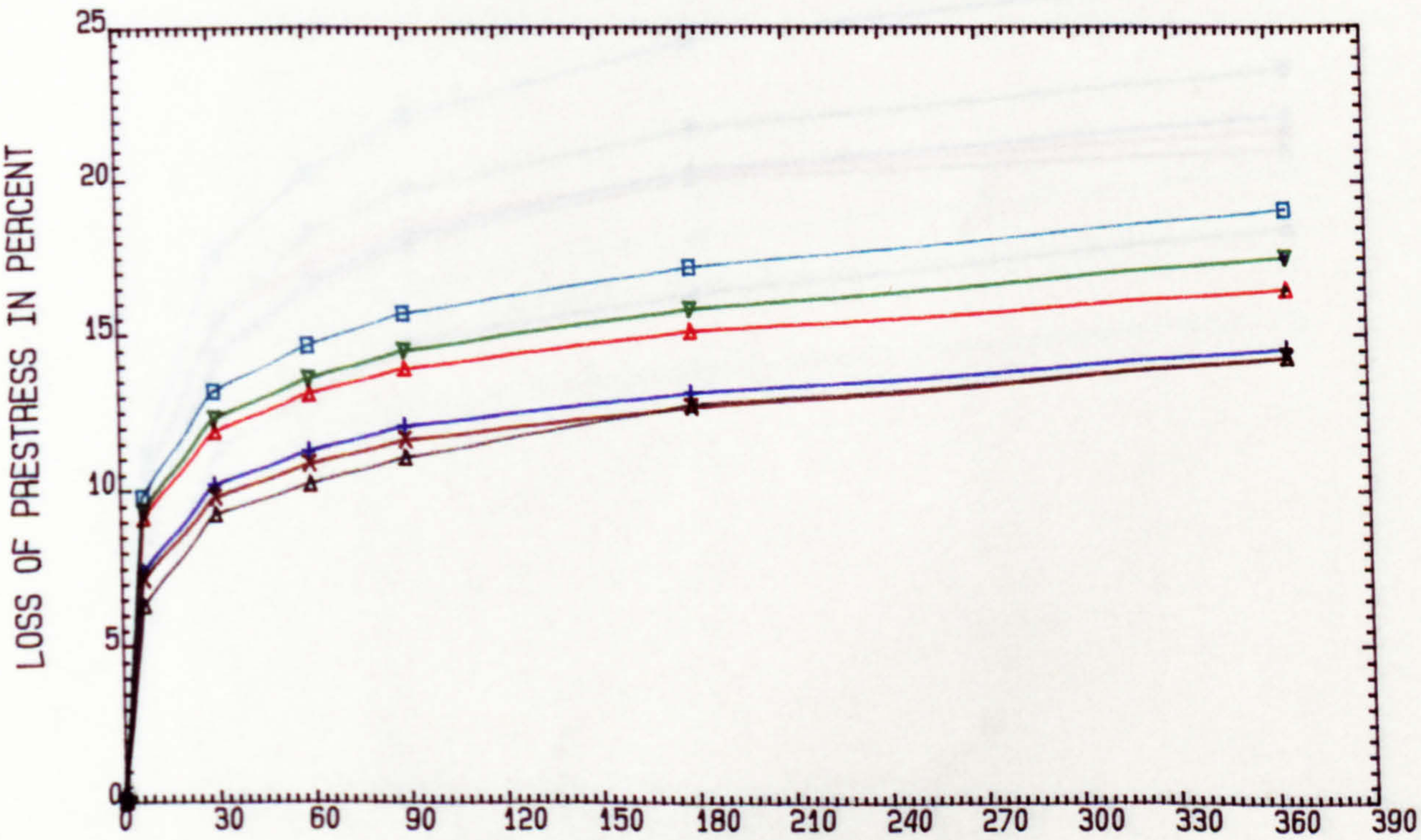

FIG. 6.36 COMPARISON OF EXPERIMENTAL AND PREDICTED TIME-DEPENDENT LOSS OF PRESTRESS BASED ON EXPERIMENTAL PARAMETERS FOR GROUTED I-BEAM (RHPC MIX) STORED IN VARIABLE ENVIRONMENT

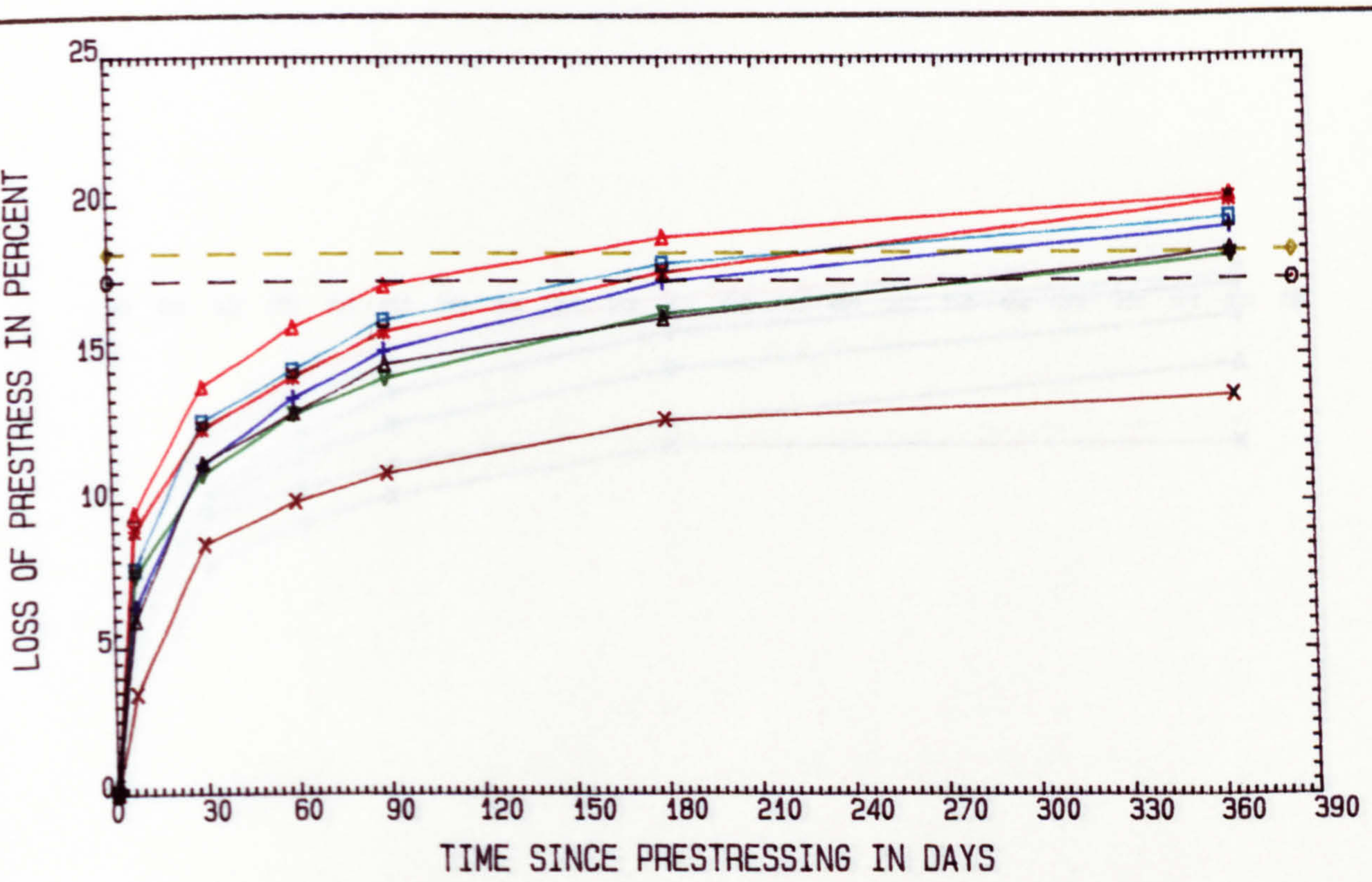

FIG. 6.37 COMPARISON OF EXPERIMENTAL AND PREDICTED TIME-DEPENDENT LOSS OF PRESTRESS BASED ON GENERAL PARAMETERS FOR GROUTED I-BEAM (OPC MIX) STORED IN CONSTANT ENVIRONMENT

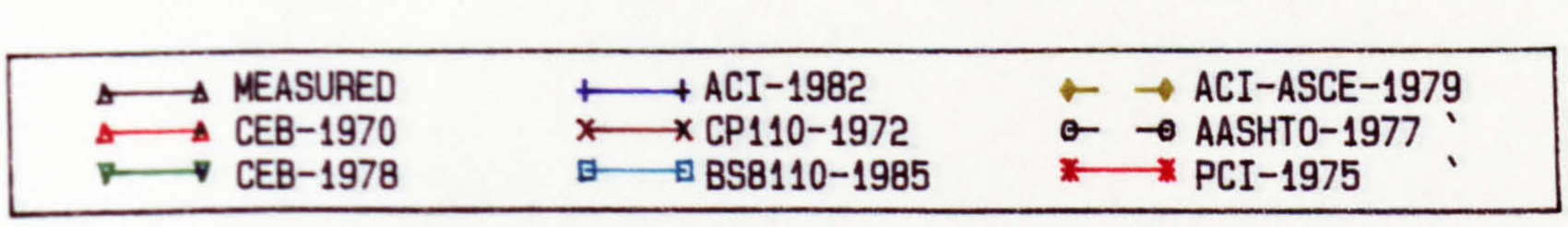

NOTE: PRESENTED VALUES OF ACI-ASCE AND AASHTO ARE FOR END OF SERVICE LIFE

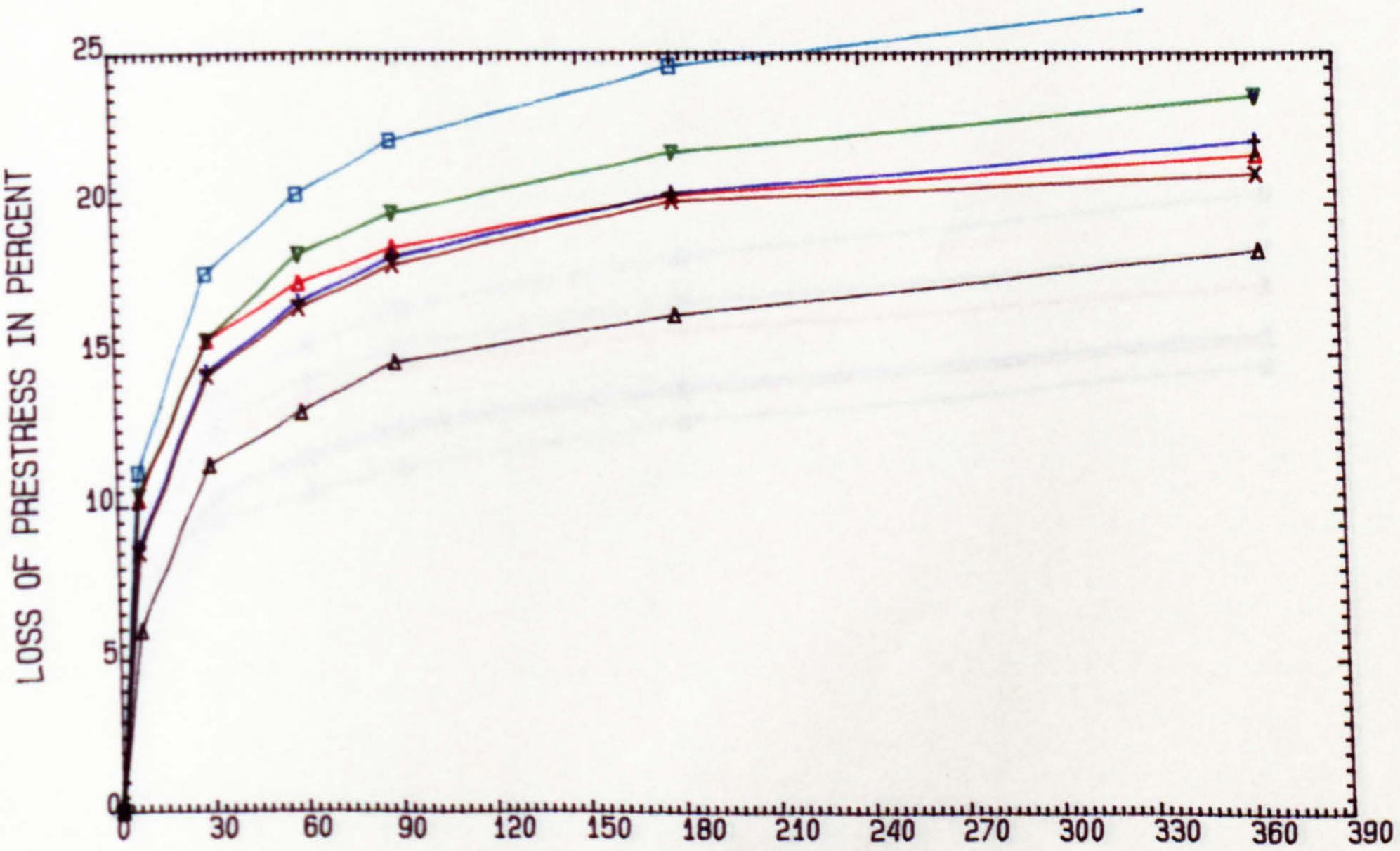

FIG. 6.38 COMPARISON OF EXPERIMENTAL AND PREDICTED TIME-DEPENDENT LOSS OF PRESTRESS BASED ON EXPERIMENTAL PARAMETERS FOR GROUTED I-BEAM (OPC MIX) STORED IN CONSTANT ENVIRONMENT

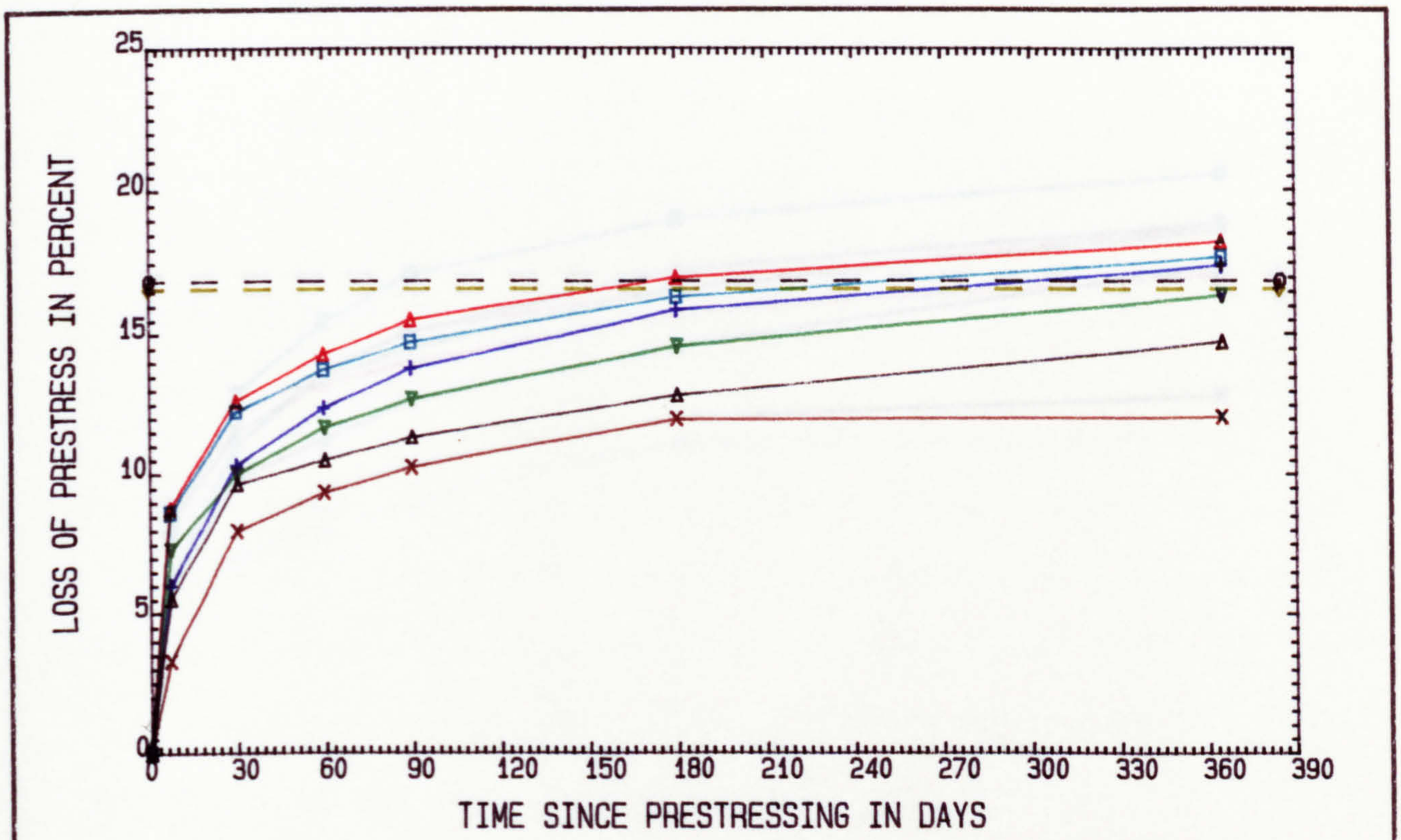

FIG. 6.39 COMPARISON OF EXPERIMENTAL AND PREDICTED TIME-DEPENDENT LOSS OF PRESTRESS BASED ON GENERAL PARAMETERS FOR GROUTED I-BEAM (OPC MIX) STORED IN VARIABLE ENVIRONMENT

NOTE: PRESENTED VALUES OF ACI-ASCE AND AASHTO ARE FOR END OF SERVICE LIFE

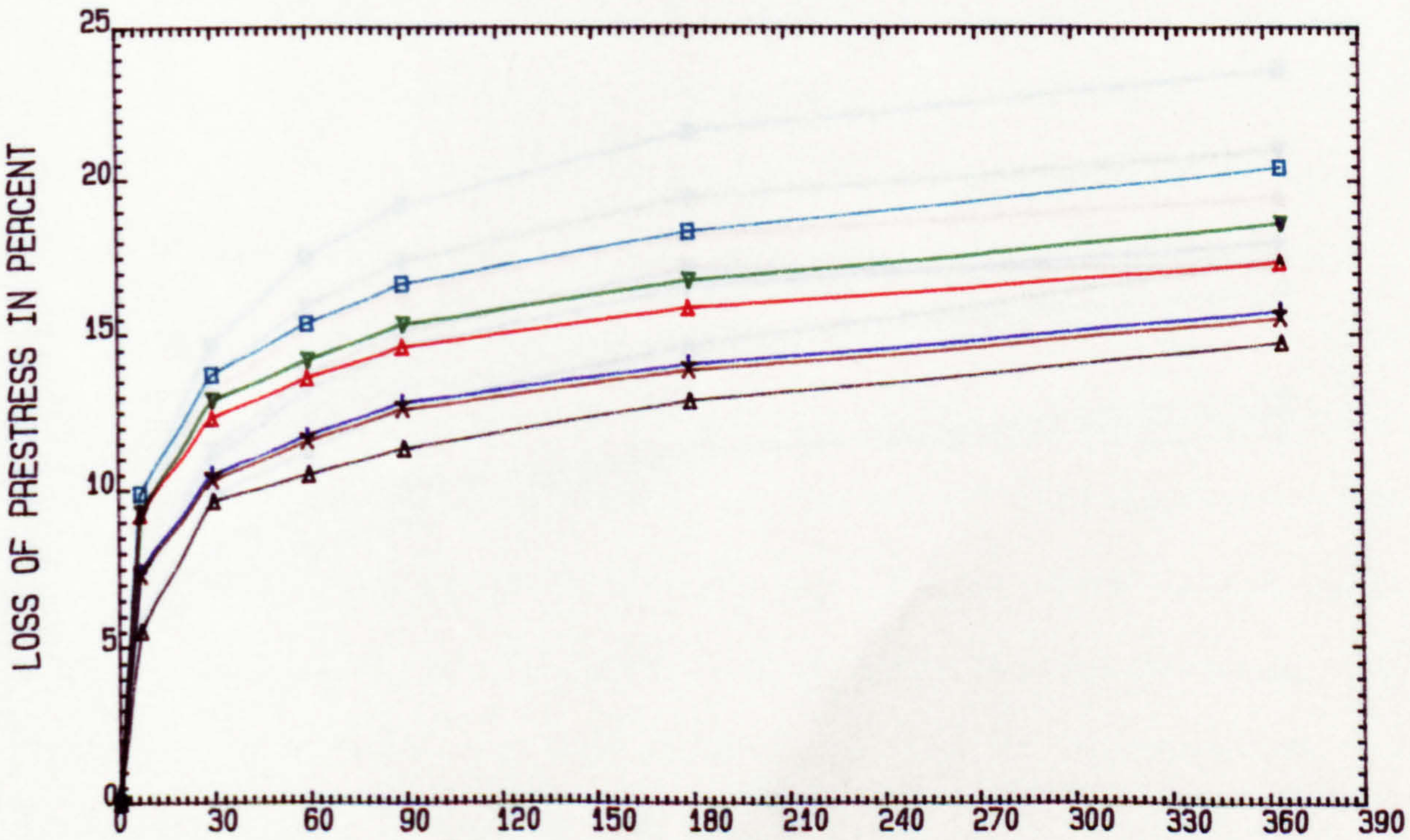

FIG. 6.40 COMPARISON OF EXPERIMENTAL AND PREDICTED TIME-DEPENDENT LOSS OF PRESTRESS BASED ON EXPERIMENTAL PARAMETERS FOR GROUTED I-BEAM (OPC MIX) STORED IN VARIABLE ENVIRONMENT

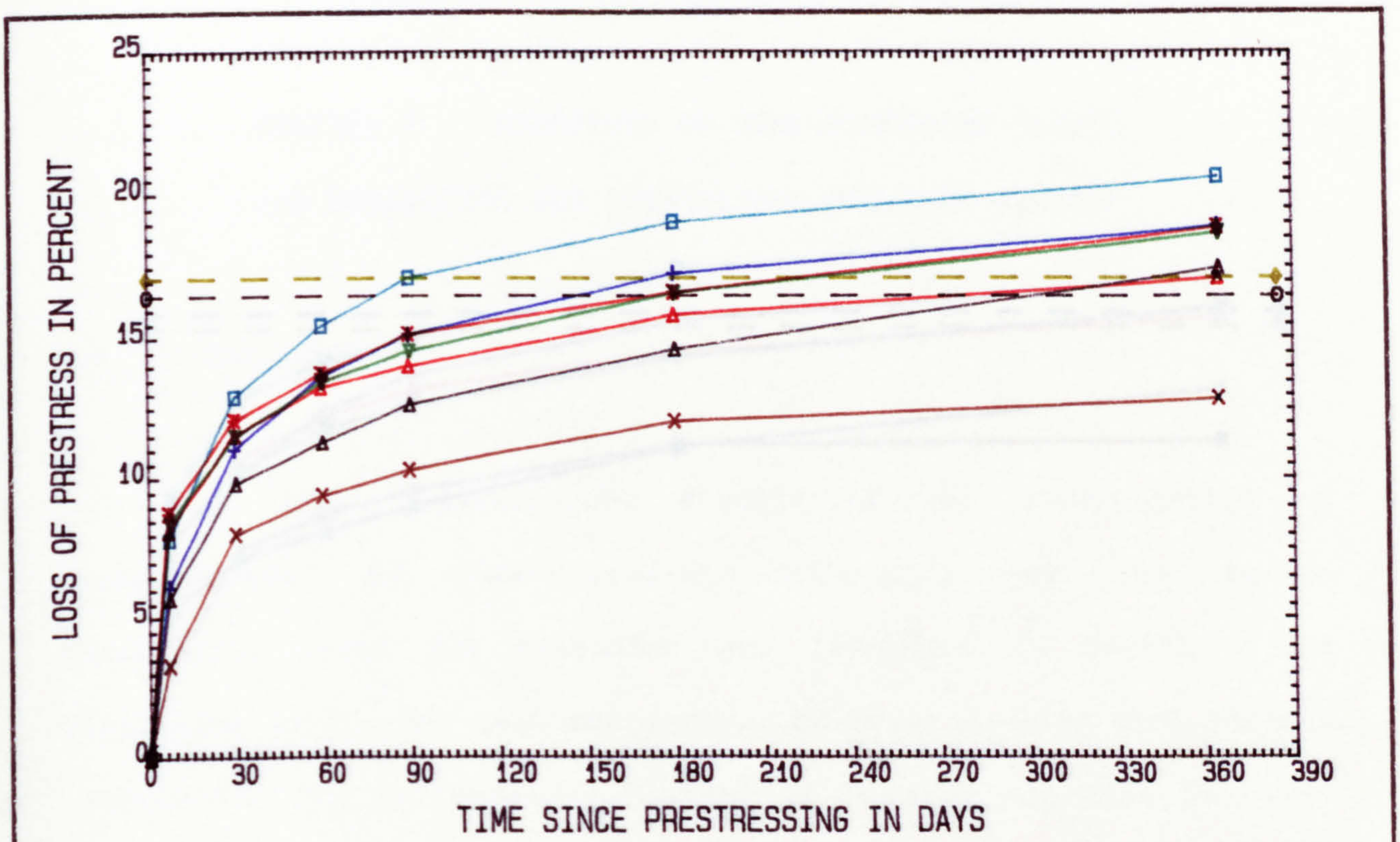

FIG. 6.41 COMPARISON OF EXPERIMENTAL AND PREDICTED TIME-DEPENDENT LOSS OF PRESTRESS BASED ON GENERAL PARAMETERS FOR GROUTED RECTANGULAR BEAM (RHPC MIX) STORED IN CONSTANT ENVIRONMENT

NOTE: PRESENTED VALUES OF ACI-ASCE AND AASHTO ARE FOR END OF SERVICE LIFE

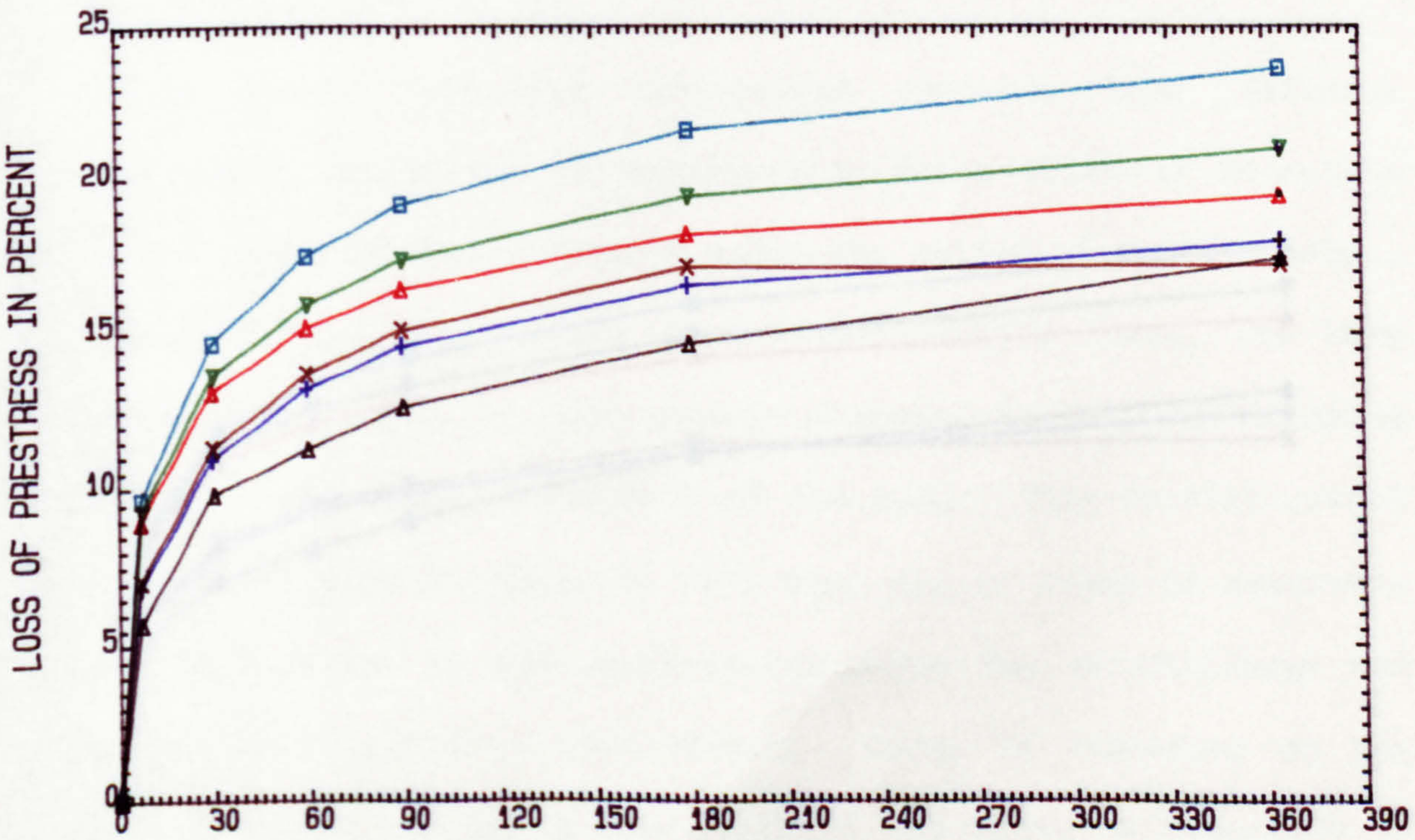

FIG. 6.42 COMPARISON OF EXPERIMENTAL AND PREDICTED TIME-DEPENDENT LOSS OF PRESTRESS BASED ON EXPERIMENTAL PARAMETERS FOR GROUTED RECTANGULAR BEAM (RHPC MIX) STORED IN CONSTANT ENVIRONMENT

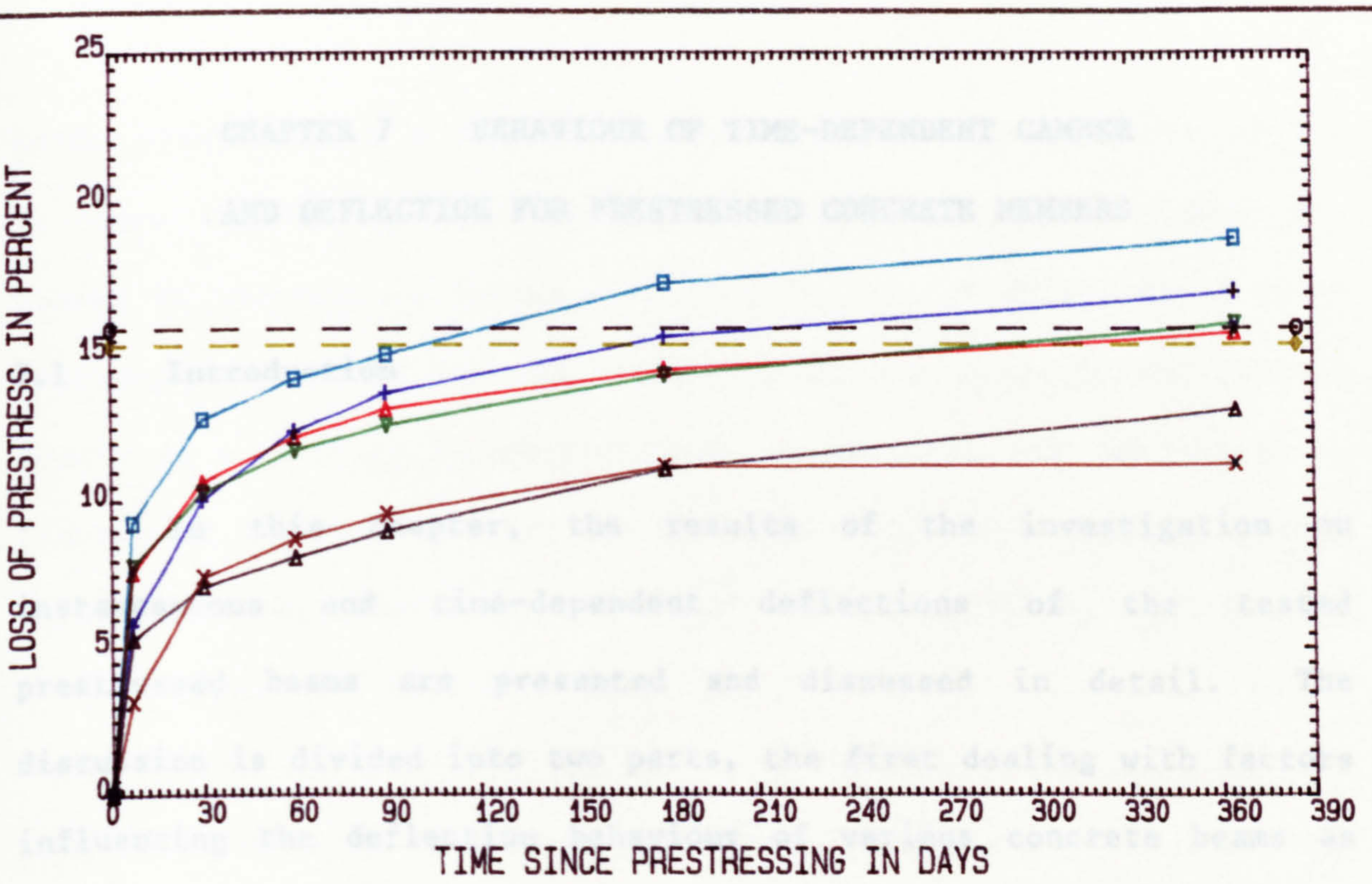

FIG. 6.43 COMPARISON OF EXPERIMENTAL AND PREDICTED TIME-DEPENDENT LOSS OF PRESTRESS BASED ON GENERAL PARAMETERS FOR GROUTED RECTANGULAR BEAM (RHPC MIX) STORED IN VARIABLE ENVIRONMENT

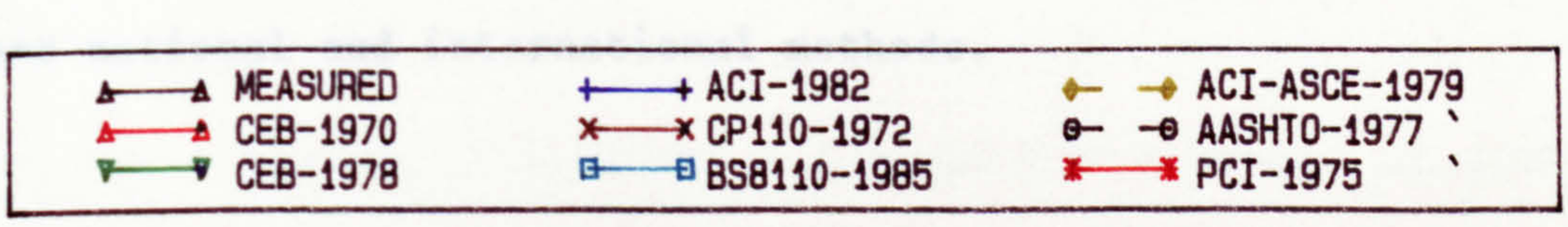

NOTE: PRESENTED VALUES OF ACI-ASCE AND AASHTO ARE FOR END OF SERVICE LIFE

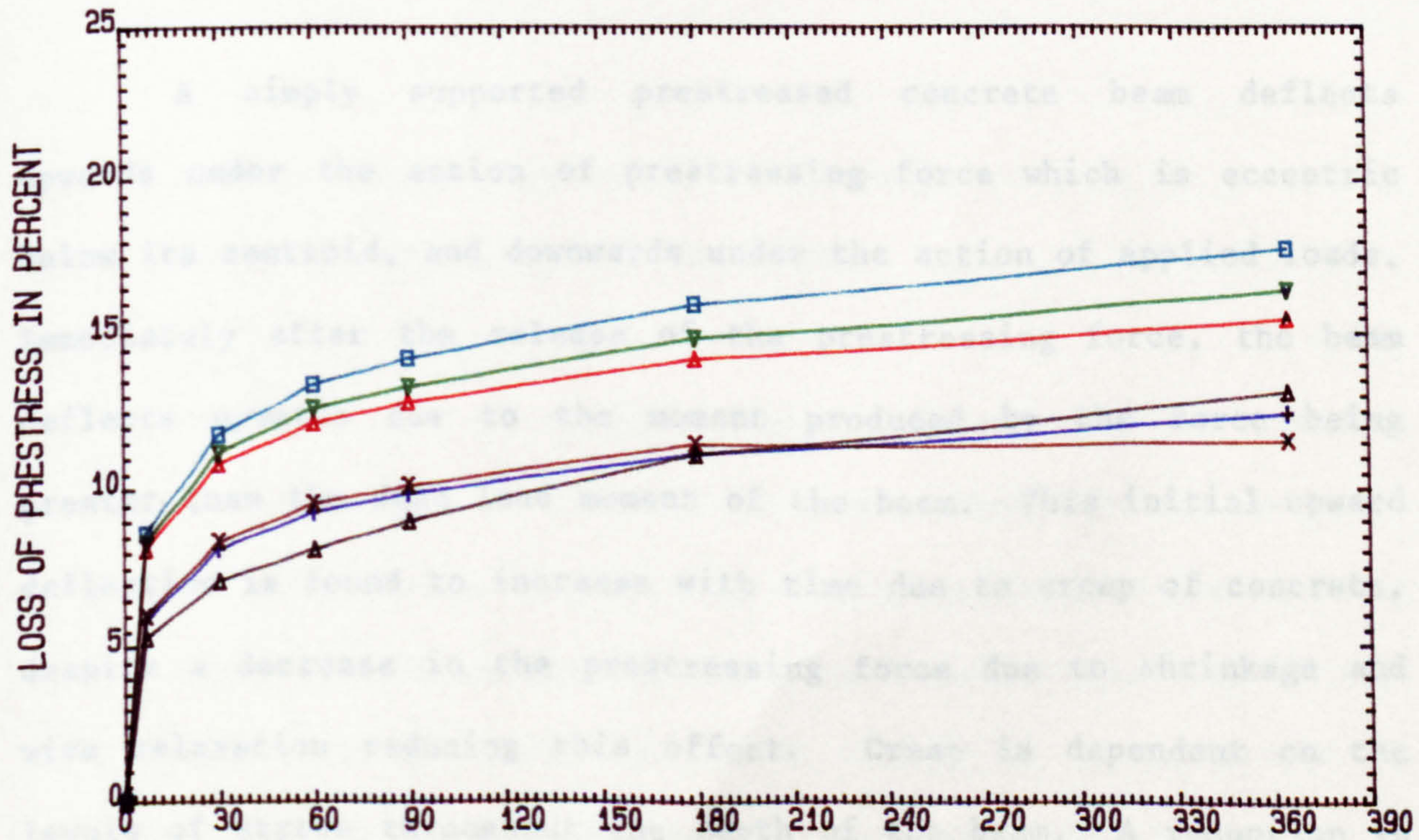

FIG. 6.44 COMPARISON OF EXPERIMENTAL AND PREDICTED TIME-DEPENDENT LOSS OF PRESTRESS BASED ON EXPERIMENTAL PARAMETERS FOR GROUTED RECTANGULAR BEAM (RHPC MIX) STORED IN VARIABLE ENVIRONMENT

CHAPTER 7 BEHAVIOUR OF TIME-DEPENDENT CAMBER AND DEFLECTION FOR PRESTRESSED CONCRETE MEMBERS

7.1 Introduction

In this chapter, the results of the investigation on instantaneous and time-dependent deflections of the tested prestressed beams are presented and discussed in detail. The discussion is divided into two parts, the first dealing with factors influencing the deflection behaviour of various concrete beams as described in Chapter Six, whilst the second part deals with a comparison between the results of tests and those predicted by current national and international methods.

7.2 Mechanism of Time-Dependent Camber and Deflection

A simply supported prestressed concrete beam deflects upwards under the action of prestressing force which is eccentric below its centroid, and downwards under the action of applied loads. Immediately after the release of the prestressing force, the beam deflects upwards due to the moment produced by the force being greater than the dead load moment of the beam. This initial upward deflection is found to increase with time due to creep of concrete, despite a decrease in the prestressing force due to shrinkage and wire relaxation reducing this effect. Creep is dependent on the levels of stress throughout the depth of the beam. A reduction in the prestressing force due to creep causes a change in the rates of creep between the top and the bottom of the beam. Thus, on the one

hand, creep causes a decrease in camber with time because of the decrease in the prestressing force, whilst on the other hand, it causes an increase in camber with time because of differential rates of creep between the top and bottom fibres due to different stress levels (i.e. creep is proportional to stress). The net change in camber due to creep is thus in the upward direction having because of higher total compressive strain at the bottom fibre, as typically shown in Fig. 6.2 (Chapter Six).

However, if the beam considered in the preceding paragraph is subjected to a sustained load, the stress distribution throughout the depth of the beam is reversed, causing an increasing downward deflection with time due to a greater creep at the top fibre. Figure 6.4 (Chapter Six) gives a typical illustration of concrete strain distribution through the mid-span section of the beam under sustained loading.

7.3 Analysis and Discussion of Test Results

7.3.1 Effect of Environmental Conditions

The influence of environmental conditions on time-dependent camber and deflection of the various prestressed concrete beams is presented in Figs. 7.1 to 7.4. By comparing the non-loaded beams with various concrete mixes and cross-sectional areas, the one-year test results reveal that the total camber of beams stored in variable humidity is about 6 to 10 percent lower than the camber of beams stored in constant humidity, as illustrated in Table 7.1. A constant environment, with 65% humidity, produced a lower effective

elastic modulus due to creep and a larger total camber and camber coefficient. It appears evident, therefore, that the total camber is noticeably insensitive to the effects of relative humidity and concrete strength in spite of the significant difference in prestress losses as discussed earlier in Section 6.2.1. The reason for this is that where there is a tendency for more creep and hence more camber, the effect is offset by a greater loss of prestress caused by both shrinkage and creep, which results in a reduction in camber. It should be pointed out that the results obtained generally confirm the findings of Branson et al. (48), but contradict the observations reported by Mossiossian (31) for different humidity conditions.

Similar trends were observed for the sustained loaded beams stored in the variable humidity environment which resulted in a reduction of 4 to 7 percent in total deflection, as shown in Table 7.2. This reduction in total deflection is believed to be associated with the higher creep at the top fibre of beams due to the service load and with the considerable difference in prestress losses found between the two environmental conditions (variation between 18 to 27%), as described earlier in Section 6.2.1.

In contrast to non-loaded and sustained loaded beams, the effect of the variable humidity condition on cyclic loaded beams reduced the total deflection considerably, viz. by 14% to 25 percent as shown in Figs. 7.1 to 7.4 and Table 7.2.

Based on the above findings it can be concluded that the

variable humidity condition (65 to 100% R.H.) tends to give lower values of total camber and deflection for different loading conditions, but it is only considered to be significant for cyclic loaded beams.

7.3.2 Effect of Loading Conditions and Shape and Size of Members

The results of different loading conditions on prestressed concrete beams of different cross-sections are also presented in Tables 7.1-7.2 and Figs. 7.1 to 7.4. As expected, the initial camber of the I-shaped beams (mean value of 0.96 mm) is greater than the rectangular beam value (mean value of 0.82 mm), since the self-weight and moment of inertia of the rectangular beams are greater.

The total camber-to-initial camber ratios and camber coefficients for various non-loaded concrete beams are presented in Table 7.1. It can be seen that the I-shaped beams have the highest total camber and camber coefficient, having total/initial camber ratios of 2.13 to 2.61 after a period of one year; by comparison, the corresponding ratios for rectangular beams were within 2.01 to 2.39. Generally, the results confirm observations reported by previous workers (12, 30, 106) who obtained similar values.

Generally speaking, the mean total camber of the non-loaded I-shaped beams is approximately 16 percent larger than the mean value of rectangular shaped beams stored in both environmental conditions. On the other hand, the total deflection variation between the two shapes of beam appears to be more significant for

sustained and cyclic loaded beams. The mean total deflection variations of sustained and cyclic loaded beams were 25 and 31 percent, respectively. This variation is thought to be associated with change of creep at the top fibre and prestress losses of each individual beam as described earlier in Chapter Six.

Table 7.2 shows the comparison of experimental time-dependent deflections for cyclic and sustained loaded beams. The total/instantaneous deflection ratios over a period of one year for various sustained loaded beams are within 1.94 to 2.47. The results seem to be within the one year values of total/instantaneous deflection ratio reported by previous investigators (12, 30, 106).

The differences between cyclic and sustained loading conditions are illustrated in Figs. 7.1 and 7.4. As expected, beams under cyclic loading give considerably lower total deflection than beams under sustained loading condition. This is believed to be caused by the lower creep values at the top fibre of the cyclic loaded beam due to a less total loading duration (viz. attributed to loading and unloading cycle). The time-dependent deflections at 365 days of cyclic loaded rectangular and I-shaped beams averaged 28 and 41 percent of the equivalent sustained loaded beams, respectively. It may also be noted that the time-dependent deflections for cyclic loaded beams stored in variable humidity were noticeably small and can be considered insignificant. This behaviour is thought to be caused by the similar values of creep at the top and bottom fibres of the cyclic loaded beams, as presented earlier in Chapter Six.

7.3.3 Effect of Concrete Mix Composition

The effect of mix composition on time-dependent camber and deflection at the end of one-year test period can be seen in Table 7.1 and 7.2. The test results reveal that the RHPC concrete beams always give lower long-term camber and deflection values than OPC concrete beams stored in different environmental conditions. The reason for that is the higher creep and prestress losses of the OPC concrete, as compared to the RHPC concrete, tends to give high upward or downward deflection depending upon the loading condition imposed. For non-loaded I-beams, stored in various environments, the average total camber at one year for RHPC beams is about 7 and 13 percent lower than for the non-grouted OPC and groupted OPC beams, respectively. This variation between the two grouting conditions is thought to be associated with variation of prestress losses as described in Chapter Six.

The results of the various concrete mixes on time-dependent deflections of cyclic and sustained loading beams are presented in Fig. 7.4 and Table 7.2. The deflection at one year for the sustained loaded rectangular beams having RHPC concrete is, on average, 12 percent lower than OPC concrete beams stored in the various environments. However, for cyclic loaded beams, the variation between the deflections of the two concrete mixes was more significant, the values for RHPC concrete beams were approximately 28 percent lower than for OPC concrete beams. It is believed again that the variation between the two concrete mixes is mainly caused by the magnitude of prestress losses and by the magnitude of creep

at the top fibre of the beams as mentioned earlier in Section 6.2.2 (Chapter Six).

The influence of PFA and the superplasticizing admixture on time-dependent camber of I-shaped beams stored in constant environment is shown in Fig. 7.5 and Table 7.1. It can be seen that the beam made from the superplasticizing admixture (NI/C3) exhibited the largest total camber at the end of the one-year test period; the total camber was nearly 7 percent greater than that of the RHPC control beam (NI/C1). This may be due to the high creep deformation at the bottom fibre of the beam made with the admixture as mentioned earlier in Section 5.2.3.1 (Chapter Five).

In the case of the beam made with PFA (NI/C4), it is surprising to find that its total camber is the lowest among all concrete beams stored in a constant environment (total/initial camber ratio of 2.2) as shown in Fig. 7.5. The total camber after one year is about 11 percent lower than the RHPC concrete control beam. For the beam (NI/C5), which contained a combination of PFA and admixture, the total camber at one year was only 4 percent lower than that of RHPC concrete control beam. The variation between the RHPC control beam and other beams having PFA and admixture is believed to be mainly associated with low creep of the PFA concrete and of the admixture and PFA concrete because a low creep at the bottom fibre of the beam tends to give a lower camber. In view of this, it can be concluded that the PFA concrete or a combination of PFA and admixture are advantageous in reducing the camber which is extremely important and beneficial for the serviceability of prestressed concrete members.

7.3.4 Duration for Stabilization

From Fig. 7.1 to 7.3, it can be seen that, for most of the unloaded beams, the camber growth with time has reached a stable stage relatively early compared with shrinkage and creep, because prestress loss resulting from the shrinkage-plus-creep causes a decrease in the camber. The variation between the 180 and 365 days camber values was very small ranging from 3 to 7 percent. Therefore, it can be concluded that the stabilization period of camber is approximately 180 days after prestressing. These results generally support the findings of previous workers (48, 53, 106). However, for the PFA concrete beam (NI/C4), it is interesting to notice that the camber growth practically ceased after 90 days (see Fig. 7.5). This early stabilization of camber is probably associated with the slow rate of creep between 90 and 365 days as shown in Fig. 5.9 (Chapter Five).

For the cyclic-loaded beams (Figs. 7.1 and 7.4), the deflection of beams stored in the constant humidity condition has practically stabilized after 180 days. On the other hand, the deflection for beams stored a in variable humidity condition has effectively ceased at the earlier age of 90 days despite the continuous decrease in prestressing force with time. This early stabilization is thought to be associated with slow rate of creep at the top and bottom fibres of the beams throughout the one-year testing period (i.e. creep at top and bottom fibres were nearly the same) as described earlier in Section 7.3.2.

In the case of the sustained loaded beams where there was a continuous loss of prestress coupled with continuous creep at the top fibre of the beams, there was no stabilization for time-dependent deflections during the first year; between 180 and 365 days, the changes in deflection were 14 to 18 percent.

This confirms recent findings of Zundelevich et al. (106) who reported a change in deflection between 180 and 300 days of 13 to 19 percent.

7.4 Comparison Between Experimental Results and Current Prediction Methods

7.4.1 Major Estimating Methods of Deflection

The comparison conducted in this investigation is limited to the major prediction methods of the present Codes and Specifications for determining the long-term deflections and camber of uncracked prestressed concrete members. Four methods are presented in the following paragraphs.

In the case of the CEB-78 model code (16), it is suggested that the total curvature is comprised of the sum of the elastic curvature and the curvature due to creep and shrinkage, i.e.

$$(1/r)_t = (1/r)_e + (1/r)_{cc} + (1/r)_{cs} \qquad \text{Eq. 7.1}$$

where $(1/r)_t$ is the total curvature,

$(1/r)_e$ is the elastic curvature (M/E_cI),

$(1/r)_{cc}$ is the creep curvature and equal to $(1/r)_e \phi_c$

where ϕ_c is the creep coefficient,

$(1/r)_{cs}$ is the shrinkage curvature and equal to $K_{cs} \varepsilon_{cs/d}$

where k_{cs} is a coefficient which depends upon the percentage of tension and compression steel in the section,

ε_{cs} is the shrinkage strain,

and d is the effective depth of member.

In the case of the ACI-82 method, the following equations are recommended for beams with straight tendons. For non-loaded beams containing prestressed steel only or containing both prestressed steel and nonprestressed tension steel, the camber or deflection at any time is computed by:

$$a_t = \overbrace{(a_i)_{F_o}}^{(1)} - \overbrace{(a_i)_D}^{(2)} + \overbrace{[-\frac{F_t}{F_o} + (1 - \frac{F_t}{2F_o})\phi(t,t_o)](a_i)_{F_o}}^{(3)} - \overbrace{(a_i)_D \phi(t,t_o)}^{(4)} - \overbrace{a_L}^{(5)}$$

Eq. 7.2

For sustained loading other than a composite slab or topping applied some time after the transfer of prestress, the deflection at any time ($a_{t,1}$) is given by:

$$a_{t,1} = \underbrace{a_t \text{ in Eq.7.2}}_{\text{Term (1-5)}} - \underbrace{(a_i)_s}_{(6)} - \underbrace{(a_i)_s \phi(t,t_o)}_{(7)} \qquad \text{Eq. 7.3}$$

Term (1) is the initial camber due to the initial prestress force after elastic loss, F_o Term (2) is the initial dead load deflection of the beam. Term (3) is the creep (time-dependent) camber of the beam due to the prestress force. Term (4) is the dead load creep deflection of the beam. Term (5) is the live load deflection of the beam. Term (6) is the initial deflection of the beam under the superimposed sustained load. Term (7) is the creep deflection of the beam under the superimposed sustained load.

In the case of the new British Code BS8110-85 (60), it is suggested that the total long-term deflection due to the prestressing force, dead load and any sustained imposed loading of uncracked members may be estimated by using an effective elastic modulus of concrete (E_{eff}) which allows for creep and given by:

$$E_{eff} = E_i/(1 + \varepsilon_{cc} E_i) \qquad \text{Eq. 7.4}$$

where E_i is the instantaneous elastic modulus

ε_{cc} is the specific creep for the period considered.

Deflections can be calculated by using simple elastic relationships such as:

$$a = Kl^2 M/E_{eff} I \qquad \text{Eq. 7.5}$$

in which a = deflection, 1 = effective span, M = moment, K = constant depending on the shape of the bending moment diagram, values for K coefficient are given in Table 3.1 (BS8110: Part 2)

and I = second moment of area of section

In the case of the PCI-1977 (107) method, suggested multipliers can be used as a guide in estimating long-time cambers and deflections for prestressed concrete member. Derivation of these multipliers is contained in a paper by Martin (108).

The long-time factor which is applied to the initial deflection caused by the dead weight of the member is gven by:

$$U_{df}=E_{ci}/E_c\ U_b$$

where E_{ci} and E_c are modulus of elasticity at the time of transfer and at 28 days, respectively

and U_b is a factor equal to 2 (no compressive reinforcement).

The multiplier which is applied to the initial deflection is:

$$m_{df} = 1 + U_{df} \qquad \text{Eq. 7.6}$$

To determine the upward component of the final camber or deflection, the multiplier which is applied to the initial camber is reduced by time-dependent prestress loss.

The long-time factor would then be:

$$U_{pf} = U_{df} P/P_o$$

in which P_o and P are prestress force at transfer and total prestress force after all losses, respectively.

The multiplier used to determine the upward (camber) component of the final camber or deflection is then:

$$M_{pf} = 1 + U_{pf} \qquad \text{Eq. 7.7}$$

For superimposed sustained dead loads, the long-time factor is given by:

$$U_{sd} = U_b$$

The multiplier which is applied to elastic deflection caused by superimposed dead load is:

$$M_{sd} = 1 + U_{sd} \qquad \text{Eq. 7.8}$$

It should be noted that the computed deflections and cambers of the PCI method is based on the 70 percent relative humidity condition.

7.4.2 Comparison Analysis and Discussion

Figure 7.6 to 7.11 présent the comparison between the

measured and predicted time-dependent mid-span camber and deflection for various beams stored in different environments. Furthermore, the comparisons of the one-year values between the measured and predicted deflections of the unloaded and loaded beam are presented in Tables 7.3 and 7.4 respectively. According to Table 7.3, it is clear that most of the prediction methods give values very close to the experimental camber values for the entire duration of the test. However, BS8110 seems to overestimate camber values for RHPC concrete beams considerably (variations of up to 36% of measured values). Both the ACI-82 and CEB-78 methods give the best predicted values with a variation within $\pm$ 14 percent of the measured values; this confirms findings reported by Zundelevich et al. (106). Furthermore, the PCI-77 method appears to give a slightly underestimated value (based on 70% relative humidity) ranging from -3 to -19 percent of the measured values. Therefore, the PCI method is conservative, especially when 65% relative humidity values are used instead of the specified 70% relative humidity. Although the BS8110 method seems to give an unconservative value for RHPC concrete beams, the method apparently gives values very close to the measured values for OPC concrete beams. It is thought that the overestimated values of camber is due to the considerable overestimation of predicted creep values of the BS8110 code as described earlier (Chapter Five).

In general, previous workers consider a sufficient accuracy of estimating camber and deflection to be 10% or 20% for practical purposes (97). As in the case of superimposed sustained loaded beams, a clear evidence of underestimation of total deflection can

be found by comparing the measured and predicted values of the various methods given in Table 7.4. It is clear that BS8110 gives generally the closest estimates of all methods, having deflections ranging from -8 to -30 percent of measured values. All the other methods seem to give a significant underestimation of deflections ranging from 26 to 52 percent of measured values.

The ACI-82 method produces underestimated values by up to 52 percent of the measured values, which confirms findings of Zundelevich et al. (106) who reported that the ACI method tends to underestimate the total deflection at one year by 36 to 42 percent of experimental values. It should be emphasized that any substantial underestimation of deflection can affect the serviceability of the concrete member and can cause significant cracks in prestressed concrete beams. Therefore, it is thought that some revision to the recent prediction methods are required to predict the time-dependent deflection caused by superimposed sustained loads. Also, more experimental tests on various factors are needed in order to find multiplier factors that can be used to modify recent methods.

The comparison between measured and predicted cambers and deflections by using the general and experimental material parameters after 365 days are presented in Table 7.5. It can be seen that when using experimental material parameters, a slight improvement in total deflection was achieved for the ACI-82 method, whereas no improvement was achieved for the other methods.

7.5 Conclusions

The behaviour of time-dependent camber and deflection of beams has been investigated by comparing identical post-tensioned beams stored in different environmental conditions.

For non-loaded beams of two different cross-sections and made from various concrete mixes,the test results over a one year period of monitoring reveals that the total camber of beams stored in a variable humidity is 6 to 10 percent lower than camber values of beams stored under constant humidity conditions. A similar trend was observed for the sustained loaded beams stored in a variable humidity in which deflection values were 4 to 7 percent lower than in a constant environment. Since such differences are small, it is concluded that the total camber or deflection is reasonably insensitive to the effects of relative humidity, as well as concrete strength, in spite of the significant difference in prestress losses. However, for a cyclic loaded beam, it has been observed that variable humidity conditions give a considerable reduction in the total deflection (a variation of 14 to 25 percent).

Test results for different shapes and sizes of concrete beams of different loading conditions indicate that the I-shaped beams give the highest camber and deflection with time. The variations between the two shapes were 16%, 25% and 31% for non-loaded, sustained loaded and cyclic loaded beams, respectively. Therefore, it is concluded that the effect of shape and size of members is more significant on camber and deflection for beams

under the cyclic and sustained loading conditions.

For the sustained loaded beams of different shapes, it was confirmed that the experimental total/instantaneous deflection ratios are in close agreement with ratios reported by previous workers (12, 30, 106).

When concrete beams are subjected to cyclic and sustained loading conditions, the test results indicate that beams under cyclic loading give a considerably lower total deflection than beams under a sustained loading condition and, in fact, the deflection is negligible under the variable humidity condition. It is concluded that the variation between the two loading conditions is more significant for the I-shaped beam which has a lower volume/surface ratio.

Investigations on the influence of concrete mix composition on time-dependent camber and deflection reveal that the RHPC concrete beams subjected to any loading condition produce lower long-term camber and deflection than OPC concrete beams stored in the same environmental conditions. The average variations between the two concrete mixes were 10%, 12% and 28% for non-loaded, sustained loaded and cyclic loaded beams, respectively. Consequently, the effect of mix composition is more significant for cyclic loading condition. Compared with RHPC control beam, the total camber of the beam with superplasticizing admixture increased by 7 percent at 365 days, whereas the one-year total camber of the PFA concrete and PFA/admixture concrete beams were less by 11 percent and 4 percent,

respectively, compared with the camber of the RHPC control beam. Therefore, it is concluded that PFA concrete, or concrete made with a combination of PFA and admixture, are beneficial for the serviceability of prestressed concrete members.

Investigation into duration of camber and deflection stabilization indicated that, for non-loaded beams, camber growth reached a stable stage at 180 days, a time which is relatively early compared to the development of shrinkage and creep. The results generally support findings reported by previous workers (48, 53, 106). It is apparent that the camber growth for PFA concrete ceases even earlier, viz. after 90 days of prestressing.

For cyclic loaded beams, the deflection in a constant humidity condition stabilizes after 180 days, whereas the deflection for beams stored in the variable humidity condition almost stabilizes at an earlier age of 90 days. For sustained loaded beams, it is concluded that there is no stabilization for time-dependent deflection during the testing period of one year.

The most recent methods of predicting time-dependent camber and deflections have been compared with each other and with the experimental results obtained from the present investigation. For non-loaded beams, it would appear that most of the prediction methods give values very close to the experimental cambers for the entire duration of the test, whereas the BS8110 overestimates camber for RHPC concrete beams considerably. Both the ACI-82 and CEB-78 methods give the best predicted values ranged within $\pm$ 14 percent of

measured values. Furthermore, the BS8110 method gives camber values for OPC concrete beams that are very close to the measured values.

In the case of sustained loaded beams, most methods underestimate the total deflection with time, but the BS8110 method is the best giving estimates of within 8 to 30 percent. It was also found that all the other methods produce significant underestimations of deflections (within 26 to 52 percent of measured values). Therefore, it is thought that some revision to the recent prediction methods is required to predict the time-dependent deflection caused by sustained load more accurately. Also more experimental testing is needed in order to find multiplier factors that can be used to allow for various factors in these methods.

Finally, when using experimental material parameters to predict time-dependent camber and deflection, a slight improvement resulted in the calculated total deflection by the ACI-82 method, but there was no improvement for the other prediction methods.

Table 7.1 - Comparison of Experimental Time-Dependent Deflections for Non-Loaded Prestressed Concrete Beams

Beam	Relative Humidity Condition	Initial Midspan Camber (mm)	Total Camber at 365 days (mm)	Ratio of Total/ Initial Camber	* Camber Coeff-icient B_t	Total Camber Ratio of Variable/ Constant Environment Beams
NGI/C1	C	0.91	2.34	2.57	1.57	0.902
NGI/V1	V	0.90	2.11	2.34	1.34	
NI/C1	C	0.93	2.21	2.38	1.38	0.923
NI/V1	V	0.92	2.04	2.22	1.22	
NGI/C2	C	1.01	2.64	2.61	1.61	0.931
NGI/V2	V	1.03	2.46	2.39	1.39	
NI/C2	C	0.99	2.38	2.40	1.4	0.911
NI/V2	V	1.02	2.17	2.13	1.13	
NI/C3	C	0.87	2.38	2.74	1.74	-
NI/C4	C	0.90	1.98	2.20	1.20	-
NI/C5	C	0.92	2.13	2.32	1.32	-
NGR/C1	C	0.83	1.98	2.39	1.39	0.941
NGR/V1	V	0.80	1.87	2.34	1.34	
NR/C1	C	0.83	1.77	2.14	1.13	0.932
NR/V1	V	0.82	1.65	2.01	1.01	

Note: C represents constant environment (65% R.H.)

V represents variable environment (From 65% to 100% R.H.)

* Camber coefficient B_t is defined as the ratio of inelastic camber to elastic camber

Designation of Beams

N = No Load/Self Wt.
C = Constant Service Load
CY = Cyclic Service Load
G = Grouted Tendons

I = I-Shape
R = Rectangular Shape
/C = Constant Environment
/V = Variable Environment

1 = RHPC Mix
2 = OPC Mix
3 = RHPC/Admixture Mix
4 = RHPC/PFA Mix
5 = RHPC/Admixture & PFA Mix

Table 7.2 - Comparison of Experimental Time-Dependent Deflections for Cyclic and Sustained Loaded Prestressed Concrete Beams

Beam	Relative Humidity Condition	* Instantaneous Midspan Deflection Due to Loading (mm)	Time-Dependent Deflection at 365 days (mm)	Total Deflection Plus Instantaneous Deflection (mm)	Ratio of Total/ Instantaneous Deflection	Total Deflection Ratio of Variable/ Constant Environment Beams
CYI/C1	C	1.10	0.91	2.01	1.82	0.76
CYI/V1	V	1.15	0.38	1.53	1.33	
CI/C1	C	1.13	1.66	2.79	2.47	0.93
CI/V1	V	1.18	1.42	2.60	2.20	
CYR/C1	C	0.92	0.39	1.31	1.42	0.86
CYR/V1	V	0.98	0.15	1.13	1.15	
CR/C1	C	0.96	1.12	2.08	2.17	0.94
CR/V1	V	1.01	0.95	1.96	1.94	
CRY/C2	C	0.97	0.56	1.53	1.58	0.75
CYR/V2	V	0.95	0.20	1.15	1.21	
CR/C2	C	0.94	1.26	2.20	2.34	0.96
CR/V2	V	1.01	1.11	2.12	2.10	

Note: * Instantaneous deflection represent the traveled distance from upward to downward deflection due to applied load

C represents constant environment (65% R.H.)

V represents variable environment (65% to 100% R.H.)

Table 7.3 - Measured and Predicted Camber of Non-Loaded Beams at the End of One-Year of Testing

Type of Beam	Method of Prediction	Initial Midspan Camber (mm)	Total Camber (mm)		Ratio of Total Computed/Measured Camber Values	
			Constant Humidity	Variable Humidity	Constant Humidity	Variable Humidity
I-Shaped Beam, RHPC Concrete Mix	Measured	0.91	2.34	2.11	-	-
	CEB-78	1.03	2.43	2.16	1.04	1.02
	ACI-82	1.04	2.52	2.41	1.08	1.14
	BS8110-85	1.14	3.04	2.87	1.30	1.36
	PCI-77 *	1.05	2.12	-	0.91	-
I-Shaped Beam, OPC Concrete Mix	Measured	1.01	2.64	2.46	-	-
	CEB-78	1.02	2.42	2.15	0.92	0.88
	ACI-82	1.04	2.49	2.37	0.94	0.96
	BS8110-85	1.13	2.70	2.44	1.02	0.99
	PCI-77 *	1.05	2.13	-	0.81	-
Rectangular Shaped Beam, RHPC Concrete Mix	Measured	0.83	1.98	1.87	-	-
	CEB-78	0.92	2.06	1.87	1.04	1.0
	ACI-82	0.94	2.18	2.09	1.10	1.11
	BS8110-85	1.02	2.68	2.54	1.35	1.36
	PCI-77 *	0.94	1.91	-	0.97	-

Note: * PCI values are based on 70% relative humidity

Table 7.4 - Measured and Predicted Deflection of Loaded Beams at the End of One-Year of Testing

Type of Beam	Method of Prediction	Total Downward Deflection (mm)		Ratio of Total Computed/Measured Deflection Values	
		Constant Humidity	Variable Humidity	Constant Humidity	Variable Humidity
I-Shaped Beam, RHPC Concrete Mix	Measured	1.66	1.41	-	-
	CEB-78	1.19	0.98	0.72	0.70
	ACI-82	1.15	1.04	0.69	0.74
	BS8110-85	1.52	1.28	0.92	0.91
	PCI-77 *	1.12	-	0.68	-
Rectangular Shaped Beam, RHPC Concrete Mix	Measured	1.12	0.95	-	-
	CEB-78	0.69	0.55	0:62	0.58
	ACI-82	0.62	0.54	0.55	0.57
	BS8110-85	0.95	0.81	0.85	0.85
	PCI-77 *	0.67	-	0.60	-
Rectangular Shaped Beam, OPC Concrete Mix	Measured	1.26	1.11	-	-
	CEB-78	0.74	0.59	0.59	0.53
	ACI-82	0.60	0.55	0.48	0.50
	BS8110-85	0.94	0.77	0.75	0.70
	PCI-77	0.68	-	0.54	-

Note: * PCI values are based on 70% relative humidity

Table 7.5 - Predicted Camber and Deflection Values at 365 days Using The General and Experimental Material Parameters

Type of Beam	Method of Prediction	Total Deflection (mm)							
		General Material Parameters				Experimental Material Parameters			
		Non-Loaded		Loaded		Non-Loaded		Loaded	
		C	V	C	V	C	V	C	V
I-Shaped Beam, RHPC Concrete Mix	Measured	2.34	2.11	-1.66	-1.41	2.34	2.11	-1.66	-1.41
	CEB-78	2.43	2.16	-1.19	-0.98	1.64	1.28	-1.0	-0.64
	ACI-82	2.52	2.41	-1.15	-1.04	2.77	2.35	-1.21	-0.89
	BS8110-85	3.04	2.87	-1.52	-1.28	1.76	1.38	-1.19	-0.74
I-Shaped Beam, OPC Concrete Mix	Measured	2.64	2.46	-	-	2.64	2.46	-	-
	CEB-78	2.42	2.15	-	-	1.85	1.44	-	-
	ACI-82	2.49	2.37	-	-	3.02	2.54	-	-
	BS8110-85	2.70	2.44	-	-	2.00	1.55	-	-
Rectangular Shaped Beam, RHPC Concrete Mix	Measured	1.98	1.87	-1.12	-0.95	1.98	1.87	-1.12	-0.95
	CEB-78	2.06	1.87	-0.69	-0.55	1.23	0.79	-0.52	-0.26
	ACI-82	2.18	2.09	-0.62	-0.54	2.18	1.73	-0.65	-0.37
	BS8110-85	2.68	2.54	-0.95	-0.81	1.31	0.85	-0.64	-0.31
Rectangular Shaped Beam, OPC Concrete Mix	Measured	-	-	-1.26	-1.11	-	-	-1.26	-1.11
	CEB-78	-	-	-0.74	-0.59	-	-	-0.58	-0.28
	ACI-82	-	-	-0.60	-0.55	-	-	-1.07	-0.41
	BS8110-85	-	-	-0.94	-0.77	-	-	-0.77	-0.37

Note: C and V are constant and variable environment, respectively

(+) and (-) signs indicate upward and downward deflection respectively.

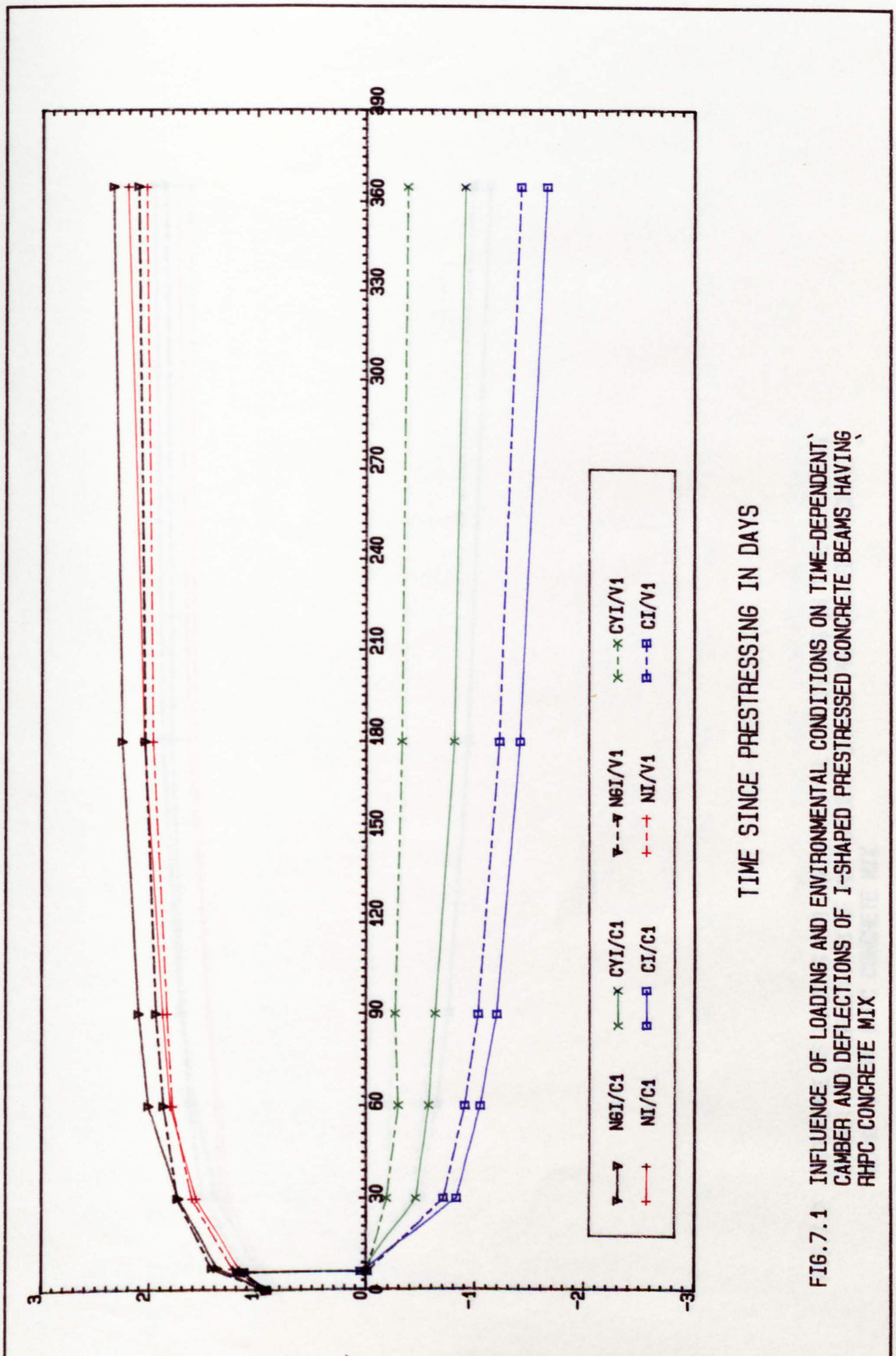

FIG.7.1 INFLUENCE OF LOADING AND ENVIRONMENTAL CONDITIONS ON TIME-DEPENDENT CAMBER AND DEFLECTIONS OF I-SHAPED PRESTRESSED CONCRETE BEAMS HAVING RHPC CONCRETE MIX

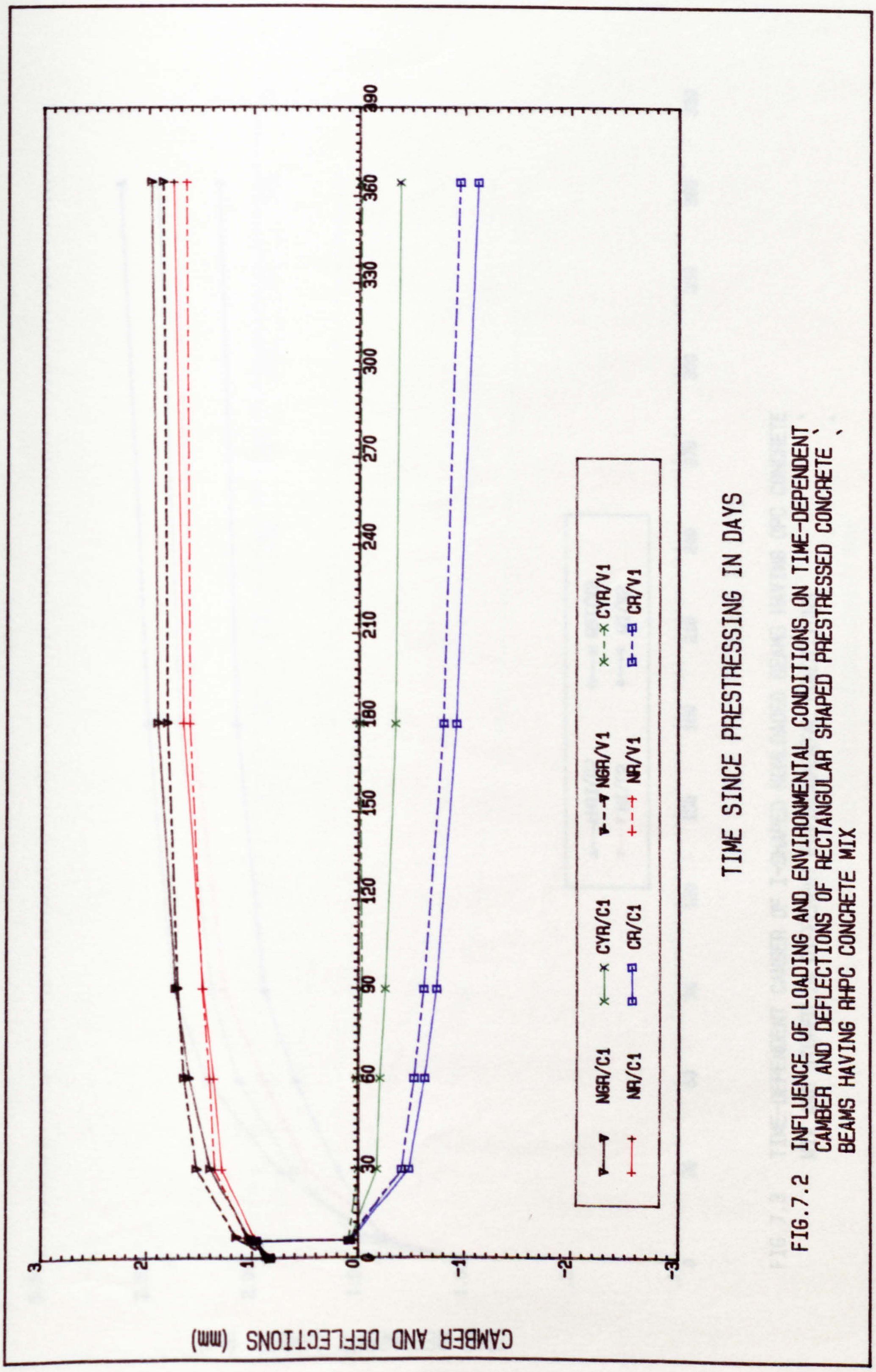

FIG.7.2 INFLUENCE OF LOADING AND ENVIRONMENTAL CONDITIONS ON TIME-DEPENDENT CAMBER AND DEFLECTIONS OF RECTANGULAR SHAPED PRESTRESSED CONCRETE BEAMS HAVING RHPC CONCRETE MIX

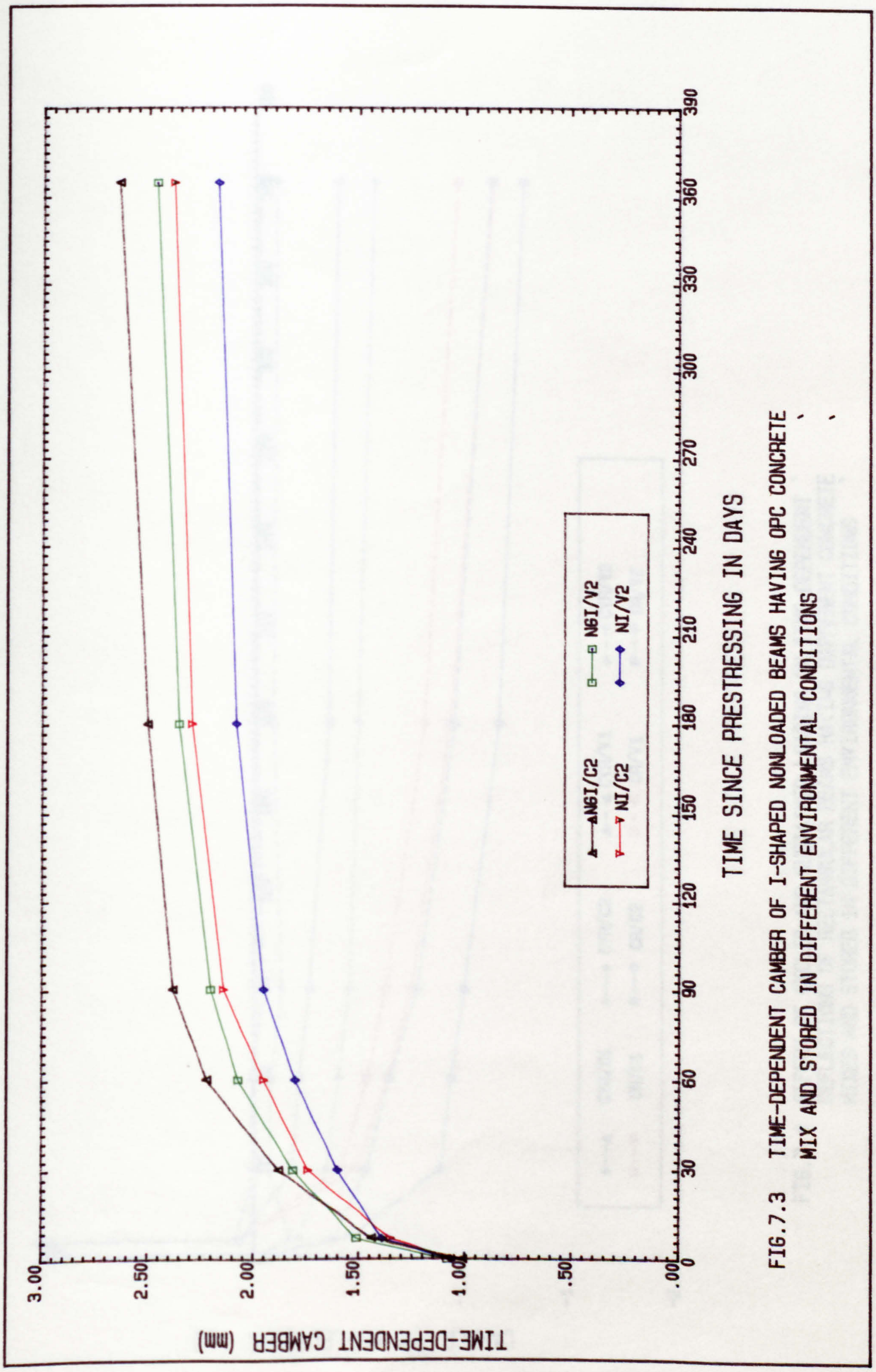

FIG.7.3 TIME-DEPENDENT CAMBER OF I-SHAPED NONLOADED BEAMS HAVING OPC CONCRETE MIX AND STORED IN DIFFERENT ENVIRONMENTAL CONDITIONS

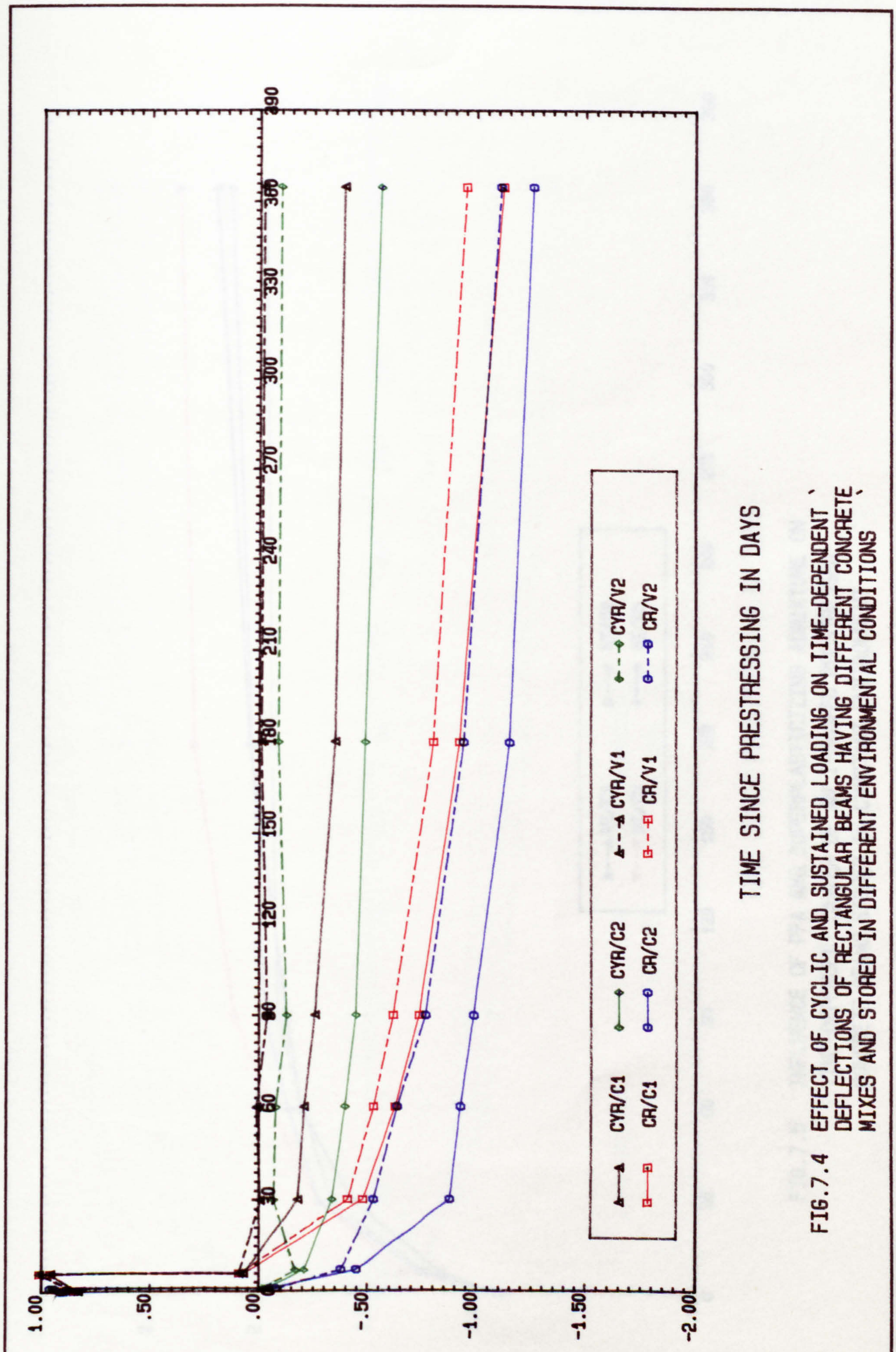

FIG.7.4 EFFECT OF CYCLIC AND SUSTAINED LOADING ON TIME-DEPENDENT DEFLECTIONS OF RECTANGULAR BEAMS HAVING DIFFERENT CONCRETE MIXES AND STORED IN DIFFERENT ENVIRONMENTAL CONDITIONS

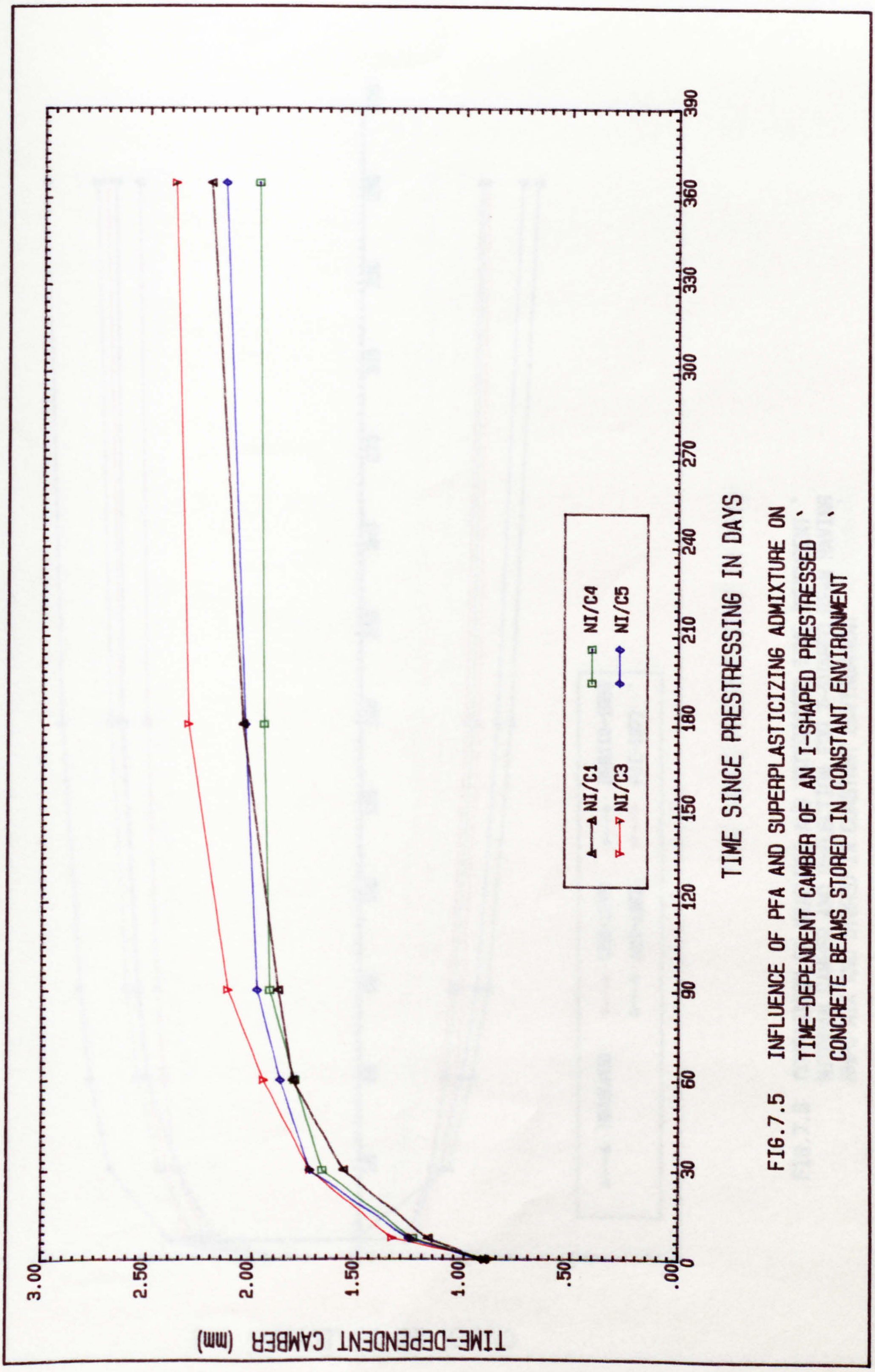
TIME-DEPENDENT CAMBER (mm)
3.00
2.50
2.00
1.50
1.00
.50
.00
0
30
60
90
120
150
180
210
240
270
300
330
360
390
TIME SINCE PRESTRESSING IN DAYS
NI/C1
NI/C2
NI/C3
NI/C4
NI/C5
INFLUENCE OF PFA AND SUPERPLASTICIZING ADMIXTURE ON
TIME-DEPENDENT CAMBER OF AN I-SHAPED PRESTRESSED
CONCRETE BEAMS STORED IN CONSTANT ENVIRONMENT

FIG.7.5

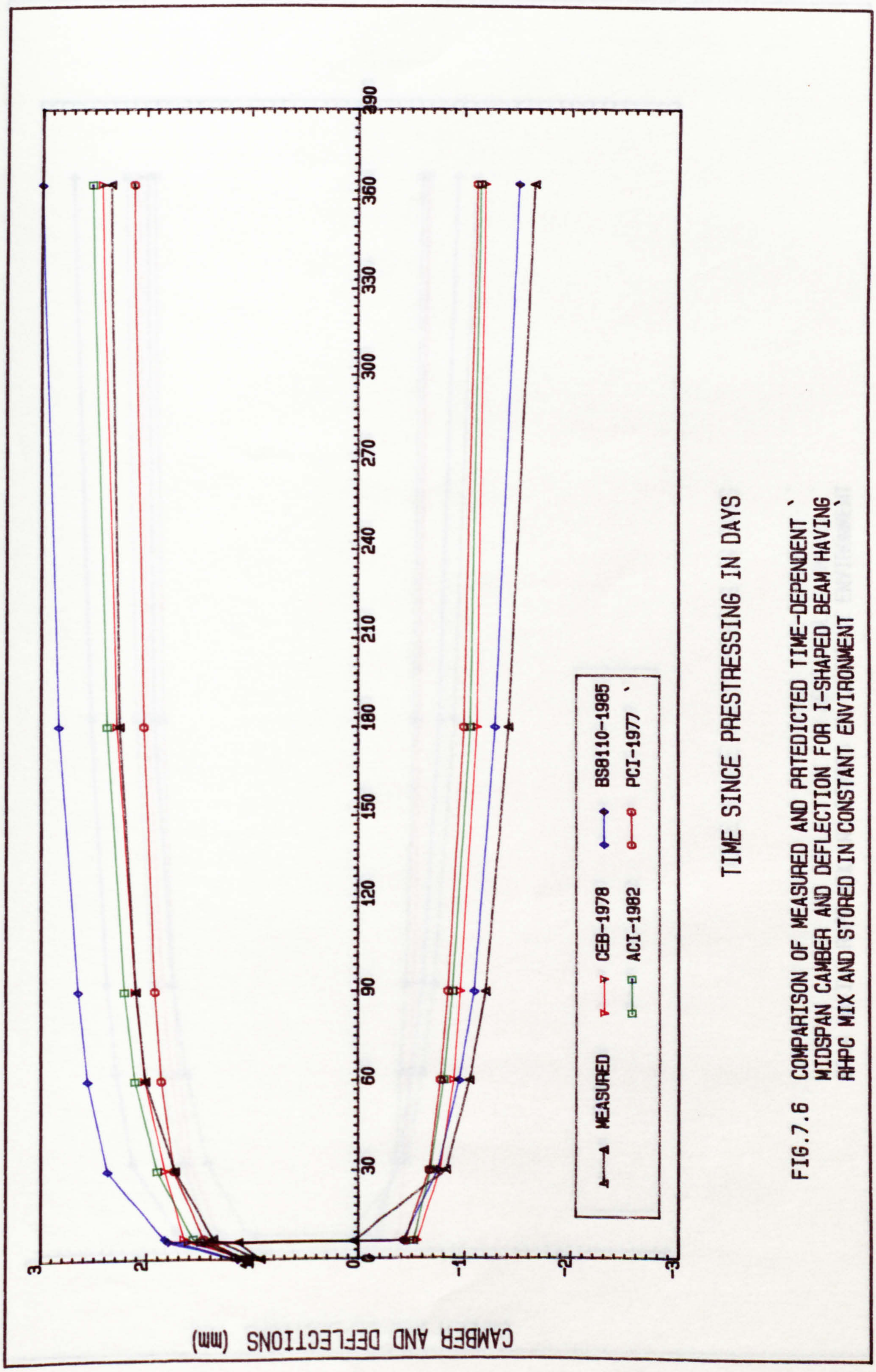

FIG.7.6 COMPARISON OF MEASURED AND PRTEDICTED TIME-DEPENDENT MIDSPAN CAMBER AND DEFLECTION FOR I-SHAPED BEAM HAVING RHPC MIX AND STORED IN CONSTANT ENVIRONMENT

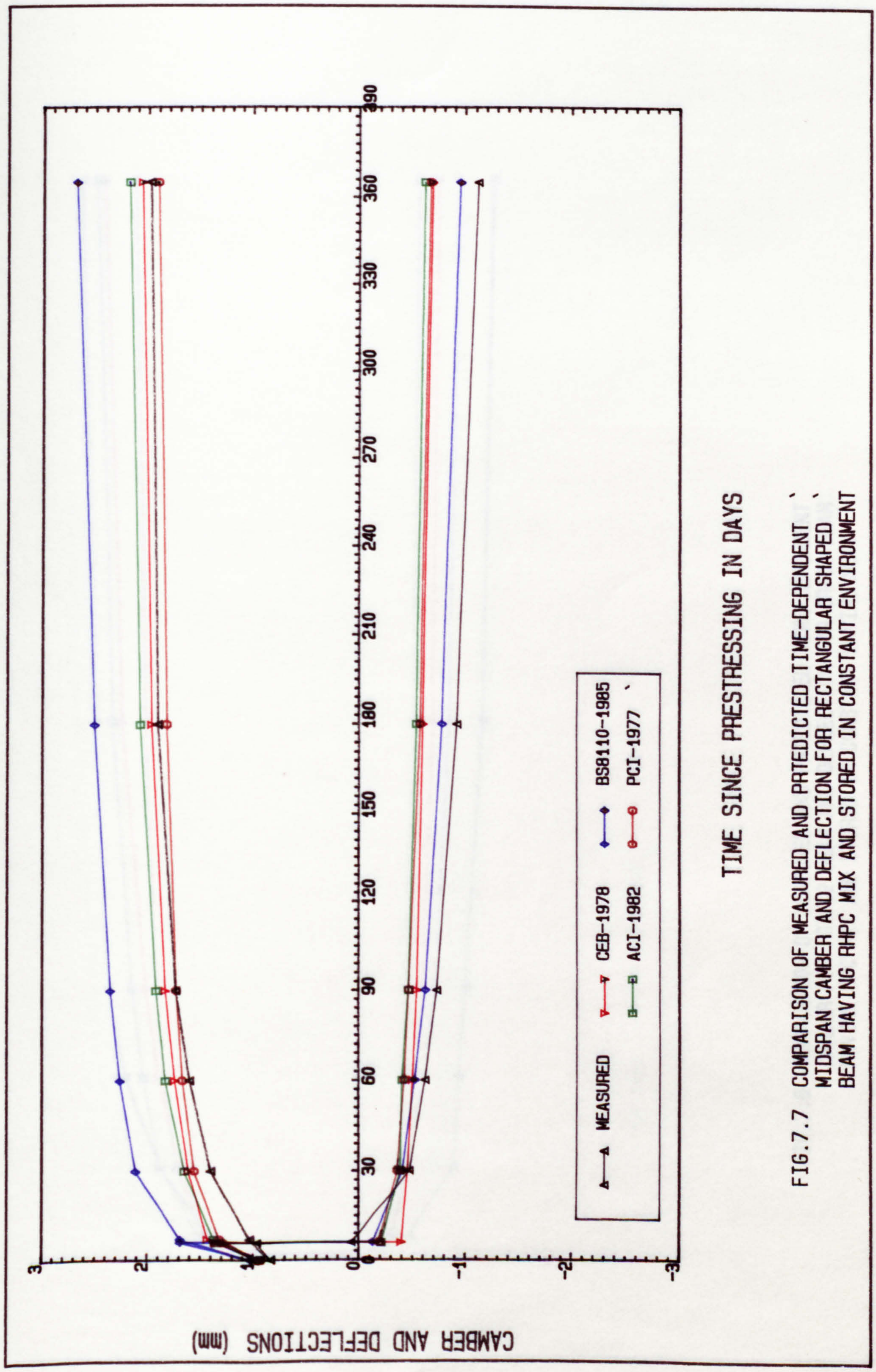

FIG.7.7 COMPARISON OF MEASURED AND PRTEDICTED TIME-DEPENDENT MIDSPAN CAMBER AND DEFLECTION FOR RECTANGULAR SHAPED BEAM HAVING RHPC MIX AND STORED IN CONSTANT ENVIRONMENT

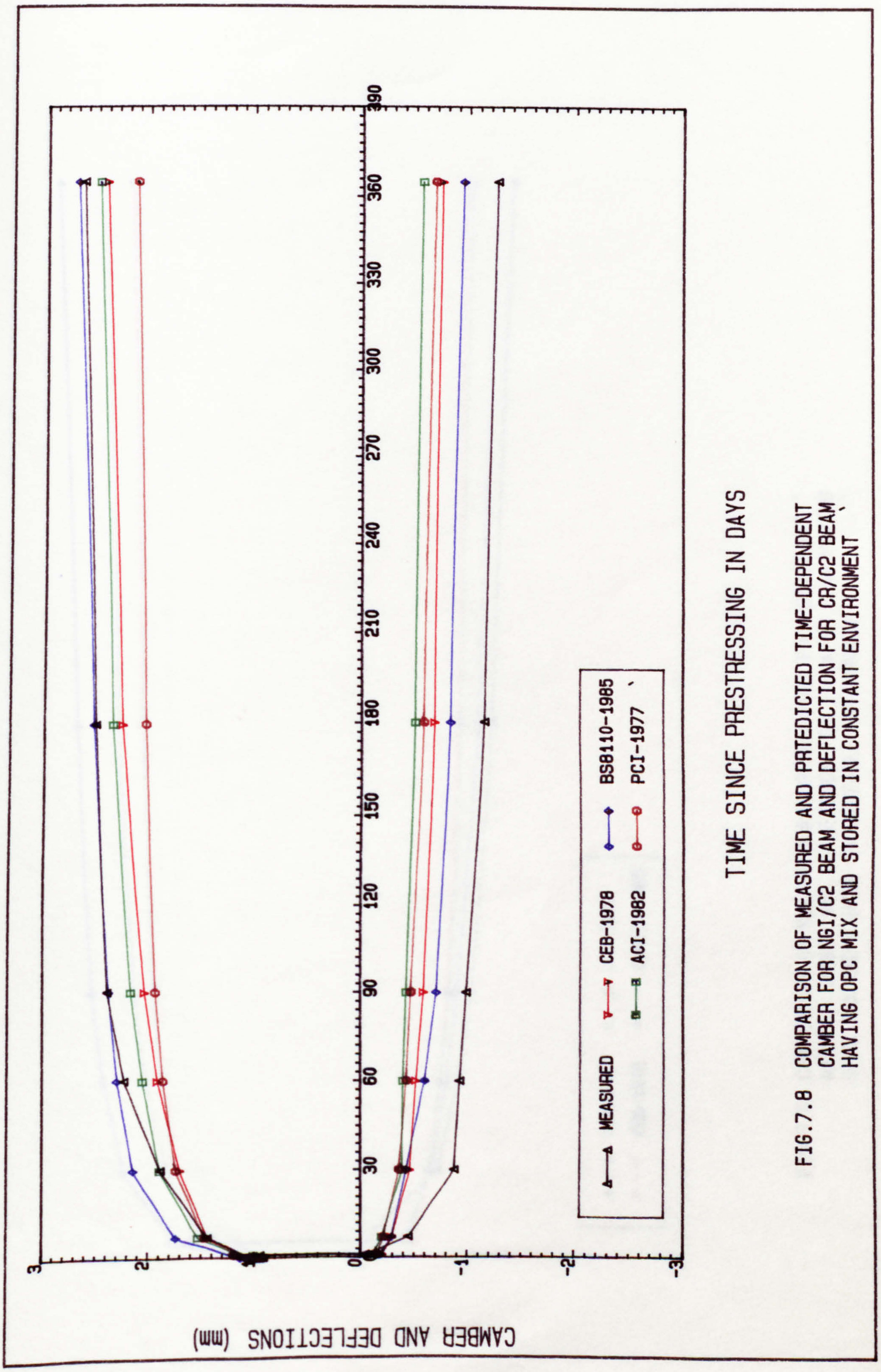

FIG.7.6.7.8 COMPARISON OF MEASURED AND PRTEDICTED TIME-DEPENDENT CAMBER FOR N6I/C2 BEAM AND DEFLECTION FOR CR/C2 BEAM HAVING OPC MIX AND STORED IN CONSTANT ENVIRONMENT

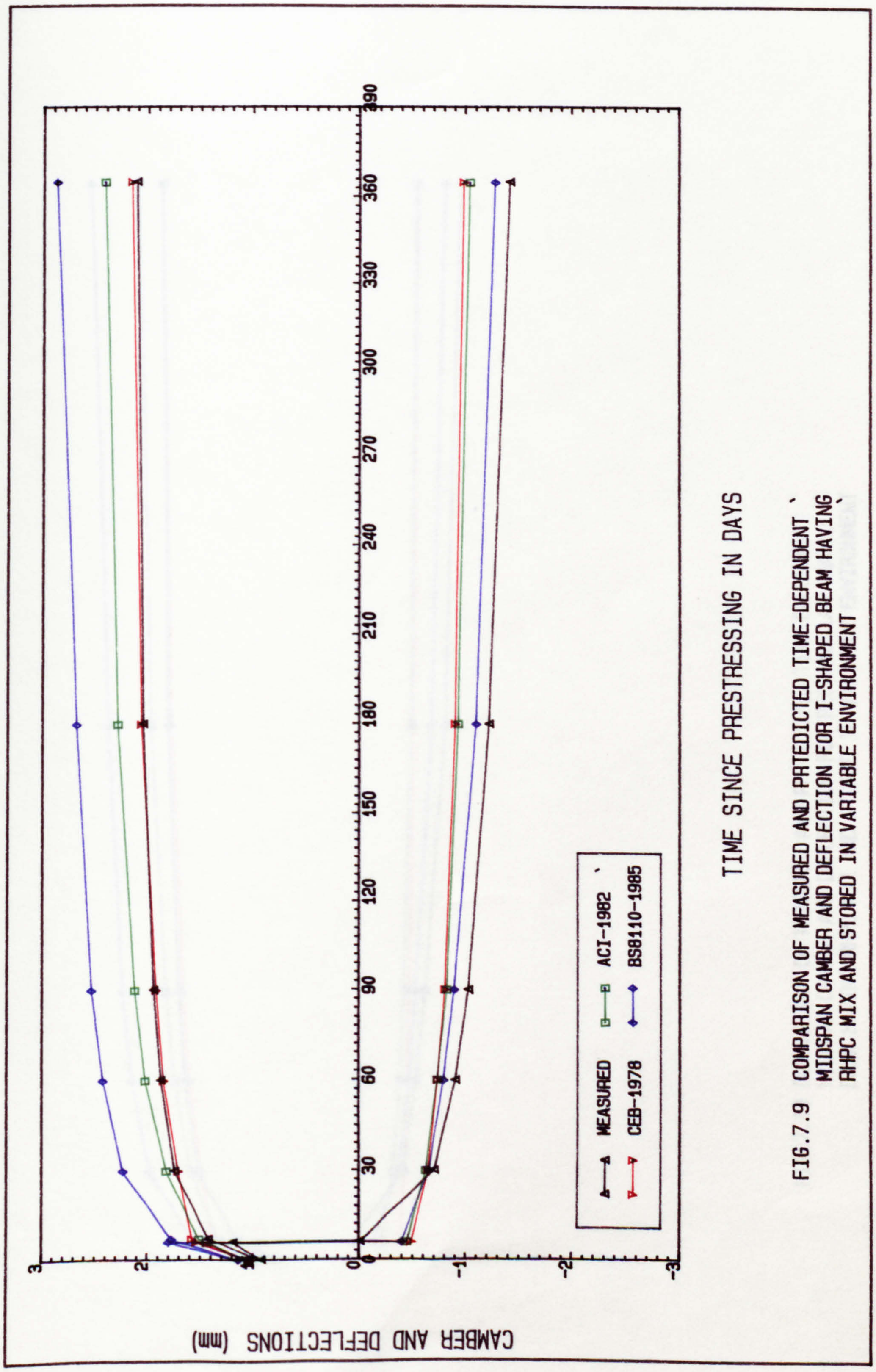

FIG.7.9 COMPARISON OF MEASURED AND PRTEDICTED TIME-DEPENDENT MIDSPAN CAMBER AND DEFLECTION FOR I-SHAPED BEAM HAVING RHPC MIX AND STORED IN VARIABLE ENVIRONMENT

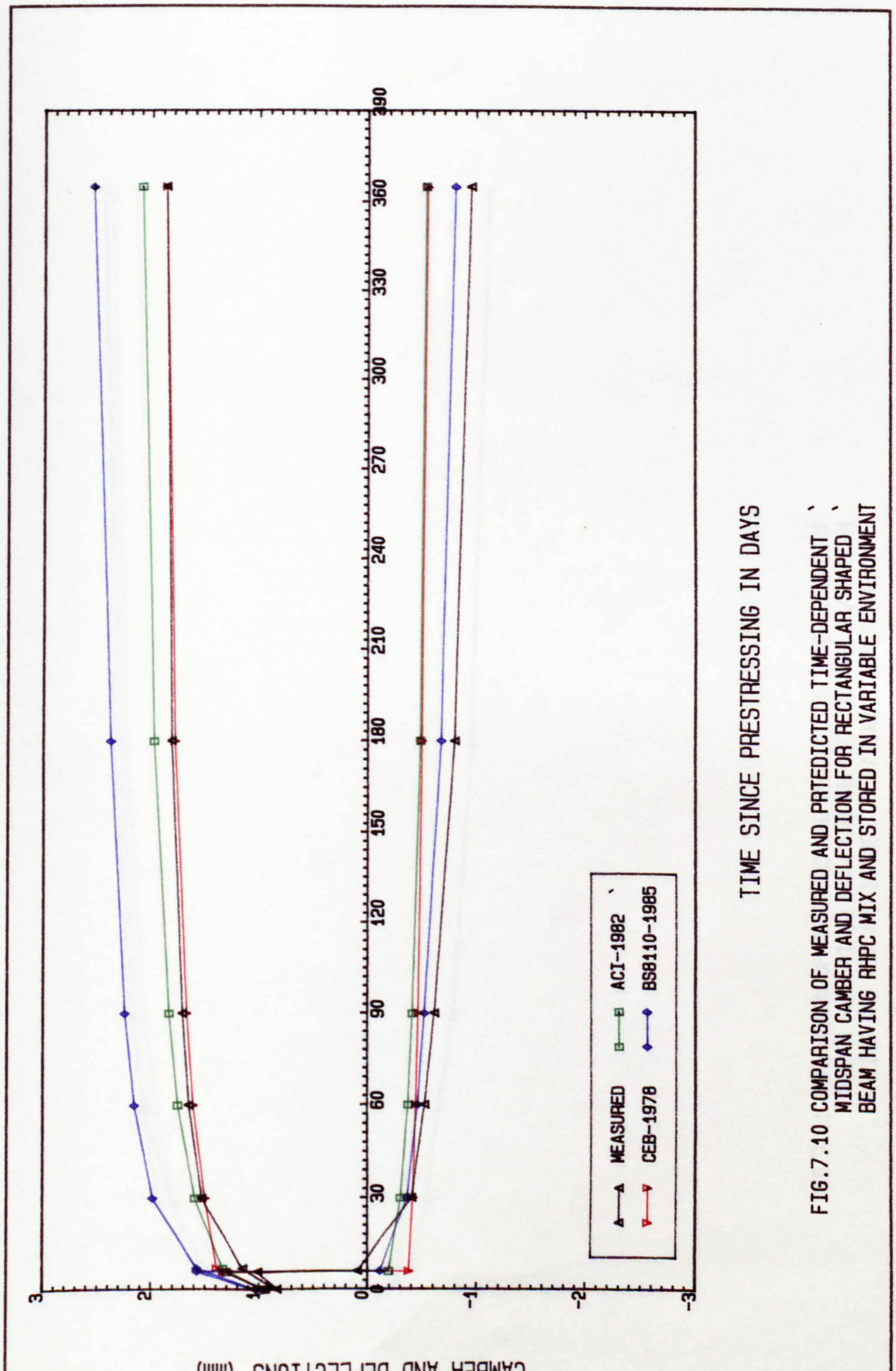

FIG.7.10 COMPARISON OF MEASURED AND PRTEDICTED TIME-DEPENDENT
MIDSPAN CAMBER AND DEFLECTION FOR RECTANGULAR SHAPED
BEAM HAVING RHPC MIX AND STORED IN VARIABLE ENVIRONMENT

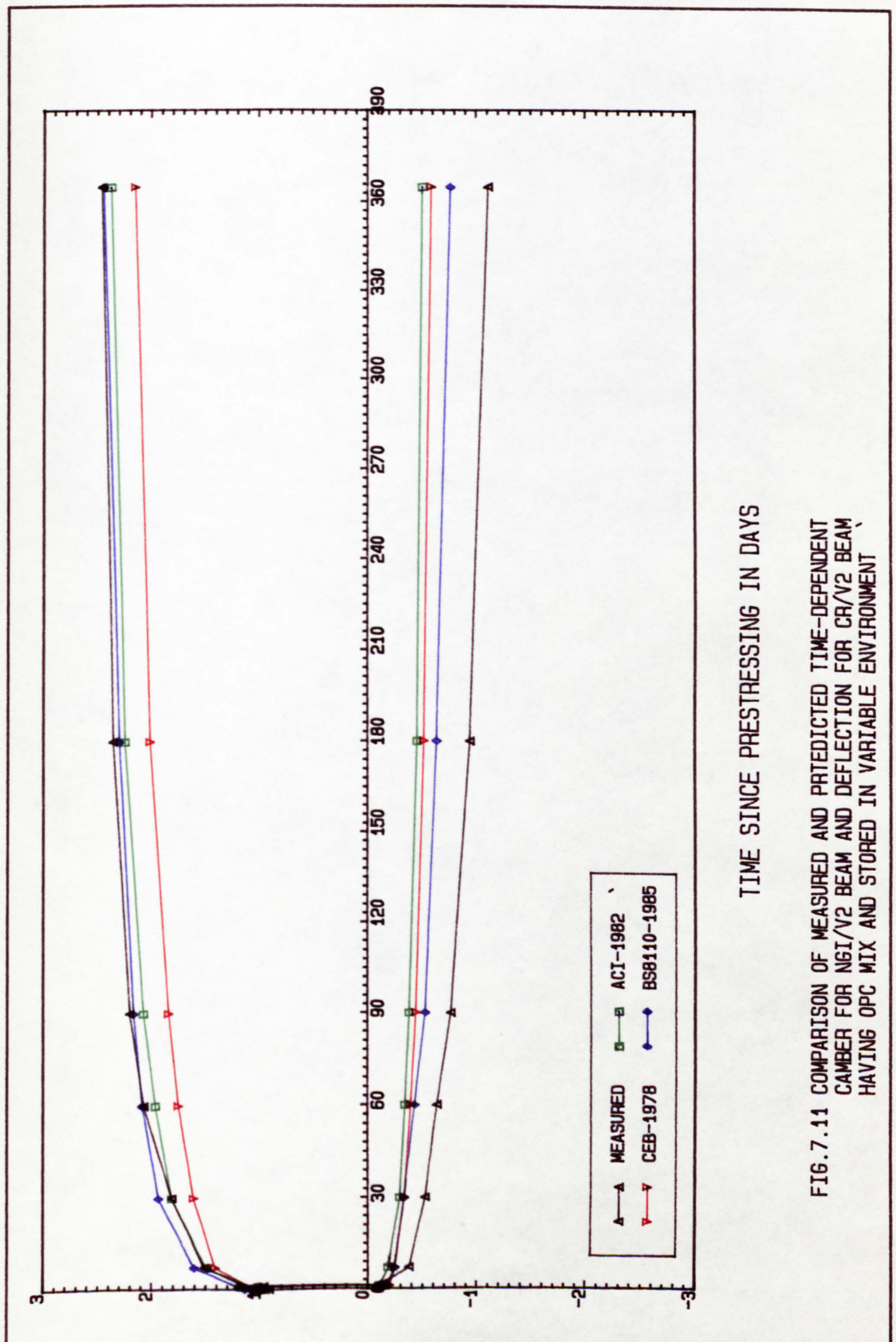

FIG.7.11 COMPARISON OF MEASURED AND PRTEDICTED TIME-DEPENDENT CAMBER FOR NGI/V2 BEAM AND DEFLECTION FOR CR/V2 BEAM HAVING OPC MIX AND STORED IN VARIABLE ENVIRONMENT

CHAPTER 8 SUMMARY OF CONCLUSIONS AND SUGGESTIONS FOR FURTHER RESEARCH

8.1 Introduction

The conclusions from this investigation are summarized in this chapter with particular reference to the objectives of the study stated in Chapter One. Suggestions for future research are also made for those aspects which may be of interest in the light of the findings from the present investigation.

8.2 Summary of Conclusions

8.2.1 Effect of Variable Environmental Conditions

(1) In the case of concrete mixes stored in varying environmental conditions, the wetting and drying cycle tends to produce a higher development of strength and modulus of elasticity with time than concrete stored in a constant drying environment, especially with OPC concrete, although such an increase is relatively small with concrete having RHPC.

(2) The effect of variable humidity decreases the one-year shrinkage in concrete to slightly more than half of the one-year shrinkage at a constant drying humidity. Variation in relative humidity also caused a reduction in creep of between 28 to 40 percent when compared with creep values in a constant drying environment.

(3) The reduction in shrinkage and creep due to the effect of variable humidity caused a significant reduction in prestress losses, averaging 20 percent (at 365 days).

(4) The total cambers and deflections of non-loaded and sustained loaded beams were found to be insensitive to the effects of relative humidity in spite of the significant variation of prestress losses between the two humidity conditions, i.e. camber and deflection values under a variable humidity condition were 4 to 10 percent lower than values under a constant humidity condition. However, for cyclic loaded beam, the variable humidity condition produced a significant reduction in total deflection (between 14 and 25 percent).

8.2.2 Effect of Loading Conditions

(1) For all prestressed concrete beams, the time-dependent concrete deformation at the tendon level was greater for non-loaded than cyclic or sustained constant loaded beams. Correspondingly, the one-year prestress losses of sustained loaded beams averaged 16 percent less than the non-loaded beams stored in the various humidity conditions. A lower prestress loss is believed to be due to a lower creep at the tendon level.

(2) There was little difference in prestress loss between cyclic and non-loading conditions. On the other hand, when beams are stored in variable humidity conditions, the effect of

cyclic loading was found to be negligible and subsequent prestress losses can be considered equal to prestress losses in the non-loaded condition.

(3) Beams under cyclic loading gave considerably lower total deflections than beams under sustained loading especially for I-shaped beams. Also, total deflection is unchanged by the effect of variable humidity. The results suggest a relatively beneficial effect of loading prestressed concrete members at early ages.

8.2.3 Effect of Shape and Size of Members

(1) When comparing the shrinkage and creep of different shapes of beam, the I-shaped beam with a lower volume/surface ratio exhibits greater shrinkage and creep than a rectangular beam with a higher volume/surface ratio. Correspondingly, the I-shaped beams exhibit higher prestress losses than rectangular-shaped beams because of the influence of volume/surface ratio on creep and shrinkage.

(2) The difference in prestress loss between the rectangular and the I-shaped beams stored in a variable environment was greater than that for beams stored in constant environment.

(3) Camber and deflection were higher for an I-shaped beam than for a rectangular shaped beam. Thus the effect of shape and size of members on camber or deflection was more significant

for beams under the cyclic and sustained loading conditions than for the non-loaded condition.

8.2.4 Effect of Concrete Mix Composition

(1) In the long term, the OPC concrete exhibits a higher creep and shrinkage than RHPC concrete in spite of the lower cement paste in the OPC concrete.

(2) In consequence, the RHPC concrete beams give slightly lower prestress losses than OPC concrete beams by 3 to 9 percent depending upon the loading and environmental conditions. On the other hand, when beams are maintained in a variable humidity and subjected to cyclic or sustained loadings, the difference between prestress losses of beams made from the two concrete mixes can be considered negligible.

(3) The long-term camber and deflection of RHPC concrete beams subjected to the various loading conditions were lower than for OPC concrete beams stored in the various environmental conditions. The average differences in camber and deflection for the two concrete mixes were 10, 12 and 28 percent for non-loaded, sustained loaded and cyclic loaded beams, respectively. The main cause of these differences is creep at the tendon level. Hence, the influence of cement type on camber and deflection is significant for a cyclic loading condition.

(4) The influence of superplasticizing admixture in RHPC concrete is to increase the creep and shrinkage, in spite of a higher early-age strength and lower water/cement ratio than the RHPC control concrete. Correspondingly, increases of 14 and 7 percent occured in prestress losses and camber at 365 days, respectively, for the non-loaded beams. The influence of the superplasticized concrete on the other loading conditions was not investigated.

(5) Compared with RHPC concrete, with or without admixture, creep and shrinkage were reduced by the use of PFA and, more so, by a combination of admixture and PFA. The one-year values of shrinkage of RHPC/PFA and RHPC/Admixture & PFA concrete were found to be 6% and 14% lower than plain RHPC concrete, respectively. However, creep of both PFA concrete mixes were found to be considerably lower than plain RHPC concrete (about 27 percent reduction in creep).

(6) Compared with the RHPC control beam, the PFA concrete and the admixture & PFA concrete produced a 7.4 and 11.5 percent reduction in one-year prestress loss, respectively. Likewise, the PFA concrete and admixture & PFA concrete beams had an 11 percent and 4 percent reduction in one-year total camber, respectively.

(7) The combination of PFA and superplasticizing admixture with RHPC give beneficial effect of high early-age and long-term strength, coupled with low shrinkage, creep, prestress

losses and camber. Such effects are of benefit in prestressed concrete applications.

8.2.5 Duration of Camber and Deflection Stabilization

(1) The camber growth of non-loaded beams had reached a stable stage at 180 days after prestresing even though creep and shrinkage were still developing. For PFA concrete, the camber growth ceased even earlier, i.e. after 90 days of prestressing.

(2) Deflections of cyclic loaded beams practically stabilized after 180 days and 90 days for the constant and variable humidity conditions, respectively. On the other hand, for sustained constant loaded beams, no stabilization of deflection was apparent during the testing period of one year.

8.2.6 Comparison Between Experimental Results and Current Preidction Methods

8.2.6.1 Elastic and Time-Dependent Deformations

(1) The ACI and CS & BS8110 methods predict the instantaneous elastic strain accurately, whereas the other prediction methods underestimate the experimental values by up to 25 percent.

(2) For shrinkage specimens with different simulated volume/surface ratios stored under a constant drying environment, the predicted shrinkage of the ACI method is practically the same as the experimental shrinkage. Other prediction methods considerably underestimate shrinkage by up to 41-68 percent, the worst prediction being that by the CS & BS8110 method. For a variable humidity environment, most prediction methods underestimate the experimental values by between 10 to 63 percent. It is concluded that by assuming a constant relative humidity for the variable environment no current prediction method is satisfactory.

(3) For swelling, CS & BS8110 and BaP methods give the best estimations for RHPC and OPC concretes, respectively.

(4) In the case of predicting basic creep, the CEB-78 method gives the best estimation, whereas the other methods overestimate basic creep considerably.

(5) For total creep in both constant or a variable environment, the ACI method, followed by CEB-78 method, give the best predictions, viz. within 24 percent of the measured total creep. All the other prediction methods generally overestimate total creep considerably. Furthermore, the recent method of Bazant et al. which accounts for cyclic humidity effects seems to overestimate the creep considerably. Use of a known elastic modulus improves predictions for most methods, the exceptions being the CEB-70 and CEB-78 methods.

(6) When the total strains (elastic plus creep plus shrinkage) are considered in a constant drying environment, the ACI, CEB-70 and BaP methods give the best predictions, whilst the CEB-78 and CS & BS8110 methods generally underestimate measured values by up to 50 percent. For the variable drying environment, it was surprisingly discovered that all prediction methods give reasonable estimates of total strains, with a slope coefficients ranging from 0.61 to 1.32.

(7) It is concluded that for both the environmental conditions used in this investigation, the ACI method gives the best overall estimation of time-dependent deformations.

8.2.6.2 Prestress Losses

(1) In the case of beams stored in a constant humidity condition, the CEB-70 and CEB-78 methods gave the best estimations of total prestress losses, followed by the ACI, BS8110 and PCI methods, respectively. For both European Codes: CEB-70 and CEB-78, prediction was within -3 to +10 percent of the measured values.

(2) The ACI method generally gave the best and the closest prediction for each individual component of total prestress loss.

(3) The British Code: BS8110 gave reasonable predictions but overestimated values by 3 to 20 percent. Since the relaxation loss was the main source of inaccuracy, a relaxation factor of 1.65 is suggested to improve predictions, instead of the 2.0 relaxation factor recently adopted by this code. A relaxation factor of 1.65 predicts relaxation and total losses to within 12 percent of the experimental values.

(4) The total predicted prestress loss of the PCI method were within 5 to 18 percent of the measured values despite the considerable underestimation of shrinkage loss.

(5) According to the previous British Code: CP110, together with ACI-ASCE and AASHTO methods, there is a substantial underestimation of total prestress losses. On the whole it was a poor estimation of shrinkage loss which caused a deterioration in the performance of each method.

(6) For beams maintained in the variable humidity condition, the prediction methods considerably overestimate the final prestress losses, with the exception of AASHTO, ACI-ASCE and CP110 methods. The AASHTO method has marginally the best performance followed by the ACI-ASCE method, which predicts within $\pm$ 9 percent of the measured values. On the other hand, the CP110 method gave a considerable underestimation of total prestress losses.

(7) When all prediction methods are compared on the basis of experimentally determined material parameters, the ACI method gave the best estimate, followed by the CP110 method; the other methods gave a significant overestimation of total prestress loss.

8.2.6.3 Camber and Deflection

(1) For the non-loaded beams, most of the methods gave predictions very close to the experimental camber values for the entire duration of the test, but BS8110 considerably overestimates camber for RHPC concrete beams. Both the ACI and CEB-78 methods gave good predicted values ranging within $\pm$ 14 percent of measured values. Furthermore, BS8110 predicted the camber very accurately for OPC concrete beams.

(2) Most methods were found to underestimate the total deflection of sustained loaded beams, BS8110 being the best with predictions being within 8 to 30 percent of the measured values.

(3) When all prediction methods are compared on the basis of experimentally determined material parameters, a slight improvement in prediction of total deflection resulted for the ACI method, but no improvement was observed for the other prediction methods.

8.3 Suggestions for Further Research

(1) Since for the various loading conditions the effect of a drying and wetting cycle on time-dependent deformations and prestress losses was significant, it would be of interest to study the effect of the actual outdoor or field conditions in the United Kingdom. Although similar conditions were simulated in the laboratory, verification of the effects of actual outdoor conditions on the properties of prestressed concrete is required.

(2) The effect of loading conditions on time-dependent prestress losses and deflections should be investigated further. In particular, the age at when external loading is imposed since early loading was found to be relatively beneficial. Furthermore, it would be of interest to study the effect of different rates of cyclic loading (such as rapidly fluctuating load) on the long-term properties of concrete members stored in various environmental conditions.

(3) Research on full-size prestressed concrete members of a large effective thickness has rarely been carried out to investigate the time-dependent prestressed losses and deflections. It would be interesting to quantify the results of the present test and those of full-size tests in order to ascertain the correct modification factors needed for present prediction methods.

(4) From the present investigation, it was found that PFA concrete, or a combination of PFA and admixture, with RHPC concrete exhibits a behaviour favourable to prestressed concrete applications. However, up to the present, tests have been limited to a constant drying environmental condition. It would be of interest to study the effects of variable environmental conditions on the time-dependent behaviour of beams made from PFA and admixtures.

(5) Further tests are required to investigate the duration of camber stabilization in particular for beams made from PFA concrete. Also, it would be of interest to investigate the camber stabilization of composite concrete structures and the effect of differential shrinkage on time-dependent camber (see Section 2.2.3).

(6) Most prediction methods gave an unreliable prediction of shrinkage in variable humidity conditions. More research is needed in this area.

(7) The BS8110 code gave an unreliable prediction of relaxation loss for class 1 relaxation wire (for post-tensioning). Further verification of the correct factor to be used for estimation is required. More research is also needed to confirm the validity of other relaxation factors presented in Table 4.6 of BS8110 (Clause 4.8.2.1).

REFERENCES

1. Ghali, A., Neville, A.M. and Jha, P.C. "Effect of Elastic and Creep Recoveries of Concrete on Loss of Prestress", Journal of the American Concrete Institute, Vol. 64, No.12, December 1967.

2. Ghali, A. and Dilger, W.H. "Rapid Accurate Evaluation of Prestress Losses", Journal of the American Concrete Institute, Vol. 70, No.69, Nov. 1973.

3. Branson, D.E. and Kripanarayanen, K.M., "Loss of Prestress, Camber and Deflection of Non-Composite and Composite Prestressed Concrete Structures", Journal of the Prestressed Concrete Institute, Vol.16, No.5, September-October 1971.

4. Glodowski, R.J. and Lorenzetti, J.J. "A Method for Predicting Prestress Losses in a Prestressed Concrete Structure", Journal of the Prestressed Concrete Institute, Vol.17, No. 2, March-April 1972.

5. Abeles, P.W. "Introduction to Prestressed Concrete", Vol. 1 and Vol. 2, Concrete Publications Limited, London, England, 1964, 1966.

6. Neville, A.M. "Creep of Concrete: Plain, Reinforced and Prestressed", North-Holland Publishing Company, Amsterdam, 1970.

7. American Concrete Institute Committee 209, "Prediction of Creep, Shrinkage and Temperature Effects in Concrete Structures", ACI Special Publication SP-27, Designing for Effects of Creep, Shrinkage, and Temperature in Concrete Structured, Detroit, Mich. 1971, pp.51-93.

8. American Concrete Institute Committee 209, "Prediction of Creep Shrinkage, and Tempertaure Effects in Concrete Structures", ACI

Special Publication SP-76, American Concrete Institute Committee 209, Designing for Effects of Creep, Shrinkage, and Temperature in Concrete Structured, Detroit, Mich. 1982, pp.193-300.

9. Neville, A.M. and Meyers, B.L. "Creep of Concrete: Influencing Factors and Prediction", ACI Symposium on Creep of Concrete, ACI SP-9, 1964.

10. Pickett, Gerald, "The Effect of Change in Moisture Content on 'The Creep of Concrete Under a Sustained Load", Proceedings of the American Concrete Institute, Vol.38, No. 4, Feb., 1942, pp.333-355.

11. Hansen, Torben, C., "Creep and Stress Relaxation of Concrete", Proceedings of the Swedish Cement and Concrete Institute, Royal Institute of Technology, Stockholm, Nr. 31, 1961.

12. Corley, W.G., Sozen, M.A. and Siess, C.P., "Time-Dependent Deflections of Prestressed Concrete Beams", Highway Research Board Bulletin 307, 1961.

13. AASHTO Specifications, "Standard Specifications for Highway Bridges", American association for State Highway and Transportation Officials, 12th ed., 1977.

14. PCI Committee on Prestress Losses, "Recommendations for Estimating Prestress Losses", J. PCI, Prestressed Concrete Institute Committee on Prestress Losses, Vol. 20, No.4, July-Aug. 1975, pp.43-75.

15. Comite Euro-International du Beton, "International Recommendations for the Design and Construction of Concrete Structures, Principles and Recommendations", European Concrete Committee-International Federation of Prestressing (CEB-FIP), Cement and Concrete Association, London, U.K., 1970.

16. Comite Euro-International du Beton, "International Recommendations for the Design and Construction of Concrete Structures, Principles and Recommendations", European Concrete Committee-International Federation of Prestressing (CEB-FIP), Cement and Concrete Association, London, U.K., 1978.

17. Gamble, B.R. and Parrott, L.J., "Creep of concrete in Compression During Dryig and Wetting", Magazine of Concrete Research, Vol. 30, No. 104, Sept., 1978, pp.129-138.

18. Neville, A.M., Dilger, W. and Brooks, J.J., "Creep of plain and structural Concrete", Construction Press, London, 1983.

19. Gamble, W., "Creep of Concrete in Variable Environments", Proc. of American Society of Civil Engineers, Structural Div., Vol. 108, No. ST10, Oct. 1982, pp.2211-2222.

20. L,Hermite, R.G. and Mamillan, M., "Further Results of Shrinkage and Creep Tests", International Conference on the Structure of Concrete, Cement and Concrete Association, London, England, 1968, pp.423.433.

21. Kingham, R.I., Fisher, J.W. and Viest, I.M., "Creep and Shrinkage of Concrete in Outdoor Exposure and Relaxation of prestressing Strand", Highway Research Board Special Report 66, American Association of State Highway Officials Road Test Technical Staff Papers, 1961, pp.103-131.

22. Troxell, G.E., Raphael, J.M. and Davis, R.E., "Long-Time Creep and Shrinkage Tests of Plain and Reinforced Concrete", Proceeding, ASTM, Vol. 58, 1958, pp.1101-1120.

23. Parrott, L.J., "Long-Term Deformation of Concrete in a Prestressed Concrete Floor", Proceedings of the Conference on Performance of Building Structures, Glasgow, Vol. 1, Mar., 1976, pp.337-351.

24. Hansen, T.G. and Mattock, A.H., "Influence of Size and Shape of Member on the Shrinkage and Creep of Concrete", Proceedings, American Concrete Institute, Vol. 63, No.2, Feb., 1966, pp.267-290.

25. Keeton, J.R., "Study of Creep in Concrete", Phase I, U.S. Naval Civil Engineering Laboratory. Technical Report R 333-1, Port Hueneme, California, Jan., 1965.

26. Lyse, I., "Shrinkage and Creep of Concrete", Journal of the American Concrete Institute, Proceedings, Vol. 56, p.775, Feb., 1960.

27. Rose, A.D., "Creep of Concrete Under Variable Stress", Journal of the American Concrete Institute, Proceedings, Vol. 54, p.739, March 1958.

28. Davis, R.E. and Davis, H.E., "Flow of Concrete under the action of sustained Loads", ACI Journal, Proc. 27, 1931, pp.837-901.

29. Bernhardt, C.J., "Creep and Shrinkage of Concrete", Materials and Structures 2, 1969, pp.145-148.

30. Breckenridge, R.A., Valent, P.J. and Bugg, S.L., "Effect of Long-Time Loads on Prestressed Concrete Beams", Tech. Rep. R-518, U.S. Naval Civil Engineering Lab., 1967.

31. Mossiossian, V., "Time-Dependent Behaviour of Noncomposite and Composite Prestressed Concrete Structures Under Field and Laboratory Conditions", Ph.D. Thesis, University of Illinois, Urbana-Champaign, 1972.

32. Hernandez, H.D., "Time-Dependent Prestress Losses in Pretensioned Concrete Construction", Ph.D. Thesis, University of Illinois at Urbana-Champaign, 1975.

33. Hummel, A., "Vom Einfluss der Zementart des Wasserzement-Verhaltiss und des Belastungsalters auf das Kriechen von Beton", Zement-Kalk-Gips, 12, No.5, 1959, pp.181-7.

34. Glanville, W.H. and Thomas, F.G., "Studies in reinforced concrete IV: Further investigations on the creep flow of concrete under load", Building Research Technical Paper No.21, Deprtment of Scientific and Industrial Research: London, 1939, 44 pp.

35. Petersen, P.H. and Watstein, D., "Shrinkage and creep in prestressed concrete", Building Science Series No.13, National Bureau of Standards: Washington DC, 1968, 12 pp.

36. Cement and Concrete Association, "Superplasticizing Admixtures in Concrete", Report of a Joint Working Party of the Cement Admixtures Association and the C. & C.A.: London, 1976, 32 pp.

37. Alexander, K.M., Bruere, G.M. and Ivanusec, I., "The creep and related properties of very high-strength superplasticized concrete", Cement and Concrete Research, 10, No.2, 1980, pp.131-7.

38. Brooks, J.J., Wainwright, P.J. and Neville, A.M., "Time-dependent behaviour of high-early-strength concrete containing a superplasticizer", Developments in the Use of Superplasticizers, American Concrete Institute Special Publication No. 68, 1981, pp.81-100.

39. Ross, A.D., "Some problems in concrete construction", Magazine of Concrete Research, 12, No. 34, 1960, pp.27-34.

40. Bamforth, P.B., "In situ measurement of the effect of partial portland cement replacement using either fly ash or ground granulated blast-furnace slag on the performance of mass concrete", Proc. ICR, Part 2, Sept. 1980, pp.777-800.

41. Gifford, P.M. and Ward, M.A., "Results of laboratory tests on lean mass concrete utilizing PFA to a high level of replacement", Int. Symp. on the Use of PFA in Concrete, Vol. 1, Eds. J.G. Cabrera and A.R. Cusens, Deprtment of Civil Engineering, University of Leeds, April 1982, pp.221-229.

42. Brooks, J.J., Wainwright, P.J. and Cripwell, J.B., Time dependent properties of concrete containing pulverised fuel ash and a superplasticizer", Ibed., pp.209-220.

43. Magura, D.D., Sozen, M.A. and Siess C.P., "A Study of Stress Relation in Prestressing Reinforcement", Journal of the Prestressed Concrete Institute, Vol. 9, No.2, April 1964.

44. Podolny, W. Jr. and Melville, T., "Understanding the Relaxation in Prestressing", Journal of the Prestressed Concrete Institute, Vol. 14, No. 4, Aug. 1969.

45. Batal, R.J. and Huang, T., "Relaxation Losses in Stress-Relieved Special Grade Prestressing Strand", Fritze Engineering Laboratory Report, No. 339, 5; April 1971.

46. Schultchen, I.C., Ying, M.T. and Huang, T., "Relaxation Behaviour of Prestressing Strands", Fritz Engineering Laboratory Report No. 339.6, March 1972.

47. Zia, P., Preston, H., Scott, N. and Workman, E., "Estimating Prestress Losses" ACI-ASCE Committee, Concrete International, June 1979, pp.32-38.

48. Branson, D.E. and Ozell, A.M., "Camber of Prestressed Concrete Beams", Journal of the American Concrete Institute, Vol. 57, No. 12, June 1961.

49. Gamble, W.L., "Field Investigation of a Continuous Composite Prestressed I-Beam Highway Bridge Location in Jefferson County", Illinois, Structural research series No. 360, University of Illinois, Urbana, Illinois, June 1970.

50. Gamble, W.L., Houdeshell, D.M. and Anderson, T.C., "Field Investigation of a Prestressed Concrete Highway Bridge Located in Douglas County", Illinois, structural research series No. 375, University of Illinois, Urbana, Illinois, Feb., 1972.

51. ACI-ASCE Joint Committee 323. "Tentative Recommendations for Prestressed Concrete", Journal of the American Concrete Institute, Vol. 54, No. 7, Jan., 1958.

52. Delare, J., "Fluage et Beton Preconstraint", RILEM Colloquim, Munich (Nov. 1958).

53. Furr, H.L., Sinno, R., Butler, H.D. and Henneberyer, W., "Prestress Loss and Camber in Highway Bridge Beam", paper presented at highway research board meeting, Washington, D.C., 1969.

54. Pauw, A., "Time Dependent Deflections of a Box-Girder Bridge", Design for Effects of Creep, Shrinkage and Temperature in Concrete Structures, American Concrete Institute Publication SP-27, 1971.

55. Gamble, W.L., "Field Investigation of Prestressed Concrete I-Beam Bridges", Colorado State University Bridge Engineering Conference, Fort Collins, Colorado, April 1970.

56. Liszka, W.Z., "Accelerated Determination of Creep of Lightweight Aggregate Concrete by the use of Elevated Temperatures", Ph.D. thesis, Dept. of Civil Engineering, The University of Leeds, August 1972.

57. Bazant, Z.P. and Panula, L., "Simplified Prediction of Concrete Creep and Shrinkage from Strength and mix", Structural Engineering, Northwestern University, Evanston, Illinois, Oct. 1978, 24 pp.

58. Concrete Society, "A simplified method for estimating the elastic modulus and creep of normal weight concrete", Training

Centre Publication No. TDH-7376, Cement and Concrete Association: London, June 1978, 1 p.

59. Concrete Society, "A simple Design Method for predicting the Elastic modulus and creep of structural concrete, London, 1978, 1 p.

60. British Standard Code of Practice, BS8110; The structural use of concrete, 1985.

61. Glucklich, J. and ISHAI, O., "Rheological behaviour of hardened cement paste under low stresses", Journal of the American Concrete Institute, Vol.57, No.46, February 1961, pp.947-964.

62. Illston, J.M., "The components of strain in concrete under sustained compressive stress, Magazine of Concrete Research, 17, No.50, 1965.

63. Illston, J.M., "Components of creep in maturing concrete", Journal of American Concrete Institute, Vol.65, No.3, March 1968, pp.219-228.

64. Rusch, H., Jungworth, D. and Hilsdorf, H., "Knitische Sichtung der Verfahren Zur Berucksichtigung der Einflusse von Krichen und Schwinden des Beton auf das Verhalten der trgwerke", Beton und Stahlbetonbau, 1973, pp.49-60, 76-86 and 152-158.

65. Parrott, L.J., "Some observations on the components of creep in concrete", Magazine of Concrete Research, Vol.22, No.72, 1970, pp.143-148.

66. Branson, D.E. and Christiason, M.L., "Time-Dependent Concrete properties Related to Design-Strength and Elastic Properties, Creep and Shrinkage", American Concrete Institute Publication, SP-27; 1971, pp.257-277.

67. Bazant, Z.P. and Wang, T., "Practical prediction of cyclic

humidity effect in creep and shrinkage of concrete", Materials and Structures (RILEM, Paris) Vol.18, No.106, 1985.

68. Muller, H.S., Hilsdrof, H.K., "Comparison of prediction methods for creep coefficients of structural concrete with experimental data", Institute fur Baustoffechnologie, university of Karlsruhe, W. Germany, 1982.

69. Brooks, J.J., "Accuracy of estimating long-term strains in concrete", Magazine of Concrete Research: Vol.36, No.128; September 1984.

70. McMillan, R.F., discussion of "Method of designing reinforced concrete slabs", by A.C. Janni, Transactions, ASCE, Vol.80, 1916, p.1738.

71. Faber, O., "Plastic Yield, Shrinkage, and other problems of concrete and their Effect on Design", Minutes of Proceedings of Institution of Civil Engineers, V. 225 port I, London, 1927.

72. Glanville, W.H., "Studies in Reinforced Concrete, III-creep or flow of concrete under load", Building Research Technical paper No.12, Department of Scientific and Industrial Research, London, 1930

73. Whitney, C.S., "Plain and Reinforced Concrete Archs", Journal of the American Concrete Institute, proceedings, Vol.28, 1932, pp.479-520.

74. Dischinger, E., "Untersuchungen uber die knicksicherheit, die elastische verformung und das kriechen des Betons bei Bogenbrllcker", Der Bauingenieur 18, No. 33/34, 35/36, 39/40, 1937, pp.487-520, 539-552, 595-621.

75. England, G.L. and Illston, J.M., "Methods of computing stresses in concrete form a history of measured strain", Civil Engineering and Public Work Review, London, Vol.60, 1965,

pp.513-517, 692-694, 846-847.

76. Nielson, L.F., "Effect of creep in uncracked composite structures of steel and concrete", Bygningestatiske Meddelelser, Vol.38, No.3, 1967, pp.65-88.

77. Nielsen, L.F., "On the Applicability of the Modified Deschninger Equations", Cement and Concrete Research, Vol.7, 1977, pp.149-160.

78. Nielsen, L.F., "The improved Dischinger Method as Related to other methods and practical Applicability", paper presented at the symposium on Design for creep and shrinkage in concrete structures, ACI fall Convention in Houston, Texas, October 1978.

79. McHenry, D., "A new aspect of creep in concrete and its application to design", Proceedings of the American Society for Testing Materials, Vol. 43, 1943, pp.1069-1086.

80. Bazant, Z.P., "Prediction of concrete creep effects using age-adjusted effective modulus method". Journal of the American Concrete Institute, Vol. 69, No. 4, April 1972, pp.212-217.

81. Trost, H., "Auswirkungen des superposions prinzips auf kriechund relaxations-probleme bei BEton und Spannbeton", Beton und Stahlbetonbau 62, 1967, Vol.62, pp.230-238, 261-269.

82. Trost, H. and Wolf, H.J., "Spannungsanderungen infolge kriechen und schwinden in beliebig bewehrten und unbestimmter Auflagerung", Final Report of the International IABSE-Symposium, Madrid, 1970, pp.405-414.

83. Bruegger, J.P., "Methods of analysis of the effects of creep in concrete structures", MSc. thesis, Deprtment of Civil Engineering, University of Toronto, August 1974.

84. Price, W.H., Factors influencing concrete strength, A.C.I.

Journal, Vol. 47, Feb. 1951, pp.417-432.

85. Neville, A.M., "Properties of Concrete", Pitman Publishing Co., London (1981), pp.779.

86. Brooks, J.J., "Prediction of Creep Recovery of Concrete from Creep in Tension and in Compression", Ph.D. Thesis, University of Leeds, 1976.

87. Davis, R.E., Troxell, G.E., "Modulus of Elasticity and Poisson's ratio for Concrete and the influence of age and other factors upon these values", Proc. ASTM, 29, Part II, pp.678-710 (1929).

88. Ghosh, R.S. and Molhotra, V.M., "Use of superplasticisers as water reducers", Cement, Concrete and Aggregates: ASTM: Vol. 1, No. 2, 56-63 pp; 1979.

89. Feldman, R.F. and Swenson, E.G., "Volume change on first drying of hydrated Portland Cement with and without admixtures", Cement and Concrete Research; Vol. 5, No. 1, 12 pp; Jan. 1975.

90. Morgan, D.R., "Possible mechanisms of influence of admixtures on drying shrinkage and creep in cement paste and concrete"; Materials and Construction; Vol. 7, No.40, 283-289, 1974.

91. Ghosh, R.S. and Timusk, J., American Concrete Institute Journal, 1981, 5, 351-357.

92. Venuat, M., Publication Technique No. 165, Centre d'Etudes et de Recherches de l'Industrie des Liants Hydrauliques, Paris, 1966, 52.

93. El-Shafey, O.A.B., "Time-Dependent Effects in Structural Concrete Members" Ph.D. Thesis, Department of Civil Engineering, University of Calgary, Alberta, August, 1979.

94. Bryant, A.H., "Creep and Shrinkage of a Bridge-Building Concrete", ACI Journal, March 1979, pp.387-403.

95. Bate, S.C.C., "The relative merits of plain and deformed wires in prestressed concrete beams under static and repeated loading", Proc. Instn Civil Engineering, 1958, 10, 473-502.

96. Hanson, J.A., "Prestress loss as affected by type of curing", Prestress Concrete Institute Journal April 1964, pp.69-93.

97. Lin, T.Y., Burns, N.H., "Design of Prestressed Concrete Structures" John Wiley & Sons, Inc., Third Edition, New York (1982) pp.646.

98. Branson, D.E., "The deformation of noncomposite and composite prestressed concrete members", ACI-(SP 43-4), 1974, pp.83-127.

99. British Standard Code of Practice, CP110, The Structural use of concrete, part 1, 1972.

100. Rowe, R., Bate, S., Cranston, W., Somerville, G., Beeby, A., Shacklock, B., Taylor, H.P.J. and Teychenne, D., "Handbook on the Unified Code for Structural Concrete (CP110: 1972)", Cement and Concrete Association, London, 1972.

101. Zia, P., Preston, H., Scott, N. and Workman, E., "Estimating Prestress Losses", (ACI-ASCE Committee on Prestressed Concrete Recommended Procedure), Concrete International, Vol. 1, No. 6, June 1979, pp.32-38.

102. Zundelevich, S., "Camber and deflection behaviour of prestressed concrete beams", Report Pb-220 043, prepared for Federal Highway Administration, Hawaii University 1971.

103. Branson, D.E., Meyers, B.L. and Kripanarayan, K., "Time-Dependent Deformation of Noncomposite and Composite Prestressed Concrete Structures": Highway Research Board, No. 324, 1970,

pp.15-43.

104. Birkenmaier, M., Nil, H., Siegwart, H.R., "Langzeitmessungen an Spannbetonbrucken", Zurich; Schweizerische Bauzeitung, Sonderdrucke aus Helf 14, 1978.

105. Stussi, F., "Zur relaxation von Stahl-drahten", IVBH Abh.19 (1959). S. 273-286, Disc. Speck. F. in 20 (1960) S.391. bis 398.

106. Zundelevich, S., Lee, D. and Chiu, A., "Camber and deflection behaviour of prestressed concrete beam made with Hawaiian aggregates", Tech. R. CE71-R1, Dept. of Civil Engineering, Univ. of Hawaii, Sep. 1971.

107. PCI Design Handbook Precast Prestressed Concrete, Second Edition, Prestressed Concrete Institute, Chicago, Illinois, 1977.

108. Martin, L.D., "A rational method for estimating Camber and deflection of Precast Prestressed Members", PCI Journal, Jan-Feb. 1977.

APPENDIX A

Table (A.1) Values of Pure Relaxation of the Steel, CEB-1970

Steel Wire Condition	in Percent
Treated rolled steel: bainitic-quenched	12 %
Oil quenched	16 %
Drawn oil	16 %
Stabilished steel	6 %

Table (A.2) Typical Loss of Prestress Ratio for Different Concretes, ACI-1982

Type of Concrete	Normal weight concrete	Sand-light weight concrete	All-light weight concrete
w in pcf, (kg/m^3)	145 (2323)	120 (1922)	100 (1602)
F_s/F_o for 3 weeks to 1 month between prestressing and sustained load application, including composite slab.	0.10	0.12	0.14
F_s/F_o -- for 2 to 3 months between prestressing and sustained load application, including composite slab.	0.14	0.16	0.18
F_u/F_o	0.18	0.21	0.23

Table (A.3) Values of $(f_{sr})_t$ and $(f_{sr})_u$ for Wires and Strands, ACI-1982

Wire or Strand		$(f_{sr})_t$ for f_{si}/f_{py} from 0.65 to .80	$(f_{sr})_u$ at $t = 10^5$ hours
Steel	Stress Relieved	$0.015\ f_{si} \times (\log_{10} t)$	$0.075\ f_{si}$
	Stabilized (low relaxation)	$0.005\ f_{si} \times (\log_{10} t)$	$0.025\ f_{si}$

Table (A.4) Shrinkage of concrete, CP110-1972

System	Shrinkage per unit length	
	Humid exposure (90 % r.h.)	Normal exposure (70 % r.h.)
Pre-tensioning: transfer at between 3 days and 5 days after concreting	100×10^{-6}	300×10^{-6}
Post-tensioning: transfer at between 7 days and 14 days after concreting	70×10^{-6}	200×10^{-6}

Table (A.5) Relaxation factors, BS8110-1985

	Wire and strand		Bar
	Relaxation class as defined in BS 5896: 1980		
	1	2	
Pre-tensioning	1.5	1.2	-
Post-tensioning	2.0	1.5	2.0

Table (A.6) Values of K_{sh} for post-tensioned members, ACI-ASCE, 1979

Time after end of moist curing to application of prestress, days	1	3	5	7	10	20	30	60
K_{sh}	0.92	0.85	0.80	0.77	0.73	0.64	0.58	0.45

Table (A.7) Values of K_{re} and J, ACI-ASCE, 1979

Type of tendon*, Grade-K_{si}	K_{re}	J
270 Grade stress-relieved strand or wire	20,000	0.15
260 Grade stress-relieved strand or wire	19,250	0.145
250 Grade stress-relieved strand or wire	18,500	0.14
240 or 235 Grade stress-relieved wire	17,600	0.13
270 Grade low-relaxation strand	5,000	0.040
250 Grade low-relaxation wire	4,630	0.037
240 or 235 Grade low-relaxation wire	4,400	0.035
145 or 160 Grade stress-relieved bar	6,000	0.05

*In accordance with ASTM A416-74, ASTM A421-76, or ASTM A722-75

Table (A.8) Values of C, ACI-ASCE, 1979

f_{pi}/f_{pu}	Stress relieved strand or wire	Stress-relieved bar or low relaxation strand or wire
0.80		1.28
0.79		1.22
0.78		1.16
0.77		1.11
0.76		1.05
0.75	1.45	1.00
0.74	1.36	0.95
0.73	1.27	0.90
0.72	1.18	0.85
0.71	1.09	0.80
0.70	1.00	0.75
0.69	0.94	0.70
0.68	0.89	0.66
0.67	0.83	0.61
0.66	0.78	0.57
0.65	0.73	0.53
0.64	0.68	0.49
0.63	0.63	0.45
0.62	0.58	0.41
0.61	0.53	0.37
0.60	0.49	0.33

Table (A.9) Creep factors for various volume to surface ratios

Volume to surface ratio, in.	Creep factor SCF
1	1.05
2	0.96
3	0.87
4	0.77
5	0.68
5	0.68

Table (A.10) Creep factors for various ages of prestress and periods of cure

Age of prestress transfer, days	Period of cure, days	Creep factor, MCF
3	3	1.14
5	5	1.07
7	7	1.00
10	7	0.96
20	7	0.84
30	7	0.72
40	7	0.60

Table (A.11) Variation of creep with time after prestress transfer

Time after prestress transfer, days	Portion of ultimate creep, AUC
1	0.08
2	0.15
5	0.18
7	0.23
10	0.24
20	0.30
30	0.35
60	0.45
90	0.51
180	0.61
365	0.74
End of service life	1.00

Table (A.12) Shrinkage factors for various volume to surface ratios

Volume to surface ratio, in.	Shrinkage factor SSF
1	1.04
2	0.96
3	0.86
4	0.77
5	0.69
6	0.60

Table (A.13) Shrinkage coefficients for various curing times, PCI-1975

Time after end of curing, days	Portion of ultimate shrinkage, AUS
1	0.08
3	0.15
5	0.20
7	0.22
10	0.27
20	0.36
30	0.42
60	0.55
90	0.62
180	0.68
365	0.86
End of service life	1.00